

The Genetics of Anthracycline-Induced Cardiotoxicity in Cancer Patients



By

HORACIA NAIDOO

NDXHOR001

SUBMITTED TO THE UNIVERSITY OF CAPE TOWN

In fulfilment of the requirements for the degree

Ph.D. (Doctor of Philosophy – Human Genetics)

Faculty of Health Sciences

UNIVERSITY OF CAPE TOWN

August 2017

Supervisor: Professor Raj Ramesar

Co-Supervisor: Professor Hannah Simonds

**Division of Human Genetics, Department of Pathology, University of Cape
Town**

The copyright of this thesis vests in the author. No quotation from it or information derived from it is to be published without full acknowledgement of the source. The thesis is to be used for private study or non-commercial research purposes only.

Published by the University of Cape Town (UCT) in terms of the non-exclusive license granted to UCT by the author.

Declaration

I, *Horacia Naidoo*, hereby declare that the work on which this dissertation/thesis is based is my original work (except where acknowledgements indicate otherwise) and that neither the whole work nor any part of it has been, is being, or is to be submitted for another degree in this or any other university.

I empower the university to reproduce for the purpose of research either the whole or any portion of the contents in any manner whatsoever.

Signature: signature removed

Date:

Abstract

INTRODUCTION: Breast cancer makes up 25% of all cancers diagnosed worldwide. Despite an increasing yearly incidence, there has been a significant decrease in mortality owing to early diagnosis and advances in treatment. Anthracycline-based chemotherapy is a relatively low cost yet highly effective anti-cancer treatment, increasing survival from 30% to >80%, presently. However, treatment efficacy is marred by the increased risk of anthracycline-induced cardiotoxicity (ACT) – estimated at 10-26%. Internationally, there has been evidence of ACT having a genetic basis.

Currently in South Africa, there is little information on ACT in cancer patients and survivors, and no information on the genetic basis of this phenomenon. Our recruitment sites in Cape Town - Groote Schuur Hospital (GSH) and Tygerberg Hospital (TBH), routinely treat hundreds of patients, notably with breast cancer, with anthracycline-based therapy every year, and provided the environment to assess ACT, as well as genetic factors which may influence this adverse drug reaction. Left ventricular ejection fraction (LVEF) acts as a surrogate measure of cardiac function in the public health-care setting.

OBJECTIVES: To provide insight into the clinical management of breast cancer patients on anthracycline-based treatment with a focus on the prevalence of ACT. To provide an index of genetic susceptibility to ACT and potentially contribute to a personalized medicine approach for a genetically diverse population.

METHODOLOGY: In the retrospective part of the study, the clinical records of cancer patients treated with anthracyclines from 2011- 2016 at the Oncology Clinic at GSH were analysed. Clinical co-morbidities such as hypertension, diabetes, pre-existing cardiac disease and smoking as well as type and dose of anthracyclines, cardiac function and patient status were assessed.

In the prospective study, breast cancer patients treated with anthracyclines, with a pre and post-treatment LVEF measure were recruited at GSH and TBH from 2013 to 2016. Patients were consented for access to both clinical information and biological material. Demographics, clinical risk factors and chemotherapeutic regimen data were analysed. LVEF, biomarkers and clinical status were also assessed in terms of reflecting ACT. In some instances certain clinical information was not available (i.e. LVEF) and out of necessity, a statistical correlation model or classifier was created in order to use available clinical data to derive missing clinical measures. Patients' DNA were analysed for seven genetic variants in the following six genes *ABCC1* (rs246221); *ABCC2* (rs17222723; rs8187710); *HNMT* (rs17583889); *NCF4* (rs1883112); *RAC2* (rs13058338) and *RARG* (rs2229774), and tested for correlation with clinical status and cardiac injury. Finally, a corollary study was conducted on a subset of patients in an attempt to determine whether cardiac biomarkers may be more sensitive measures of cardiotoxicity.

RESULTS & DISCUSSION: In the retrospective cohort (n=402) 19.7% of patients showed diminished cardiac function. Logistic regression showed that the following predictors: type of first line chemotherapy, and total dose significantly contributed to the ACT phenotype as measured by change in LVEF.

In the prospective patients (n=272), 14% were affected with ACT, with an increased likelihood of cardiotoxicity in the Indigenous African population. Logistic regression showed that both total anthracycline dose and change in LVEF were predictive of ACT. In the association study of prospective patients, only the *RARG rs2229774* variant was significantly associated with patient ACT status (p=0.049, Chi-Square Test).

Forty-two patients were assessed for the β -Natriuretic Peptide (BNP) biomarker and showed limited utility in correlating clinical status and/or LVEF decrease in all patients except Indigenous Africans indicating potential increased susceptibility of population group to ACT.

LVEF was found to be unreliable as significant LVEF decreases did not always correlate with cardiac impairment and vice-versa. Changes in routine clinical patient management and overburdening of the nuclear medicine department also translated to only one LVEF measure being obtained in some instances. The statistically derived classifier for missing indicators of heart function was useful, but will require refinement.

CONCLUSIONS AND RECOMMENDATIONS: Despite the inability of genotype as a predictor of ACT in this study, the increased susceptibility in the Indigenous African population to ACT as well as increased BNP levels after chemotherapy requires a closer look. The interrogation of Indigenous African patient genomes for novel variants of susceptibility to ACT are recommended; this requires building up of a substantial cohort from this population group, which would likely require collaboration with health care institutions in one of the other provinces of South Africa e.g. Eastern Cape, KwaZulu-Natal and/or Gauteng. Both this study and literature recommend the need for clinical trials for new and existing drugs on local African populations for both safety and efficacy.

Furthermore, the BNP biomarker may be better suited to the prediction of irreversible cardiac damage rather than early cardiotoxicity. Troponin, released in response to cardiomyocyte death, may be a more sensitive biomarker in predicting ACT. Similarly, the inherent variability and lack of sensitivity of LVEF as a measure of cardiac function warrants the consideration of alternatives such as echocardiography or tissue-doppler imaging.

Findings derived from this study indicate the need for refined patient management of ACT in a South African population to potentially allow for treatment with minimised risk and event-free breast cancer survival.

Acknowledgements

“Courtesies of a small and trivial character are the ones which strike deepest in the grateful and appreciating heart.” – Henry Clay

While this PhD may have my name on it, it would have not been possible without the kindness and selfless contribution of others – for which I am both immeasurably and eternally grateful.

Firstly, to my parents Ravi and Shereen, no words can express the gratitude I have to both of you for the life you have blessed me with. The hard work and sacrifice undertaken and the motivation and love that you have given has resulted in a life with endless possibilities and for that I thank you...I only hope that I can one day bestow these same kindnesses on both of you for there is no one more deserving. I love you both so much.

Della and Tash, my lovely sisters – one here and one in heaven, thank you for always being your big sister's greatest supporters. Della, thank you for your generosity of spirit and being the most fun person I know – being with you is like a holiday and I love you for it.

Michael, my love – in the journey of the PhD, I never expected to find you and I am so grateful that I did. Not only have you given me greater resilience in pursuing my dreams but you have inadvertently brought out the best version of me and for that I thank you.

To my friends – Amy, Khalil, Lindie, Shareefa, Maryam, Tasneem and Marelize who have loyally supported and encouraged me from the side-lines. Our friendship transcends distance and time – thank you. Shareefa (Dr Dalvie), thank you for being a most trusted PhD ally- without your editing, advice and incredible teaching I would be lost.

To the kindness of the selfless ones, those who take a moment to pause in their busy lives to ensure you are assisted is akin to a gratefully received miracle. Alvera, thank you for both always dropping everything to help me and your sage advice; Lara, Eve and Dr Van Wijk at the Groote Schuur Hospital LE33 Clinic for making my hospital visits a happy and productive one; Dr Pieter Barnardt at Tygerberg Hospital for being an incredibly proficient research collaborator; Dr Ferial Azibani and Professor Karen Sliwa for your kind collaborative efforts; Professors Jacquie Greenberg and Collet Dandara for always providing support and a listening ear and Heidi Paulse, our saint in the front office – thank you.

To my supervisors Professor Raj Ramesar and Hannah Simonds, thank you for your expertise and support allowing for the completion of my PhD. Professor Ramesar, thank you for giving me the opportunity of a lifetime and allowing me to grow – my time at HumGen has been an incredibly happy one. Professor Simonds, you are an inspiration for women in medicine and science, thank you for all your help in my PhD journey.

To the National Research Foundation and the UCT Funding Office, without your steadfast financial contribution this PhD would not be possible – thank you.

To all the patients and their families who so kindly consented to be a part of this study – thank you. I sincerely hope that this work will ultimately contribute to better clinical outcomes in the future.

Finally, I must express my gratitude to God for a life with an abundance of blessings.

Table of Contents

Declaration	ii
Abstract	iii
Acknowledgements.....	v
List of Figures	xii
List of Tables	xv
Abbreviations.....	xvii
Chapter 1: Preface.....	1
1.1 Thesis Statement:.....	1
1.2 Project Summary:	1
1.3 Motivation:	1
1.4 Research Related Aims and Objectives:.....	3
Chapter 2: Introduction	6
2.1 Retrospective Patient Analysis	6
2.1.1 Definition of Breast Cancer	6
2.1.2 Incidence of Breast Cancer.....	6
2.1.3 Types of Breast Cancers	8
2.1.4 Breast Cancer Staging and Classification	10
2.1.5 Treatment of Breast Cancer.....	15
2.2 Prospective Patient Analysis.....	16
2.2.1 Anthracycline-based Chemotherapy	16
2.2.2 Modalities to Assess Cardiac Function	26
2.2.3 Management of Cardiotoxicity	30
2.3 Genetics of Cardiotoxicity	32
2.3.1 Characterisation of Specific Genes.....	38
2.4 Economic Implications of Cardiac Failure compared to Preventative Measures	41
2.4.1 Comparison of Preventative Measures, Sensitive Assessment Modalities and Treatment for Cardiac Failure	41
Chapter 3: Patients, Materials and Methods	43

3.1	Retrospective Cohort.....	43
3.1.1	Setup of Database.....	43
3.1.2	Collection of Data	43
3.1.3	Statistical Analyses.....	44
3.2	Literature Mining.....	45
3.3	Prospective Study: Selecting Genes/SNPs of Interest	45
3.3.1	Pathway-based Approach.....	45
3.3.2	Gene Annotation.....	45
3.3.3	Selected Genes of Interest	46
3.4	Prospective Study: Patient Recruitment.....	48
3.4.1	Recruitment Protocol and Ethics.....	48
3.4.2	Procurement of Clinical Information from Patient Folders	48
3.5	Patient Sample	49
3.6	DNA isolation.....	49
3.6.1	Principle of DNA Isolation using Promega Maxwell® 16 DNA Purification Kit:.....	49
3.6.2	Principle of DNA Isolation using 'Salting-Out' Technique:	50
3.6.3	Quantification of DNA:	51
3.6.4	DNA Integrity Gels.....	52
3.7	Polymerase Chain Reaction (PCR).....	53
3.7.1	Principle of PCR	53
3.7.2	Primer Design for PCR	54
3.7.3	Optimisation: Singleplex and Multiplex	57
3.7.4	Technique of PCR	60
3.7.5	Agarose Gel Electrophoresis	62
3.8	Genotyping	62
3.8.1	Genotyping by the SNaPshot® Multiplex Assay	62
3.8.2	Genotyping by TaqMan™ SNP Genotyping Assay	70
3.9	Sequencing	72

3.9.1	Principle of Sequencing	72
3.9.2	Technique of Sanger Sequencing.....	73
3.10	Statistical Analysis	75
Chapter 4:	Results	78
4.1	Retrospective Cohort Analysis	78
4.2	Prospective Cohort Analysis	87
4.2.1	Recruitment.....	87
4.2.2	Procurement of Clinical Information from Patient Folders.....	87
4.2.3	Statistical Analysis	90
4.3	Patient Sample.....	93
4.3.1	DNA isolation	93
4.3.1.1	Spectrophotometry for quantitation of DNA	94
4.3.1.2	Assessment of DNA Integrity	94
4.4	Selected Genes of Interest.....	95
4.4.1	Gene Annotation	95
4.5	PCR	95
4.5.1	Optimisation: Singleplex and Multiplex PCR.....	95
4.5.1.1	Temperature Gradient.....	95
4.5.1.2	Magnesium Gradient.....	96
4.5.1.3	Additives	97
4.5.1.4	Touchdown PCR.....	97
4.5.2	Optimised Multiplex PCRs.....	98
4.6	Genotyping.....	100
4.6.1	Optimisation of the SNaPshot® Multiplex System	100
4.6.2	Optimisation of the TaqMan™ SNP Genotyping Assay	101
4.6.3	Genotyping of patient samples	102
4.6.4	Validation Sequencing	102
4.7	Statistical Analysis	104
4.7.1	Genotype and Allele frequencies.....	104

4.7.2	Association testing	108
Chapter 5: Discussion.....		112
5.1	Summary of Main Findings.....	112
5.2	Retrospective Cohort Analysis	113
5.3	Prospective Cohort Analysis	116
5.4	Study Limitations.....	120
5.5	Recommendations	121
5.6	Future Directions.....	121
Chapter 6: Supplementary Study – Testing of Biomarkers as a Measure of Cardiac Injury.....		123
6.1	Introduction:	123
6.1.1	Brain Type Natriuretic Peptide (BNP)	123
6.1.2	Troponin T.....	125
6.1.3	Suppression of Tumorigenicity 2 (ST2)	127
6.2	Materials and Methods:	127
6.2.1	The Study Cohort:	127
6.2.2	Determination of cardiac biomarker of injury levels using peripheral blood	127
6.2.2.1	Principle of ELISA	128
6.2.2.2	Technique of Detection of N-terminal pro B-Type Natriuretic Peptide (NT-proBNP) using a Competitive ELISA.....	129
6.2.2.3	Statistical Analysis for the determination of NT-proBNP levels	129
6.3	Results:	130
6.3.1	Determination of cardiac biomarker of injury levels using EDTA-plasma	130
6.3.2	NT-pro B-Natriuretic Peptide (NT-proBNP) concentration	130
6.3.3	Statistical Analysis	133
6.3.4	Correlation between Routine Measures, Biomarkers and Cardiac Function Decline	138
6.4	Discussion.....	141

6.4.1	Study Limitations:.....	143
6.4.2	Recommendations:	144
Chapter 7: Concluding Remarks		145
References		146
Appendices		155
Appendix A: Gene Annotation and Primer Design Protocol		155
Appendix B: Informed Consent.....		158
Appendix C: Ethics Approval – UCT		160
Appendix D: Ethics Approval – GSH		161
Appendix E: Ethics Approval – SUN/TBH.....		162
Appendix F: Reagent Preparation		163
Appendix G: Multiplex PCR Protocol		165
Appendix H: Patient DNA Isolations		167
Appendix I: Spectrophotometric quantitation of DNA		174

List of Figures

Figure 1: Graphical representation of the initiation of the PhD project	3
Figure 2: Experimental steps taken towards fulfilment of aims and objectives	4
Figure 3: Global incidence and mortality of breast cancer	7
Figure 4: Illustration of breast tissue showing comparison between ductal and lobular carcinoma.....	8
Figure 5: Inflammatory Breast Cancer	9
Figure 6: Two-dimensional structure of Doxorubicin	17
Figure 7: Chemical structure of doxorubicin and epirubicin	17
Figure 8: Comparison of a normal heart and a heart in congestive failure	19
Figure 9: Cardiomyocyte showing mechanism of action of anthracycline.....	25
Figure 10: Representation of pathways showing candidate genes involved in the metabolism of doxorubicin in a cancer cell	33
Figure 11: Representation of transport and metabolism of doxorubicin.....	34
Figure 12: Representation of candidate genes involved in the metabolism of doxorubicin	34
Figure 13: Representation of GeneRuler™ 100bp Plus DNA Ladder (Molecular Weight Marker)	53
Figure 14: Diagrammatic illustration of PCR	54
Figure 15: Diagrammatic representation of touchdown PCR	59
Figure 16: Diagrammatic Representation of SNaPshot® Genotyping	63
Figure 17: GeneScan™ 120 Liz™ Size Standard	69
Figure 18: Analysis settings on GeneMapper v4.1 software	69
Figure 19: Graphical representation of Taqman™ SNP Genotyping Assay	70
Figure 20: Example of an Allelic Discrimination plot	72
Figure 21: Histogram of retrospective cohort illustrating proportion of patients and their age at diagnosis (n=402)	78
Figure 22: Patient Clinical Status (Cardiac impairment/dysfunction: affected vs unaffected) of retrospective cohort after chemotherapy	81
Figure 23: Histogram of the age at diagnosis of patients in the prospective cohort (n=272).....	88
Figure 24: Clinical status (Cardiac impairment/dysfunction: affected vs unaffected) of Patients in Prospective Cohort.....	91
Figure 25: Difference between actual and predicted post-chemo LVEF measures in prospective patients.....	93
Figure 26: Assessment of DNA Integrity using agarose gel electrophoresis...	94

Figure 27: Multiplex optimisation using a temperature gradient.....	95
Figure 28: Singleplex optimisation using a magnesium chloride (MgCl ₂) gradient	96
Figure 29: Singleplex optimisation of ABCC2 rs17222723 using additives.....	97
Figure 30: Multiplex optimisation of ACO1 rs867469, ABCC1 rs246221 and ABCC2 rs17222723	98
Figure 31: Optimised multiplex PCR showing the amplification of HNMT rs17583889 and ABCC2 rs8187710.....	98
Figure 32: Optimised multiplex PCR showing the amplification of RAC2 rs13058338 and NCF4 rs1883112.....	99
Figure 33: Optimised multiplex PCR showing the amplification of ABCC1 rs246221 and ABCC2 rs17222723.....	99
Figure 34: Electropherogram illustrating determination of genotypes for both HNMT rs17583889 and ABCC2 rs8187710.....	100
Figure 35: Electropherogram illustrating determination of genotypes for both NCF4 rs1883112 and RAC2 rs13058338	100
Figure 36: Electropherogram illustrating determination of genotypes for both ABCC1 rs246221 and ABCC2 rs17222723.....	101
Figure 37: Quantification & Allelic Discrimination Plots.....	101
Figure 38: Representation of electropherogram, sequence coverage and sequence derived from Sanger sequencing	102
Figure 39: Representation of nucleotide blast results for ABCC2 rs8187710 validating both the target gene and corresponding SNP.....	103
Figure 40: LD plot and Haplotype analysis generated by the SHEsis program	108
Figure 41: Natriuretic peptides involved in Cardiac Failure	123
Figure 42: Natriuretic peptides ANP, BNP and CNP	124
Figure 43: Visualization of cardiac muscle and Troponin molecules	126
Figure 44: Generalized principles of the four types of ELISAs	128
Figure 45: Comparison of baseline BNP concentrations in both the MA and IA cohorts with the exclusion of hypertensive patients	134
Figure 46: BNP Concentration of the entire cohort before (pre) and after (post) chemotherapy	135
Figure 47: BNP Concentration of the non-hypertensive patients before and after chemotherapy	136
Figure 48: Comparison of BNP levels at baseline (pre) and after (post) chemotherapy for both MA and IA patients	136

Figure 49: Comparison of BNP levels at baseline and after chemotherapy for both MA and IA patients	137
Figure 50: Comparison of change in BNP based on both patient status and severity score	139
Figure 51: Comparison of change in BNP in both IA and MA affected and unaffected individuals	140
Figure 52: BNP changes in patients with baseline cardiac incidental finding	141

List of Tables

Table 1: Clinical Classification of breast cancer	12
Table 2: Staging of breast cancer based on TNM Classification.....	14
Table 3: Types of Anthracycline-Induced Cardiotoxicity	19
Table 4: Studies illustrating dose-dependent cardiotoxicity	22
Table 5: Left Ventricular Ejection Fraction and its Interpretation	27
Table 6: Genes and SNPs associated with anthracycline-induced cardiotoxicity	37
Table 7: Details of SNPs for further study of anthracycline-induced cardiotoxicity in patient cohort.....	47
Table 8: Custom-designed PCR Primers.....	56
Table 9: Conditions of PCR reaction required for optimisation of annealing temperature.....	57
Table 10: Conditions of Touchdown PCR reaction	60
Table 11: Optimised Multiplex Conditions	60
Table 12: Prescribed reagents and concentrations for a standard PCR.....	61
Table 13: Prescribed reagents and concentrations for a touchdown PCR.....	61
Table 14: Labelled ddNTPs, their fluorescent dyes and colours that determine genotype.....	63
Table 15: Pre-designed TaqMan™ SNP Genotyping Assay.....	65
Table 16: Custom-designed Primers for Genotyping using the SNaPshot® Multiplex System	66
Table 17: Reagents required for the purification of PCR products	67
Table 18: Reagents required for the SNaPshot Multiplex Assay	68
Table 19: Reagents required for the automated electrophoresis run	68
Table 20: Preparation of reaction mix for the wet DNA method	71
Table 21: Labelled ddNTPs, their fluorescent dyes and colours that determine genotype.....	73
Table 22: Primers utilised for validation of genotyping using Sanger sequencing	74
Table 23: Reagents required for validation of genotyping using Sanger Sequencing	74
Table 24: Demographic characteristics of the retrospective patients cohort ..	79
Table 25: Type and Stage of Cancer of Patients in the Retrospective Cohort ..	80
Table 26: Patients classified according to clinical manifestations	81
Table 27: The effect of severity score on LVEF post chemotherapy	82

Table 28: Prediction of LVEF post-chemo measure using population group, type of first-line chemotherapy and severity score	83
Table 29: Logistic Regression Coefficients used to determine Odds Ratios of covariates for Patient Clinical Status	86
Table 30: Demographic characteristics of patients in the Prospective cohort	88
Table 31: Type and Stage of Cancer of Patients in the Prospective Cohort.....	89
Table 32: Incidental cardiac findings derived from baseline cardiac function.	90
Table 33: Logistic Regression Co-efficients used to determine Odds Ratios using Clinical-based Covariates	92
Table 34: Distribution of genotypes and minor allele frequencies.....	105
Table 35: Patient population allele frequencies and Pearson’s Chi-Square test for HWE	106
Table 36: Testing for LD of genetic variants using R and SHESIS.....	107
Table 37: Logistic Regression Co-efficients used to determine Odds Ratios using Genotype to Predict Outcome	109
Table 38: Logistic Regression Co-efficients used to determine Odds Ratios using Genotype and Dose Covariates.....	110
Table 39: Overview of genetic variants, their genetic model and contribution to phenotype	111
Table 40: Clinical, demographic and experimental information for patients assessed for BNP levels	131
Table 41: Comparison of median baseline BNP concentrations before the administration of anthracycline based chemotherapy.....	134
Table 42: Severity Score established using LVEF measure and patient clinical phenotype	138
Table 43: Patients with baseline cardiac incidental findings analysed for both BNP levels and clinical status	140

Abbreviations

4PL	Four parameter logistic regression
5FU	5-Fluorouracil
<i>ABCC1/2</i>	ATP binding cassette subfamily C member 1/2, gene
<i>ABCB4</i>	ATP binding cassette subfamily B member 4, gene
AC	Adriamycin and Cyclophosphamide
ACE	Angiotensin Converting Enzyme Inhibitor
<i>ACO1</i>	Aconitase 1, gene
ACT	Anthracycline-Induced Cardiotoxicity
ADMET	Absorption, Distribution, Metabolism, Elimination and Toxicity of drug
ADR	Adverse Drug Reaction
AKR	Aldo/keto Reductase, enzyme
<i>AKR1A1</i>	Aldo-keto reductase family 1 member A1
AJCC	American Joint Committee on Cancer
AT	Adenine-Thymine
ATP	Adenosine Triphosphate
BLAST	Basic Local Alignment Search Tool
BMI	Body Mass Index
BNP	Brain type Natriuretic Peptide (NT-proBNP, alternate form)
<i>CAT</i>	Catalase, gene
CBR	Carbonyl Reductase, enzyme
<i>CBR3</i>	Carbonyl reductase 3, gene
CF	Cardiac Failure
CI	Confidence Intervals
CMR	Cardiac Magnetic Resonance
CRAN	Comprehensive R Archive Network
CT	Computerized Tomography
CTCAE	Common Technology Criteria for Adverse Events
<i>CYBA</i>	Cytochrome b-245 alpha chain, gene
DCIS	Ductal Carcinoma In Situ
DMSO	dimethyl sulfoxide
DNA	Deoxyribonucleic Acid
dNTPs	deoxynucleotides

ddNTPs	dideoxynucleotides
DOX	doxorubicin (Adriamycin)
DTT	dithiothreitol
ECHO	Echocardiography
EDTA	Ethylenediaminetetraacetic Acid
EF	Ejection Fraction
EIA	Enzyme Immunoassays
ELISA	Enzyme-Linked Immunosorbent Assays
EPI	Epirubicin (4-Epi-Adriamycin)
EPR	Electronic Patient Records
ER	Estrogen Receptor
ERNA	Equilibrium Radionuclide Angiography
Exo1	Exonuclease 1
FastAP	Alkaline Phosphatase
FDA	Food and Drug Administration
FS	Fractional Shortening
GC	Guanine-Cytosine
GSH	Groote Schuur Hospital
<i>GSTP1</i>	Glutathione S-transferase pi 1, gene
GTP	Guanosine triphosphate
GUI	Graphical User Interface
GWAS	Genome Wide Association Studies
HER2	Human Epidermal Growth Factor 2
HFE	Haemochromatosis, gene
HIV	Human Immunodeficiency Virus
<i>HNMT</i>	Histamine N-methyltransferase, gene
HREC	Human Research Ethics Committee
HRPO	Horseradish Peroxidase, enzyme
HSP20	Heat Shock Protein 20
HWE	Hardy-Weinberg Equilibrium
IDC	Invasive or Infiltrating Ductal Carcinoma
IDT	Integrated DNA Technologies
ILC	Invasive or Infiltrating Lobular Carcinoma
<i>IREB2</i>	Iron Responsive Element Binding Protein 2, gene

IRES	Iron Responsive Elements
LCIS	Lobular Carcinoma In Situ
LD	Linkage Disequilibrium
LV	Left Ventricle/Ventricular
LVEF	Left Ventricular Ejection Fraction
MAPK	Mitogen Activated Protein Kinase
MGB	Minor Groove Binding
MgCl ₂	Magnesium Chloride
MRD	Minimal Residual Disease
MRI	Magnetic Resonance Imaging
MUGA	Multigated Acquisition Scan
NADPH	nicotinamide adenine dinucleotide phosphate, enzyme
NCBI	National Center for Biotechnology Information
<i>NCF4</i>	Neutrophil cytosolic factor 4, gene
NOS	Not otherwise specified
NTC	No template control
OD	Optical Density
PCR	Polymerase Chain Reaction
PR	Progesterone Receptor
<i>RAC2</i>	Ras-related C3 botulinum toxin substrate 2, gene
<i>RARG</i>	Retinoic acid receptor gamma, gene
RNA	Ribonucleic Acid
RNS	Reactive Nitrogen Species
ROS	Reactive Oxygen Species
RFU	Relative Fluorescent Units
SDS	Sodium Dodecyl Sulfate
<i>SLC28A3</i>	Solute Carrier Family 28 Member 3, gene
SNP	Single Nucleotide Polymorphism
SQ	Sizing Quality
ST2	Suppression of Tumorigenicity 2, cytokine
<i>Taq</i>	<i>Thermus Aquaticus</i> , enzyme
TBE	Tris-Borate-EDTA, buffer
TBH	Tygerberg Hospital
TC	Docetaxel and Cyclophosphamide

TE	Tris-EDTA, buffer
T _m	Melting Temperature
TMB	3,3',5,5'-Tetramethylbenzidine, substrate
TNBC	Triple Negative Breast Cancer
TNM	Staging of Cancer System (Primary Tumour, Regional Lymph nodes, Metastasis)
UMIC	Upper Middle Income Country
UP	Uncoupling Proteins
USA	United States of America
UV	Ultraviolet

Chapter 1: Preface

1.1 Thesis Statement:

Anthracycline-induced cardiotoxicity, while dose-dependent, may be attributed to inherent genetic differences in treated patients.

1.2 Project Summary:

This project focused on the genetic susceptibility of cardiotoxicity in breast cancer patients receiving specific types of anthracycline treatment (Adriamycin/doxorubicin and epirubicin). Patients were assessed at Groote Schuur (GSH) and Tygerberg (TBH) Hospitals. Variable drug response from patients were corrected for co-morbidities and dosage and attributed to genetic make-up. Hence, the genetic susceptibility of individual patients to anthracycline-induced cardiotoxicity was ascertained using variant detection to ultimately allow for the individualisation of patient treatment especially focusing on highly-susceptible patients. Ultimately, the goal was to identify susceptible patients before treatment towards reducing or eliminating anthracycline-induced cardiotoxicity during or after treatment and to prevent long-term irreparable and sometimes life-threatening cardiac damage in cancer survivors.

1.3 Motivation:

The motivation for this study was: (i) the record of international findings pertaining to differential responses to anthracycline, (ii) reports of the cardiotoxicity of anthracyclines, and (iii) the complete lack of information on patients/populations in South Africa (and particularly taking into account the widespread use of anthracyclines in the treatment of cancers, nationally). Consultations with clinical caregivers e.g. radiation oncologists and surgeons revealed both the concerning occurrence of cardiac events in chemotherapy patients as well as the lack of means for clinically stratifying these patients based on risk of adverse drug events before chemotherapy exposure. The anecdotal data stemmed from routine clinical patient interactions and from interrogating a retrospective database to assess the trend, if any, in all patients exposed to anthracycline-based treatment.

Retrospective data collection (2011-2016) indicated that approximately 20% of all patients treated with anthracycline-based chemotherapy at GSH experienced decreased cardiac

function (as measured by pre and post treatment left ventricular ejection fraction) or even death due to cardiac damage. This prompted an extensive literature review which confirmed the incidence of cardiotoxicity due to anthracycline-based chemotherapy in cancer patients to be between 10-26% ^{1,2}.

Chemotherapy, specifically anthracycline-based chemotherapy, has been widely accepted to have an increased risk for dose-dependent cardiotoxicity particularly in patients of advanced age with pre-existing conditions such as hypertension, diabetes and cardiac disease. Therefore, safe administration would be ideally, to patients who have been clinically stratified as “low risk” and at doses within a “safe” range. The Food and Drug Administration (USA) prescribes a safe range of cumulative dosage at 300-450mg/m² for doxorubicin ^{3,4}. However, approximately 21% of all patients treated with anthracyclines at cumulative doses of less than 300mg/m² still experience cardiotoxicity despite the prescribed “safe” dosage threshold ⁵.

The stratification of patients with increased susceptibility for developing ACT is still considerably challenging despite cognizance of both the clinical risk factors and dose-dependent association. Consequently, previous studies have been conducted, investigating the genetic basis of cardiotoxicity attributed to anthracyclines. Genetic variants involved in the absorption, distribution, metabolism, elimination and toxicity of the drug have been implicated in the predisposition to ACT ⁶⁻¹⁰.

The majority of studies, with the exception of Aminkeng *et al.* ^{6,7} have investigated the genetic basis of ACT in either European and/or Caucasian populations. Previous studies have shown increased adverse drug reactions, reduced drug efficacy and poorer survival in African populations for various drugs and attributed this to pharmacogenomic heterogeneity ^{6,11}. The positive outcomes of clinical trials and previous genetic ACT associations ought not to be readily extrapolated to our unique local populations in South Africa [especially the Indigenous African (IA) and Mixed Ancestry (MA) groups]. Therefore, a comprehensive investigation into the genetic basis of anthracycline-induced cardiotoxicity in our local populations as well the evaluation of routine clinical management was warranted.

Ideally, this individualized gene-based approach could allow for specific thresholds for therapeutic dosage safety and the pharmacological prevention of cardiac deficit ¹². Clinical observations of cardiotoxicity during routine clinical management of breast cancer patients followed by the establishment of a retrospective database to validate these claims warranted the initiation of the PhD study whereby literature was extensively reviewed and a prospective cohort established to elucidate the genetic basis of ACT in our local populations. Recruited

patients (GSH and TBH) had biological specimens (peripheral blood before and after chemotherapy) and hospital records assessed to establish a model of susceptibility to ACT. This process is illustrated in Figure 1.

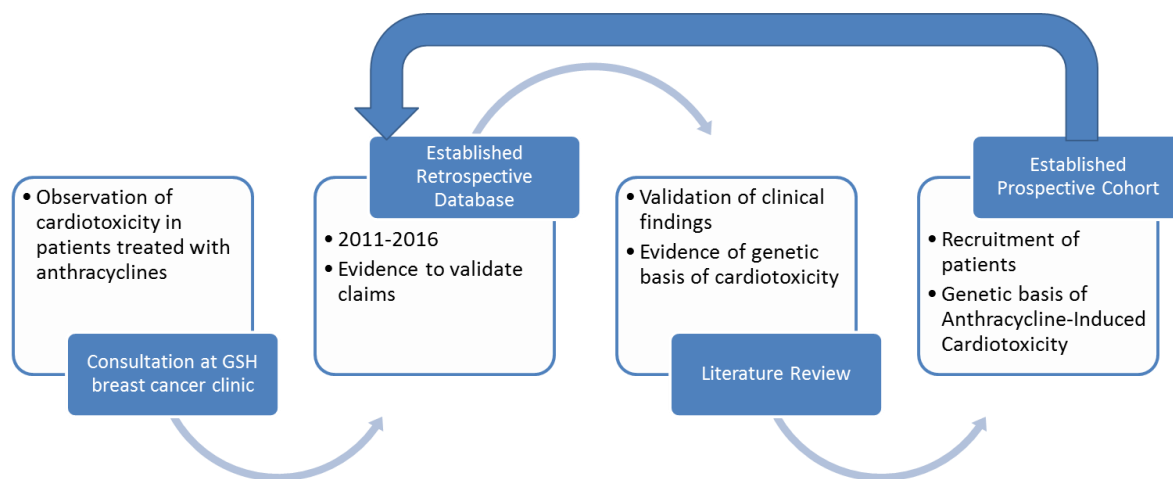


Figure 1: Graphical representation of the initiation of the PhD project

1.4 Research Related Aims and Objectives:

- To assess the effect of anthracycline treatment, if any, on cardiac function using various clinical modalities and patient clinical evaluation using both retrospective and prospective patient data
- To determine the cardiotoxic effects of anthracyclines (both clinical and molecular) in the unique local populations – IA and MA, and the genes responsible for this susceptibility
- To provide tools for the creation of a model of risk for susceptibility to anthracycline-induced cardiotoxicity before the initiation of treatment

In the fulfilment of the aims and objectives of this study, this study was conducted as illustrated in Figure 2:

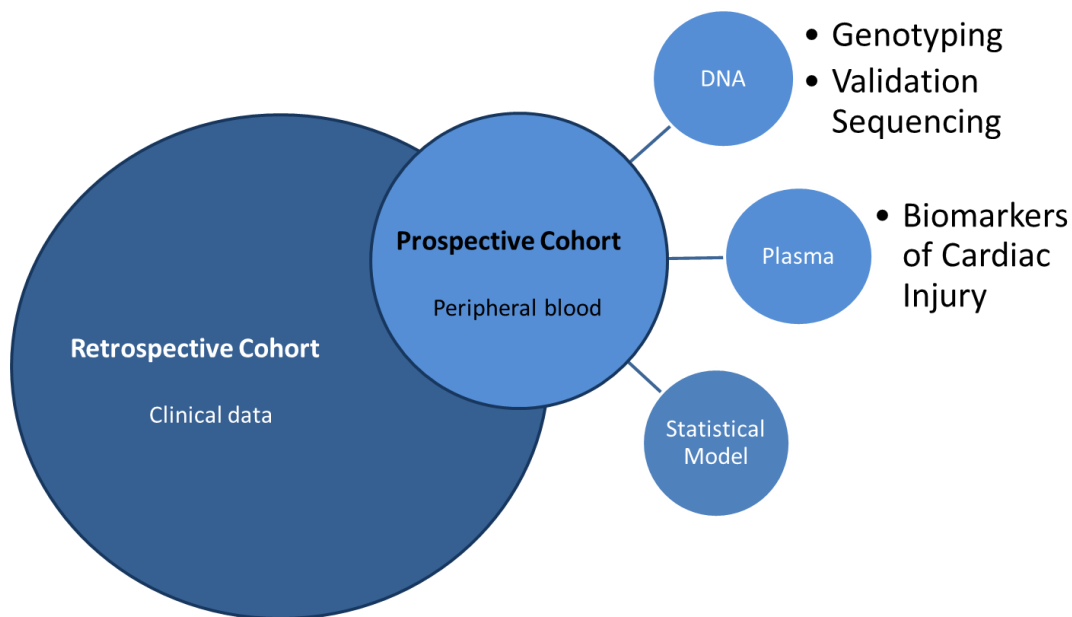


Figure 2: Experimental steps taken towards fulfilment of the project aims and objectives

The establishment of the retrospective cohort allowed for the collection of clinical data of patients at GSH from 2011-2016. The prospective cohort was partially derived from this cohort as well as from TBH (from 2013-2016) and peripheral blood from consented patients was for purposes of genotyping candidate markers. Genotyping for variants associated with anthracycline-induced cardiotoxicity, assessment of levels of cardiac injury using biomarkers and evaluation of clinical data allowed for a comprehensive profile on each patient. Retrospective cohort data allowed for the creation of a statistical model that allowed for inferences to be made in the prospective cohort. Essentially this model may predict risk of anthracycline-induced cardiotoxicity specific to population group before the administration of chemotherapy.

It is important to note that all patients in both the retrospective and prospective cohorts have cancer and that their clinical status (affected or unaffected) refers to their cardiac impairment/dysfunction due to anthracycline-based chemotherapy.

This thesis is divided into seven chapters: this introductory chapter is followed by a literature review with sub-sections on:

- The elements involved in the analysis of the retrospective cohort such as types of breast cancers, staging and classification and treatment regimens,
- Anthracycline based chemotherapy - efficacy, mechanism of action, risks involved, methods of detection of ACT and the genetics of cardiotoxicity, and

- The evaluation of modalities used to assess cardiac function. This is followed by Chapter 3: Patients, Materials and Methods where all experimental methods are outlined systematically.
- Subsequently, in Chapter 4: Results will comprise the analysis of the entire cohort based on clinical data followed by the analysis of molecular data derived from the sub-cohort, with biological specimens as well as the development of a correlation model to predict cardiac function in lieu of missing clinical data
- This is followed by Chapter 5: Discussion which will focus on the entire cohort's clinical data and its implications; trends and associations observed from experimental work and recommendations for both clinical management and future studies.
- Chapter 6: Cardiac biomarker study which includes the introduction, materials and methods, results and discussion and recommendations,
- Chapter 7: Conclusions from both the retrospective and prospective study as well as the biomarker study

Chapter 2: Introduction

2.1 Retrospective Patient Analysis

Breast cancer patients in the Western Cape follow a fast track referral service from both public (government) and private hospitals in the province.

Government or public hospital patients attend a breast surgical outpatient clinic and are urgently referred to the Radiation Oncology Outpatient clinics at both GSH and TBH if found to have a breast carcinoma. Private hospital patients undergo a full workup, mammogram and histology before being referred to these outpatient clinics. Private patients utilise this facility if their medical insurance funds are depleted or if they require a second medical opinion.

Once referred to the Oncology Clinic, the patients are reviewed by a multi-disciplinary team and a decision is made regarding treatment options. This may include surgery with a mastectomy or lumpectomy followed by adjuvant chemotherapy, radiotherapy, and hormonal therapy, where appropriate. Alternatively, patients are treated with neoadjuvant chemotherapy which is usually followed by a surgical intervention. Patients are followed up after chemotherapy is complete to assess if they need further treatment, alternative treatment or palliative options.

This review will elucidate the intricacies of a patient's cancer diagnosis and management, with a focus on breast cancer and anthracycline-based chemotherapy and its association with cardiotoxicity. There will be further exploration into the modalities used for the assessment of cardiac function and the genetics of anthracycline-induced cardiotoxicity. In addition the economic implications of a cancer diagnosis with the eventuality of a potentially fatal adverse drug reaction will be considered.

2.1.1 Definition of Breast Cancer

Breast cancer is defined as uncontrolled cellular growth culminating in a malignant tumour with the ability to metastasize to different parts of the body¹³. Breast cancer occurs most frequently in women, however it does also occur in men (i.e. approximately 1% of all cases of breast cancer)¹⁴.

2.1.2 Incidence of Breast Cancer

In 2012, global statistics indicate that about 14.1 million people are diagnosed with cancer annually, with a mortality of 8.2 million per annum¹⁵.

Breast cancer was reported to be the second most common cancer, occurring in 25% of cancer diagnoses, worldwide, and the most common cause of cancer-related death in women in both developing and developed nations¹⁵.

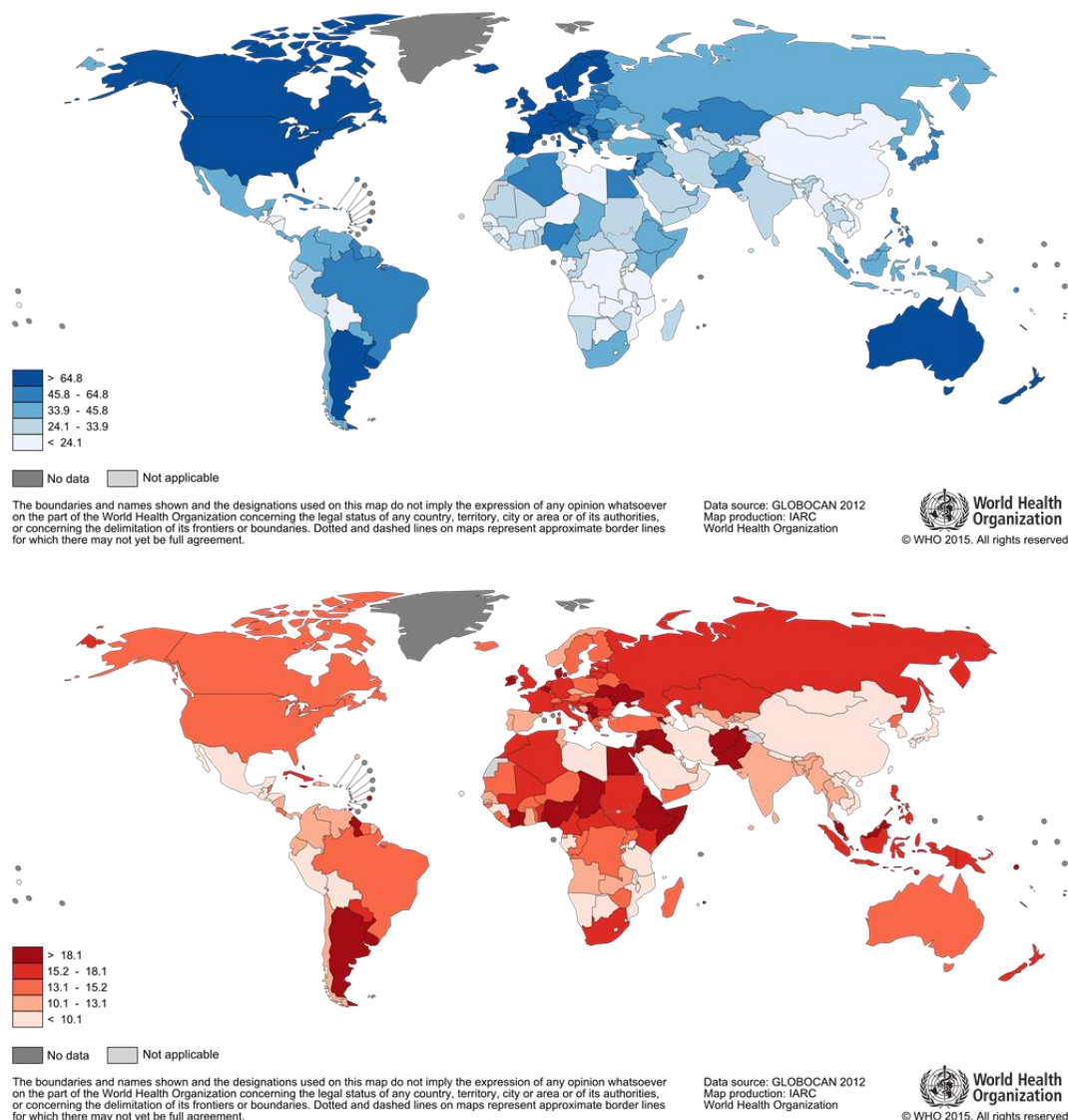


Figure 3: Global incidence (blue) and mortality (red) of breast cancer according to the World Health Organization¹⁵

Despite the increased incidence, there has been a significant decrease in mortality owing to early diagnosis and recent advances in treatment¹⁶. Mortality of breast cancer patients in the USA for the periods 1975-1977 compared to 1999-2005 decreased from 68% to 50%, per annum¹⁷. Nearly 90% of all women diagnosed with breast cancer will have a survival period of 5 years or longer¹⁸.

Developing nations are reported to have more cases and deaths due to breast cancer compared to developed nations (Fig. 3).

Currently, approximately 500 new cases of breast cancer are diagnosed and/or treated annually at each of the oncology facilities at GSH and TBH.

Patients' breast tissue are biopsied to determine the type, grade and stage of breast cancer which are informative for subsequent clinical management and may have prognostic implications.

2.1.3 Types of Breast Cancers

Variants of breast cancer are attributed to cellular morphology. Specifically, carcinomas initiate in the epithelial cells in breast tissue, adenocarcinoma initiates in glandular tissue and sarcomas originate in muscle, fat or connective tissue cells¹³.

2.1.3.1 Carcinoma In Situ

Carcinoma *in situ* may be regarded as non-invasive or pre-invasive breast cancer; the majority of women with early diagnoses have either ductal carcinoma *in situ* (DCIS) or lobular carcinoma *in situ* (LCIS)¹³. DCIS originates in the cells lining the milk ducts whereas LCIS originates in the milk-producing glands of the breast tissue. Carcinoma *in situ*, by definition, does not metastasize but does possess the capacity to develop into invasive disease.

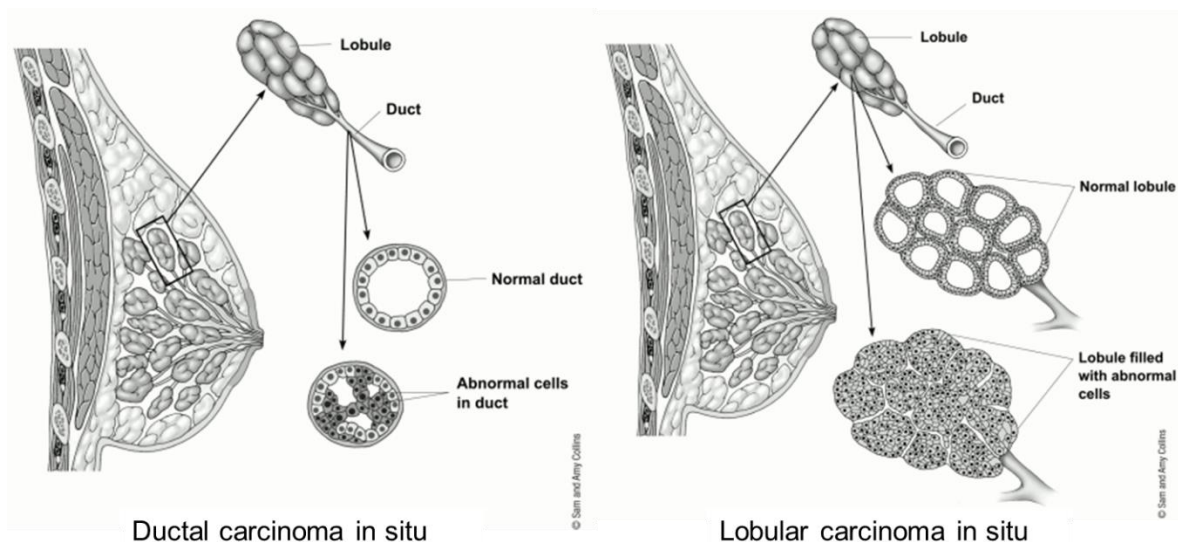


Figure 4: Illustration of breast tissue showing a comparison between ductal and lobular carcinoma *in situ* (Image adapted from¹³)

2.1.3.2 Invasive or Infiltrating Ductal Carcinoma (IDC)

IDC is the most common type of breast cancer. It has the capacity to initiate in the milk duct, breach the wall of the milk duct, and to subsequently grow in the surrounding fatty tissue ultimately metastasizing to other parts of the body by utilizing the lymphatic system or blood stream¹³.

2.1.3.3 Invasive or Infiltrating Lobular Carcinoma (ILC)

Approximately 1 in 10 of all invasive breast cancers are ILC ¹³, which like IDC, have the ability to metastasize to other parts of the body.

2.1.3.4 Inflammatory Breast Cancer

Inflammatory breast cancer is rare occurring in 1-3% of all breast cancer cases and is challenging to diagnose as there is no discrete tumour mass present¹³. Instead, the skin on the breast appears to be thick and pitted like an orange peel (“peau d’orange”) and this is attributed to cancer cells blocking lymph vessels in the skin. Difficulty in diagnosis due to its atypical presentation may negatively impact prognosis¹³.

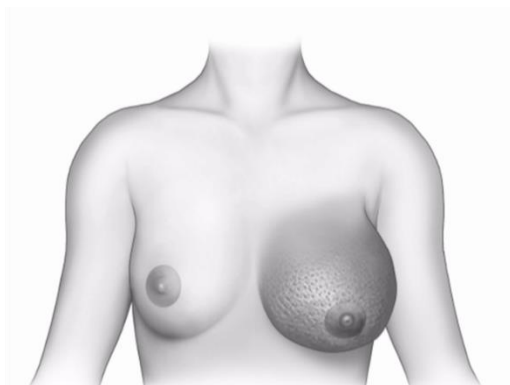


Figure 5: Inflammatory Breast Cancer presenting with the “peau d’orange” appearance (Image adapted from ¹³)

2.1.3.5 Paget Disease of the Nipple

This type of cancer accounts for only about 1% of all breast cancer diagnoses and originates in the milk ducts, progresses to the skin of the nipple and areola resulting in red, itchy, bleeding or oozing nipples¹³. Paget’s disease is optimally treated with a mastectomy.

2.1.3.6 Phyllodes Tumour (PT)

PT is a fairly rare type of tumour that develops in the connective tissue of the breast. Malignant phyllodes tumours are treated with surgery and chemotherapy if they are metastatic¹³.

2.1.3.7 Angiosarcoma

This type of cancer originates in the blood or lymph vessels, very rarely in the breast tissue and can spread rapidly. Angiosarcomas may occur as a complication of radiation therapy, or in some cases, in the tissues of the arms of women who have had lymph node surgery and subsequent lymphoedema¹³.

2.1.3.8 Invasive Breast Carcinoma

The following types of invasive cancer have a good prognosis compared to IDC: Adenocystic carcinoma, adenosquamous carcinoma (low-grade), medullary carcinoma, mucinous carcinoma, papillary carcinoma and tubular carcinoma ¹³.

However the following types of invasive cancers have a poor prognosis compared to IDC: Metaplastic carcinoma, Micropapillary carcinoma and Mixed Carcinoma (both ductal and lobular) ¹³.

Nevertheless all these subtypes are treated similarly to IDC.

Breast cancer may also be classified according to rate of growth and ability to metastasize, as well as molecular markers in or on cells. While tumour grading and staging determine whether or not neoadjuvant or adjuvant therapy will be utilised, the presence/absence of hormone receptors may direct appropriate treatment.

2.1.4 Breast Cancer Staging and Classification

Breast cancer grading is based on histological features which indicate the rate of growth and the likelihood of metastasis. Grade 1 indicates well-differentiated cancer cells, Grade 2 indicates moderately-differentiated cells whereas Grade 3 indicates poorly-differentiated cancer cells that grow and metastasize rapidly ¹³.

While grading is informative, breast cancer staging is crucial as it quantifies the extent of 'spread' of the cancer, which, in turn, has ramifications on prognosis and treatment options. A standardized staging system that is used routinely is the American Joint Committee on Cancer (AJCC) TNM Staging System ¹⁹. Clinical staging is determined using physical examination,

biopsy and imaging test results. Pathologic staging includes clinical staging as well as surgical and histological results and is therefore more accurate.

The T, N and M staging/classification of cancers denote the following:

Primary Tumour (T), numbered 0-4, describes tumour size and spread to the skin or chest wall whereby higher T numbers describe larger tumours or a greater degree of spread.

Regional Lymph Nodes (N), numbered 0-3, describes whether cancer has spread to axillary or internal mammary lymph nodes and how many are affected.

Metastasis (M), numbered 0 or 1, indicates whether distant metastases has occurred (i.e. M=1).

Table 1: Clinical Classification of breast cancer allowing for determination of T,N and M

TNM	Clinical Classification ^{19,20}
Primary Tumour	
Tx	Unable to assess primary tumour
T0	No primary tumour found
Tis	Carcinoma <i>in situ</i> (ductal or lobular) or Paget's Disease of the nipple without tumour
T1	Tumour dimension ≤ 2cm:
T1a	Tumour dimension ≤ 0.5cm
T1b	0.5cm < Tumour dimension < 1cm
T1c	1cm < Tumour dimension < 2cm
T2	2cm < Tumour Dimension < 5cm
T3	Tumour Dimension > 5cm
T4	Tumour with extension to the chest wall or skin:
T4a	Extension to chest wall
T4b	Oedema, ulceration of the skin or satellite skin nodules on the same breast
T4c	Both T4a and T4b
T4d	Inflammatory carcinoma
Nearby Lymph Nodes	
Nx	Unable to assess regional lymph nodes
N0	No regional lymph node metastasis
N1	Metastasis to 1-3 axillary lymph node/s and/or detectable number of cancer cells in internal mammary lymph nodes
N1mi	Micrometastases in 1-3 axillary lymph nodes <2mm across
N1a	Metastasis to 1-3 axillary lymph nodes with at least one area >2mm across
N1b	Metastasis to internal mammary lymph nodes
N1c	N1a and N1b apply
N2	Metastasis to 4-9 axillary lymph node/s or cancer-enlarged internal mammary lymph nodes
N2a	Metastasis to 4-9 axillary lymph nodes with at least one area >2mm across
N2b	Metastasis to internal mammary lymph nodes causing enlargement

Table 1 continued. Clinical Classification of breast cancer allowing for determination of T,N and M

N3a	Metastasis to 10/+ axillary lymph nodes with at least one area >2mm across or metastasis to lymph nodes under clavicle with at least one area >2mm across
N3b	Metastasis in at least 1 axillary lymph node >2mm across and enlarged internal mammary lymph nodes or
	Metastasis in 4/+ axillary lymph nodes with at least one area >2mm across and detectable amounts of cancer in internal mammary lymph nodes (determined by sentinel node biopsy)
N3c	Metastasis to lymph nodes above clavicle with at least one area >2mm across
Metastasis	
MX	Unable to assess distant metastasis
M0	No distant metastasis present
M1	Distant metastasis present

The T, N and M numbers allow for the determination of stage grouping whereby therapeutic decisions can be made. The staging ranges from Stage 0 (non-invasive cancer) to Stage I (least advanced) to Stage IV (most advanced).

After the comprehensive classification of breast cancer using clinical/pathological staging (Table 1 and 2), it is further characterised by the utilisation of hormone receptors and Human Epidermal Growth Factor 2 (*HER2/neu*) status.

Hormone receptors are intracellular proteins that have an effect on cancer cell growth ¹³. Breast cancer cells may have oestrogen receptors (ER positive) and/or progesterone receptors (PR positive). Breast cancers may also be ER and PR negative. While hormone-receptor positive cancers have slower growth, they tend to recur; they are however amenable to hormonal therapy whereas hormone-receptor negative cancers are not ¹³. Menopausal women are more likely to have hormone receptor-positive cancers while hormone receptor-negative cancers are more likely to occur in premenopausal women ¹³.

A cell surface receptor protein routinely tested for, is *HER2/neu* which promotes cancer cell growth at increased levels ¹³. *HER2* positive cancers result in cancers that grow and spread aggressively, however, they generally respond favourably to therapies targeting the *HER2/neu* protein ¹³.

Low levels of *HER2* coupled with the absence of both ER and PR hormone receptors result in triple negative breast cancer (TNBC) which not only favours younger women of African American/Latina descent but also tends to proliferate and metastasize rapidly ¹³. Patients with

TNBC have limited therapeutic options as they are not responsive to both hormonal and HER2-targeted therapies, however chemotherapy can still be utilised.

Table 2: Staging of breast cancer based on TNM Classification

Staging	TNM Classification ²⁰
Stage 0	Tis, N0, M0 Breast carcinoma <i>in situ</i> (DCIS & LCIS): pre-cancer or early cancer of the breast
Stage IA	T1, N0, M0 Tumour dimension < 2cm across with no lymph node or distant metastasis
Stage IB	T0 or T1, N1mi, M0 Tumour dimension < 2cm across with micrometastasis in 1-3 axillary lymph nodes and no distant metastasis
Stage IIA	T0-1, N1, M0 Tumour dimension < 2cm across and metastasis in 1-3 axillary lymph nodes or detectable number of cancer cells in internal mammary lymph nodes or both of the above T2, N0, M0 2cm < Tumour Dimension > 5cm with no lymph node or distant metastasis
Stage IIB	T2, N1, M0 2cm < Tumour Dimension > 5cm with metastasis in 1-3 axillary lymph nodes or detectable number of cancer cells in internal mammary lymph nodes but no distant metastasis T3, N0, M0 Tumour Dimension > 5cm with no lymph node or distant metastasis
Stage IIIA	T0-2, N2, M0 Tumour dimension <5cm with metastasis in 4-9 axillary lymph nodes or detectable number of cancer cells in internal mammary lymph nodes but no distant metastasis T3, N1-2, M0 Tumour dimension >5cm with metastasis in 1-9 axillary lymph nodes or internal mammary lymph nodes but no distant metastasis
Stage IIIB	T4, N0-2, M0 Tumour grown into chest wall or skin and no metastasis to lymph nodes (N0) or metastasis in 1-3 axillary lymph nodes and micrometastasis in internal mammary lymph nodes (N1) or metastasis in 4-9 axillary lymph nodes and internal mammary lymph nodes (N2). No distant metastasis (M0)
Stage IIIC	T(any), N3, M0 Tumour dimension of indeterminate size or cannot be located and one of the following: metastasis to 10/+ axillary lymph nodes or to lymph nodes above clavicle or below clavicle or axillary lymph nodes and enlargement of internal mammary lymph nodes or 4/+ axillary lymph nodes and micrometastasis to internal mammary lymph nodes (N3). No distant metastasis
Stage IV	T(any), N(any), M1 Metastasis to organs or lymph nodes away from the breast

2.1.5 Treatment of Breast Cancer

Factors such as breast cancer type, stage and patient clinical comorbidities generally determine the type of treatment administered. Breast cancers may be treated locally (direct involvement of only the tumour) and/or systemically (therapy is effected via the bloodstream)¹³. Patients will often receive combination therapies to eradicate cancer cells and/or prevent recurrence.

Treatment strategies may include ¹³:

1. Surgery –

Surgical treatments involve either breast-conserving surgery whereby only the tumour is removed and normal breast tissue is conserved, or a mastectomy whereby the entire breast and surrounding tissues are removed. Axillary nodes are cleared at the time of surgery.

2. Radiation Therapy –

Radiation therapy is often utilized after surgery. High energy gamma rays with the capacity to eradicate cancer cells are delivered from outside the body from a linear accelerator.

3. Hormonal Therapy –

Patients with hormone receptor-positive breast cancers are treated with systemic therapies that prevent oestrogen from attaching to hormone-receptors thereby either slowing or stopping further cancer cell growth. Hormone therapy may be used before and after surgery as well as for cancer recurrence.

4. Targeted Therapy –

Targeted therapies leverage specific qualities of cancer cells i.e. cell-surface protein to prevent further growth and metastasis. While chemotherapy destroys all rapidly growing cells, including normal cells, targeted therapy has greater anticancer specificity, and they tend to have less severe side effects.

5. Chemotherapy –

Chemotherapy is administered either orally or intravenously and can be effected in a multitude of ways in breast cancer patients: before surgery to reduce tumour mass to allow for a more

successfully operable tumour (neoadjuvant); after surgery to minimise recurrence via minimal residual disease (MRD) (adjuvant) and as palliative therapy in patients with advanced disease to alleviate symptoms and prolong survival ^{13,21}.

Routinely used chemotherapies include: Anthracyclines, Taxanes, 5-fluorouracil (5FU), Cyclophosphamide and Carboplatin. Combinations of the various types of chemotherapy are administered to increase their anti-neoplastic activity - however this also increases the propensity of developing adverse drug reactions (ADRs).

2.2 Prospective Patient Analysis

2.2.1 Anthracycline-based Chemotherapy

Currently, anthracyclines are one of the most widely used and effective anti-cancer treatments and have been used routinely for more than 50 years ²². While neoadjuvant chemotherapy is frequently recommended in sub-Saharan Africa (67%), first-line chemotherapy consisting of anthracycline-based chemotherapy is used in 60% of breast cancer patients, which translates to approximately 60,000 patients in Africa per year ^{15,23}. Not only are they first-line regimens for breast cancer but also for leukaemia, lymphoma and sarcomas ¹². Anthracyclines are a class of anti-tumour drugs administered to both adult and paediatric patients with soft-tissue sarcomas, and solid or haematologic cancers ²⁴.

2.2.1.1 Types of Anthracyclines

Anthracycline-based regimens include: doxorubicin (Adriamycin®), 4-Epi-doxorubicin or epirubicin (Ellence®), Daunorubicin, L-asparaginase, and Mitoxantrone ³.

- **Doxorubicin**

Doxorubicin was first extracted in the 1960's from the bacterium, *Streptomyces peucetius var. caesius*, and was utilised from the 1970's for routine clinical use ²⁵⁻²⁷. The drug is used in the treatment of various cancers which include: breast, lung, gastric, ovarian, thyroid, Hodgkin's and non-Hodgkin's lymphoma, multiple myeloma, sarcoma and paediatric cancers ²⁷.

The doxorubicin compound has an aglyconic and sugar moiety – the aglycone consists of a tetracyclic ring and quinone-hydroquinone groups, a methoxy substituent and a side chain with a carbonyl group ²². The daunosamine sugar molecule is attached by a glycosidic bond to a ring and consists of a 3-amino-2,3,6-trideoxy-L-fucosyl moiety ²².

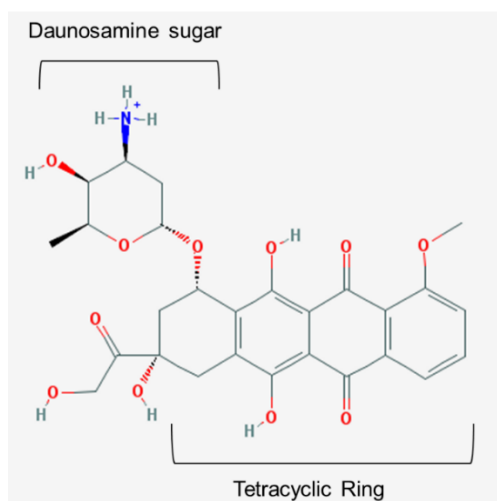


Figure 6: Two-dimensional structure of Doxorubicin ²⁸

- **Epirubicin**

Epirubicin is a semi-synthetic derivative of doxorubicin and is created by the epimerization of the hydroxyl group in a daunosamine carbon ²². The effect of this change is a shorter terminal half-life and increased total body clearance, however the mode of action and antineoplastic activity remains the same as doxorubicin ^{22,26}.

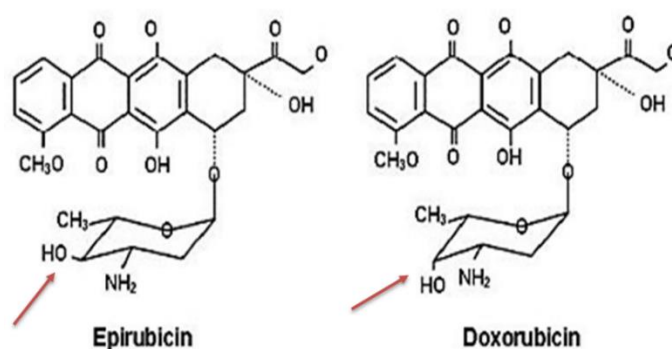


Figure 7: Chemical structure of structurally similar doxorubicin and epirubicin – Reorientation of the hydroxyl group (OH) in the 4' position of the daunosamine ring contributes to different pharmacological effects and safety profiles ²⁹

This allows for the use of higher cumulative doses of epirubicin compared to doxorubicin ³⁰.

- **Daunorubicin**

Daunorubicin, isolated from the bacterium *Streptomyces peucetius*, is used in the treatment of leukaemia and other neoplasms. Daunorubicin's antineoplastic activity may be attributed to DNA intercalation and the inhibition of topoisomerase II. Additionally Daunorubicin may affect the regulation of gene expression and produce free radical damage to DNA ³¹.

- **Valrubicin**

Valrubicin, a semi-synthetic analog of doxorubicin, is primarily used to treat bladder cancer ³². It is administered via direct infusion into the bladder where it easily penetrates into cells. Its anti-tumour activity is due to its ability to cause chromosomal damage and arrest cell cycle in G2 achieved by DNA intercalation and the inhibition of nucleosides into nucleic acids ³².

- **Mitoxantrone**

Mitoxantrone is an antineoplastic agent used to treat leukaemia, lymphomas and multiple sclerosis. It has the ability to intercalate into DNA, interfere with RNA and inhibit topoisomerase II enabling it to be used in treatment of progressive or relapsed leukaemia, lymphoma and multiple sclerosis ³³.

2.2.1.2 Efficacy

Anthracyclines are arguably one of the most effective anticancer therapies ever developed ³⁰. Doxorubicin is particularly effective in treating aggressive lymphomas, Hodgkin's disease, soft tissue carcinomas, childhood solid tumours and breast cancer ³⁴.

Routine anthracycline administration has resulted in cancer survival increasing from 30% in the 1960's to about 80% presently ^{26,35}. More than 70% of childhood cancer patients will survive at least five years as a result of the use of anthracyclines ³⁶.

However tumour resistance and drug toxicity may hinder antineoplastic activity.

2.2.1.3 Risks

Although generally efficacious, chemotherapy may cause patients to exhibit signs of toxicity or cancers may be refractory to treatment ²¹. While some common side effects attributable to doxorubicin may be managed with medical intervention e.g. nausea, vomiting, stomatitis, alopecia, gastrointestinal disturbances, pyrexia, hyperpigmentation of the nails and conjunctivitis; some reactions to the drug are far more serious, namely: neurologic impairment, cumulative cardiotoxicity and bone marrow aplasia with subsequent granulocytopenia, neutropenia, thrombocytopenia and anaemia ²². Undoubtedly, one of the most challenging sequelae of anthracycline-based chemotherapy is cardiotoxicity ^{9,16,18,24}.

The risk of anthracycline-induced cardiotoxicity (ACT) is reported to be between 10-26% with a mortality rate of more than 20% ^{1,2}. ACT can be identified in the following ways: either as acute, early or late cardiotoxicity ^{22,24-26,37}. Acute ACT, occurs in 11% of patients, is dose-independent, clinically manageable and generally reversible ^{9,38}. It may present during

treatment as arrhythmias which include sinus tachycardia, premature ventricular contractions and ventricular tachycardia, bradycardia, coronary syndromes, dilated cardiomyopathy or rarely, acute cardiac failure. Early cardiotoxicity is defined as occurring within one year of treatment whereas late cardiotoxicity is defined as occurring after one year of treatment. Both early and late-onset cardiotoxicity (also referred to as chronic cardiotoxicity) are dose-dependent ^{39,40}. Chronic ACT may present as progressive left ventricular dysfunction, cardiomyopathies and subsequent death due to cardiac failure (CF) ^{9,25,26,37,39,41}.

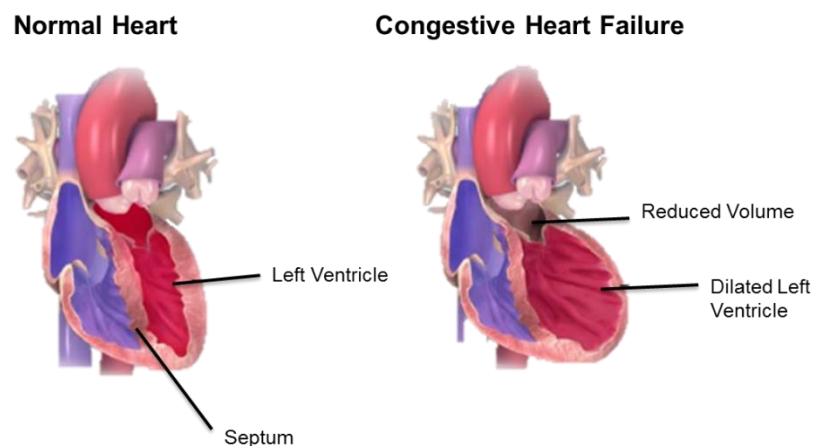


Figure 8: Stylised comparison of a normal heart and a heart in congestive failure (Image adapted from ⁴²). Progressive muscle weakness in a congested heart results in the inability of a dilated left ventricle to pump adequate blood throughout the body

Table 3 below compares the types of ACT, hallmark clinical features and prognosis in both adults and children.

Table 3: Types of Anthracycline-Induced Cardiotoxicity – Features and Prognosis

	Acute Cardiotoxicity	Early Cardiotoxicity	Late Cardiotoxicity
Onset	Within 1 st week of treatment	<1 year after treatment	≥1 year after treatment
Clinical Features in Adults	Arrhythmias, acute cardiac failure	Dilated cardiomyopathy	Dilated cardiomyopathy
Clinical Features in Children		Restrictive and/or dilated cardiomyopathy	Restrictive and/or dilated cardiomyopathy
Prognosis	Generally reversible	May be progressive	May be progressive

Adapted from Raj *et al.* (2014) ²⁴

Clinical cardiac phenotypes referred to in Table 3 are described below in greater detail:

Arrhythmias describe abnormal heart rhythm that can either be too fast (tachycardia) or too slow (bradycardia or brachycardia) that may result in symptoms of fatigue and dizziness ⁴³.

Dilated cardiomyopathy occurs when the left or both ventricles dilate resulting in impaired systolic function that may present with symptoms of CF and/or arrhythmia and systemic embolism. Symptomatic therapy which includes diuretics, beta blockers and angiotensin converting enzyme (ACE) inhibitors may be administered. Extreme cases may warrant cardiac transplantation ⁴³.

Restrictive cardiomyopathy is characterised by both normal or reduced diastolic or systolic volumes and normal thickness of the ventricular wall. While restrictive cardiomyopathy of the left ventricle may present with pulmonary congestion and/or mitral regurgitation, restrictive cardiomyopathy of the right ventricle may present with increased jugular venous pressure, hepatomegaly and tricuspid regurgitation ⁴³. Diuretics may improve the condition but advanced disease has a poor prognosis.

Cardiotoxicity may range from the fairly innocuous swelling of the sarcoplasmic reticulum, cytoplasmic vacuolization, myofibrillar degeneration, myocyte disruption to the severity of fibrosis, systolic/diastolic dysfunction and CF ^{26,39}. The range of cardiac damage may explain the types of ACT – while cardiac remodelling and subsequent contractile dysfunction, largely due to fibrosis, accounts for both chronic and acute ACT; late onset ACT may be attributed to cumulative cardiac damage coupled with the inability of cardiomyocytes to rebound from toxicity ¹².

The progressive nature of irreversible cardiotoxicity may be of greatest burden to children, adolescents and long term cancer survivors ^{36,41}. Approximately one out of eight childhood cancer survivors have been reported to experience severe cardiac disease later in life – with an average time between diagnosis and cardiomyopathy of 9.4 years; this risk increases significantly with increased cumulative dose ^{24,44}. When childhood cancer survivors were compared to their siblings, they were found to have a significantly higher incidence of CF, myocardial infarction, pericardial disease and valvular abnormalities – cardiac events which increased in likelihood over a 30 year period after initial cancer diagnosis ⁴⁵. Specifically, a study by Grenier *et al.* ⁴⁶, showed that almost 65% of all long term childhood cancer survivors, treated with anthracyclines, showed left ventricle (LV) contractile dysfunction and that heart transplantation was common in young adults who experienced cardiotoxicity.

In terms of breast cancer, increased survival due to therapy translates to a significant number of survivors with impaired cardiac function or the potential to develop cardiomyopathies. Currently, in the USA alone, it is estimated that there may be more than 2 million cancer survivors at risk of delayed anthracycline cardiotoxicity ¹⁷. This increased risk combined with family history of cardiovascular heart disease and unhealthy lifestyle choices can severely compromise quality and quantity of life.

The incidence and severity of ACT may be increased due to a multitude of risk factors such as higher cumulative dose, increased individual dose, younger or older age at diagnosis, female sex, pre-existing cardiovascular disease such as hypertension, ischaemic, myocardial or valvular disease, metabolic disorders, genetic factors (i.e. trisomy 21, African Ancestry), mediastinal radiation therapy, and shorter infusion time ^{9,10,24,26,36,47,48}. Risk factors worth consideration due to their effect on cardiac health include: smoking, consumption and/or use of alcohol, energy drinks, stimulants, prescription and illegal drugs ²⁴. Impaired cardiac function may be caused by complications arising from viral infection, pregnancy, arrhythmia, and anaemia – therefore, a combination of predisposing medical conditions coupled with cardiotoxic chemotherapy increases the risk of developing ACT.

Nevertheless, cardiovascular disease (CVD) is a leading cause of long-term morbidity and mortality amongst cancer patients ^{49,50}.

2.2.1.4 Dose

Numerous studies have shown that cumulative dose is strongly associated with the risk of developing ACT ^{3,5,9,24,25,36,40,44,51-53}.

While the USA's Food and Drug Administration (FDA) has stipulated that total cumulative doses exceeding 550 mg/m² results in permanent cardiac damage, there are still patients who experience symptoms of cardiac failure below this prescribed "safe" anthracycline dose ^{3,53}. Conversely, there are also patients who can tolerate anthracyclines (without cardiotoxicity) with cumulative doses exceeding 1000 mg/m².

Table 4 which is a summary of previously published work shows the risk of cardiotoxicity attributed to varying cumulative doses and in some instances the type of anthracycline-based therapy.

Table 4: Studies illustrating dose-dependent cardiotoxicity experienced by patients treated with anthracyclines

Study	Therapy	Cumulative Doses and Subsequent Risk of Cardiotoxicity					
		≥ 150 mg/m ²	250 mg/m ²	350 mg/m ² (+/-)	450 mg/m ²	550 mg/m ² (+/-)	>600 mg/m ²
Raj <i>et al.</i> 2014 24		7%	9%	18%	38%	65%	
Volkova <i>et al.</i> 2011 25		0.2% (CF)		1.6% (CF)	3.3% (CF)	8.7% (CF)	
Von Hoff <i>et al.</i> 1979 40	DOX			3% (CF)		7.5% (CF)	
Swain <i>et al.</i> 2003 53	DOX			5% (CF)		26% (CF)	48% (CF)
Ryberg <i>et al.</i> 1998 52	EPI						1.9-4% (CF)
Kumar <i>et al.</i> 2012 5	DOX		21%				
Deng <i>et al.</i> 2007 9						26% (CF)	

It is important to clearly delineate how cardiotoxicity and/or CF was defined – Von Hoff *et al.*⁵⁴ described the event as clinical symptoms of CF exhibited by the patient after the administration of doxorubicin^{40,51}. Swain *et al.*⁵³ defined CF as fulfilling two of the following requirements: cardiomegaly on chest x-ray, basilar rates, S₃ gallop, or paroxysmal nocturnal dyspnoea, orthopnoea or significant dyspnoea following exertion⁵³. Ryberg *et al.*⁵² specified that patients deemed as having CF fulfilled the following requirements: a history of breathlessness, clinical signs of CF such as dyspnoea and/or congestion on the chest X-ray and/or peripheral oedema, cardiomegaly with/without pulmonary congestion/pleural effusion on an X-ray and/or abnormal left ventricular ejection fraction (LVEF) where LVEF < 46% or a decrease of > 15% (post-treatment compared to pre-treatment) and if possible, an abnormal echocardiography (ECHO).

While risk of CF and/or cardiotoxicity risk is inconsistent between studies, it shows that there is no “safe” dose of anthracyclines and furthermore that the dose-dependent association with cardiomyopathy may limit therapeutic potential⁴⁴. The disparities in some instances (as shown in Table 4) in terms of cardiac risk at specific cumulative doses can be explained by the varying definitions of CF and/or cardiotoxicity adopted by the authors, as well as the type of anthracycline-based treatment administered.

While doxorubicin is effective against a wide variety of tumours, 4-epi-doxorubicin or epirubicin is estimated to be about 30% less cardiotoxic due to differences in the manner in which they are metabolized ^{10,26,35} – this is discussed in greater detail later in the chapter.

While anthracycline-based therapy alone is damaging to the cardiac muscle structure and function, the combination of anthracyclines with other therapies (i.e. combination therapy) may carry a greater risk of cardiac failure in cancer patients ²⁴.

2.2.1.5 Combination Therapy

The overall risk of ACT may be significantly increased when radiation therapy and/or other agents such as targeted drugs are utilized together with an anthracycline-based regimen.

Radiation therapy, if administered in an irradiation field covering parts of the heart, may exacerbate symptoms of ACT and long term cardiac risk – this has been shown to be associated with a high cumulative anthracycline dose with radiation ^{16,24,51}. Wang *et al.*⁴⁴ demonstrated that the risk of cardiomyopathy may be increased by up to 3-fold if anthracycline-based therapy was combined with chest irradiation. However, more recent modes of chest wall irradiation such as intensity-modulated radiation therapy may avoid significant damage to the heart ⁵¹.

Targeted drugs including the anti-HER2 antibody (trastuzumab) and inhibitor (lapatinib) when combined with anthracyclines have increased anti-cancer activity but potentially significant cardiotoxic effects. The risk of cardiac dysfunction increases from 10% to 28% when anthracyclines are combined with trastuzumab ^{16,17,39}. Trastuzumab administered alone, impairs myocyte contractility causing short-term, reversible damage; however in combination with anthracyclines, it causes impairment to myocytes' homeostatic mechanisms and survival pathways ultimately contributing to myocyte loss and causing long term cardiac damage ¹⁷. Other potential contributors to cardiotoxicity include taxanes, platinum drugs, fluoropyrimidines, vinca alkaloids and nitrogen mustard analogues ²⁷. While combination therapy is often necessary in cancer patients with a poor prognosis, this has to counterbalance with the increased risk of ACT ¹⁸.

While ACT generally presents with symptoms indicative of cardiac dysfunction, numerous studies have found cancer patients with subclinical damage that could not be routinely detected yet later manifested as cardiovascular heart disease ^{9,40,48,55}. Patients with subclinical damage still receiving doxorubicin may have severely compromised left ventricular function that can contribute to further damage and CHF ^{17,39}. Compensatory mechanisms such as

tachycardia or shortness of breath after minimal exertion may precede CF, and are signs to be looked out for ¹⁷. It has been reported that subclinical cardiac abnormalities may occur in more than 50% of all patients treated with anthracyclines, suggesting that reported rates (10-30%) may be underestimating actual cardiotoxicity rates ^{9,40,55}.

Previous attempts to stratify patients based on co-morbidities and clinical factors into risk groups for developing ACT have proved to be unsuccessful. It is therefore necessary to take a comprehensive patient history to avoid exacerbating existing cardiac damage with anthracycline based treatment, but also to attempt to elucidate the underlying mechanisms of drug-related injury ^{9,10,24,26,47,48}.

2.2.1.6 Mechanism of Action

The mechanism of action of anthracyclines involves damage to tumour DNA via intercalation of the drug between bases and effectively blocking the synthesis of DNA and/or RNA ^{2,24}. Furthermore, anthracyclines inhibit the action of topoisomerase II, an enzyme necessary for DNA replication, which contributes to both cellular apoptosis and the inhibition of cancer cell replication ⁵⁶. The subsequent generation of semiquinone free radicals and oxygen-free radicals further damages DNA, proteins and cellular membranes ^{21,24}.

The mechanism of action of anthracyclines may also explain the damage inflicted on cardiomyocytes and subsequent chronic cardiomyopathies and CF (Fig. 9) ^{2,16,22,27,48,56}.

Anthracyclines are able to bind to both nuclear and mitochondrial DNA and interfere with the transcription of genes and cellular replication. While Topoisomerase II inhibition is effective for tumour eradication, it is detrimental for healthy cardiomyocytes ⁵⁶. The inhibition of Topoisomerase II in cardiomyocytes activates DNA cleaving caspases (caspase 3 and caspase 9), which contribute to myofibril and troponin damage ⁵⁶. Troponin is a myofibrillar protein that regulates cardiac muscle contraction ⁵⁷. Dysfunction and/or damage may result in impaired cardiac function.

The metabolism of doxorubicin may additionally explain further cardiac insult whereby doxorubicin undergoes a two-electron reduction to the alcohol metabolite – doxorubicinol and a one electron reduction to the semiquinone radical coupled with the generation of reactive oxygen species (ROS) ^{26,27}. The two-electron reduction of the carbonyl group in the anthracycline side chain is catalysed by nicotinamide adenine dinucleotide phosphate (NADPH)-dependent reductases, carbonyl reductases (CBR) and aldo/keto reductases (AKR) and results in the accumulation of alcoholic metabolites. These alcoholic metabolites not only

impair cardiomyocyte contractility by inhibition of the Ca^{2+} and Na^+/K^+ pump and depleting Adenosine Triphosphate (ATP) but also disturb cardiac iron homeostasis^{47,56,58}. This disturbance occurs when anthracyclines bind cellular iron resulting in a doxorubicin-iron complex that generates free radicals and is damaging to DNA, intracellular proteins and membrane lipids^{25,39}. Consequently, there is a direct correlation between the myocardial accumulation of alcoholic metabolites and the onset of cardiomyopathy^{25,26,47,58}.

Furthermore, the one electron reduction of the quinone moiety in the tetracyclic ring of the anthracycline is catalysed by oxidoreductases and produces a semiquinone radical capable of regeneration and production of ROS. ROS has been previously implicated in contributing to membrane and DNA damage, oxidative stress and cellular apoptosis and ultimately, to the progression of cardiomyopathies to CF^{26,27,39,41,47}.

Increased nitric oxide production due to doxorubicin metabolism also results in the creation of reactive nitrogen species (RNS) which together with ROS may further impair cardiac function by: (i) contributing to the disruption of cardiac gene expression and apoptosis, and (ii) affecting mitochondrial function and energy generation^{16,17,26}. The intercalation of anthracyclines into mitochondrial DNA and their affinity for cardiolipins (inner mitochondrial-membrane specific phospholipid) further compromises mitochondrial enzyme activity and subsequent function^{22,59}. The oxidation of cell membrane lipids, DNA degradation, mitochondrial defects and dysfunction of enzymes containing sulfhydryl groups may all be attributed to ROS and contribute to chronic cardiotoxicity³⁴. The initiation of apoptosis is also due to the release of cytochrome C due to oxidant stress as well as p38 MAPK activation²⁵.

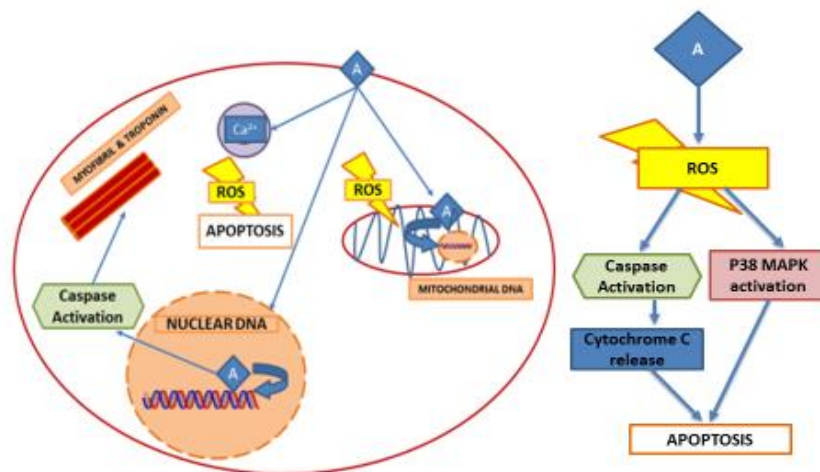


Figure 9: Illustration of a cardiomyocyte showing mechanism of action of anthracycline and potential cellular damage (Image adapted from Sandhu *et al.* 2014⁵⁶ and Volkova *et al.* 2011²⁵)

As previously mentioned, epirubicin is less cardiotoxic than doxorubicin due to differences in their intracellular distribution and metabolism. While doxorubicin localises in the mitochondria, epirubicin is found in cytoplasmic organelles where it undergoes a one-electron reduction with little ROS produced and limited two-electron reductions further reducing the amount of alcoholic metabolites produced ^{26,35}. Despite these advantages, epirubicin does still accumulate in the heart allowing for direct interaction with vulnerable cardiomyocytes ²⁶.

Cardiac cells are vulnerable due to their high metabolic activity, weak antioxidant defences and high cardiolipin concentration for which anthracyclines have a great affinity ^{17,22,26,37,39}. Cardiomyocytes are also post-mitotic cells with limited regeneration ability, therefore, anthracycline-induced cardiac damage is often irreversible ²². A barrage of cardiac insults including: depleted cardiac stem cells, impaired DNA synthesis, gene expression and cell signalling contributing to damage in the sarcoplasmic reticulum, mitochondria and sarcomeres inevitably results in chronic cardiomyopathy ²⁴.

These mechanisms of action and pathways may aid in the differentiation of cardiovascular phenotypes based on the type of damage inflicted on cardiomyocytes ultimately allowing for a delineation between genetic and ischaemic cardiomyopathy that could be utilized in the genetic determination of cardiac risk ^{16,24}. Therefore, ACT can be categorized as either Type I or II, where Type I consists of irreversible, cardiac damage contributing to cardiomyocyte death, compared to Type II which includes damage caused by combination therapies and may be reversible due to benign myocyte impairment ^{25,60}. Type I damage is attributed to ROS generation by anthracyclines resulting in cardiac cell damage and myocyte loss compared to Type II damage which may be due to competition for binding therapeutic targets (i.e. HER2 protein by trastuzumab) therefore affecting cardiomyocyte growth, repair and survival ^{10,25,60}. As a result, Type I damage is often associated with long-term cardiotoxicity.

2.2.2 Modalities to Assess Cardiac Function

Not only does reduced reporting of cardiac events and inherent clinical differences in cancer patients contribute to determining accurate estimates of ACT but the variance and low sensitivity of routinely used detection modalities may further compound the issue ²⁴.

In the routine clinical setting cardiotoxicity is detected using LVEF derived from a number of modalities, including ECHO and clinical examination. However these methods are rarely able to detect early stage or subclinical cardiotoxicity ³⁹. Other tests utilised to monitor anthracycline-induced cardiotoxicity include: equilibrium radionuclide angiocardiology

(ERNA), endomyocardial biopsy and indium-111 antimyosin imaging, magnetic resonance imaging (MRI), tissue-doppler imaging and biomarkers ^{39,61-64}.

2.2.2.1 Left Ventricular Ejection Fraction (LVEF)

LVEF is a measure of the amount of blood being pumped out of the main pumping chamber of the heart, the left ventricle with each contraction. A healthy heart pumps more than half the heart's blood volume with each beat and is quantified as a percentage ⁶⁴.

Table 5: Left Ventricular Ejection Fraction and its Interpretation ⁶⁴

Ejection Fraction	Interpretation
55-70%	Normal/ Healthy heart
40-55%	Below Normal
<40%	May indicate heart failure
≤35%	Risk of life-threatening irregular heartbeats

Table 5 shows ejection fraction measurements and their interpretations – while a lowered LVEF indicates compromised cardiac function due to damaged cardiac muscle or disease, a patient with diastolic failure can have a normal or preserved ejection fraction ¹⁷. CF can either be attributed to systolic CF whereby the left ventricle muscle contracts inadequately resulting in reduced oxygenated blood being pumped throughout the body or to diastolic CF where contraction of the heart is normal but ventricles are impaired not allowing sufficient blood into the heart ⁶⁴. Nevertheless, a patient with an EF of less than 35% is at risk of sudden cardiac arrest or cardiac death due to irregular heartbeats ⁶⁴.

In the context of anthracycline-based chemotherapy, baseline LVEF is determined prior to treatment and again after three or four cycles where patients with an LVEF greater than 50% at baseline are deemed healthy and subsequently amenable to treatment ^{10,39}. However, a decrease in LVEF of greater than 10% from baseline to after treatment, or an LVEF of less than 50% may indicate the onset of cardiotoxicity and treatment should either be discontinued or substituted ^{37,39}. Moderate decreases (≤10%) in LVEF do not necessarily denote CF or impaired muscle function and may be stabilized with the discontinuation of treatment ²⁵.

LVEF is therefore a commonly utilised and accepted physiologic measure of cardiac function in patients receiving anthracycline-based chemotherapy and may be determined using ERNA or a multigated acquisition scan (MUGA), ECHO, cardiac catheterization, computerized tomography (CT) scan or an MRI ^{39,64}.

- ***Equilibrium Radionuclide Angiography (ERNA)***

ERNA came into prominence in the 1970s as a reliable method for the quantification of LVEF⁶⁵. ERNA also known as a MUGA scan, involves the use of a radionuclide agent such as technetium-99m to tag patient red blood cells which are then re-injected followed by gated-image acquisition⁶⁵.

Gated-image acquisition occurs when the patient's cardiac rhythm is at rest and 300-600 heartbeats are assessed over a period of 5-10 minutes – this together with 3 standardised views of the heart and a count-based algorithm allows for the determination of LVEF⁶⁵.

The advantages of this technique are its non-invasive nature and high reproducibility, whereas its disadvantages include the limitation of clinical benefit compared to exposure to radiation, difficulty in obtaining image acquisition angles and problematic gating due to patient arrhythmias⁶⁵.

- ***Echocardiography (ECHO)***

ECHO is a modality for the determination of LVEF that is similarly non-invasive, more sensitive and avoids radiation exposure^{65,66}.

ECHO employs the use of sound waves or ultrasound to visualise the heart in real time and may be two dimensional (2D ECHO) or three dimensional (3D ECHO). Doppler ECHO or tissue doppler imaging makes use of pulsed wave Doppler⁶¹. 2D ECHO enables the visualization of real-time motion of the heart's structures whereas 3D ECHO enables the visualization of the heart's structure and function in greater depth⁶⁷. The more sensitive Doppler ECHO shows the flow of blood through the heart's chambers and valves allowing for the quantitation of blood pumped out with each beat and subsequent function of the heart⁶⁷.

While ECHO is a technique that can be used to detect structural abnormalities and evaluate cardiac function, determinations of LVEF are often an approximation³⁹. Generally an LVEF, derived using an ECHO, of less than 40% and/or fractional shortening (FS) of less than 28% is regarded as left ventricular dysfunction⁶⁸. Childhood cancer survivors' echocardiograms have shown reduced LV fractional shortening related to the cumulative dose of doxorubicin, however significant reductions in LV fractional shortening were also observed in some treated with low doses, emphasising that there was no safe dose of doxorubicin²⁴.

Even though studies have found Doppler ECHO to be a highly sensitive measure of myocardial strain and 3D ECHOs to be superior to 2D ECHOs; echocardiography was prone

to intra- and inter operator variability as well as being fairly expensive (to be taken into account especially in a resource-poor setting) ^{16,66,67}.

Nevertheless, 3D ECHOs were found to be comparable to cardiac magnetic resonance techniques.

2.2.2.2 Cardiac Magnetic Resonance (CMR) Imaging

Cardiac Magnetic Resonance (CMR), utilises a magnetic field together with radio frequency impulses to produce a highly detailed image of the heart.

Although infrequently used, it is both non-invasive, highly sensitive and superior to cardiac nuclear imaging (ERNA/MUGA) and therefore considered the gold standard for the assessment of LV function ^{65,69}. The determination of LVEF and volumes using CMR have been found to be highly reproducible and accurate ^{65,69}. Limitations, however, include the high cost and expertise required to operate an MRI machine, irregular heartbeats affecting the image quality and the time taken to perform the imaging ⁷⁰.

Despite the various modalities to assess LVEF, it has low sensitivity as an early predictor of cardiomyopathy especially when patients have acute reversible damage that may be timeously treated ^{18,37,65,69}. A number of alternatives exist for assessing cardiac function with greater sensitivity; similarly alternative measures of early cardiac dysfunction need to be assessed – these include endomyocardial biopsies, Indium-111 antimyosin and cardiac biomarkers.

2.2.2.3 Endomyocardial Biopsy

An endomyocardial biopsy consists of the invasive removal of a right ventricular endomyocardium sample ³⁹. Biopsies performed after early doxorubicin treatment may show cell disruption and loss with histopathologic changes as previously observed in specimens of patients treated with doses as low as 240mg/m² ^{17,25}. However this technique can be expensive, risky and may confer inconclusive findings ³⁹.

2.2.2.4 In-111 Antimyosin

In-111 antimyosin is a tracer used for the imaging of conditions such as myocarditis, cardiomyopathy, cardiac transplant rejection and doxorubicin-induced cardiotoxicity; while it is highly sensitive to early onset cardiotoxicity, it can be expensive, technically challenging and time-consuming ^{39,65}.

Therefore there is a need for a sensitive yet fairly inexpensive and efficient, non-invasive measure of cardiac injury.

2.2.3 Management of Cardiotoxicity

ACT can be reduced or prevented in a number of ways which include: drug dose control; the use of less toxic natural derivatives, tumour-targeted formulations or cardio-protective agents; continuous infusion to reduce peak plasma drug levels; the delayed administration of trastuzumab after anthracycline treatment and administering a non-anthracycline based regimen ^{17,26,39,71}.

2.2.3.1 Dose Control

As previously discussed, the recommended cumulative dose for doxorubicin is 240-360mg/m² and 450-600mg/m² for epirubicin; as is obvious – different individuals may tolerate relatively low doses – below the optimum therapeutic range ^{17,39}. Therefore, despite the setting of an arbitrarily low dosage to prevent cardiotoxicity, there is no safe dose of anthracycline. Also, despite the association between high cumulative doses and increased risk of ACT, long-term follow-up studies have shown subclinical dysfunction and CF in cancer survivors administered even at low doses of anthracyclines ^{12,24}.

2.2.3.2 Natural Derivatives

While doxorubicin is naturally occurring, a semisynthetic derivative – epirubicin, was discovered to be less cardiotoxic yet equally efficacious in both animal models and *in vivo* studies. However clinical trial data has not been definitive in relative cardiotoxicities of the two anthracyclines ^{22,72-74}.

As previously discussed in this chapter, epirubicin has been utilized in high risk patients and often at higher cumulative doses.

2.2.3.3 Tumour-targeted Formulations

Tumour-targeted formulations endeavour to prevent the uptake of anthracyclines by cardiac cells and improve tumouricidal activity ^{37,72,75}. These formulations have two modes of action: active targeting - whereby there is specific tumour recognition by the carrier, and passive targeting, where there is preferential drug distribution such as the liposomal encapsulation. This process prevents interaction of anthracyclines with the heart, by virtue of the large size of their liposome 'covers', making them unable to fit into tight capillaries, thereby reducing

cardiotoxicity^{75,76}. Studies of the liposomal formulations of doxorubicin have shown promise in reducing cardiotoxicity in the clinical setting, while also suggesting it may be a better alternative to both conventional doxorubicin and epirubicin^{22,37,72}.

2.2.3.4 Cardio-protective Agents

Numerous agents may confer cardio-protection to patients who are at risk of ACT and subsequent HF. Dexrazoxane, a derivative of ethylenediaminetetraacetic acid (EDTA), is an iron-chelator that has emerged with the most promise^{10,24,27,37,76}. Dexrazoxane binds free and/or loosely bound cellular iron or iron from anthracycline-iron complexes therefore preventing iron-catalysed ROS damage. Cardio-protection is evidenced by the stable or non-increased Troponin T levels in patients treated with anthracyclines^{17,22,26}.

There has been evidence of an association between dexrazoxane use and impaired efficacy of anthracyclines, lower response rates, and significant haematologic and gastrointestinal tract toxicity, however other studies have found that dexrazoxane conferred long-term cardio-protection without compromising oncologic efficacy^{17,24,27,39}. Based on this contentious evidence, dexrazoxane is cautiously administered only when the cumulative dose of anthracyclines is maximized^{17,27,39}.

Routinely prescribed cardiac medications for asymptomatic left ventricular dysfunction or cardiac failure which include: β -blockers, angiotensin-converting enzyme inhibitors, angiotensin receptor blockers, diuretics, nitrates and hydralazine may, if prescribed early enough achieve complete cardiac recovery¹⁶. Another agent, heat-shock protein 20 (HSP20), has shown protection against doxorubicin-induced apoptosis and may have potential as a cardio-protector²². Angiotensin-converting inhibitors such as enalapril, which usually improve both LV structure and function, had a temporary effect on patients with CF, as well as worsened long-term cancer survivors' conditions after 6-10 years²⁴.

Despite the challenges associated with cardio-protective agents, they may confer benefit given the progressive nature of ACT evidenced by the significant number of cancer survivors suffering from cardiac failure refractory to treatment or needing cardiac transplantation^{10,37}.

2.2.3.5 Continuous Infusion

Due to risk of ACT being dose-dependent, another strategy to decrease risk of cardiac injury is to reduce peak plasma levels of doxorubicin by increasing the duration of infusion without reducing the overall dose i.e. continuous infusion⁷⁷. While continuous infusion compared to

bolus infusion of doxorubicin has been shown to reduce cardiotoxicity in adults; this was not the case in children even when it was combined with the cardio-protectant, dexrazoxane ^{24,77}.

2.2.3.6 *Delayed Administration of trastuzumab*

While trastuzumab markedly improves breast cancer survival, it also aggravates ACT increasing cardiac risk by 27% when combined with anthracyclines; this is why its delayed administration is recommended ^{16,78}.

The reason for not administering trastuzumab with anthracyclines is that trastuzumab acts as a modulator of ACT when administered at the same time as anthracyclines and has the ability of further damaging already vulnerable myocytes ⁷⁸.

2.2.3.7 *Non-Anthracycline Based Regimen*

In patients where the risk of cardiomyopathy and/or CF is too high without compromising treatment efficacy [with risk mitigation strategies such as dose control], other non-anthracycline based regimens may be considered ⁷⁶. Studies have shown superior disease-free survival and lower rates of CF in patients treated with four cycles of TC (docetaxel and cyclophosphamide) compared to four cycles of AC (adriamycin and cyclophosphamide) ⁷⁶.

The prevention of anthracycline-induced cardiotoxicity while maintaining anti-tumour efficacy is an important consideration especially in long term cancer survivors such as childhood cancer patients. However, since the mechanism of drug-induced cardiac damage is not fully understood, understanding the process of metabolism of anthracyclines may explain cardiotoxicity. It is therefore not unreasonable to presume that the genes coding for enzymes involved in anthracycline metabolism may be determinants of cardiac damage ³⁴.

2.3 *Genetics of Cardiotoxicity*

Since there is compelling evidence that genetic factors play a role in the effectiveness of chemotherapy as well as adverse drug reactions, there is strong motivation to investigate pharmacogenetic associations with treatment outcomes ^{7,8,55}. The field of pharmacogenetics seeks to explain the genetic contribution to variable drug responses - in this instance the variability in an individual's response to anthracyclines ^{9,13}. Observed variability in patient drug response as well as fairly inconclusive risk associations with clinical co-morbidities suggests that there is very likely to be a genetic predisposition/susceptibility to ACT. Therefore, polymorphisms in pathway-based genes involved in drug absorption, distribution, metabolism,

elimination and toxicity (ADMET) may allow for the elucidation of genetic response to cardiotoxicity and subsequently allow for the individualisation of treatment and to minimise event-free survival^{10,55,79}.

The function of proteins involved in drug ADMET may be affected by amino acid changes due to genetic alterations. However, not all genetic mutations trigger an amino acid change- these changes may range from them being functionally neutral to deleterious⁸⁰. A synonymous genetic variant comprises a sequence change without any change to the encoded amino acid⁸¹. Missense variants result in a sequence change where the encoded amino acid is changed but the length is preserved⁸¹. An intronic variant may have the potential to also affect gene regulation⁸¹. There is growing evidence that variants which are not overtly functional (e.g. nonsense or missense) may well occur in intergenic and intronic regions, but be very important from a regulatory perspective⁸².

Returning to ACT - previously genetic variants have been found to potentially modify the association between dose-dependence and cardiotoxicity as indicated by inter-individual variability⁴⁴.

Candidate genes involved in the metabolism of doxorubicin were first investigated (Fig.10) followed by anthracycline-based drug transport within a cell (Fig.11) and its metabolism in a cardiomyocyte and subsequent adverse drug reactions (Fig.12).

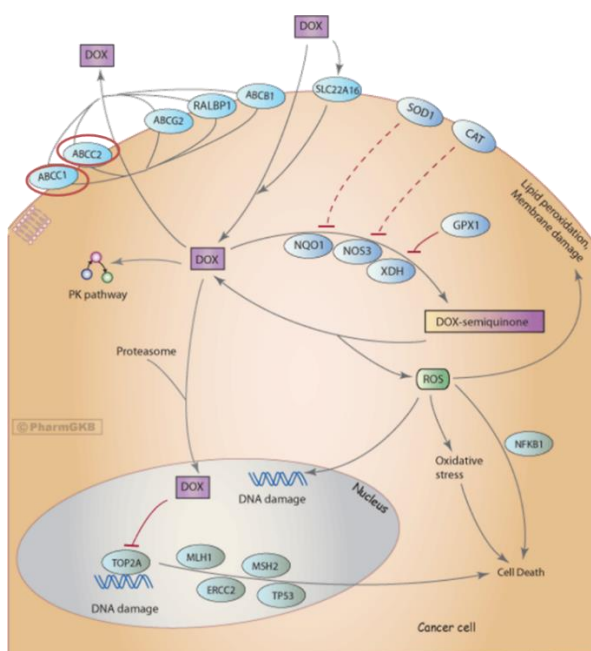


Figure 10: Representation of pathways showing candidate genes involved in the metabolism of doxorubicin in a cancer cell⁸³- courtesy of www.pharmgkb.org

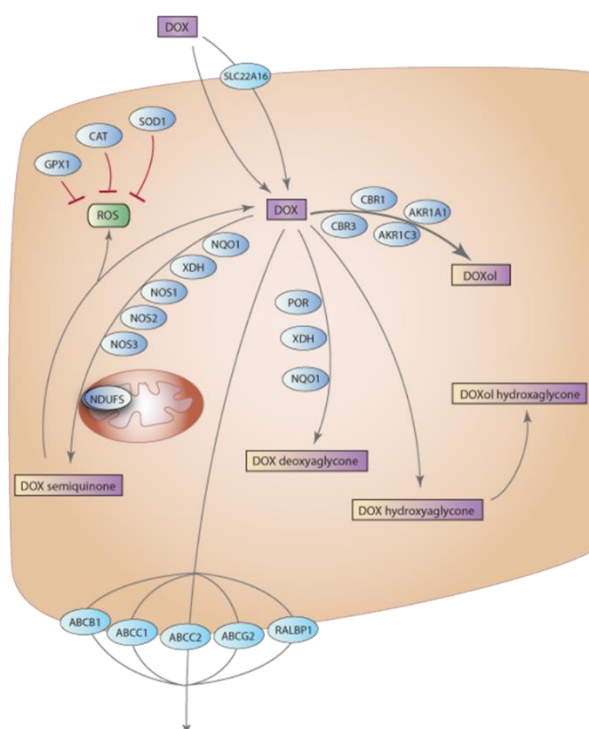


Figure 11: Representation of transport and metabolism of doxorubicin⁸³ – courtesy of www.pharmgkb.org

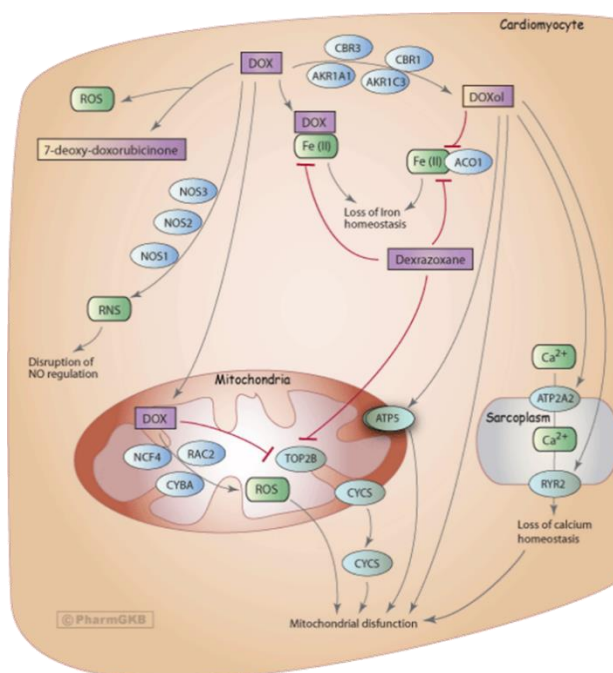


Figure 12: Representation of candidate genes involved in the metabolism of doxorubicin and subsequent adverse reactions in a cardiomyocyte⁸³ – courtesy of www.pharmgkb.org

Therefore, a candidate gene approach that focused on genes involved in drug ADMET as well as in the mechanism of cardiomyocyte injury would allow for a plausible investigation into the following:

1. Aldo-keto reductases are NADPH-dependent oxidoreductases involved in the metabolism of Doxorubicin ³⁴. They are involved in the reduction of aldehydes and ketones into primary and secondary alcohols that are eventually eliminated from the body ³⁴. The formation of doxorubicinol (an alcohol metabolite) therefore requires input from the following genes: *AKR1C3*, *AKR1A1*, *CBR1* and *CBR3* ^{27,34}.
2. CBRs are also involved in converting anthracyclines to alcohol metabolites which may be cardiotoxic. Therefore, the *CBR3* V244M variant (rs1056892) may be associated with ACT ^{26,47,68}. This single nucleotide polymorphism (SNP) encodes for a valine to methionine substitution at position 244 and has been found at varying frequencies in different population groups ²⁶. While *CBR3* and *HAS3* (rs2232228) may have a dose-modifying risk of ACT- patients homozygous for the *CBR3* V224M G allele and the *HAS3* A allele were previously shown to be susceptible to cardiotoxicity, even at fairly low doses (101-150mg/m²), ACT was also induced at high doses of anthracyclines (>250mg/m²) irrespective of the *CBR3* genotype but not for the *HAS3* AA genotype ^{44,68}. *CBR3* expression is regulated by the transcription factor, nuclear factor like-2 (nrf2), which controls genes that protect against oxidative stress and may provide the link between ROS-cardiomyocyte damage and *CBR3* expression.
3. Genes involved in the oxidation reaction and production of ROS and deactivation of ROS include NADPH dehydrogenases, namely *NCF4*, *CYBA* and *RAC2*, *nitric oxide synthases*, *xanthine oxidase*, *glutathione peroxidase*, *catalase* and *superoxide dismutase* ²⁷. NADPH oxidases may play a crucial role in oxidative cardiac damage, remodelling and contractile dysfunction, and are therefore of importance for the development of ACT ¹². Specifically, *NCF4* rs1883112, was found to be strongly associated with cardiac interstitial fibrosis (a common feature of cardiomyopathy) while patched myocardial necrosis (infarcted myocardium causing a necrotic patch) was associated with *CYBA* rs4673 ¹².
4. Due to the ability of doxorubicin to destroy topoisomerase II, leading to DNA damage and cell death, genes involved in the DNA repair pathway may be of interest and include: *TOP2A*, *MLH1*, *MSH2*, *TP53* and *ERCC2* ²⁷.
5. Uncoupling proteins (UCP) are members of the family of mitochondrial transport proteins that maintain the mitochondrial membrane. Decreased UCP expression was

found to be associated with both increased mitochondrial ATP production and ROS production; potentially increasing the likelihood of ACT²⁴. Therefore polymorphisms in the genes coding for UCPs may have a bearing on genetic predisposition to cardiotoxicity.

6. Recently, it was found that African American ancestry and mutation in the Haemochromatosis gene (*HFE*) may increase predisposition to ACT²⁴.

Due to the advances in the development of bioinformatics tools and ever decreasing costs of next generation genomic technologies, genome wide association studies (GWAS) have helped to identify novel SNPs that may predict ACT⁴⁴. Wang *et al.*⁴⁴ focused on the validation of a novel SNP involved in a gene-environment interaction; specifically its ability to modify the dose-dependent risk of cardiomyopathy. SNP rs1786814 in the *CELF4* gene was successfully associated, validated and replicated and showed that cardiomyopathy was rare and not dose-dependent in patients with the AA genotype⁴⁴. Patients with the GG genotype however, exposed to a cumulative anthracycline dose of 300 mg/m², had a more than 10-fold risk of cardiomyopathy compared to their GA/AA counterparts⁴⁴. Furthermore, an association was found between the *CELF4* (rs1786814) GG genotype and more than one splicing variant of *TNNT2*; the gene that encodes cardiac troponin T, a biomarker of myocardial damage⁴⁴. More than one cardiac troponin T variant results in a temporally-split myofilament response to calcium and subsequent decreased myocardial contractility and ventricular function⁴⁴. Splicing of *TNNT2* during development results in the inclusion of alternative exon 5 which subsequently results in an additional 10 amino acids into the protein ultimately pre-empting cardiac dysfunction⁴⁴.

Similarly, Aminkeng *et al.*⁷ conducted a GWAS study on childhood cancer patients treated with anthracyclines and found a novel variant, *RARG* rs2229774, to be associated with ACT. The *RARG* variant impairs transcriptional regulation of *Top2b*, which encodes DNA topoisomerase – a target of anthracyclines^{7,84}. A study by Zhang *et al.*⁸⁵ showed that in mice, the cardiomyocyte-specific deletion of *Top2b* which encodes for topoisomerase IIB resulted in a protective effect. Cardiomyocytes were safe from DNA double-strand breaks and transcriptome changes generally inflicted by doxorubicin thereby preventing defective mitochondrial biogenesis and ROS formation. This ultimately protected these mice from developing doxorubicin-induced progressive cardiac failure.

Other SNP risk variants include: *SLC28A3* rs7853758 which was found to be strongly associated with ACT; *UGT1A6* rs6759892; *ABCB4* rs1149222; *ABCC1* rs4148350 and *HNMT*

rs17583889¹⁰. Specifically, *SLC28A3* rs7853758 (L461 L) and *UGT1A6* rs17863783 (V209 V) have been previously associated with ACT in paediatric cancer patients⁸⁴. While neither of these variants are expressed in the heart, it is surmised that their associations with ACT may indicate indirect effects on cardiac tissue⁸⁴. The variant *UGT1A6* rs17863783 (V209 V) has been linked to impaired drug metabolism possibly due to its reduced glucuronidation activity *in vitro*⁸⁴. A reduction in glucuronidation results in the accumulation of reactive oxygen species and toxic alcohol metabolites. The variant *SLC28A3* rs7853758 (L461 L) has been shown to have reduced expression in cell lines and subsequent reduced exposure to anthracyclines which may confer a protective effect⁸⁴. This is due largely to *SLC28A3*'s role as a drug transporter.

A number of genes and SNPs or variants within or in the vicinity of these genes, as shown in Table 6, have been associated with either a protective or increased risk effect related to anthracycline-induced cardiotoxicity^{8,10,27,55,79}:

Table 6: Genes and SNPs that have been previously associated with anthracycline-induced cardiotoxicity

Gene	Variant	CHR	Position	Functional Annotation	Alleles
<i>ABCC1</i>	rs45511401	16	16173232	Exon Missense	G/T
	rs4148350	16	16170477	Intron	G/T
	rs246221	16	16138322	Exon	T/C
<i>ABCC2</i>	rs17222723	10	101595996	Exon Missense	T/A
	rs8187710	10	101611294	Exon Missense	G/A
<i>ABCB4</i>	rs1149222	7	87073775	Intron	G/T
<i>ACO1</i>	rs867469	9	32383708	5' near gene	G/A
<i>AKR1A1</i>	rs2229540	1	46032311	Exon Missense	A/G
<i>CAT</i>	rs10836235	11	34460704	Intron	C/T
<i>CBR3</i>	rs1056892	21	37518706	Exon Missense	G/A
<i>CYBA</i>	rs4673	16	88713236	Exon Missense	T/C
<i>GSTP1</i>	rs1695	11	67352689	Exon Missense	A/G
<i>HFE</i>	rs1800562	6	26092913	Intron	A/G
<i>HNMT</i>	rs17583889	2	138746039	Intron	C/A
<i>IREB2</i>	rs17483548	15	78730313	5' near gene	G/A
<i>NCF4</i>	rs1883112	22	20219009	5' near gene	G/A
<i>RAC2</i>	rs13058338	22	20597907	Intron	A/T
<i>RARG</i>	rs2229774	12	53211761	Exon Missense	G/A
<i>SLC28A3</i>	rs7853758	9	86900926	Exon	G/A

2.3.1 Characterisation of Specific Genes

- **ABCC1**

ATP binding cassette subfamily C member 1 (ABCC1) is located on chromosome 16p13.11 and encodes for a transporter involved in intra- and extra- cellular membrane transport ^{81,86}. ABCC1 also confers anti-cancer drug resistance due to its role in the transmembrane movement of substances.

ABCC1 acts as both a transporter and inhibitor for 69 clinically approved drugs including doxorubicin, methotrexate, lamivudine and docetaxel utilized in diverse clinical applications ranging from cancer to HIV ⁸⁶.

- **ABCC2**

ATP binding cassette subfamily C member 2 (ABCC2) is located on chromosome 10q24.2 and similar to *ABCC1*, encodes for the transmembrane transport of substances and additionally contributes to drug resistance ^{81,86}.

ABCC2 has a role as a transporter in the metabolism of 102 approved drugs including doxorubicin, docetaxel, methotrexate and cisplatin ⁸⁶.

- **ABCB4**

ATP binding cassette subfamily B member 4 (ABCB4) is located on chromosome 7q21.12 and encodes for a membrane-associated protein involved in both the transport of substances across the cellular membrane as well as the transport of phospholipids from liver hepatocytes into bile ^{81,86}.

ABCB4 has a role as an antagonist and transporter in the metabolism of drugs ⁸⁶.

- **ACO1**

Aconitase 1 (ACO1) is located on chromosome 9p21.1 and encodes for a protein with enzymatic functions essential to the regulation of iron levels inside cells. ACO1 protein binds to iron-responsive elements (IRES) to target mRNA when iron levels are low ^{81,86}.

- **AKR1A1**

Aldo-keto reductase family 1 member A1 (AKR1A1) is located on chromosome 1p34.1 and encodes for an aldo/keto reductase that catalyzes the NADPH-dependent reduction of aldehydes to their specific alcohols ^{81,86}.

AKR1A1 plays a role in the metabolism of various drugs including both doxorubicin and daunorubicin ⁸⁶.

- **CAT**

Catalase (CAT) is a gene located on chromosome 11p13 that encodes for a key antioxidant enzyme involved in defence against oxidative stress ^{81,86}. This enzyme converts ROS to water and oxygen thereby preventing toxicity. CAT also promotes the growth of T-cells, B-cells, myeloid leukaemia cells, melanoma cells, mastocytoma cells and fibroblasts ⁸⁶.

CAT plays a role in the metabolism of substances including ethanol and anthracyclines ⁸⁶.

- **CBR3**

Carbonyl reductase 3 (CBR3) is located on chromosome 21q22.12 and encodes for a NADPH-dependent oxidoreductase involved in the catalysis of carbonyl compounds to specific alcohols ^{81,86}.

CBR3 is involved in the metabolism of doxorubicin and other anthracyclines in both the cardiomyocyte and in cancer cells ⁸⁶.

- **CYBA**

Cytochrome b-245 alpha chain (CYBA) is located on chromosome 16q24.2 and encodes the light chain (alpha subunit) of cytochrome b which is a critical component of the membrane-bound oxidase of phagocytes that generate superoxide ^{81,86}.

CYBA plays a role in the metabolism of drugs that includes doxorubicin as well as in oxidative stress and the response to ROS ⁸⁶.

- **GSTP1**

Glutathione S-transferase pi 1 (GSTP1) is located on chromosome 11q13.2 and encodes enzymes that play a critical role in detoxification, xenobiotic metabolism as well as susceptibility to cancer and other diseases ^{81,86}.

GSTP1 has an enzymatic role in the metabolism of drugs as well as in cellular response to stress and the detoxification of ROS ⁸⁶.

- **HFE**

Hemochromatosis (HFE) is located on chromosome 6p22.2 and encodes for a protein that regulates iron absorption by binding the transferrin receptor ^{81,86}. Defects in this gene result in the recessive condition, hereditary haemochromatosis, which is an iron-storage disorder ⁸⁶.

HFE has been implicated in ACT due to its role in the regulation of iron levels – HFE deficient cells allow for increased levels of doxorubicin-iron complexes and subsequent cardiac injury⁸⁷.

- **HNMT**

Histamine N-methyltransferase (HNMT) is located on chromosome 2q22.1 and encodes for an enzyme involved in methyl group transfer; the dysregulation of which contributes to the development of cancer^{81,86}.

Due to its role in regulating histamine levels and subsequent regulation of the airway response to histamine, HNMT is involved in the metabolism of drugs as diverse as amodiaquine (anti-inflammatory and anti-malarial) as well as anthracyclines⁸⁶.

- **IREB2**

Iron Responsive Element Binding Protein 2 (IREB2) is located on chromosome 15q25.1 and encodes for an RNA-binding protein that binds to iron-responsive elements in ferritin thereby inhibiting mRNA degradation^{81,86}.

The role of IREB2 in cellular iron homeostasis and as a modifier for HFE, influences haemochromatosis as previously mentioned, and may therefore contribute to ACT due to the regulation of cellular iron and its propensity to form doxorubicin-iron complexes⁸⁶⁻⁸⁸.

- **NCF4**

Neutrophil cytosolic factor 4 (NCF4) is located on chromosome 22q12.3 and encodes for a regulatory protein component of the NADPH-oxidase that produces superoxide and plays a crucial role in host cell defence^{81,86}.

Furthermore, due to NADPH-oxidase being involved in oxidative cardiac damage and remodelling, NADPH-oxidase polymorphisms have been implicated in the predisposition to ACT, as discussed earlier in the chapter^{12,86}.

- **RAC2**

Ras-related C3 botulinum toxin substrate 2 (RAC2) is located on chromosome 22q21.3 and encodes for small, plasma membrane-associated guanosine triphosphate (GTP) proteins where it regulates various cellular responses such as secretion, phagocytosis and cell polarization as well as the generation of ROS together with NADPH-oxidase^{81,86}.

- **RARG**

Retinoic acid receptor gamma (RARG) is located on chromosome 12q13.13 and encodes for retinoic acid receptors involved in various biological processes including the regulation of gene expression ^{81,86}.

- **SLC28A3**

Solute Carrier Family 28 Member 3 (SLC28A3) is located on chromosome 9q21.32 and encodes for a nucleoside transporter that regulates multiple cellular processes including the transport and metabolism of nucleoside drugs such as anthracyclines ^{81,86}.

Measures to either prevent or mitigate the onset of ACT have been discussed in detail in this chapter – while they have advantages and disadvantages, it is often their financial cost that prevent many of them being utilized in favour of managing the patient's cancer as a first priority. The next section will discuss the long term cost of employing this strategy.

2.4 Economic Implications of Cardiac Failure compared to Preventative Measures

South Africa, as a developing nation (UMIC) with a stretched healthcare budget and a discrepancy between private and public healthcare, needs an approach that is financially feasible without compromising patient need ^{89,90}. As previously mentioned, CVD is a leading cause of non-cancer related morbidity and mortality which can significantly increase the public health financial burden ^{49,50}.

2.4.1 Comparison of Preventative Measures, Sensitive Assessment Modalities and Treatment for Cardiac Failure

In 2004 medical imaging was one of the highest costs claimed from medical insurance – this was attributed to both high patient demand and increased diagnostic accuracy ⁸⁹.

Picano *et al.* ⁸⁹ showed that by using an echocardiogram as a cost comparator of 1, the CT is 3.1x, cardiac MRI 5.51x and 19.96x for a right or left heart catheterization. The cost of an echocardiogram is approximately \$2275 in the United States ⁹¹ (+/- R31 631.00 in SA, according to the current exchange rate, although SA costs were not available. The cost of determining LVEF using ERNA or MUGA is approximately \$573 (+/- R7984.00) per scan. Economic costs aside, each modality must be carefully considered in terms of sensitivity, inter-operator variability and if applicable, radiation dose.

Comparatively, the cost of assessing cardiac injury using biomarkers were as follows: BNP was found to be between \$200- \$1000 per test (+/- R2790- R13 948) and Troponin was found to be between \$45- \$95 per test (+/- R628- R1325) ^{92,93}.

While lower and middle income countries struggle to manage chronic diseases such as hypertension and diabetes, the subsequent health and economic burden of cardiac disease increases ⁹⁴. Adverse drug reactions such as ACT may add considerable strain to this.

Breast cancer screening together with a mastectomy, chemotherapy, radiation and targeted therapy (inpatient and outpatient treatment) is incredibly expensive and can be upwards of R500 000 per patient ⁹⁵. The average cost of anthracycline was estimated at approximately R1300.00 compared to the relatively cardio-safe alternative, liposomal encapsulated doxorubicin at approximately R131 575 per patient ^{96,97}. Dexrazoxane, the cardio-protector that would be administered together with the anthracycline-based chemotherapy costs approximately \$5661.77 per patient (+/- R78 960.00) and may be a cheaper alternative to the liposomal encapsulated doxorubicin ⁹⁸.

However, in comparison to the estimated lifetime cost of the implications of CF of \$109 451 (+/- R1 526 639), the more expensive therapeutic options may be comparatively cheaper when faced with the risk of HF due to ACT ⁹⁹. Especially since it is estimated that amongst breast cancer survivors, CVD is the largest contributor to non-cancer related mortality – approximately 35% in cancer survivors over the age of 50 years ⁵⁰.

The Present Study

With the above narrative setting the scene for the need to do further research on ACT in the diverse populations of South Africa, the objectives that were targeted for the research were as follows:

- To assess the effect of anthracycline treatment, if any, on cardiac function using various clinical modalities and patient clinical evaluation, using both retrospective and prospective patient data
- To determine the cardiotoxic effects of anthracyclines (both clinical and molecular) in the unique local populations – IA and MA, and the genes responsible for this susceptibility
- To provide tools for the creation of a model of risk for susceptibility to anthracycline-induced cardiotoxicity before the initiation of treatment

Chapter 3: Patients, Materials and Methods

3.1 Retrospective Cohort

This study was initiated following anecdotal reports of cardiotoxicity during or after routine anthracycline-based treatment for patients with cancer. Adequate evidence had to be found from patients who were previously treated to necessitate a comprehensive study involving patient recruitment and subsequent biological specimens.

3.1.1 Setup of Database

Ethical approval was granted from both the University of Cape Town (UCT) and GSH (HREC Ref 650/2012) for this review. A Microsoft Excel database was established utilising records derived from GSH Pharmacy of all patients prescribed anthracyclines from 2011-2016, regardless of type of cancer. Patient information was limited to patient name, demographics, hospital number, prescription date and type of anthracycline administered. Hospital numbers were imported into the spreadsheet and duplicates were tagged and removed. The database was password protected and only accessed by the principal investigator. All data analysis was presented after patients were de-identified.

3.1.2 Collection of Data

Demographic information, patient history and clinical management details are recorded in paper-based patient folders specific to the clinic where the patient is receiving treatment. Therefore, imported hospital numbers in the patient database were used to find ID numbers specific to patient folders in the outpatient Oncology Clinic at GSH. Hospital Radiotherapy (RT ID) numbers are managed electronically on 'Clinicom' and Electronic Patient Records (EPR). RT ID numbers enabled the physical location of patient folders which are divided according to year and patient surname; deceased and alive patient folders are filed separately.

Data was collected from patient folders, EPR and 'Clinicom' to populate the following fields: age, sex, population group, type and stage of cancer, HIV status, type of chemotherapy/regimen, number of cycles and cumulative dose, LVEF before and after chemotherapy using ERNA, body surface area (BSA) and whether the patients experienced any signs or symptoms related to cardiotoxicity or CF.

Baseline cardiac assessments together with clinical history were utilized to eliminate cardiac impairment unrelated to cardiotoxicity. Acute cardiotoxicity, which is both rare and reversible, typically occurs within a week of treatment and while transient, may present as sinus tachycardia, ventricular tachycardia, transient arrhythmia, pericarditis-myocarditis syndrome and acute LV failure⁷⁶. Early onset ACT which occurs within a year of treatment, and late onset ACT, which occurs more than a year after treatment, presents with ventricular dysfunction, CF and arrhythmias^{7,36}.

Furthermore grading of the ACT was based on the Common Technology Criteria for Adverse Events v3.0 (CTCAE) and definitions in the literature^{7,10,51}. Patients with no signs or symptoms of cardiac impairment were graded as 0. Whereas, patients with chest pain, shortness of breath and/or palpitations without LVEF decline were graded as 1; patients with chest pain, shortness of breath and/or palpitations with LVEF decline <10% were graded as 2; patients with a suspected CCF, LV dilation and increased Troponin T were graded as 3; and patients with CF, MI and/or decline in LVEF $\geq 10\%$ were graded most severe, as 4. Therefore, early or late onset ACT was determined by a LVEF decrease of more than 10%⁷⁶ determined by ERNA and/or clinical symptoms pertaining to cardiac impairment (shortness of breath, chest pain, and effort intolerance) or cardiac failure and/or the grading determined by the CTCAE report. The association of cumulative anthracycline dose with ACT was also utilized to further stratify patients as low risk ($\leq 250\text{mg/m}^2$ for doxorubicin and $< 400\text{mg/m}^2$ for epirubicin) and high risk ($> 250\text{mg/m}^2$ for doxorubicin and $> 400\text{mg/m}^2$ for epirubicin), the type of anthracycline was also taken into account - with doxorubicin denoting increased toxicity compared to epirubicin^{7,26,58}. This data contributed to the building of the correlation model discussed later in the chapter.

3.1.3 Statistical Analyses

Data from folders, specifically for patients treated for cancer from 2011-2015, were collected and analysed using GraphPad Prism 5¹⁰⁰ and R programming language and scripting¹⁰¹. Graphs were generated using both Microsoft Excel, GraphPad Prism 5 and R programming language.

Analysis of variance (ANOVA) type II tests were used to determine significance of certain variables (i.e. age, pre-existing clinical conditions, type of chemotherapy etc.) to the post LVEF measures.

3.2 Literature Mining

Literature was extensively mined focusing on textbooks and journal articles. Google Scholar alerts were established using keywords “anthracycline”, “cardiotoxicity” and “anthracycline-induced cardiotoxicity” to allow for the procurement of updated literature. Abstracts from conference proceedings were also useful in keeping the literature current.

3.3 Prospective Study: Selecting Genes/SNPs of Interest

The value of SNPs in this study were to elucidate whether heritable genetic variation had an association with ACT¹⁰². SNPs are distinguished from rare variations by having a minor allele frequency (MAF) of more than 1%^{102,103}.

This candidate gene study utilized both, SNPs found to have an association with risk of anthracycline-induced cardiotoxicity from previous studies, as well as genes of interest derived from PharmGKB (www.pharmgkb.org, date accessed 2014/07/10).

3.3.1 Pathway-based Approach

Genes involved in the metabolism of anthracyclines, especially those with cardiomyocyte involvement, were selected for further interrogation. Hence the pathway-based approach was utilized. PharmGKB (www.pharmgkb.org, date originally accessed 2013/09/11) was extensively accessed to better understand the metabolism of both doxorubicin and epirubicin, and to select the genes and variations that impact drug response.⁸³

3.3.2 Gene Annotation

The purpose of gene annotation is to provide gene descriptions, identify coding regions and to relay functional significance.

Gene annotation in this instance was performed by using two online databases, the National Centre for Biotechnology Information (www.ncbi.nlm.nih.gov) and Ensembl (www.ensembl.org) as well as a specifically designed script¹⁰⁴ using Practical Extraction and Report Language (Perl Version 5). The information derived from gene annotation allowed for the design of polymerase chain reaction (PCR) primers described later in the chapter.

NCBI and Ensembl were used to gather information, specifically the gene and transcript ID, DNA sequence of interest, as well as the orientation of the strand. This information was edited and saved as SEQ files. The PerlV5 script ¹⁰⁴ was then run on these files using command line programming and the output analysed for both gene characterisation and primer design (Appendix A).

3.3.3 Selected Genes of Interest

Table 7 details the 19 SNPs that were interrogated further in prospectively recruited patient samples.

Table 7: Details of SNPs for further study of anthracycline-induced cardiotoxicity in patient cohort

Gene	Gene Name	rs ID	Variant	Genomic Location/ Co-Ordinates	Functional Significance	Pharmacokinetic/ dynamic effect
ABCB4	ATP-Binding Cassette, Sub Family B, Member 4	rs1149222	G	7: 87073775(+)	ADME* processes	
ABCC1	ATP-Binding Cassette, Sub Family C, Member 1	rs45511401	T	16: 16173232(+)	ADME processes	Resistance to anticancer drugs
ABCC1		rs4148350	T	16: 16170477(+)		
ABCC1		rs246221	C	16:16138322 (+)		
ABCC2	Multidrug Resistance Protein 2	rs17222723	A	10: 101595996(+)	Efflux Transporter of cytotoxic agents out of cell	Increased risk ACT ¹⁰⁵
ABCC2		rs8187710	A	10: 101611294(+)		
ACO1	Aconitase 1	rs867469	A	9:32383708 (+)	Regulation of cellular iron levels	Affects iron homeostasis ⁸³
AKR1A1	Aldo-Keto Reductase Family 1, Aldehyde Reductase	rs6690497	C	1:46032321(+)	NADPH-dependent reduction of substrates to alcohols	Altered efficiency of metabolism of anthracyclines ^{86, 34}
AKR1A1		rs2229540	G	1:46032311 (+)		
CAT	Catalase	rs10836235	T	11: 34460704(+)	Defence against oxidative stress	Impaired catalase activity increases ROS damage ⁸⁶ ; CC genotype associated with ACT ¹⁰⁶
CBR3	Carbonyl Reductase 3	rs1056892	A	21: 37518706(+)	Enzymatic reduction of compounds to alcohols	Associated with ACT associated CF ⁴⁷
CYBA	Cytochrome b-245, alpha polypeptide	rs4673	T	16: 88713236(+)	Critical component of NADPH oxidase (p22-phox) that produces superoxide	Missense mutation; Minor allele (T) associated with ACT ⁸
GSTP1	Glutathione S-Transferase Pi 1	rs1695	G	11: 67352689(+)	Role in detoxification	
HNMT	Histamine N-Methyltransferase	rs17583889	A	2: 138746039(+)	Metabolism of Histamine	
IREB2	Iron-Responsive Element Binding Protein 2	rs17483548	A	15:78730313 (+)	Regulation of cellular iron levels	Affects iron homeostasis
NCF4	Neutrophil cytosolic factor 4	rs1883112	A	22: 20219009(+)	Component of NADPH oxidase (p40-phox) that generates reactive oxidant intermediates	Downregulation of oxidase
RAC2	Ras-related C3 botulinum toxin, substrate 2	rs13058338	A	22: 20597907(+)		Increased risk ACT ¹⁰⁵
RARG	Retinoic Acid Receptor, Gamma Integrin, Beta 7	rs2229774	A	12:53211761(+)	Ligand dependent transcriptional regulator ⁸⁶	Impaired <i>Top2B</i> regulation ⁷
SLC28A3	Solute Carrier Family 28, Member 3	rs7853758	A	9: 86900926(+)	Nucleoside transporter in many tissues including the heart ¹⁰	Minor allele (A) protective against ACT ¹⁰

*Absorption, Distribution, Metabolism and Elimination (ADME)

3.4 Prospective Study: Patient Recruitment

3.4.1 Recruitment Protocol and Ethics

Patients were recruited from outpatient breast cancer clinics at GSH for the period from May 2013 – March 2016 and TBH for the period from May 2015 – March 2016. Patients eligible for the study were anthracycline-treatment naïve who were to commence anthracycline-based chemotherapy for breast cancer. Informed patients were consented (Appendix B), peripheral blood samples were procured at specific time points (before the commencement of chemotherapy and after 3 or 4 cycles of chemotherapy) and patients' clinical management was closely monitored for the duration of the study.

Ethical approvals (Appendix C, D and E) were received from the Human Research Ethics Committees (HREC) at the UCT and GSH (HREC 650/2012) and the University of Stellenbosch and TBH (HREC S15/02/032) and the study was conducted in accordance with the Declaration of Helsinki ¹⁰⁷.

3.4.2 Procurement of Clinical Information from Patient Folders

Recruited patients' clinical information were collected from treating oncologists, patient folders and online data management systems specific to each hospital (for GSH – 'Electronic Patient Records' and 'Clinicom'; and at TBH – Enterprise Content Management). Patients were de-identified and assigned laboratory numbers - only the principal investigator had access to identifying patient information.

Demographic information (age, sex, population group, family history of cancer or cardiac disease, weight, height), pre-existing conditions (hypertension, diabetes, cardiac disease, cholesterol), lifestyle factors (smoking and HIV status, chronic medication) and factors pertaining to the cancer diagnosis and treatment (type and stage of cancer, post or pre-operative status, treatment regimen and dose, cardiac monitoring) – was recorded in an access controlled database.

Transient acute ACT was excluded as patients had follow-up cardiac measures assessed more than 21 days after treatment. Baseline cardiac assessments together with clinical history were utilized to eliminate cardiac impairment unrelated to cardiotoxicity.

Furthermore, grading of the ACT was established using the CTCAE and literature findings. As with the retrospective cohort, patients with a grading of higher than 3 after administration of anthracyclines were deemed as serious ACT. Early or late onset ACT was determined by a decrease of more than 10% in LVEF ⁷⁶ determined by either ERNA, MUGA or ECHOs and/or clinical symptoms pertaining to cardiac impairment (shortness of breath, chest pain, effort intolerance) or cardiac failure and/or the grading determined by the CTCAE Report and literature findings. This data together with the data from the retrospective cohort, was utilised to create the correlation model to extrapolate cardiac function in the absence of a clinical measure/function (i.e. missing LVEF).

3.5 Patient Sample

Peripheral whole blood (3ml) was collected in Greiner Bio-One Vacuette Venous Blood Tubes (Lavender K₃EDTA) from patients. The additive, EDTA, binds calcium ions resulting in the inhibition of the coagulation cascade ¹⁰⁸. These blood tubes enable an intact and stable specimen to be collected for both DNA and RNA isolation.

3.6 DNA isolation

3.6.1 Principle of DNA Isolation using Promega Maxwell® 16 DNA Purification Kit:

The Promega Maxwell® 16 Instrument (Promega, USA) together with the DNA Purification Kit enable the isolation of DNA by the utilisation of paramagnetic particles allowing for the subsequent capture, washing and elution of DNA. The prepared reagent cartridges and automated purification allowed for DNA isolation to be completed in approximately 45 minutes.

3.6.1.1 Technique of DNA Isolation using Promega Maxwell® 16 DNA Purification Kit:

DNA was isolated using the Promega Maxwell® 16 DNA Purification Kit (Promega, USA) according to manufacturer's instructions. Briefly, the peripheral blood sample was centrifuged at 2500 rpm for 10 minutes resulting in the separation of three layers – plasma, buffy coat and erythrocyte layers. The utilisation of the buffy coat enables an enrichment of the white blood cells, however, the yield may be affected by other factors such as sample quality and patient total white blood cell count.

A volume of 1ml of the buffy coat layer was centrifuged at 3000 rpm for 10 minutes. A total of 500ul of the leukocyte-enriched fraction was then added to the first well of the Maxwell extraction cartridge and a plunger was added to the last well. The cartridge was placed on the Promega Maxwell® 16 platform and blue elution tubes were placed in the elution tube slots as indicated on the instrument. The elution tubes were filled with 300ul of Elution Buffer and the automated purification run was selected.

After the isolation, the blue elution tubes were placed in a Magnetic Elution Tube Rack where residual Magnesil® particles were removed. Eluted sample was then pipetted into a clean 1.5 ml microfuge tube, quantified and its integrity assessed before being stored at -12°C for downstream applications.

The Promega Maxwell® 16 DNA Purification Kit, while time-efficient, resulted in purified DNA of a relatively low concentration.

3.6.2 Principle of DNA Isolation using ‘Salting-Out’ Technique:

The majority of samples in this study were extracted using the ‘salting-out’ technique¹⁰⁹ to ensure highly concentrated DNA samples that would be utilisable for downstream applications involving PCR, genotyping and sequencing.

This technique, adapted from Miller’s salting out method¹⁰⁹, involves the removal of erythrocytes from the DNA-containing leukocytes in a peripheral blood sample, which are then lysed using cell-lysis solution. The cell-lysis solution contains detergents and salts that disintegrate the cellular membrane and subsequently liberate the DNA. The denaturation of proteins occurs by the addition of Sodium Dodecyl Sulfate (SDS) and Proteinase K. Specifically a detergent, SDS, results in the solubilisation of proteins and lipids that make up the cellular membrane; Proteinase K, an enzyme, is used to digest proteins thereby eliminating protein contamination from DNA samples as well as preventing DNA degradation by the inactivation of nucleases. Subsequent incubation at 37°C for 48 hours allows for complete cell lysis. Sodium Chloride (NaCl) was then added to precipitate DNA – the neutralization of the negative charge of DNA decreases the solubility of DNA in water. The availability of Na⁺ monovalent cations allows for further precipitation of the nucleic acids. Excess salts were removed by the addition of 70% ethanol and then air dried to remove excess ethanol. The pellets were resuspended in Tris-EDTA (TE) buffer (Appendix F) to prevent further degradation to the DNA.

Briefly, the peripheral blood sample was centrifuged at 2500 rpm for 10 minutes forming distinct layers of plasma, buffy coat containing leukocytes and platelets and erythrocytes. A volume of 500ul of the buffy coat together with 900ul of Red Blood Cell Lysis Buffer (RBC Lysis Buffer) (Appendix F) were vortexed. After incubation at 37°C for an hour, and further centrifugation at 2500 rpm for 10 minutes the resulting supernatant was discarded. A further 2ml of the RBC Lysis Buffer was added to the pellet, vortexed and centrifuged at 2500 rpm for 10 minutes with the supernatant again discarded. 600ul of Cell Lysis solution, 20ul of 20% SDS and 2ul of Proteinase K (20mg/ml) was added to the pellet, incubated at 37°C overnight and then vortexed to dissolve the pellet. A total of 400ul of 6M NaCl was added, the sample was vortexed and then centrifuged at 2500rpm for 15 minutes. The supernatant was then transferred to a clean microfuge tube and 100ul of absolute ethanol was added and the tube inverted until the DNA was visibly aggregated. The sample was then centrifuged at 10000 rpm for 2 minutes, the subsequent supernatant discarded and the pellet left to air dry for 2 hours. The pellet was finally resuspended in 200ul 1x TE Buffer (Appendix F), quantified spectrophotometrically, and integrity assessed before downstream applications.

3.6.3 Quantification of DNA:

Concentration and purity were determined using the Nanodrop™ ND-1000 Spectrophotometer (Nanodrop Technologies, USA). DNA concentration is determined by the measurement of ultraviolet light absorbance at 260nm with an absorbance unit or OD being determined using the following formula:

$$O.D = c \times l \times \epsilon$$

where c = concentration, l = path length and ϵ = extinction co-efficient

The purity of DNA was assessed using ratios based on the following: A230 is the wavelength for maximum organic solvent absorbance; A260 is the wavelength for maximum DNA absorbance and A280 is the wavelength for maximum protein absorbance. Therefore, protein and organic solvent contamination are detected by measuring the ratios of A260/A280 and A260/A230 respectively. An A260/280 ratio of ≈ 1.8 and an A260/230 ratio of 2-2.2 are representative of DNA of adequate purity.

Non-degraded DNA samples were diluted to a working concentration of 100ng/ul and stored at 4°C for downstream experiments.

3.6.4 DNA Integrity Gels

3.6.4.1 Principle of Agarose Gel Electrophoresis

The integrity of DNA was assessed using agarose gel electrophoresis ¹¹⁰. Agarose, derived from seaweed, forms a matrix composed of interlinking polysaccharide chains. When in an electric field negatively charged DNA molecules travel through matrix pores toward the anode. Tris-Borate-EDTA (TBE) buffer (Appendix F) is the medium in which the gel is run.

DNA fragments may be separated by size as a result of larger fragments migrating slower across the gel than smaller ones. The separation of fragments with similar sizes may be achieved with a higher percentage agarose gel – the increased resolution is due to pores in the matrix being smaller. A nucleic acid stain allows for the visualisation of DNA fragments by fluorescing under ultraviolet light while a specific molecular weight marker or ‘ladder’ electrophoresed alongside the samples of interest allows for the determination of DNA fragment size in neighbouring wells. Sharp, well-defined bands close to the well indicated DNA of adequate concentration and integrity whereas blurry bands indicated potential degradation.

Potentially degraded DNA samples were not discarded due to the high sensitivity of downstream applications such as PCR. Failure to amplify, or in other downstream application, in some cases, could be correlated with degradation of DNA as evident on the gel.

3.6.4.2 Method of Agarose Gel Electrophoresis

Briefly, 500ng of DNA and 2ul of 6x Loading Dye (ThermoScientific, USA) were loaded onto a 1% agarose (Seakem[®] LE Agarose, Lonza, USA) gel immersed in 1x TBE Buffer. The gel was solidified with the addition of nucleic acid stain, SYBR[®]Safe (Life Technologies, USA) (1ul/10ml). 10ul of molecular weight marker, GeneRuler[™] 100bp Plus DNA Ladder (ThermoScientific, USA) together with 2ul of loading dye was loaded separately to gauge the size of genomic fragments in adjacent lanes. Electrophoresis of the fragments at 90V for 60 minutes allowed for adequate resolution of fragments for their visualisation under UV light using the UVIPro Gold transilluminator and UVIPro version 12.3 software (UVITec Limited, UK).

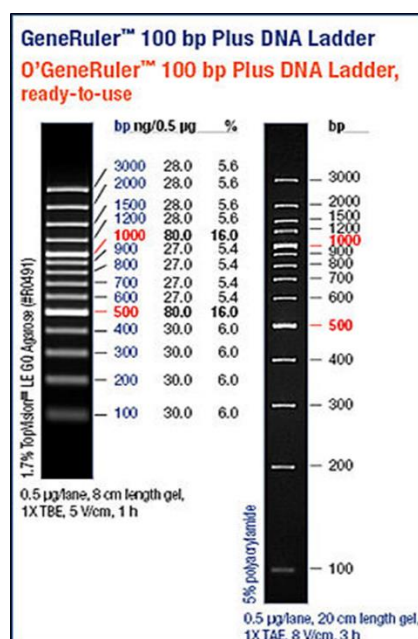


Figure 13: Representation of GeneRuler™ 100bp Plus DNA Ladder (ThermoScientific, USA) Molecular Weight Marker and its utilisation in the estimation of nucleotide fragment size ¹¹¹

3.7 Polymerase Chain Reaction (PCR)

3.7.1 Principle of PCR

PCR allows for the specific amplification of regions of DNA using two flanking oligonucleotide primers, a thermostable *Taq* polymerase derived from the thermophilic microorganism *Thermus aquaticus*, and repeated cycles of heat denaturation, annealing of primers to complementary regions and subsequent extension of the primers using deoxynucleotides (dNTPs) which act as the building blocks of the new strands ¹¹². The region of amplification lies between the two primers and each cycle of amplification effectively doubles the number of products achieving exponential, highly specific amplification of a specific DNA region ¹¹². *Taq*, is heat-resistant and therefore able to withstand repeated cycles of denaturation at high temperatures without its function being compromised ¹¹². Generally 25-30 cycles with denaturation at 95°C, annealing at 50-60°C and extension at 68-72°C ensure optimal *Taq* polymerase function (Fig. 14) as well as reaction yield ^{112,113}.

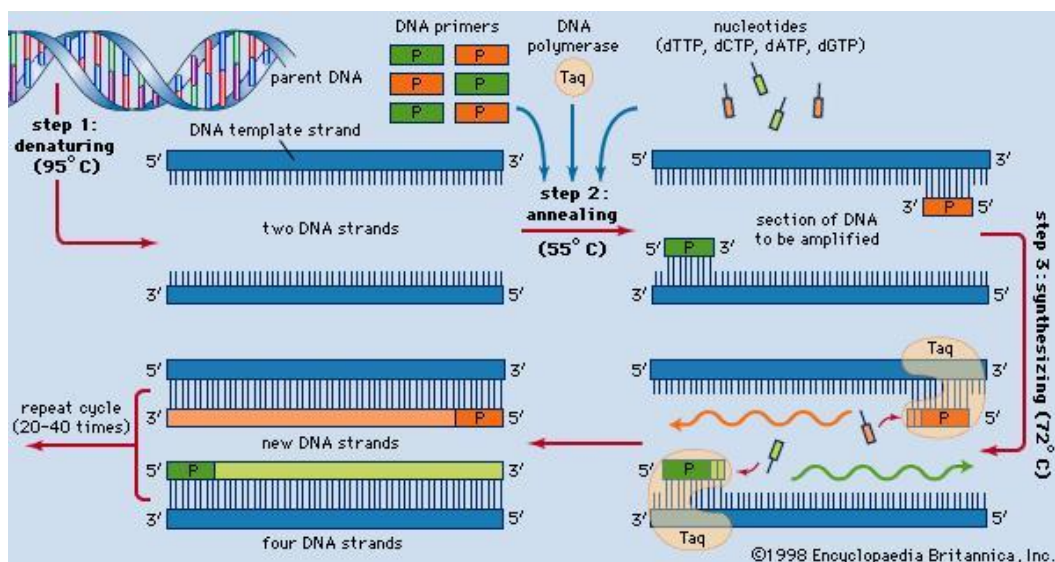


Figure 14: Diagrammatic illustration of PCR and subsequent exponential doubling of amplified DNA ¹¹³

The high rate of efficiency of amplification also requires the addition of a negative control (sterile H₂O instead of template DNA) as a measure of contamination with an extraneous source of template DNA. A successful PCR free from contamination will have an unamplified negative control.

3.7.2 Primer Design for PCR

As previously mentioned, primers are crucial to the successful and specific amplification of a DNA region of interest. Primers are short oligonucleotide sequences that are complementary to flanking regions of a sequence of interest and their competent design significantly contributes to both specificity and yield of the PCR reaction.

Primers were designed by using the following databases: Primer3 version 0.4.0 (<http://bioinfo.ut.ee/primer3-0.4.0/>, date accessed 2013/11/06), Integrated DNA Technologies (IDT) OligoAnalyzer version 3.1 (<http://eu.idtdna.com/calc/analyser>, date accessed 2013/11/06) and NCBI Primer-BLAST (<http://www.ncbi.nlm.nih.gov/tools/primer-blast/>, date accessed 2013/11/06).

Primer3 is an automated program that identifies primer pairs that may be utilised to amplify a specific DNA region of interest. These primer pairs are determined using certain specifications such as primer melting temperature (T_m), primer size and the molar concentrations of Guanine and Cytosine in a sequence (GC% content). Specifically, conditions adhered to for primer design in this study were as follows:

primer size of 20-24 base pairs in length, primer melting temperature of 50-60°C with a maximum temperature difference between the two primers of no more than 3°C, a GC content of 50-60% and a maximum permitted mononucleotide repeat length of 3 (Max Poly-X).

IDT OligoAnalyzer was then utilized to detect secondary structures such as hairpins, self-dimers and heterodimers that may be produced during the PCR reaction. The forward and reverse primers are both individually assessed, specifically for primer sequence complementarity that may hinder the efficient extension of the PCR product. Primer pairs were rejected if: the hairpin T_m was close to the primer T_m and if the Delta G (ΔG) is smaller than -4. The ΔG represents the amount of energy required to break a secondary structure and the lower the value, the higher the energy requirement.

Primer pairs that met specific criteria after Primer3 and IDT OligoAnalyzer analyses were then submitted to NCBI Primer-BLAST to ensure that primer pairs would bind specifically to the target region and that the likelihood of mismatches to other regions in the genome were unlikely.

Often singleplex PCR reactions, where one target region is amplified at a time, can be both time-consuming and expensive. Therefore multiplex PCR reactions are a feasible alternative, primer design however has to be minimally amended whereby: primer pairs at the same T_m are grouped together and their product size ranges altered so that there can be an approximately 100bp size difference that can be elucidated on a gel. These multiplex primers are then analysed using IDT OligoAnalyzer for complementarity to each other by assessing the forward primer of one of the pairs together with the reverse and other primer pairs for potential secondary structures.

Primers were resuspended in 1x TE buffer. 100uM stock solutions were made using 1x TE buffer whereas 10uM working solutions were made using sterile H₂O.

$\alpha \text{ ul of TE buffer required} = 10 \times \text{nanomoles of oligonucleotide}$

Primer working solutions were stored at 4°C and stock primer solutions were stored long-term at -20°C.

Table 8 lists the seventeen primer pairs that were designed for PCR using the approaches previously described.

Table 8: Custom-designed PCR Primers for the Amplification of Target Regions containing the SNP of interest

GENE	dbSNP ID	FORWARD PRIMERS	TM	GC%	REVERSE PRIMERS	TM	GC%	PRODUCT SIZE
ABCB4	rs1149222	CATGTTGTAGCCAGACTGAG	54.28	50	GGACCTGGAATGTCACAA	54.95	50	703
ABCC1	rs246221	AGGACCTTGTCTGAAGTCAC	54.13	50	TGGAGACATCTGGCTATGAG	56.31	50	595
ABCC1	rs4148350	GACTTAGCTTACCCATCTGGAC	57	50	CTCCTAACAGTGGGATACACAG	56.37	50	333
ABCC1	rs45511401	GTCCTCTCCTTTTCAGACCTT	54.98	50	GTCCTCATCCTACCTTGATAGC	56.94	50	492
ABCC2	rs8187710	GCTGTTTGGAGATGATAGGC	57.36	50	GGTAGTAGGTTTCATGGGTGTTC	57.46	50	572
ABCC2	rs17222723	CCTTAGGAGGTTTGGAGACT	55.04	50	CCTGTGAGATAGGGTGTGTT	54.97	50	761
ACO1	rs867469	CAGTATGACAGGGAAGGTGTAG	56.37	50	CTAGATGAAAGGTGGTGAGG	54.78	50	307
AKR1A1	rs2229540 rs6690497	GGTGACAGTAGAAGGCTGAA	55.45	50	TCAGGTACAGGTCCAGATACTC	55.85	50	489
CAT	rs10836235	CCAATCAGAAGGCAGTCCTC	59.8	55	GTGCTGGAGACCTCAAGATT	56.86	50	699
CBR3	rs1056892	CCAGTGGTTGTACCTCTGTGA	58.63	52.38	CTCCGAAGCAGACGTTTACC	59.88	55	505
CYBA	rs4673	GAGCTTGTTTTCTCACTTGG	57.51	50	GTGTTCTCAGCCTTGATGTG	56.76	50	680
GSTP1	rs1695	ACTGAGACCCACTGAGGTTA	54.65	50	AGGAGATCAGAAACCACCAG	56.71	50	637
HNMT	rs17583889	GACCTGAATAAGAGCACAGC	55.09	50	GACCTCAAGTGATCTGCCTA	55.36	50	325
IREB2	rs17483548	GACAGGAGATAATGCTGGGTAG	57.84	50	GGGAGGAAAGAAGGAAGCAG	60.32	55	646
NCF4	rs1883112	CCTGTGAGAGAATGTAGTAGGG	55.6	50	CCACTTCCTTGATGTCAGTC	55.55	50	725
RAC2	rs13058338	TGAGAACCAAGACCTGACTG	56.28	50	AAGGCTAGATCCTGTTACCC	55	50	341
SLC23A3	rs7853758	CATCACCAAGTCTGAACTCC	55.55	50	AACCTATGAGTCTGGCAACC	56.7	50	476

*TM= melting temperature

3.7.3 Optimisation: Singleplex and Multiplex

PCR optimisation is a crucial step in experimentation before the primers, designed *in silico*, are used routinely on patient DNA.

Various parameters such as annealing temperature, magnesium concentration, additives and modification of the PCR conditions were altered to facilitate optimisation. Furthermore, after PCR was optimised for primers in singleplex, those with similar T_m 's were optimised in multiplex.

3.7.3.1 Temperature Gradient

The first step for PCR optimisation was a temperature gradient. This determines the optimum annealing temperature for each primer set and in this study a range between $T_m - 5^\circ\text{C}$ and $T_m + 5^\circ\text{C}$ was utilised. The annealing temperature producing the most specific yet highest yield of product for each primer set, visualised on an agarose gel, was then utilized for routine PCRs.

Table 9: Conditions of PCR reaction required for optimisation of annealing temperature

PCR Step	Cycles	Time (mm:ss)	Temperature ($^\circ\text{C}$)
Initial Denaturation	1	3:00	94
Denaturation	30	00:30	94
Annealing		00:30	$T_m \pm 5^\circ\text{C}$
Extension		1:30	72
Final Extension	1	10:00	72

If the temperature gradient resulted in inadequate PCR product yield then the Magnesium Chloride concentration was changed to achieve optimal amplification.

3.7.3.2 Magnesium Chloride (MgCl_2) Gradient

MgCl_2 enhances the activity of *Taq* polymerase however while it is a valuable cofactor and catalyser, it may compromise specificity. Too little MgCl_2 may result in no PCR product whereas too much MgCl_2 may result in non-specific PCR products. A delicate balance between amplification efficiency (yield) and specificity must be maintained.

Generally a PCR requires 1.5-2mM of MgCl_2 for efficient amplification which is usually contained in the reaction buffer. The 5X Green GoTaq® Reaction Buffer (Promega, USA) was utilized for all PCR reactions and contained 1.5mM of MgCl_2 per reaction. However, there were instances requiring additional MgCl_2 for optimal amplification.

The MgCl_2 concentration may be as high as 4mM and a gradient was established starting at 1.5mM (in the reaction buffer) and increased by 0.5mM increments. MgCl_2 concentrations where amplification of DNA resulted in both adequate yield and discernible specificity were maintained for routine PCRs.

There may be PCR reactions that despite the altering of annealing temperature and MgCl_2 concentrations result in persistent non-specificity or non-amplification due to their propensity to form secondary structures or due to inherent high GC content ¹¹⁴. An excess of these nitrogenous bases, by virtue of their three hydrogen bonds, have greater stability of structure and may accumulate resulting in problematic denaturation and truncated PCR products. Therefore, certain additives were added to increase specificity and efficiency.

3.7.3.3 Additives

Certain target regions of DNA may prove to be difficult perhaps because of GC content, and would therefore require addition of specific agents to the reaction mix to achieve amplification. Commonly used agents include: dimethyl sulfoxide (DMSO), Betaine, Glycerol and dithiothreitol (DTT).

Betaine and DMSO function as PCR enhancers especially in GC rich regions where primer annealing is in competition with the formation of secondary structures ¹¹⁴ as previously discussed. Betaine, an isostabilizing agent, enhances denaturation and ensures that there is an equal contribution of both GC and Adenine-Thymine (AT) base pairing to the DNA duplex further increasing stability ¹¹⁵. DMSO facilitates denaturation by disrupting base pairing ¹¹⁵. The reducing compound, DTT, breaks disulphide bonds facilitating primer annealing to the template while stabilizing the DNA polymerase ¹¹⁴. Glycerol acts as a stabilizing agent by improving the thermal stability of *Taq* polymerase ¹¹⁶. Some additives may be added singularly but other agents needed to be added in combination (i.e. DTT and Betaine) to produce a discernible improvement in amplification efficiency.

While amplification efficiency is important, it should not be at the cost of specificity. Touchdown PCR is a technique that decreases non-specific amplification while increasing efficiency.

3.7.3.4 Touchdown PCR

Touchdown PCR is the stepwise reduction of the annealing temperature for each cycle (Fig.15) ¹¹⁴. The initial annealing temperature is approximately 5°C above the

annealing temperature of the primers and progressively decreases to a lower annealing temperature, usually in increments of 0.5°C ¹¹⁷. Non-specific annealing occurs at lower temperatures however with touchdown PCR, an initial higher annealing temperature translates to very specific binding of primer to template allowing for an accumulation of specific DNA products, before the lower temperatures are reached ¹¹⁷. At the lower temperatures, the amplification efficiency is increased as specificity of binding decreases, however, the accumulation of specific PCR products outnumbers the non-specific products ¹¹⁷. This technique is generally longer than a standard PCR.

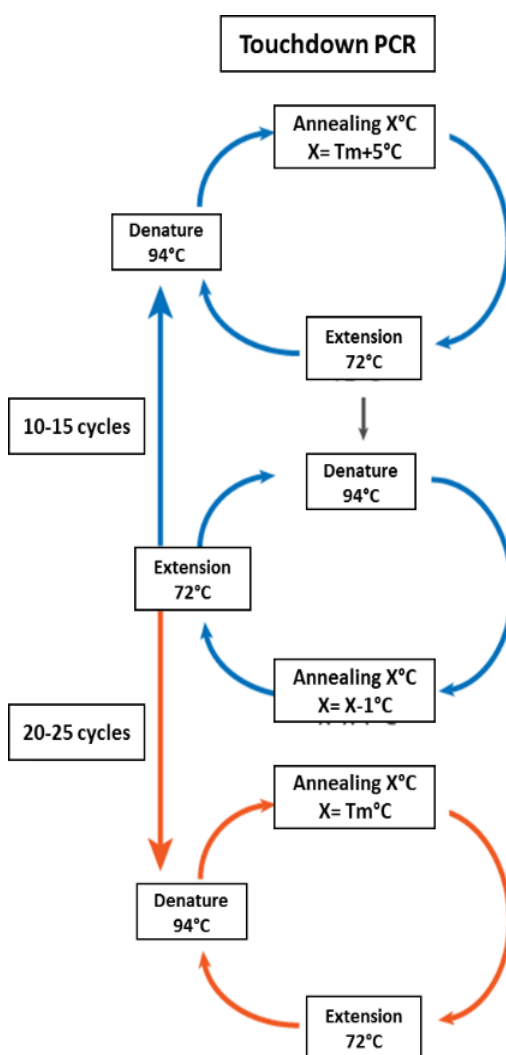


Figure 15: Diagrammatic representation of touchdown PCR adapted from ¹¹⁸

The conditions of an optimised Touchdown PCR reaction are outlined in Table 10.

Table 10: Conditions of Touchdown PCR reaction

PCR Step	Cycles	Time (mm:ss)	Temperature (°C)
Initial Denaturation	1	03:00	94
Denaturation 1	30	00:30	94
Annealing 1		00:30	T _m + 5°C -0.5°C per cycle
Extension 1		00:30	72
Denaturation 2	30	00:30	94
Annealing 2		00:30	55
Extension 2		00:30	72
Final Extension	1	05:00	72

3.7.4 Technique of PCR

Target regions of DNA were amplified using multiplex PCR reactions that had been optimised using healthy control DNA as previously mentioned.

Table 11: Optimised Multiplex Conditions

Multiplex	Amplification region	Size of fragment (bp)	T _m (°C)
Multiplex 1	<i>HNMT</i> rs17583889	325	55
	<i>ABCC2</i> rs8187710	572	
Multiplex 2	<i>RAC2</i> rs13058338	341	56
	<i>NCF4</i> rs1883112	725	
Multiplex 3	<i>ABCC1</i> rs246221	595	65*
	<i>ABCC2</i> rs17222723	761	

*Touchdown PCR with the addition of glycerol

A total of 100ng of DNA was amplified using the conditions described below. Table 12 shows an optimised PCR for both Multiplex 1 and Multiplex 2. Detailed protocols for optimized PCRs are included in the appendix (Appendix G).

Table 12: Prescribed reagents and concentrations for a standard PCR (Multiplex 1 and 2)

Reagents	Stock Concentration	Working Concentration	Volume (ul) – 1x
5X Green GoTaq® Reaction Buffer (Promega)	5x	1x	5
MgCl ₂	50mM	1mM	1.5
dNTPs	5mM	200uM	1
Forward Primer	20µM	10pmol	0.5
Reverse Primer	20uM	10pmol	0.5
Sterile water			15.4
<i>Taq</i> polymerase	5U	0.02U	0.1
DNA template	100ng	100ng	1
Total			25

Table 13 shows the reagents and concentrations for an optimised touchdown PCR with an additive for Multiplex 3.

Table 13: Prescribed reagents and concentrations for a touchdown PCR (Multiplex 3)

Reagents	Stock Concentration	Working Concentration	Volume (ul) – 1x
5X Green GoTaq® Reaction Buffer (Promega)	5x	1x	5
MgCl ₂	50mM	1mM	1.5
dNTPs	5mM	200uM	1
Forward Primer	20uM	10pmol	0.5
Reverse Primer	20uM	10pmol	0.5
Sterile water			15.15
Glycerol			0.25
<i>Taq</i> polymerase	5U	0.02U	0.1
DNA template	100ng	100ng	1
Total			25

The 5X Green GoTaq® Reaction Buffer (Promega, USA) was specifically utilised as it contains two dyes, blue and yellow, which allows for monitoring of migration during agarose gel electrophoresis without the addition of a loading dye.

3.7.5 Agarose Gel Electrophoresis

The success of a PCR was determined by using agarose gel electrophoresis similar to the technique used to assess DNA integrity as previously mentioned in the chapter. The multiplex PCRs were all assessed on a 3% (w/v) agarose gel electrophoresed at 120V for 1 hour or until the line of migration was close to the end of the gel.

Sharp, well-defined bands at the expected molecular weight, measured by a GeneRuler™ 100bp Plus DNA Ladder (ThermoScientific, USA) run alongside the samples, indicated a successful amplification. Bands that were missing, faint or non-specific indicated an unsuccessful PCR. Amplification in the negative control indicated contamination of the PCR and the PCR products were not subsequently run in downstream applications such as genotyping and sequencing. Non-amplification or repeated faint bands prompted an increase in DNA template from 100ng to 200ng per reaction.

Adequate PCR products were then used for downstream genotyping.

3.8 Genotyping

Genotyping enables the elucidation of genetic variants by interrogation of the genotype or DNA sequence.

In this study, the SNaPshot® Multiplex System for SNP Genotyping Assay (Thermofisher Scientific, USA) on the 3130xl Genetic Analyzer (Applied Biosystems, USA) was utilized for 6 out of the 7 SNPs studied. *RARG* rs2229774 was genotyped using the TaqMan® SNP genotyping assay (Thermofisher Scientific, USA).

3.8.1 Genotyping by the SNaPshot® Multiplex Assay

3.8.1.1 Principle of Genotyping by SNaPshot®

The SNaPshot® System for SNP Genotyping Assay has the capability of detecting SNPs by using single base extension and termination ¹¹⁹. A single oligonucleotide primer binds to a complementary template in the presence of DNA polymerase and fluorescently labelled dideoxynucleotides (ddNTPs). There is single base extension of the primer by the polymerase – the fluorescently labelled ddNTP (ddGTP, ddCTP, ddATP, ddUTP) terminates extension by virtue of the absence of a 3'-hydroxyl group preventing the formation of a phosphodiester bond with another nucleotide (Fig.16).

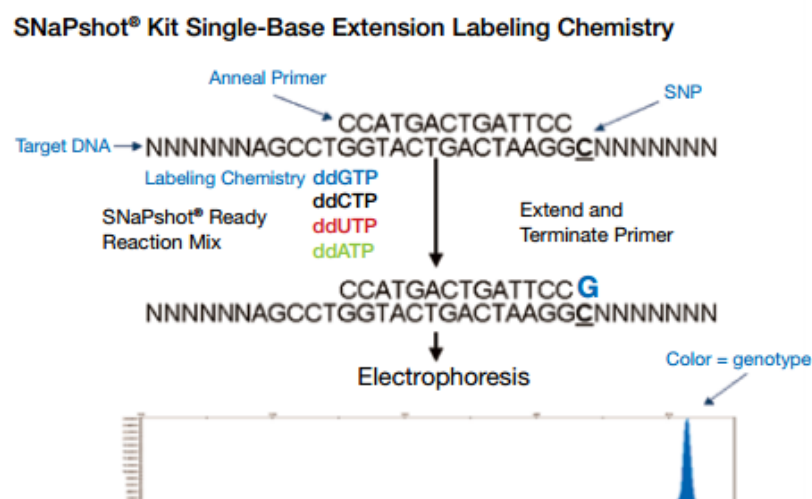


Figure 16: Diagrammatic Representation of the Principle of SNaPshot® Genotyping ¹¹⁹

The incorporated ddNTP's fluorescence is quantified on an electropherogram generated by automated electrophoresis and a genotype can be subsequently called

¹¹⁹.

Table 14: Labelled ddNTPs, their fluorescent dyes and colours that determine genotype

ddNTP	Dye	Expected Colour
Adenine (A)	dR6G	Green
Cytosine (C)	dTAMRA™	Black
Guanine (G)	dR110	Blue
Thymine (T)	dROX™	Red

The GeneMapper® software version 4.1 allows for the analysis of genotyping data generated by the SNaPshot® Genotyping Assay and the ABI3130xl Genetic Analyzer (Applied Biosystems, USA).

Successful genotyping requires primer specificity – this was achieved by precise genotyping primer design described below.

3.8.1.2 Primer Design for SNaPshot® Genotyping

Genotyping primer design is similar to PCR primer design described earlier in the chapter. However there are minor modifications.

Genotyping primers were designed by using the following databases: IDT OligoAnalyzer version 3.1 (<http://eu.idtdna.com/calc/analyzer>, date accessed

[2014/06/24](#)) and NCBI Nucleotide-BLAST (https://blast.ncbi.nlm.nih.gov/Blast.cgi?PAGE_TYPE=BlastSearch, date accessed [2014/06/24](#)). Either a forward or reverse primer was designed for the region amplified by PCR for genotyping by SNaPshot®. The genotyping assay was multiplexed, therefore primer lengths had to be at least 25 nucleotides long and differed by at least 4-6 nucleotides to prevent overlap – non-homologous nucleotides were added to the 5' end, where necessary. The recommended annealing temperature of the SNaPshot® control primer is 50°C therefore the annealing temperature of the primer should be at least 50°C.

The amplified region was analysed *in silico*, the position of the SNP noted and either 25 nucleotides upstream or downstream of it was highlighted as a potential forward or reverse primer, respectively. This region of potential primer was then analysed using IDT OligoAnalyzer: for hairpin structures, the T_m of the secondary structures should not be similar to the primer T_m; for self-dimer, the ΔG should not be smaller than -4 and for the heterodimer, the other primers to be utilised in the multiplex should be analysed whereby if the ΔG is smaller than -4, the primer may be accepted and allowed to be assessed by NCBI Nucleotide-Blast. It is important to note that if a reverse primer is designed, this region must be reverse complemented resulting in the complement SNP being detected.

Primers were multiplexed and therefore submitted to Autodimer software (<http://yellow.nist.gov:8444/dnaAnalysis/primerToolsPage.do>, date accessed [2014/06/30](#)) to ensure that the primers would not form hairpins or primer-dimers.

Genotyping primers were not designed for the following SNPs due to failure to amplify: *ABCB4* rs1149222; *IREB2* rs17483548 and *SLC23A3* rs7853758.

Genotyping primers for the TaqMan™ SNP Genotyping Assay (Table 15) were not designed for *RARG* rs2229774 as these were pre-designed by ThermoFisher Scientific (Applied Biosystems, USA).

Table 15: Pre-designed TaqMan™ SNP Genotyping Assay

GENE	RS ID	PRIMER CONC		CONTEXT SEQUENCE
		FORWARD	REVERSE	
RARG	rs2229774	36uM	36uM	GGCATTGGGGTGGGGACCAGGCTGC[A/G]A GGAGTCATCCTCAAACATTTCAGG

Table 16 shows the genotyping primers designed as outlined previously.

Table 16: Custom-designed Primers for Genotyping using the SNaPshot® Multiplex System (ThermoFisherScientific, Applied Biosystems, USA)

GENE	dbSNP ID	PRIMER	TM ¹	GC% ²	LENGTH (BASES)	DIRECTION	CHANGE	CHANGE IF REVERSE
ABCC1	rs246221	AGA TCC TTG GAG GAG TAC AC	53.2	50	20	Reverse	.	A/G
ABCC1	rs4148350	GCA GGC AAG GCT GCT GTA ACT TAC AAT	61.6	50	28	Reverse	.	C/A
ABCC1	rs45511401	TAA TCA CCT TCT CCA TCC CCG AAG	58.1	50	24	Forward	G/T	.
ABCC2	rs8187710	GGC GGC ACA AGA CAA CGG GAA GAT TAT AGA GT	64.1	50	32	Forward	G/A	.
ABCC2	rs17222723	GC ATT CTG GTT GGT GTC AAT CCT C	58.2	50	24	Reverse	.	A/T
ACO1	rs867469	CGG CGT ACA AGT AAA GAA TAT TAC C	53.7	40	25	Reverse	.	C/T
AKR1A1	rs2229540	CTA CGA TTG ATT GTG CTG CTA TCT ACG GCA	61.4	46.7	30	Forward	A/G	.
AKR1A1	rs6690497	AAG GTG CTA TCT ACG GCA ATG AGC CTG A	62.9	50	28	Forward	G/C	.
CAT	rs10836235	TAT TAG GCG TCG GCA AGT AAA GGC CCG GCT TC	67.2	56.3	32	Forward	C/T	.
CBR3	rs1056892	ATT ATC AGG TCT CAG CCC CCT CCT CCA	64.1	55.6	27	Reverse	.	C/T
CYBA	rs4673	ACA TCA CCA CGG CGG TCA TGT	61.6	57.1	21	Reverse	.	A/G
GSTP1	rs1695	GCG ATT ACA TAC GTT GCC TCC GCT GCA AAT AC	63.8	50	32	Forward	A/G	.
HNMT	rs17583889	GGT CCG AAC AGC ATG GGT GAA TGT TT	61.6	50	26	Forward	C/A	.
NCF4	rs1883112	GAC ATA GGT CAC AAG ACA CCC TGA TG	58.8	50	26	Forward	G/A	.
RAC2	rs13058338	CAT AGT GGT CTC TGG GTT CCT TGA ATG C	60.7	50	28	Forward	A/T	.

¹TM= melting temperature; ²GC% = percentage Guanine and Cytosine content

3.8.1.3 Technique of the SNaPshot® System

The ABI Prism SNaPshot® System (ThermoFisherScientific, Applied Biosystems, USA) technique consisted of three experimental procedures conducted sequentially: purification of PCR products, the SNaPshot® PCR reaction followed by the purification of the SNaPshot® PCR products before automated electrophoresis on the ABI 3130xl Genetic Analyzer (ThermoFisherScientific, Applied Biosystems, USA).

Table 17 shows the reagents and volumes required for purification or “clean-up” of PCR products before the SNaPshot® reaction.

Table 17: Reagents required for the purification of PCR products for genotyping

Reagents	X1 (ul)
FastAP	1.5
Exonuclease 1 (Exo1)	0.1
Sterile water	13.4
PCR product	5
Total	20

Alkaline Phosphatase (FastAP) (ThermoFisher Scientific, USA) dephosphorylates all blunt, 5' and 3' ends at 37°C and was inactivated at 75°C ¹²⁰. This enzyme together with Exo1, was necessary for the purification of PCR products where excess dNTPs, unbound primers, enzymes and failed PCR products were removed to prevent interference of genotyping primer annealing during the subsequent SNaPshot® reaction. The reaction cycling conditions were 37°C for 1 hour followed by 75°C for 15 minutes. A negative control was also purified and subject to downstream experiments to exclude contamination.

Purification of PCR products was followed by the SNaPshot® PCR reaction where a single primer was utilized to detect a SNP (Table 18). The reaction was multiplexed and as a result, the corresponding primers were mixed and primer volume was taken from this mixture as shown below.

Table 18: Reagents required for the SNaPshot Multiplex Assay

Reagents	X1 (ul)	Cycling Conditions
SNaPshot Reaction Mix	1	<div> <div>96°C for 10s</div> <div>50°C for 5s</div> <div>60°C for 30s</div> <div>Hold of 4°C</div> </div> <div> <div>25 cycles</div> </div>
Primers	1	
Sterile water	3	
Purified PCR product	5	
Total	10	

This reaction was followed by a second purification of products where 1ul of FastAP (ThermoFisher Scientific, USA) was added to each sample including the negative control thereby allowing for genotyping of sequences not inhibited by excess primers or extraneous PCR products not bound by primer. Samples were then placed in a thermal cycler with cycling conditions as follows: 37°C for 1 hour followed by 75°C for 15 minutes.

Samples were then submitted for automated electrophoresis and the subsequent generation of an electropherogram and genotype. Automated electrophoresis was conducted on the ABI 3130xl Genetic Analyzer (Applied Biosystems, USA) and the reaction prepared as described below (Table 19).

Table 19: Reagents required for the automated electrophoresis run

Reagents	X1 (ul)
120 LIZ™ Size Standard	0.3
Hi-Di™ Formamide	8.7
PCR product	1
Total	10

The reaction components were denatured at 95°C for 5 minutes followed by being placed on an ice-block at -20°C for 2 minutes before electrophoresis could occur.

The GeneScan™ 120 LIZ™ Size Standard (ThermoFisher Scientific, USA) utilises five dyes to enable sizing of small fragments (15-120 nucleotides). The size standard which consists of nine single-stranded DNA fragments at 15, 20, 25, 35, 50, 62, 80, 110 and 120 nucleotides in length, are labelled with the LIZ™ fluorophore ¹²¹. The highly deionized Hi-Di™ Formamide (ThermoFisher Scientific, USA) enabled the resuspension of samples to facilitate capillary electrophoresis.

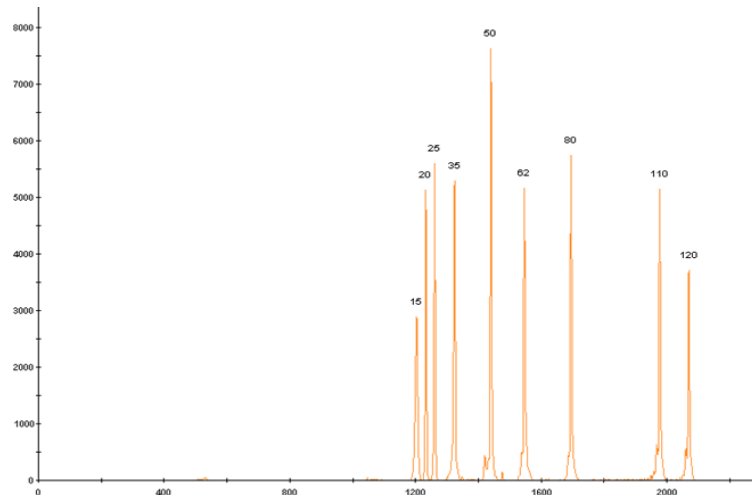


Figure 17: GeneScan™ 120 Liz™ Size Standard whereby nine DNA fragments were utilized to size small stretches of DNA to determine genotype

Results generated by the ABI 3130xl Genetic Analyzer (Applied Biosystems, USA) were analysed using the GeneScan Software run on the GeneMapper (version 4.1). The initial analysis required the setup of an analysis method, kit, panel, bin set and markers were determined. These settings allowed for the peak height and quality which were measured in relative fluorescent units (RFU), experiment type and type of alleles at specific positions that would be expected to be set. Analysis of subsequent experiments utilised these established settings. Similarly, the accurate sizing standard for each sample was crucial to the calling of the alleles and subsequent determination of the genotype. Failed sizing quality (SQ) was often due to the sizing standard being inaccurately assigned and could be manually amended to allow for the genotype to be called (Fig.18).

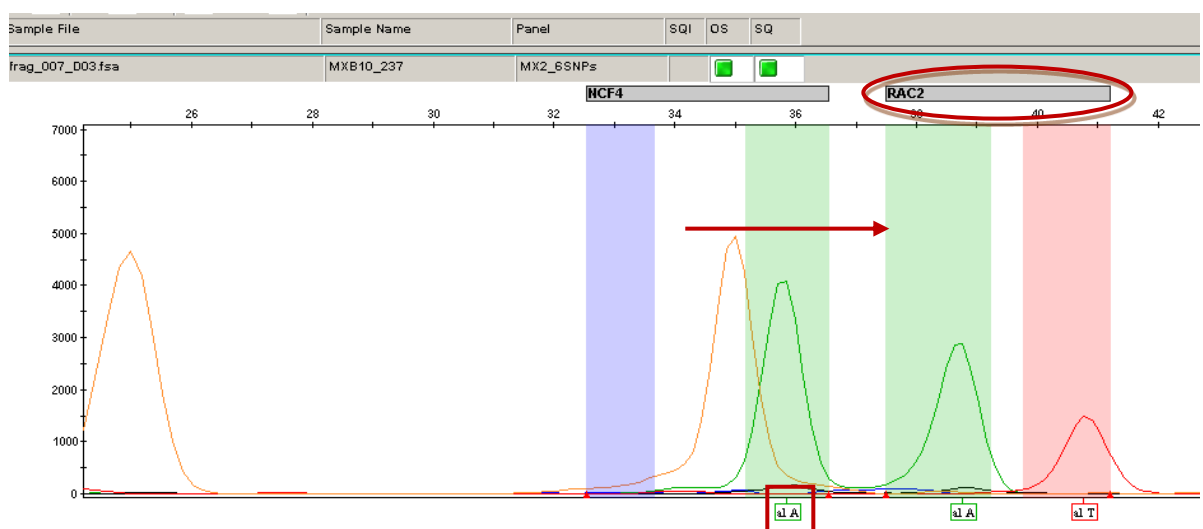


Figure 18: Analysis settings on GeneMapper v4.1 software allowing for subsequent routine genotyping calling (Red circle indicates SNP, red arrow indicates bin determining type and position of allele expected, red box shows automated allele calling)

Samples, despite being amplified by PCR, which failed to be accurately genotyped in multiplex were repeated and genotyped in singleplex.

The second technique of genotyping utilized was the TaqMan™ SNP Genotyping Assay (ThermoFisherScientific, Applied Biosystems, USA) outlined below.

3.8.2 Genotyping by TaqMan™ SNP Genotyping Assay

3.8.2.1 Principle of Genotyping by TaqMan™ SNP Genotyping Assay

A predesigned TaqMan™ SNP Genotyping Assay was utilized for the elucidation of *RARG* rs2229774. TaqMan™ Assays are relatively costly but have a quick turnaround time – this SNP (*RARG* rs2229774) was found to have an association with ACT in childhood cancer patients from a GWAS only in 2015 ⁷ and was later included in our cohort. TaqMan™ assays utilize 5' nuclease chemistry whereby a VIC® dye-labelled probe and FAM™ dye-labelled probe together with minor groove binding (MGB) technology, fluorescent dyes and target specific PCR primer pairs allow for the amplification and detection of polymorphisms in purified DNA samples (Fig. 19) ¹²². Probe and primer sets allow for increased specificity – specifically, MGB probes improve allelic discrimination due to increased binding stability between MGB probe and DNA template and the incorporation of a non-fluorescent quencher improves signal-to-noise ratios ¹²². The exonuclease cleavage of an allele-specific 5' dye label allows for the generation of a detectable signal ¹²².

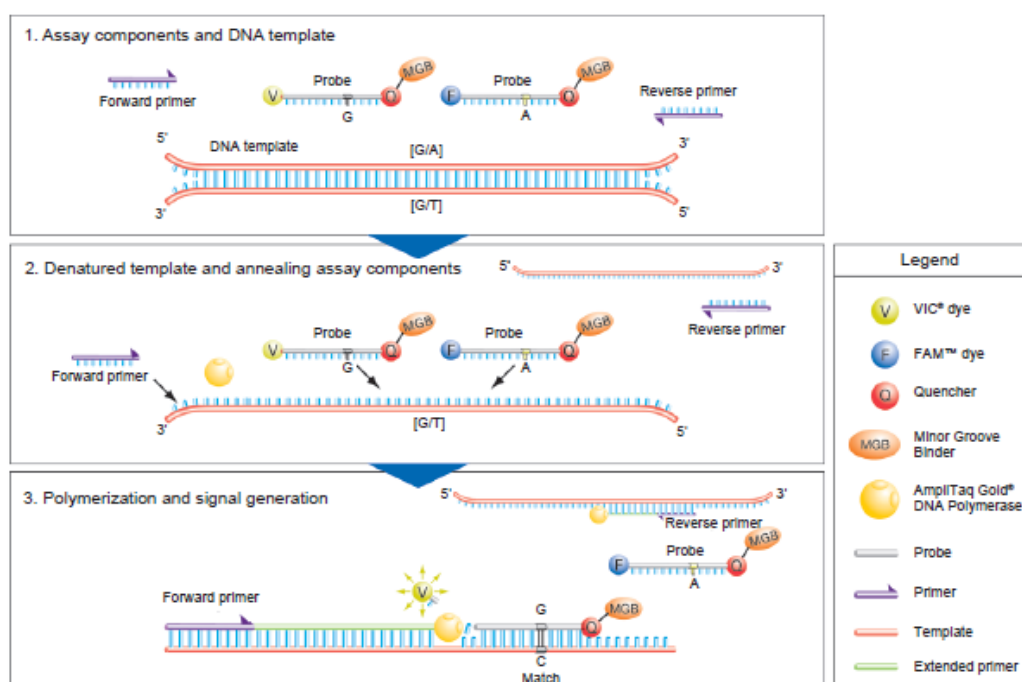


Figure 19: Graphical representation of Taqman™ SNP Genotyping Assay ¹²²

3.8.2.2 Optimisation of TaqMan™ SNP Genotyping Assay

Genotyping utilising the TaqMan™ SNP Genotyping Assay (ThermoFisherScientific, Applied Biosystems, USA) only required optimisation in terms of delineating whether the assay allowed for amplification of sample and the ideal volume of DNA to be added. Therefore, control DNA was utilized for the optimisation of this assay before it was routinely applied to all patient samples.

3.8.2.3 Technique of TaqMan™ SNP Genotyping

Components of the TaqMan™ SNP Genotyping Assay (primers and probes), TaqMan™ Genotyping Master Mix and purified genomic DNA (1-20ng) were required for the detection of this SNP. TaqMan™ Assay was diluted to 20X working solution using 1x TE Buffer (Appendix F) and stored as multiple aliquots at -15 to -25°C in the dark due to their fluorescent probes being light-sensitive.

Each reaction plate had DNA samples that were to be interrogated for the SNP of interest and two no-template controls (NTCs). A 96 well plate with a total reaction volume of 10ul was utilized (Table 20).

Table 20: Preparation of reaction mix for the wet DNA method ¹²²

<u>Reagents</u>	<u>Volume (ul) – 1x</u>
2X TaqMan® Genotyping Master Mix	5
20X Assay Working Stock	0.5
Nuclease-free water	2.5
Total volume per well	8
DNA (100ng/ul)	2
Total volume per well	20

The 2X TaqMan™ Genotyping Master Mix was added to the 20X Assay Working Stock and nuclease-free water, vortexed and centrifuged. 8ul of this mixture was pipetted into the MicroAmp® Optical 96-Well Reaction Plate wells, covered with MicroAmp® Optical Adhesive Film and centrifuged to eliminate air bubbles. DNA was diluted with nuclease-free water to ensure a concentration of 100ng/ul – 2ul of DNA was added to the required well ensuring a reaction concentration of 20ng/ul. The plate was covered with MicroAmp® Optical Adhesive Film and centrifuged.

The samples were cycled on the CFX96™ Real-Time PCR Detection System (Bio-Rad, USA) with the following conditions: enzyme activation at 95°C for 10 minutes followed by 40 cycles of denaturation at 95°C for 15 seconds followed by annealing and extension at 60°C for 1 minute.

Data generated was analysed using the TaqMan™ Genotyper Software and results were represented as a scatter plot (Allele 1 [VIC® dye] vs Allele 2 [FAM® dye]) where each point denoted an individual well (Fig.20). The NTCs were assigned as such to allow for a baseline correction for each run allowing for greater accuracy of allele calls.

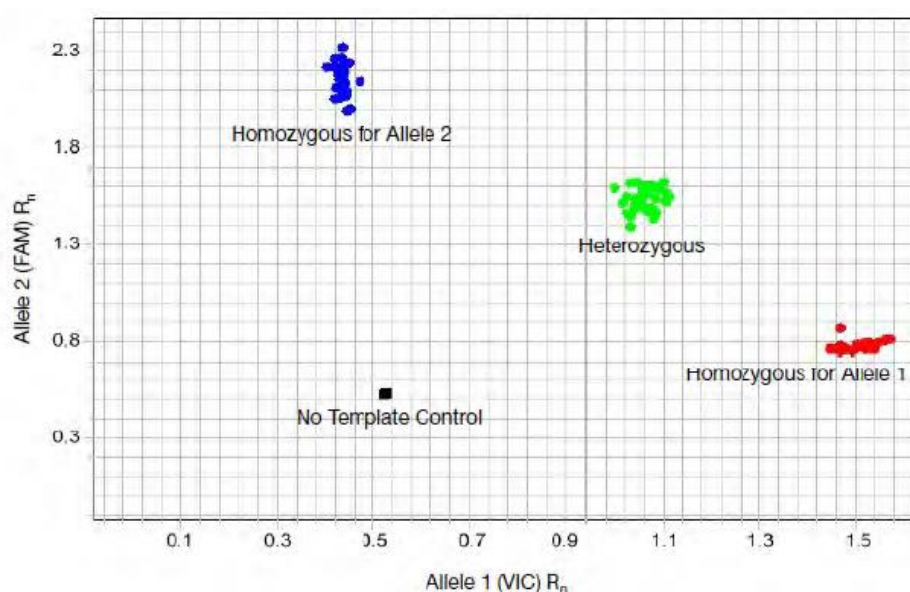


Figure 20: Example of an Allelic Discrimination plot ¹²²

3.9 Sequencing

Sanger sequencing ¹²³, as the gold standard for variant detection, was employed to confirm genotype findings using the SNaPshot® Technique. A random sample of 5% of the total cohort were sequenced – a technique that is both scientifically accurate and economical.

Generally statistical significance is achieved when the calculated probability (p) of the null hypothesis (H_0) being true is less than the significance level of 5% or 1% for greater stringency therefore 5% of our cohort was selected for validation sequencing for each variant.

3.9.1 Principle of Sequencing

Sanger sequencing ¹²³ also known as Direct Cycle sequencing, involves the utilisation of a single primer, dNTPs and fluorescently labelled ddNTPs. While dNTPs allow for

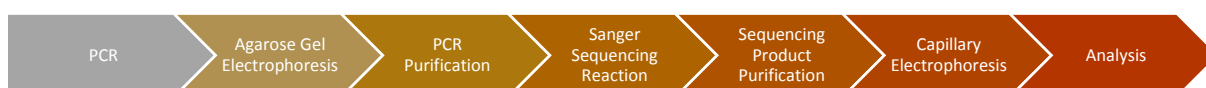
fragment extension by *Taq* polymerase, ddNTPs by virtue of an absent 3'-hydroxyl group will terminate further extension ¹²³. This method ensures that with a sufficiently high concentration of PCR products as a starting template and a specific ratio of dNTPs to ddNTPs that fragments covering the entire amplicon are generated. These fragments all terminate with a fluorescently labelled ddNTP that can be differentiated by a coloured dye (Table 21).

Table 21: Labelled ddNTPs, their fluorescent dyes and colours that determine genotype

ddNTP	Dye	Colour
Adenine (A)	dR6G	Green
Guanine (G)	dR110	Blue
Cytosine (C)	dTAMRA™	Black
Thymine (T)	dROX™	Red

After denaturation, the fragments can be separated according to size by capillary electrophoresis, which includes a laser that both excites and detects fluorescent labels. Capillary electrophoresis has the ability to discriminate between single nucleotide differences. The pattern of bands that result would generate a full sequence of the amplicon – a graphical representation called an electropherogram.

3.9.2 Technique of Sanger Sequencing



Variants were specifically amplified by primer-specific PCR and amplification confirmed by agarose gel electrophoresis as previously described.

PCR products were then purified from unincorporated dNTPs and single stranded primers using 1ul of FastAP, 0.2ul of Exonuclease I (ExoI), 3.8ul of sterile H₂O and 5ul of PCR product in a single total volume of 10ul. The reactions were then incubated at 37°C for 1 hour followed by an enzymatic degradation at 75°C for 15 minutes on the BioRad Thermal Cycler (BioRad, USA).

Purified PCR products were then combined with components of the BigDye® Terminator v3.1 Cycle Sequencing Kit (Life Technologies, USA), either the forward or

reverse primer (Table 22) and sterile distilled water to a total volume of 10ul specifically described in Table 23.

Table 22: Primers utilised for the validation of genotyping results using Sanger sequencing

GENE	RS ID	PRIMER	DIRECTION	SIZE (BP)	TM (°C)	NO. OF SAMPLES
ABCC1	rs246221	AGGACCTTGTCTGAAGTCAC	Forward	595	56	14
ABCC2	rs8187710	GGTAGTAGGTTTCATGGGTGT TC	Reverse	572	56	14
ABCC2	rs17222723	CCTGTGAGATAGGGTGTGTT	Reverse	761	60*	13
HNMT	rs17583889	GACCTGAATAAGAGCACAGC	Forward	325	57	13
NCF4	rs1883112	CCACTTCCTTGATGTCAGTC	Reverse	725	56	13
RAC2	rs13058338	TGAGAACCAAGACCTGACTG	Forward	341	57	14
RARG	rs2229774	GAGGGAGCCGGTTAGATCA G	Reverse	464	59	14

*Touchdown PCR

Depending on the brightness of band visualized on the agarose gel, concentration of the product and the volumes of both purified PCR product and BigDye ® Terminator Cycle Sequencing Mix could be modified. The volume of the distilled water was then amended accordingly allowing the total volume to remain at 10ul.

Table 23: Reagents required for the validation of genotyping using Sanger Sequencing

Reagents	Concentration	Volume (µl) – 1x
BigDye ® Terminator Cycle Sequencing Mix	-	~ 2
BigDye ® Terminator Dilution Buffer	5X	2
Forward/Reverse Primer	20uM	0.5
Sterile distilled H ₂ O	-	3.5
PCR Product	-	~2
Total Volume		10

~ variable volume dependent on amplification of product

Sanger sequencing reaction conditions include: PCR template denaturation at 98°C for 5 minutes followed by 35 cycles of fragment denaturation at 96°C for 30 seconds,

primer annealing at 55°C for 15 seconds and product extension at 60°C for 4 minutes on the ABI Thermal cycler.

Sequencing product purification was achieved by using ethanol precipitation, whereby negatively charged DNA would precipitate in the presence of absolute ethanol due to its interaction with salt ions ¹²⁴. The salt ions are subsequently removed by 70% ethanol which simultaneously maintains the DNA in its state of precipitation. Briefly, 2.5ul of sodium acetate (0.36M, pH 5.21) and 30ul of absolute ethanol was added to 10ul of sequencing product, vortexed and incubated overnight at -22°C. This was then centrifuged at 10 000 rpm for 10 minutes, the supernatant discarded and 50ul of 70% ethanol added to the precipitate. The sample was then centrifuged at 10 000 rpm for 10 minutes, the supernatant discarded and air-dried for an hour. The purified sequencing product was then resuspended in 10ul of sterile H₂O.

The purified sequencing product was then separated according to size using capillary electrophoresis. 5ul of the sequencing product was combined with 8ul of Hi-Di formamide (ThermoFisher Scientific, Applied Biosystems, USA) in a single well in a MicroAmp plate, denatured at 95°C for 5 minutes on a thermal cycler, snap-frozen on an ice-block and then loaded onto an ABI3130xl Genetic Analyzer (Applied Biosystems, USA). Electropherograms and product sequences were subsequently produced by the Genetic Analyzer for further analysis. BioEdit Sequence Alignment Editor, Version 7.1.3.0 ¹²⁵ was utilized for comparative sequence alignment.

3.10 Statistical Analysis

Retrospective cohort analysis, prospective cohort analysis and the analysis of genotypes and their association with clinical phenotypes were conducted using Microsoft Excel, GraphPad Prism version 5 and R programming Language version 3.2.1 (GUI) ¹⁰¹. The “Genetics” package and all its ‘imports or depends’ were also downloaded from the Comprehensive R Archive Network (CRAN) mirror (<https://cran.r-project.org/mirrors.html>).

Continuous variables such as age were analysed by deriving the mean and median and performing a Shapiro-Wilk test for normality. The Shapiro-Wilk test is a test of normality with the assumption that the population is normally distributed.

Chi-square tests were used to test for significant differences in categorical variables and depending on the nature of both the independent and dependent variables (categorical, ordinal, interval or normal), either the t-test, Wilcoxon-Mann Whitney Test, one-way ANOVA, Kruskal Wallis or logistic regression was utilized ^{126,127}. Chi-

square tests were used to either compare observed data with expected data based on a specific hypothesis i.e. the “goodness of fit” between observed and expected data and/or test for independence whereby a test would show whether two attributes occur independently ¹²⁸. Statistical significance was defined as $p < 0.05$. The correlation of data was achieved by the use of a multivariable, binomial logistic regression model. Estimates derived from the logistic regressions were used to compute odds ratios where $OR = 1$ denotes no effect to outcome; $OR > 1$ shows exposure associated with increased likeliness of outcome and $OR < 1$ shows exposure associated with decreased likeliness of outcome ¹²⁹.

It was determined that logistic regression would be the more robust of the two analyses (Chi-square vs logistic regression) based on the following rationale: chi-square was defined as a descriptive test much like a correlation that would be suited to describing the strength of a relationship. Logistic regression however was defined as a means to model the determinants of and predict the likelihood of an outcome. For the purposes of this study, we wished to explicitly define dependent variables and make predictions (likelihood of developing ACT) and found logistic regression to be most statistically appropriate.

The absence of post-treatment LVEF measures in the prospective cohort and subsequent change in LVEF prompted the design of a statistical model whereby the scoring system developed in this study allowed for inferences to be made on potential LVEF changes.

Retrospective data ($n=402$) with two LVEF measures and subsequent change in LVEF; a severity score (0-4) based on clinical indicators of cardiac dysfunction/impairment; type of first-line chemotherapy and population group were used to predict post LVEF where there was only one LVEF value. This model was tested in the prospective cohort ($n=87$) where patients had two measures of LVEF for robustness. The predictive model was then used on the prospective sub-cohort with missing post chemotherapy LVEF measures ($n=185$).

For single marker analyses: chi-square tests were performed using a threshold of $p < 0.05$ for the comparison of population groups for genotypic distribution, minor allele frequencies and clinical and demographic characteristics; however, to correct for multiple testing, Bonferroni correction was utilised with a more stringent p-value ($p < 0.0167$ for significance) ¹³⁰. The rationale for using a threshold of $p < 0.05$ was based on p-values for replication of previously associated variants was set to $P < 0.05$ based on the existing evidence for prior associations.

Linkage Disequilibrium (LD) tests and Haplotype Analysis were conducted using the SHEsis program and R programming Language version 3.2.1^{101,131,132}. Furthermore, markers were assessed whether they were in Hardy-Weinberg Equilibrium (HWE) and if in HWE then a Pearson's chi square test was used for independence¹³⁰. Gross deviations from HWE may indicate genotyping errors. For LD, if $D' = +1$, then there is no evidence for recombination between the markers; however, a high D' together with similar allele frequencies may indicate markers that are inherited together (i.e. in LD); if Δ^2 or $r^2 = 1$ then the markers may be surrogates for each other and if Δ^2 or $r^2 = 0$ then the markers are in equilibrium. Similarly for HWE, the Chi-square goodness of fit test is employed to determine if the observed population is significantly different from the expectations of HWE – again the significance level of $p < 0.05$ is utilized.

The successful utilization of the methods outlined in this chapter produced the experimental findings and analyses which will be described in the subsequent results chapter.

Chapter 4: Results

4.1 Retrospective Cohort Analysis

Data from the records of a total of 402 retrospective cancer patients who had attended the Oncology Clinic at GSH from 2011 - 2016 were captured on an Excel spreadsheet and analysed. The patients had all been treated with anthracyclines and had at least two measures of LVEF.

In terms of population group (or ethnicity), the cohort comprised of 24 Caucasians (CA), 95 IA and 283 patients of MA; 395 of the 402 patients were females and 7 were males.

A histogram (Fig. 21) was used to illustrate patient age at diagnosis. The median age at cancer diagnosis was 51 years (range: 27 to 77 years). Analysis by population group (or ethnicity) showed that IA patients had a younger median age at diagnosis of 44 years, compared to their MA (52 years) and CA (51 years) groups.

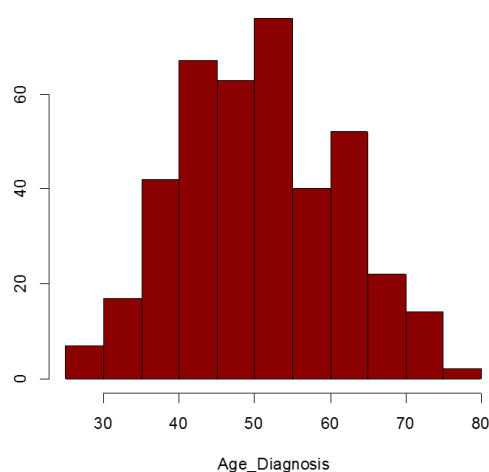


Figure 21: Histogram of retrospective cohort illustrating proportion of patients and their age at diagnosis (n=402)

The Shapiro-Wilk test showed that age at diagnosis was not normally distributed ($W=0.98958$, $p=0.006$).

Table 24 shows the demographic characteristics of the retrospective patient cohort.

Table 24: Demographic characteristics of the retrospective patients cohort (n=402)

	MA (n=283)	IA (n=95)	CA (n=24)	Combined (n=402)
Sex (Female:Male)	278 : 5	93 : 2	24 : 0	395 : 7
Median Age at Diagnosis (years)	52	44	51	51
Body Surface Area*	1.77	1.86	1.80	1.8
HIV Status (Negative: Positive: Unknown)	117 : 2 : 164 (0.41/0.007/0.59)	45 : 10 : 40 (0.47/0.11/0.42)	10 : 0 : 14 (0.42/0/0.58)	172 : 12 : 218 (0.43/0.03/0.54)
Tobacco Smoking (No: Yes: Unknown)	168 : 107 : 8 (0.59/0.38/0.03)	84 : 10 : 1 (0.88/0.11/0.01)	12 : 11 : 1 (0.50/0.46/0.04)	264 : 128 : 10 (0.66/0.32/0.02)
Hypertension (No: Yes: Unknown)	165 : 118 : 0 (0.58/0.42/0)	62 : 33 : 0 (0.65/0.35/0)	16 : 8 : 0 (0.67/0.33/0)	243 : 159 : 0 (0.60/0.40/0)
Diabetes (No: Yes: Unknown)	240 : 43 : 0 (0.85/0.15/0)	83 : 12 : 0 (0.87/0.13/0)	23 : 1 : 0 (0.96/0.04/0)	346 : 56 : 0 (0.86/0.14/0)
Cardiac Disease (No: Yes: Unknown)	266 : 17 : 0 (0.94/0.06/0)	91 : 4 : 0 (0.96/0.04/0)	24 : 0 : 0 (1.00/0/0)	381 : 21 : 0 (0.95/0.05/0)

* Body surface area (BSA) in females is considered normal at approx. 1.6m² and in males at approx. 1.9m² ¹³³

The average BSA used to determine accurate treatment dose, was higher than the “normal” for females at 1.6m² for all population groups and even higher for IA females (1.86m²).

Clinical characteristics demonstrated that 159 patients were hypertensive (40%), 56 patients were diabetic (14%) and that 21 had pre-existing cardiac disease (5%). Of the self-reported 128 smokers in the cohort (32%), CA patients were proportionally the highest (46%) (although the sample size was small: n=24). MA patients, proportionally, had the highest incidence of hypertension (42%), diabetes (15%) and pre-existing cardiac disease (6%), compared to IA (35%, 13% and 4%, respectively) and CA subjects (33%, 4% and 0%, respectively).

Table 25 shows the type and stage of cancer for patients in the retrospective cohort.

Table 25: Type and Stage of Cancer of Patients in the Retrospective Cohort (n=402)

<u>Type of Cancer</u>	<u>Stage of Cancer</u>									
	<u>IA</u>	<u>IB</u>	<u>IIA</u>	<u>IIB</u>	<u>IIIA</u>	<u>IIIB</u>	<u>IIIC</u>	<u>IV</u>	<u>Unknown</u>	<u>Total</u>
DCIS or LCIS	9	0	19	13	11	11	0	3	1	67
IDC	16	0	52	60	44	61	7	10	2	252
ILC	1	0	7	2	2	8	1	1	0	22
Inflammatory	0	0	0	0	0	0	0	0	0	0
Invasive	2	1	2	2	1	3	0	0	0	11
BC NOS*	1	0	3	5	1	12	0	3	0	25
Metastatic	0	0	0	3	3	2	0	8	0	16
Other	0	0	0	2	1	1	0	2	3	9
Total	29	1	83	87	63	98	8	27	6	402

*BC NOS = Breast Cancer, not otherwise specified

The most frequently diagnosed type of cancer was infiltrating ductal carcinoma (63% of the entire cohort) with the majority of patients diagnosed at stage IIIB (i.e. 24% of all invasive or infiltrating ductal carcinoma patients). Inflammatory breast cancer was not diagnosed in this cohort.

In terms of first-line chemotherapy – 138 patients (34%) were on doxorubicin and 264 (66%) were on epirubicin. The median administered dose of doxorubicin was 450mg/m² (range 75 - 690mg/m²) compared to the median dose of 680mg/m² of epirubicin (range 75 – 1200mg/m²). Population stratification revealed that, proportionately, more CA patients (42%) were on doxorubicin compared to MA (36%) and IA (26%) patients. Furthermore, the CA sub-cohort received higher median doses of doxorubicin (539mg/m²) than the MA (449mg/m²) and IA (456mg/m²) groups, respectively, which would seemingly place CA patients at a higher risk of ACT compared to their MA and IA counterparts.

The median change in LVEF (between the two measured time-points) was a decrease of 3% (range: decrease of -21% to an increase of +18%) after chemotherapy. A significant decrease in LVEF (of ≥10%) was noted in 56 patients (56/402= 14%), yet only seven of these patients (7/56= 12.5%) had definitive clinical symptoms after treatment. Conversely, of the 79 (79/402 = 19.7%) patients with the clinical status of “affected” (with potential or confirmed ACT), only 56 (70.8%) had a significant LVEF decline.

In terms of patient cardiac clinical status after treatment, there were 79 (19.7%) affected and 323 (80.3%) unaffected (normal cardiac function) subjects. Patient

clinical status was stratified according to population group and is illustrated below (Fig.22).

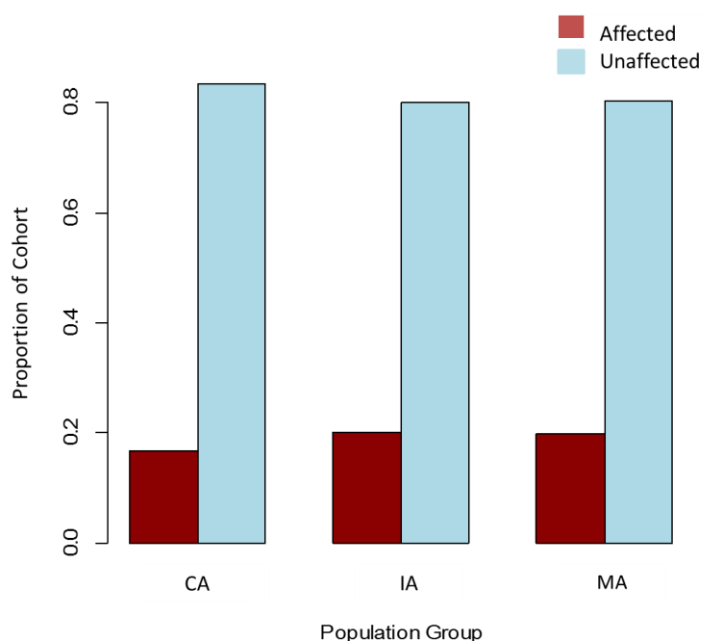


Figure 22: Patient Clinical Status (Cardiac impairment/dysfunction: affected vs unaffected) of retrospective cohort after chemotherapy stratified by population group and illustrated as relative proportions

Figure 22 shows minimal differences ($p=0.9977$), between the population groups in terms of patient clinical status after chemotherapy. Approximately 20% of IA subjects, 19.8% of MA and 16.7% of CA subjects had clinical signs of CF. By using the score or classifier developed for this study, the delineation is illustrated in Table 26:

Table 26: Patients classified according to their clinical manifestations and subsequent score

Score	Score Indication	Patients' Score
0	Normal cardiac function	323 (80%)
1	Chest pain, SOB and/or palpitations without LVEF decline	1 (0.2%)
2	Chest pain, SOB and/or palpitations with non-significant LVEF decline	13 (3%)
3	Suspected CCF and/or LV dilation and/or raised troponin T and/or cardiomegaly	5 (1%)
4	Congestive heart failure or myocardial infarction and/or significant LVEF change (>10%)	60 (15%)

The severity score had a very significant effect on LVEF post chemotherapy measures (Table 27).

Table 27: The effect of severity score on LVEF post chemotherapy measures

	Severity 0	Severity 1	Severity 2	Severity 3	Severity 4
<i>n</i>	323	1	13	5	60
Effect	+3.33	+6.54	−1.61	−2.03	−6.23

The LVEF post chemotherapy is higher for severity score zero and lower for severity score 4. The particularly high effect for severity score 1 is due to the fact that there is only a single observation and this patient has higher LVEF post chemo though still in the normal range.

ANOVA type II tests showed that the following variables did not have a statistically significant effect on the LVEF post-chemotherapy measure: age, age at diagnosis, sex, cancer type, cancer stage, hypertension, diabetes, cardiac disease, smoking status, HIV status, number of cycles for first-line chemotherapy, type of first and second-line chemotherapy, number of cycles for second-line chemotherapy and total dose of doxorubicin. However, the severity score was found to significantly contribute to the LVEF post-chemotherapy measure ($p=2.2e^{-16}$) and the LVEF pre-chemotherapy measure together with population group significantly contributed to the LVEF post-chemotherapy measure ($p=0.0036$). The type of first-line chemotherapy together with LVEF pre-chemotherapy measure did not significantly contribute to the LVEF post-chemotherapy measure ($p=0.093$).

The LVEF pre-chemotherapy measure when combined with severity score, population group and type of first-line chemotherapy had a significant effect on the prediction of LVEF post-chemo (Table 28).

Table 28: Prediction of LVEF post-chemo measure using population group, type of first-line chemotherapy and severity score

						Severity	Chemo regime 1	Population group	
$LVEF_{post}$ =		$3.11 - 12.48$ $+ 1.09LVEF_{pre}$	$\left\{ \right.$	-15.91 $+ 0.24LVEF_{pre}$	$= 1.33LVEF_{pre}$ $- 21.95$	0	AC	CA	
					$= 1.33LVEF_{pre}$ $- 26.89$	2			
					$= 1.33LVEF_{pre}$ $- 27.31$	3			
					$= 1.33LVEF_{pre}$ $- 31.51$	4			
				$+3.31$ $- 0.05LVEF_{pre}$	$= 1.04LVEF_{pre}$ $- 2.73$	0	CAF		
					$= 1.04LVEF_{pre}$ $- 7.67$	2			
					$= 1.04LVEF_{pre}$ $- 8.09$	3			
					$= 1.04LVEF_{pre}$ $- 12.29$	4			
				$+3.52$ $- 0.05LVEF_{pre}$	$= 1.04LVEF_{pre}$ $- 2.52$	0	EC		
					$= 1.04LVEF_{pre}$ $- 7.46$	2			
					$= 1.04LVEF_{pre}$ $- 7.88$	3			
					$= 1.04LVEF_{pre}$ $- 12.08$	4			
				$+9.08$ $- 0.14LVEF_{pre}$	$= 0.95LVEF_{pre}$ $+ 3.04$	0	FEC		
					$= 0.95LVEF_{pre}$ $- 1.90$	2			
					$= 0.95LVEF_{pre}$ $- 2.32$	3			
					$0.95LVEF_{pre} - 6.52$	4			
					$= 1.09LVEF_{pre}$ $- 6.04$	0	Other		
					$= 1.09LVEF_{pre}$ $- 10.98$	2			
					$= 1.09LVEF_{pre}$ $- 11.40$	3			
					$= 1.09LVEF_{pre}$ $- 15.60$	4			
		$3.11 + 11.98$ $+ 0.68LVEF_{pre}$		-15.91 $+ 0.24LVEF_{pre}$	$= 0.92LVEF_{pre}$ $+ 2.51$	0	AC		IA
					$= 0.92LVEF_{pre}$ $- 2.43$	2			

--	--	--	--	--	--	--	--	--	--	--	--	--	--	--	--	--	--	--	--	--	--	--	--	--	--	--	--	--	--	--	--	--	--	--	--	--	--	--	--	--	--	--	--	--	--	--	--	--	--	--	--	--	--	--	--	--	--	--	--	--	--	--	--	--	--	--	--	--	--	--	--	--	--	--	--	--	--	--	--	--	--	--	--	--	--	--	--	--	--	--	--	--	--	--	--	--	--	--	--	--	--	--	--	--	--	--	--	--	--	--	--	--	--	--	--	--	--	--	--	--	--	--	--	--	--	--	--	--	--	--	--	--	--	--	--	--	--	--	--	--	--	--	--	--	--	--	--	--	--	--	--	--	--	--	--	--	--	--	--	--	--	--	--	--	--	--	--	--	--	--	--	--	--	--	--	--	--	--	--	--	--	--	--	--	--	--	--	--	--	--	--	--	--	--	--	--	--	--	--	--	--	--	--	--	--	--	--	--	--	--	--	--	--	--	--	--	--	--	--	--	--	--	--	--	--	--	--	--	--	--	--	--	--	--	--	--	--	--	--	--	--	--	--	--	--	--	--	--	--	--	--	--	--	--	--	--	--	--	--	--	--	--	--	--	--	--	--	--	--	--	--	--	--	--	--	--	--	--	--	--	--	--	--	--	--	--	--	--	--	--	--	--	--	--	--	--	--	--	--	--	--	--	--	--	--	--	--	--	--	--	--	--	--	--	--	--	--	--	--	--	--	--	--	--	--	--	--	--	--	--	--	--	--	--	--	--	--	--	--	--	--	--	--	--	--	--	--	--	--	--	--	--	--	--	--	--	--	--	--	--	--	--	--	--	--	--	--	--	--	--	--	--	--	--	--	--	--	--	--	--	--	--	--	--	--	--	--	--	--	--	--	--	--	--	--	--	--	--	--	--	--	--	--	--	--	--	--	--	--	--	--	--	--	--	--	--	--	--	--	--	--	--	--	--	--	--	--	--	--	--	--	--	--	--	--	--	--	--	--	--	--	--	--	--	--	--	--	--	--	--	--	--	--	--	--	--	--	--	--	--	--	--	--	--	--	--	--	--	--	--	--	--	--	--	--	--	--	--	--	--	--	--	--	--	--	--	--	--	--	--	--	--	--	--	--	--	--	--	--	--	--	--	--	--	--	--	--	--	--	--	--	--	--	--	--	--	--	--	--	--	--	--	--	--	--	--	--	--	--	--	--	--	--	--	--	--	--	--	--	--	--	--	--	--	--	--	--	--	--	--	--	--	--	--	--	--	--	--	--	--	--	--	--	--	--	--	--	--	--	--	--	--	--	--	--	--	--	--	--	--	--	--	--	--	--	--	--	--	--	--	--	--	--	--	--	--	--	--	--	--	--	--	--	--	--	--	--	--	--	--	--	--	--	--	--	--	--	--	--	--	--	--	--	--	--	--	--	--	--	--	--	--	--	--	--	--	--	--	--	--	--	--	--	--	--	--	--	--	--	--	--	--	--	--	--	--	--	--	--	--	--	--	--	--	--	--

					$= 0.81LVEF\ pre + 0.24$	4		
					$+3.52$			
					$- 0.05LVEF\ pre$			
					$= 0.81LVEF\ pre + 10.01$	0		
					$= 0.81LVEF\ pre + 5.07$	2		
					$= 0.81LVEF\ pre + 4.65$	3		
					$= 0.81LVEF\ pre + 0.45$	4		
					$= 0.72LVEF\ pre + 15.57$	0		
					$+9.08$			
					$- 0.14LVEF\ pre$			
					$= 0.72LVEF\ pre + 10.63$	2		
					$= 0.72LVEF\ pre + 10.21$	3		
					$= 0.72LVEF\ pre + 6.01$	4		
					$= 0.86LVEF\ pre + 6.49$	0		
					$= 0.86LVEF\ pre + 1.55$	2		
					$= 0.86LVEF\ pre + 1.13$	3		
					$= 0.86LVEF\ pre - 3.07$	4		

*Grey font indicates little data and should be ignored.

Logistic regression was then performed with patient clinical status as the outcome and severity score and/or classifier and additional variables listed in Table 29, as the predictors.

Table 29: Logistic Regression Coefficients used to determine Odds Ratios of covariates for Patient Clinical Status

Covariates	Test Statistic	Odds Ratio [^]	p-value
		1.00	
Age at Diagnosis	0.019	(0.98-1.02)	0.985
Gender- Male	-2.245	(0.03-0.81)	0.025*
	-----	-----	-----
Population Group_CA (ref)	-0.370	0.81 (0.23-2.25)	0.711
Population Group_MA		0.80	
Population Group_IA	-0.369	(0.21-2.43)	0.712
Hypertension	0.063	1.02 (0.62-1.69)	0.950
Diabetes Mellitus	-0.722	0.78 (0.41-1.58)	0.470
Pre-existing Cardiac Disease	-0.491	0.77 (0.29-2.42)	0.623
Smoking Status	0.666	1.2 (0.71-2.09)	0.506
First line Chemotherapy	2.587	1.94 (1.17-3.20)	0.009*
Total doxorubicin dose	5.175	1.008 (1.005-1.01)	2.28e ⁻⁰⁷ *
Total epirubicin dose	5.857	1.004 (1.003-1.005)	4.72e ⁻⁰⁹ *
Total anthracycline dose	2.127	1.001 (1.000-1.003)	0.003*
Change in LVEF	8.98	1.63 (1.48-1.83)	<2e ⁻¹⁶ *
Score (0-4)	-0.003	1.88 ⁺	0.998

*statistically significant with a p-value threshold of <0.05; [^]univariate odds ratios with 95% CI; *sample size too small for CI

The logistic regression analyses indicate that patients on first-line chemotherapy had nearly twice the odds of developing the outcome (OR=1.94, 95%CI, p=0.009). HPT has an OR of 1 indicating no association, while smoking has an OR of 1.2, this is not significant. Only those predictors with a statistically significant p-value were

considered for the multivariable model. Predictor variables were computed in multiple combinations and only the change in LVEF remained statistically significant when computed with other variables (p value=0.000164, OR=1.7).

4.2 Prospective Cohort Analysis

4.2.1 Recruitment

Of the 275 patients originally recruited in the prospective study, three were removed for various reasons, including a change in treatment regimen, a cerebrovascular accident (CVA/stroke) and the development of herpes zoster. One patient was recruited in the cardiology clinic after suffering a myocardial infarction due to chemotherapy – only the post-chemotherapy sample was procured.

Patients deemed to have sufficient chemotherapy for quantifiable effect, despite regimen switches or incomplete regimen, were extensively interrogated. Thirty-seven patients had only one sample procured (pre-chemotherapy). Three patients deceased before a second sample could be procured. Seven patients either discontinued or switched chemotherapeutic regimen. Twenty-seven patients were lost to follow-up despite the majority of them completing chemotherapy. After completion of the study, 25 patients (9.2%) were deceased due to cancer progression, CF or treatment-related mortality. Seventeen of the deceased patients (68%) were from GSH and eight (32%) were from TBH. Ultimately, 272 of the original 275 patients were genotyped and analysed.

4.2.2 Procurement of Clinical Information from Patient Folders

The median age of the prospective patient cohort was 50 years (range 25 - 77 years). This was comparable to the retrospective cohort (median age: 51 years, and range 27 to 77 years). The Shapiro-Wilk test showed that age of the prospective cohort was normally distributed ($W=0.99222$, p -value =0.1641). IA patients were diagnosed at a median age of 44 years compared to their MA (51 years) and CA (59 years) counterparts. This was very similar to the data from the retrospective cohort for IA patients who had a median age at diagnosis of 44 years, compared to their MA (52 years) counterparts. The prospective cohort showed that the CA patients were appreciably older at diagnosis (59 years) than both the IA and MA groups

The histogram below (Fig.23) illustrates the age at diagnosis of patients in the prospectively analysed cohort.

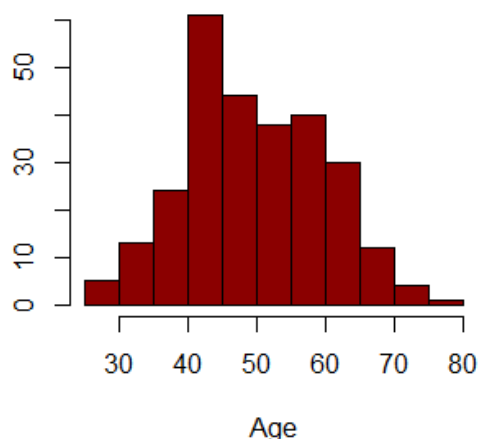


Figure 23: Histogram of the age at diagnosis of patients in the prospective cohort (n=272)

All patients recruited in the study were female, diagnosed with breast cancer and anthracycline-based treatment naïve. The average BSA, used to determine accurate treatment dose, was higher than the “normal” at 1.6m² for all population groups and to a greater degree for both CA (1.84) and IA (1.81) patients. Table 30 outlines the demographic characteristics of the patients in the cohort in greater detail.

Table 30: Demographic characteristics of patients receiving anthracycline-based chemotherapy in the prospective cohort

	MA (n=215)	IA (n=47)	CA (n=10)	Combined (n=272)
Sex (Female:Male)	215 : 0	47 : 0	10 : 0	272 : 0
Median Age at Diagnosis (years)	51	44	59	50
Body Surface Area*	1.74	1.81	1.84	1.76
HIV Status (Negative: Positive: Unk)	193 : 5 : 17 (0.90/0.02/0.08)	27 : 20 : 0 (0.57/0.43/0)	10 : 0 : 0 (1/0/0)	230 : 25 : 17 (0.85/0.09/0.06)
Tobacco Smoking (No: Yes: Unknown)	122 : 77 : 16 (0.57/0.36/0.07)	41 : 5 : 1 (0.87/0.11/0.02)	6 : 3 : 1 (0.60/0.30/0.1)	169 : 85 : 18 (0.62/0.31/0.07)
Hypertension (No: Yes: Unknown)	116 : 99 : 0 (0.54/0.46/0)	33 : 14 : 0 (0.70/0.30/0)	4 : 6 : 0 (0.40/0.60/0)	153 : 119 : 0 (0.57/0.43/0)
Diabetes (No: Yes: Unknown)	190 : 25 : 0 (0.88/0.12/0)	46 : 1 : 0 (0.98/0.02/0)	9 : 1 : 0 (0.90/0.10/0)	245 : 27 : 0 (0.90/0.10/0)
Cardiac Disease (No: Yes: Unknown)	200 : 14 : 1 (0.93/0.065/0.005)	41 : 6 : 0 (0.87/0.13/0)	10 : 0 : 0 (1.00/0/0)	251 : 20 : 1 (0.92/0.07/0.004)

* BSA in females is considered normal at approx. 1.6m²

The majority of patients in the cohort were HIV negative (85%); however further analysis revealed that a significant number of IA patients were HIV positive (43%) compared to MA patients (2%) and Caucasian patients (0%). Conversely in terms of smoking, hypertension and diabetes, IA patients self-reported the lowest incidence – with smokers (11%), hypertensives (30%) and diabetics (2%) compared to MA patients – smokers (36%), hypertensives (46%) and diabetics (12%) and Caucasian patients – smokers (30%), hypertensives (60%) and diabetics (10%).

Despite the majority of patients not having any pre-existing cardiac disease (92%), early measures of cardiac function before administration of chemotherapy revealed minor abnormalities in approximately 5% of patients. IA patients had the highest incidence of pre-existing cardiac disease (13%).

Table 31 shows both the type and stage of breast cancer of all the patients in the cohort.

Table 31: Type and Stage of Cancer of Patients in the Prospective Cohort (n=272)

<u>Type of Cancer</u>	<u>Stage of Cancer</u>									
	<u>IA</u>	<u>IB</u>	<u>IIA</u>	<u>IIB</u>	<u>IIIA</u>	<u>IIIB</u>	<u>IIIC</u>	<u>IV</u>	<u>Unknown</u>	<u>Total</u>
DCIS or LCIS	2	0	7	9	7	9	1	0	0	35
IDC	8	2	45	53	30	42	9	2	2	193
ILC	0	0	3	4	2	4	0	1	0	14
Inflammatory	0	0	0	0	0	2	0	0	0	2
Invasive	0	0	3	3	2	2	0	0	0	10
BC NOS*	1	0	1	0	1	3	0	0	0	6
Metastatic	0	0	1	0	2	3	0	5	1	12
Total	11	2	60	69	44	65	10	8	3	272

*BC NOS – Breast Cancer, not otherwise specified

As with the retrospective cohort, the most frequently diagnosed type of cancer was IDC (71% of the entire cohort) with the majority of these patients diagnosed at stage IIB (27% of all IDC patients). Inflammatory breast cancer was diagnosed most infrequently at only 0.7% of the cohort, consistent with the rare presentation of this subtype in the general population (Table 31).

Fifteen patients who were assessed at baseline before the administration of chemotherapy were found to have incidental cardiac findings (Table 32). One patient had an inconclusive LVEF measure.

Of the 15 patients who were found to have some measure of cardiac impairment/dysfunction before the start of chemotherapy – 20% were IA and 80% of

were MA, approximately reflecting the relative distribution of the ethnicities in the total cohort.

Table 32: Incidental cardiac findings derived from routine assessment of baseline cardiac function before commencement of anthracycline-based chemotherapy contrasted with baseline LVEF

<u>Cardiac Incidental Findings</u>	<u>LVEF (%)</u>	<u>Population Group</u>
Rhythm abnormality	52	IA
Mild cardiomegaly	60	IA
Rhythm abnormality	-	MA
Aortic Regurgitation	60	MA
Impaired relaxation indicated by diastolic filling pattern	55	MA
Left ventricular hypertrophy	70	MA
Cardiomegaly with pericardial effusion	54	MA
Left ventricular hypertrophy; elevated left atrial filling pressures; mildly dilated left atrium	60	MA
Wall motion impairment	55	MA
Left ventricular hypertrophy with normal diastolic filling pattern	55	IA
Impaired relaxation of left ventricle	55	MA
Impaired relaxation with elevated left atrial filling pressures	55	MA
Aortic regurgitation; impaired relaxation of left ventricle; early mild pulmonary hypertension	60	MA
Tricuspid regurgitation	60	MA
Left ventricular hypertrophy	55	MA

4.2.3 Statistical Analysis

Patient status was deemed either affected or unaffected with signs or symptoms of ACT. There were 38 affected (14% of the cohort) and 234 unaffected patients at the conclusion of chemotherapy in the prospective cohort. However this clinical status could be considered provisional as unaffected patients may have subclinical damage that may manifest later.

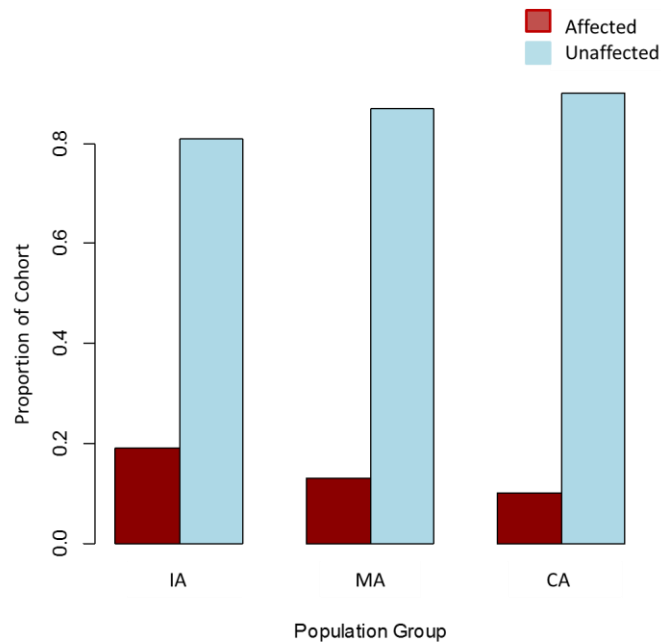


Figure 24: Clinical status (Cardiac impairment/dysfunction: affected vs unaffected) of Patients stratified by Population Group in Prospective Cohort

Clinical status (Cardiac impairment/dysfunction: affected vs unaffected) differed between population groups ($p=0.5116$), where 19% of IA patients were classified as affected compared to 13% of MA and 10% of CA indicating that IAs may have increased sensitivity to ACT (Fig.24).

The score or classifier was established to allow for patients with missing post-treatment LVEF ($n=185$) to be assessed in cardiac terms with 0 being 'normal' and 4 being 'most severely affected'. The differences between the population groups was found to be statistically significant (Chi-square, $p=0.036$).

Table 33: Logistic Regression Co-efficients used to determine Odds Ratios using Clinical-based Covariates

Covariates	Test Statistic	Odds Ratio[^]	p-value
Age	-0.610	0.99 (0.96-1.02)	0.542
Population Group_IA (ref)	-----	-----	-----
Population Group_MA	1.085	1.58 (0.66-3.5)	0.278
Population Group_CA	0.677	2.13 (0.33-41.9)	0.498
Hypertension	-1.184	0.66 (0.33-1.31)	0.236
Diabetes Mellitus	0.450	1.33 (0.44-5.82)	0.653
Pre-existing Cardiac Disease	-0.131	0.92 (0.29-4.08)	0.896
Smoking Status	0.144	1.06 (0.51-2.29)	0.886
Change in LVEF	3.891	1.65 (1.34-2.25)	9.99e ^{-05*}
Total Dose of Anthracycline-Based Chemotherapy	2.400	1.002 (1.0004-1.004)	0.0164*
Change in LVEF and Total Dose	3.769	1.704 (1.36-2.39)	0.000164*

*statistically significant; [^]odds ratios with 95% CI

Gender was not used as a covariate due to all the patients in the prospective cohort being female.

Therefore, based on both the OR and p-values, the change in LVEF and total dose of anthracycline-based chemotherapy significantly increased the likelihood of cardiotoxicity.

The change in LVEF as a predictor of the outcome of ACT, meant that missing LVEF measures needed to be addressed. A simple model was established whereby patients with missing variables (i.e. LVEF post-chemo) could be estimated using the clinical classifier/score developed during this study as well as population group and type of first-line chemotherapy regimen.

Retrospective data (n=402) where two LVEF measures, together with qualitative and quantitative cardiac data, where available, (and scored from 0-4) was used to create a formula that was validated on prospective patients (n=87) with both pre and post-chemo LVEF measures. The formula was then applied to prospective patients (n=185) with only one LVEF measure (pre-chemo) to predict post-chemo LVEF

measures. The difference between actual and predicted post-chemo LVEF measures is illustrated in Figure 25.

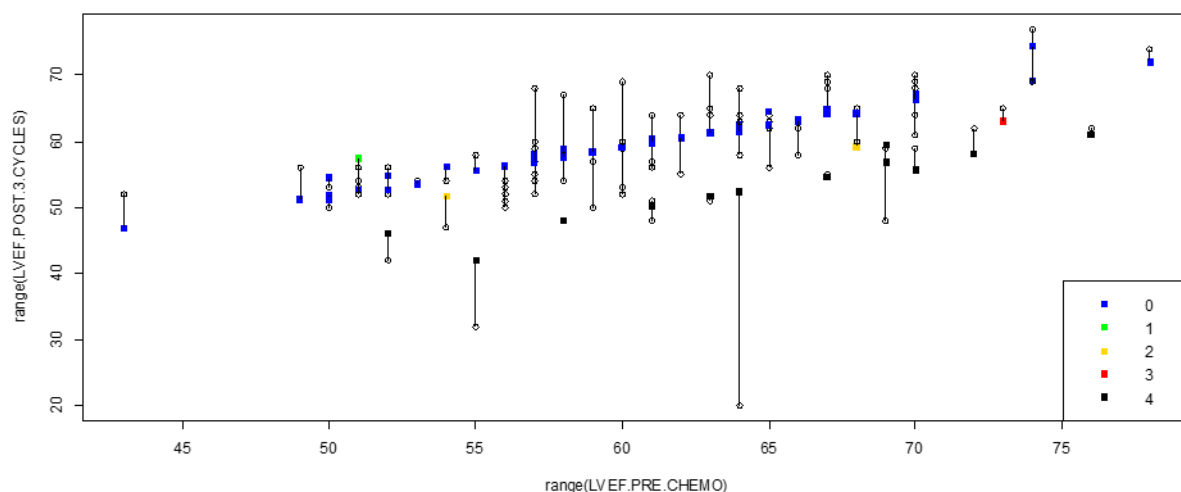


Figure 25: Difference between actual and predicted post-chemo LVEF measures in prospective patients (n=87) – Observed LVEF measures are represented as open circles with predicted values colour-coded according to severity score

A cut-off of 4% was utilized as literature indicates that measurements of LVEF accounting for both inter-operator variability and repeat testing on the same patient are acceptable if in the range of 2-4% ¹³⁴.

Therefore the proposed model indicates an 82% accuracy rate in predicting post-chemo LVEF and can be used for missing variables (LVEF measure) for the rest of the prospective patient cohort.

4.3 Patient Sample

4.3.1 DNA isolation

DNA was isolated from 275 patient samples using the Promega Maxwell® 16 DNA Purification Kit and the salting out method. The Promega Maxwell® 16 DNA Purification Kit had a quick turnaround time but produced low yields of isolated DNA.

DNA was successfully isolated from 274 patients, only one patient had insufficient white blood cells for the isolation of DNA. All patient DNA, after being quantified using spectrophotometry, was stored at -20°C until required for downstream applications (Appendix H, Table 1). The majority of patient samples taken after chemotherapy were stored as buffy coats and isolated as needed.

4.3.1.1 Spectrophotometry for quantitation of DNA

All DNA samples were spectrophotometrically quantified before PCR (Appendix I, Fig. 1) and a total of 86 of the 274 patient DNA samples had concentrations less than 100ng/ul – the optimal concentration for PCR. This was noted in anticipation of potential failure to amplify.

4.3.1.2 Assessment of DNA Integrity

The integrity of the patient DNA was assessed using agarose gel electrophoresis (Fig.26). Low molecular weight DNA or degraded DNA appeared as a smear on the gel whereas intact DNA appeared as a sharp band proximal to the loading well.

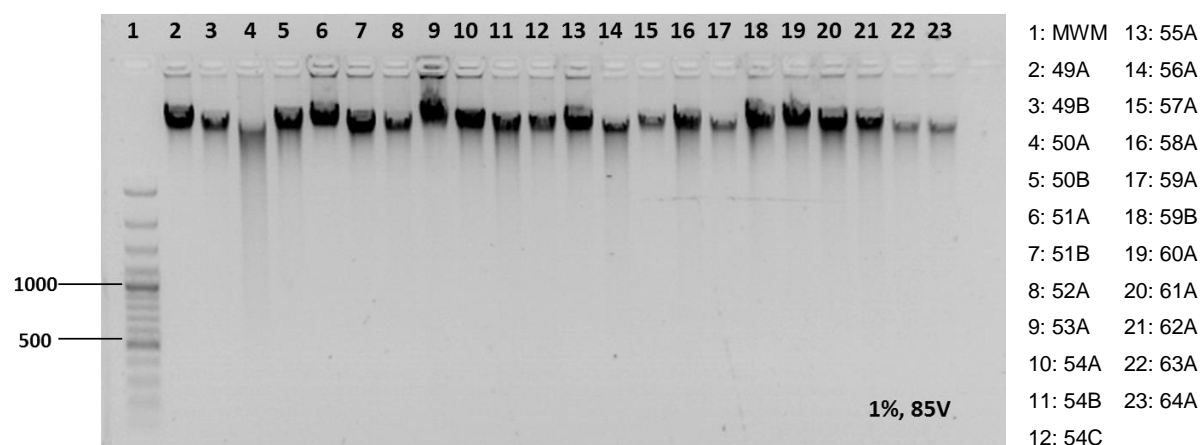


Figure 26: Assessment of DNA Integrity using agarose gel electrophoresis. Patient DNA samples were electrophoresed at 85V for 2 hours on a 1% (w/v) agarose gel (Seakem® LE Agarose, Lonza, USA) stained with SYBR®Safe (Life Technologies, USA) and visualized under UV light. The molecular weight marker (MWM) used was the GeneRuler™ 100bp Plus DNA Ladder (ThermoScientific, USA).

This DNA integrity gel (Fig.26) indicates that the majority of the patient DNA samples are utilisable for downstream applications. However the smeared band for sample 50A (lane 4) and the feint bands for samples 63A and 64A (lanes 22 and 23) may be partially degraded and/or of relatively low concentration. Spectrophotometry shows that sample 50A (lane 4) has a sufficiently high concentration (452.16 ng/ul) therefore is likely to be degraded. Both samples 63A (25.1 ng/ul) and 64A (29.8 ng/ul) have low concentrations which explains the feint band visualized on the gel.

Cumulatively, 22 samples had either very low concentrations and appeared on the gel as feint bands or were partially degraded and appeared on the gel as smears. Nevertheless all 22 samples were amplified using PCR – only six samples exhibiting

partial degradation and two samples with very low concentrations were problematic to amplify and genotype.

4.4 Selected Genes of Interest

Genes of interest were selected using both a pathway-based⁸³ and candidate gene/marker approach based on previous studies^{10,12,27,34,47,106,135-137}.

Initially, 19 SNPs in 15 genes described in Table 7 were selected using a candidate gene approach. However, after approximately 70 patients were genotyped, genotypes appeared to be monomorphic for some of the SNPs, therefore only seven SNPs (*ABCC1* rs246221; *ABCC2* rs17222723; *ABCC2* rs8187710; *HNMT* rs17583889; *NCF4* rs1883112, *RAC2* rs13058338 and *RARG* rs2229774) that showed both heterozygosity and association with the cardiac phenotype were further interrogated for all patient samples (Table 7).

4.4.1 Gene Annotation

The output derived from Appendix J Figure 1, allowed for both the confirmation of the genetic location of the SNP as well as the design of primers found later in the chapter (Appendix J, Figure 1).

4.5 PCR

4.5.1 Optimisation: Singleplex and Multiplex PCR

4.5.1.1 Temperature Gradient

The first PCR optimisation step was establishing a good melting temperature where there would be optimal yield of specific product.

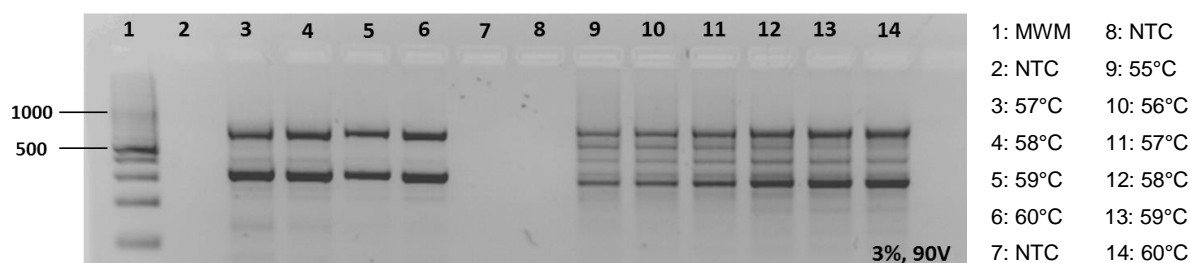


Figure 27: Multiplex optimisation using a temperature gradient and visualized by agarose gel electrophoresis. Control DNA (C18F) was amplified for *ABCC1* rs4148350 (333bp) and *CYBA* rs4673 (680bp) [lanes 2-6] and *ACO1* rs867469 (307bp) and *ABCC2* rs17222723 (761bp) [lanes 8-14] and were electrophoresed at 90V for 2 hours on a 3% (w/v) agarose gel (Seakem® LE Agarose, Lonza, USA); MWM = GeneRuler™ 100bp Plus DNA Ladder

The first multiplex involving the amplification of both *ABCC1* rs4148350 (333bp) and *CYBA* rs4673 (680bp) on a temperature gradient between 57-60°C showed greatest specificity and efficiency at $T_m=60^\circ\text{C}$ (lane 6). Temperatures lower than 60°C resulted in non-specific amplification (lanes 3-5). The second multiplex involving the amplification of both *ACO1* rs867469 (307bp) and *ABCC2* rs17222723 (761bp) showed increased yield of both regions as the temperature increased, however, non-specific amplification persisted (lanes 9-14). There was no amplification in both NTCs (lanes 2 and 8) therefore contamination of the PCRs were unlikely.

4.5.1.2 Magnesium Gradient

The optimisation of the concentration of magnesium to remove any non-specific amplification (Fig.28)

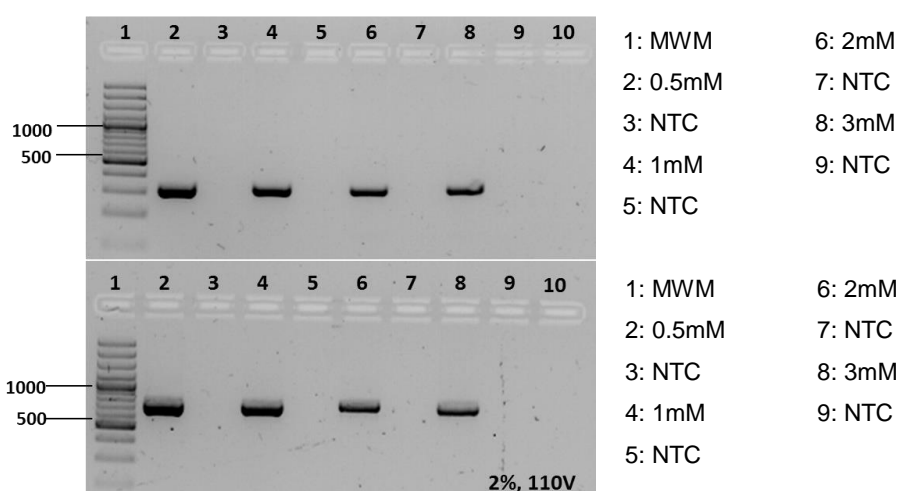


Figure 28: Singleplex optimisation using a magnesium chloride (MgCl_2) gradient and visualized by agarose gel electrophoresis. Control DNA (C18F) was amplified for *ABCC1* rs4148350 (333bp) [top gel] and *NCF4* rs1883112 (725bp) [bottom gel] and were electrophoresed at 110V for 1 hour on a 2% (w/v) agarose gel (Seakem® LE Agarose, Lonza, USA); MWM = GeneRuler™ 100bp Plus DNA Ladder (ThermoScientific, USA); NTC= no template control

Amplification for both *ABCC1* rs4148350 (333bp) [top gel – lanes 2-9] and *NCF4* rs1883112 (725bp) [bottom gel – lanes 2-9] were optimised using an MgCl_2 gradient with concentrations at 0.5mM (lanes 2 & 3), 1mM (lanes 4 & 5), 2mM (lanes 6 & 7) and 3mM (lanes 7 & 8). Amplification for both *ABCC1* rs4148350 (top gel) and *NCF4* rs1883112 (bottom gel) had optimum yield and specificity at an MgCl_2 concentration of 1-2mM (lanes 4 & 6). NTCs for each sample showed no amplification therefore contamination was unlikely.

4.5.1.3 Additives

Alterations to the annealing temperature and $MgCl_2$ concentration did not always guarantee an optimised PCR, therefore, the addition of certain additives were utilized to improve specificity (Fig.29).

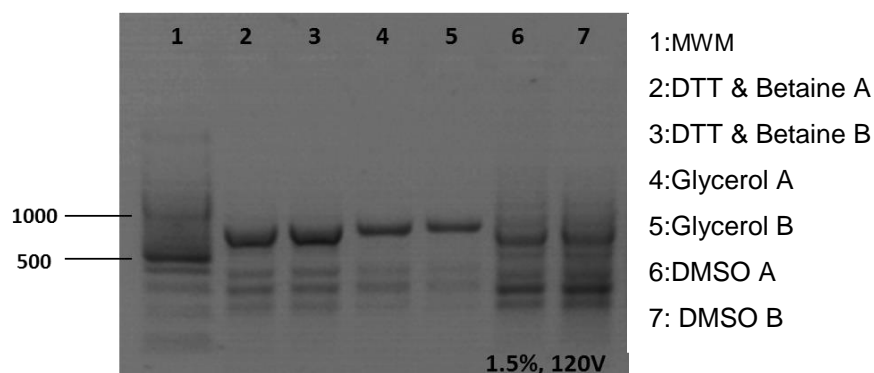


Figure 29: Singleplex optimisation of ABCC2 rs17222723 (761bp) using additives (Dithiothreitol (DTT), Betaine, Glycerol and dimethyl sulfoxide (DMSO)) and visualized by agarose gel electrophoresis. Control DNA (C18F) was amplified for ABCC2 rs17222723 (761bp) in duplicate (A & B) and were electrophoresed at 120V for 40 minutes on a 1.5% (w/v) agarose gel (Seakem® LE Agarose, Lonza, USA); MWM = GeneRuler™ 100bp Plus DNA Ladder (ThermoScientific, USA)

Amplification of ABCC2 rs17222723 (761bp) showed least non-specificity with the addition of Glycerol (Lanes 4 & 5). The addition of both DTT and Betaine (Lanes 2 & 3) was less successful – while the target region was amplified at a sufficiently high yield, there were three non-specific bands. The addition of DMSO (Lanes 6 & 7) was the least successful- there were multiple bands of non-specific amplification with one of the bands having as high a yield as the target region. This challenging PCR required further optimisation whereby non-specific amplification was eliminated.

4.5.1.4 Touchdown PCR

Touchdown PCR allows for the both the amplification of difficult to amplify regions as well as the elimination of non-specific products.

Previously, the addition of glycerol showed a reduction in non-specific amplification however some measure of non-specificity persisted. Touchdown PCR (Fig.30), eliminated non-specific bands and the yield of the target PCR products was high (lanes 8 & 9) compared to the temperature gradient (lanes 3-6) where non-specificity is most apparent at lower temperatures. There was no amplification in either of the two NTCs indicating the absence of contamination.

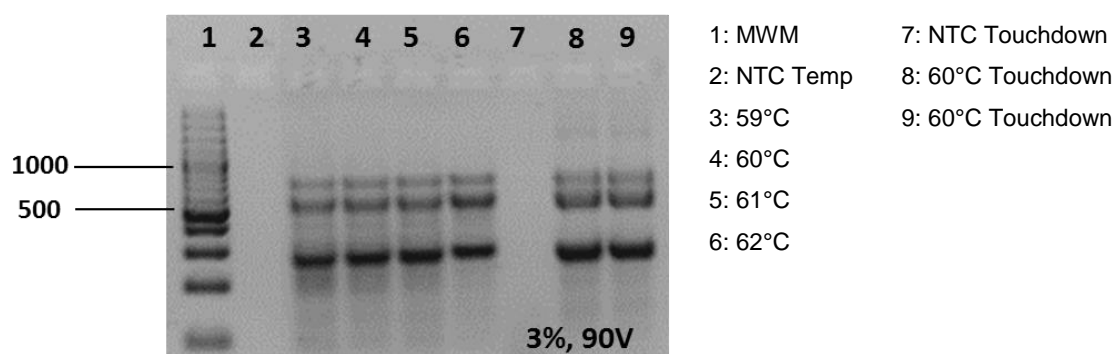


Figure 30: Multiplex optimisation of *ACO1* rs867469 (307bp), *ABCC1* rs246221 (595bp) and *ABCC2* rs17222723 (761bp) using the additive Glycerol and comparing a temperature gradient (59°C-62°C: lanes 3-6) to touchdown PCR performed at 60°C (lanes 7-9) and visualized by agarose gel electrophoresis. Control DNA (C18F) was amplified in a multiplex PCR for *ACO1* rs867469 (307bp), *ABCC1* rs246221 (595bp) and *ABCC2* rs17222723 (761bp) and were electrophoresed at 90V for 2 hours on a 3% (w/v) agarose gel (Seakem® LE Agarose, Lonza, USA); MWM = GeneRuler™ 100bp Plus DNA Ladder (ThermoScientific, USA); NTC = no template control

While the annealing temperature of 62°C for a standard PCR (lane 6) also showed reduced non-specific amplification, the intensity of the bands which represent amplified target regions was greater in the touchdown PCR (lanes 8-9) indicating greater yield of product and therefore greater overall efficiency. Hence the amplification of these regions was optimised with the addition of glycerol and utilizing a touchdown PCR.

4.5.2 Optimised Multiplex PCRs

All samples (lanes 2-16) amplified specifically for both target regions – *HNMT* rs17583889 (325bp) and *ABCC2* rs8187710. There was no amplification in the NTC therefore contamination was unlikely (Fig.31).

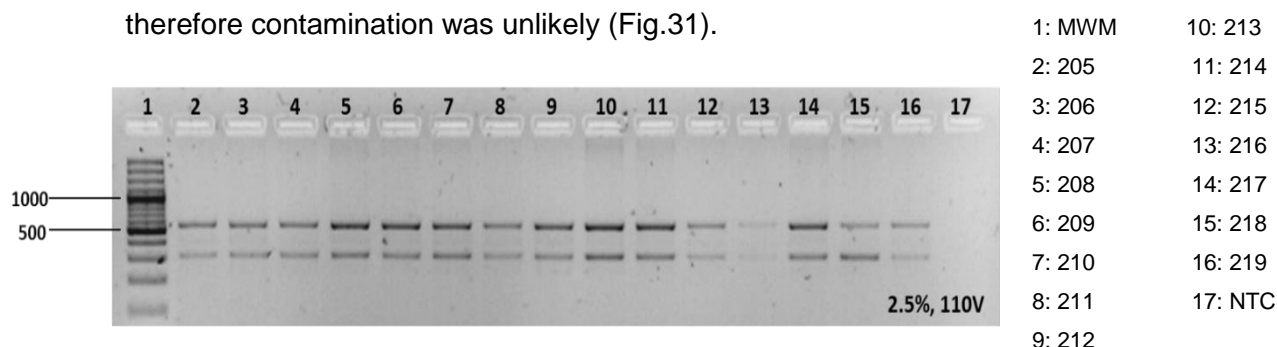


Figure 31: Optimised multiplex PCR showing the amplification of *HNMT* rs17583889 (325bp) and *ABCC2* rs8187710 (572bp) performed at 55°C and visualized by agarose gel electrophoresis. Patient DNA was amplified in a multiplex PCR for *HNMT* rs17583889 (325bp) and *ABCC2* rs8187710 (572bp) and were electrophoresed at 110V for 1.5 hours on a 2.5% (w/v) agarose gel (Seakem® LE Agarose, Lonza, USA); MWM = GeneRuler™ 100bp Plus DNA Ladder (ThermoScientific, USA); NTC = no template control

All samples (lanes 2-16) amplified specifically and efficiently for both target regions – *RAC2* rs13058338 (341bp) and *NCF4* rs1883112 (725bp). There was no amplification in the NTC therefore contamination was unlikely (Fig.32).

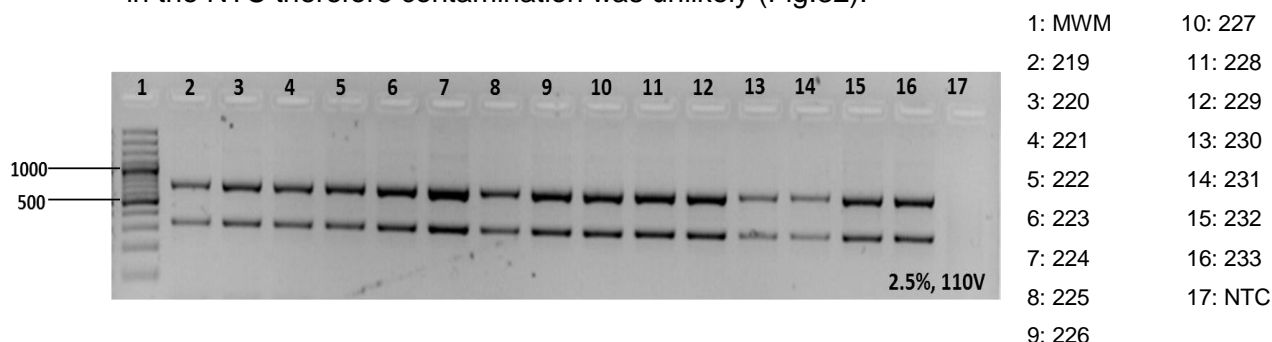


Figure 32: Optimised multiplex PCR showing the amplification of *RAC2* rs13058338 (341bp) and *NCF4* rs1883112 (725bp) performed at 56°C and visualized by agarose gel electrophoresis. Patient DNA was amplified in a multiplex PCR for *RAC2* rs13058338 (341bp) and *NCF4* rs1883112 (725bp) and were electrophoresed at 110V for 1.5 hours on a 2.5% (w/v) agarose gel (Seakem® LE Agarose, Lonza, USA); MWM = GeneRuler™ 100bp Plus DNA Ladder (ThermoScientific, USA); NTC = no template control

All samples (lanes 2-16) amplified specifically and efficiently for both target regions – *ABCC1* rs246221 (595bp) and *ABCC2* rs17222723 (761bp). There was no amplification in the NTC therefore contamination was unlikely (Fig.33).

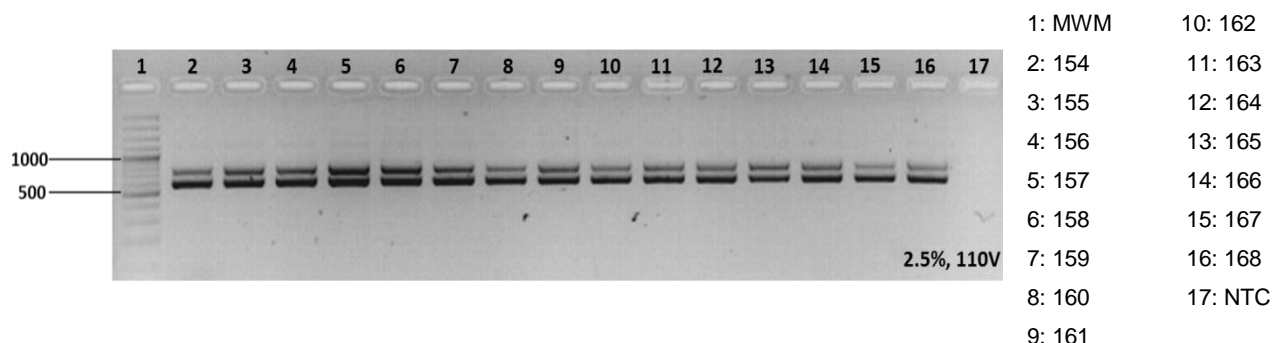


Figure 33: Optimised multiplex PCR showing the amplification of *ABCC1* rs246221 (595bp) and *ABCC2* rs17222723 (761bp) performed using a Touchdown PCR at 60°C with the addition of glycerol and visualized by agarose gel electrophoresis. Patient DNA was amplified in a multiplex PCR for *ABCC1* rs246221 (595bp) and *ABCC2* rs17222723 (761bp) and were electrophoresed at 110V for 1.5 hours on a 2.5% (w/v) agarose gel (Seakem® LE Agarose, Lonza, USA); MWM = GeneRuler™ 100bp Plus DNA Ladder (ThermoScientific, USA); NTC = no template control

4.6 Genotyping

4.6.1 Optimisation of the SNaPshot® Multiplex System

Multiplex PCRs were optimised for genotyping using the SNaPshot® System (ThermoFisherScientific, Applied Biosystems, USA). Patient ACT 107.1NOM was genotyped for both *HNMT* rs17583889 and *ABCC2* rs8187710 and found to be a C/C homozygote and a G/A heterozygote respectively (Fig.34).

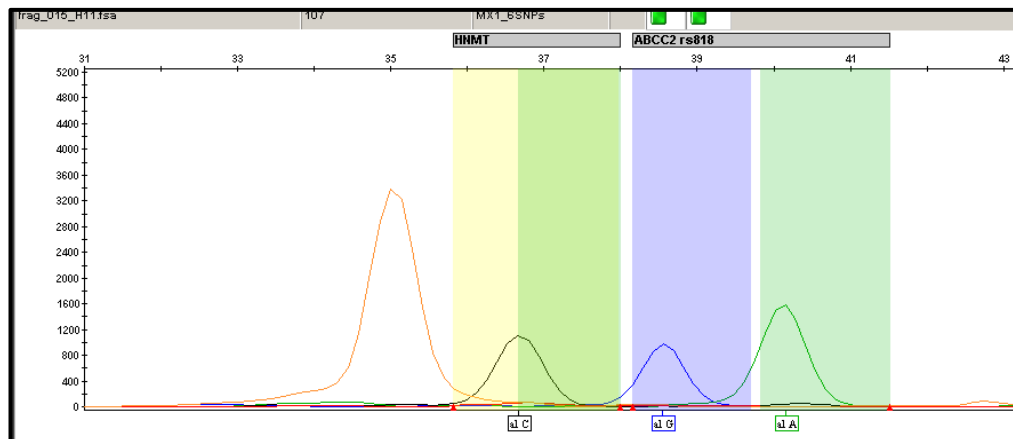


Figure 34: Electropherogram illustrating determination of genotypes for both *HNMT* rs17583889 (black peak C/C) and *ABCC2* rs8187710 (blue and green peaks G/A) derived from GeneMapper (version 4.1 using the ABI3130xl Genetic Analyzer (Applied Biosystems, USA). The orange peak indicates the GeneScan™ 120 LIZ® Size Standard (35 nt).

Patient ACT 257.1ANN was genotyped for both *NCF4* rs1883112 and *RAC2* rs13058338 and found to be a G/A heterozygote and an A/T heterozygote respectively (Fig.35).

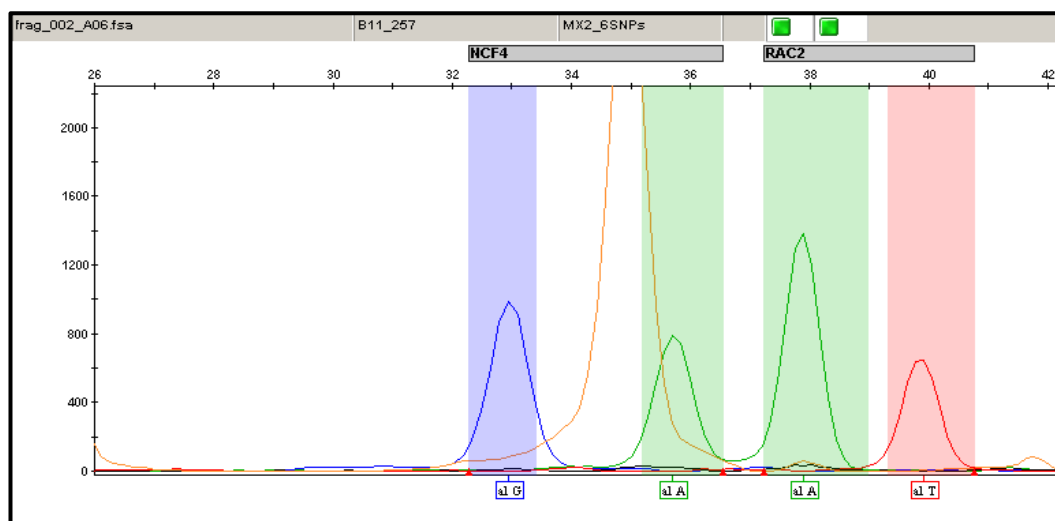


Figure 35: Electropherogram illustrating determination of genotypes for both *NCF4* rs1883112 (blue and green peaks G/A) and *RAC2* rs13058338 (green and red peaks A/T) derived from GeneMapper (version 4.1 using the ABI3130xl Genetic Analyzer (Applied Biosystems, USA). The orange peak indicates the GeneScan™ 120 LIZ® Size Standard (35 nt)

Patient ACT 200.1KAR was genotyped for both *ABCC1* rs246221 and *ABCC2* rs17222723 and found to be a G/A heterozygote and an A/T heterozygote respectively (Fig.36).

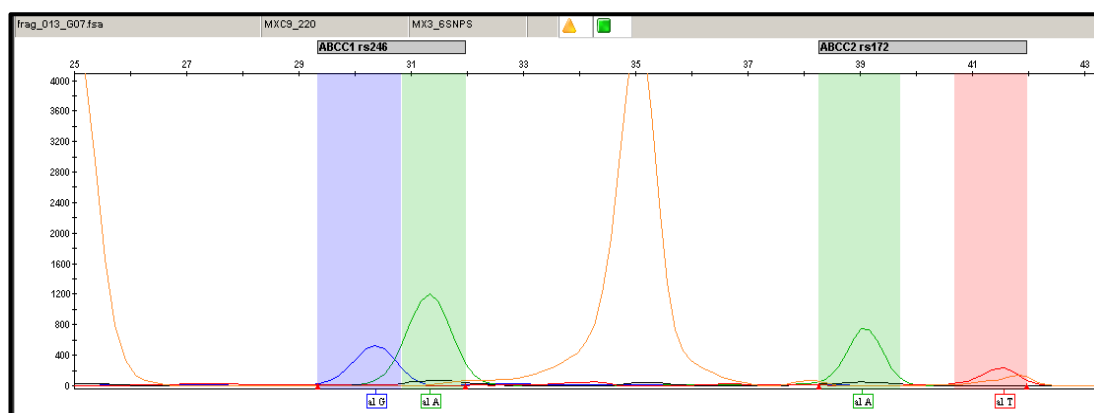


Figure 36: Electropherogram illustrating determination of genotypes for both *ABCC1* rs246221 (blue and green peaks G/A) and *ABCC2* rs17222723 (green and red peaks A/T) derived from GeneMapper (version 4.1 using the ABI3130xl Genetic Analyzer (Applied Biosystems, USA). The orange peak indicates the GeneScan™ 120 LIZ® Size Standard (35 nt)

4.6.2 Optimisation of the TaqMan™ SNP Genotyping Assay

The concentration and integrity of the control DNA was adequate (124ng/ul) for the optimisation of the assay (Appendix H, Fig. 2). The assay was optimised by the utilization of varying concentrations of DNA to delineate the optimal volume of DNA needed for a distinct genotype to be called.

Control DNA Sample (C35F) was genotyped as a heterozygote (A/G) indicated by the blue arrow in Figure 37. The optimal volume was determined to be 2-3ul at a concentration of 100ng/ul.

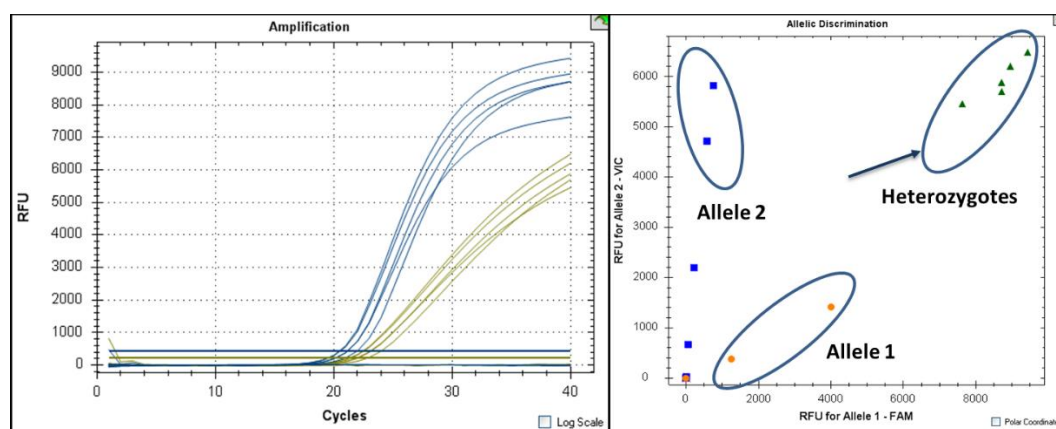


Figure 37: Quantification & Allelic Discrimination Plots generated from the CFX™ Real-Time PCR Detection System together with the TaqMan™ Genotyper Software

4.6.3 Genotyping of patient samples

Nineteen SNPs in fifteen genes, described in Table 7, were selected using a candidate gene approach. However, only seven SNPs were interrogated for all patient samples: *ABCC1* rs246221; *ABCC2* rs17222723; *ABCC2* rs8187710; *HNMT* rs17583889; *NCF4* rs1883112, *RAC2* rs13058338 and *RARG* rs2229774.

Genotypes were derived for the following number of patients: *ABCC1* rs246221 (n=270), *ABCC2* rs17222723 (n=260), *ABCC2* rs8187710 (n=267), *HNMT* rs17583889 (n=250), *NCF4* rs1883112 (n=259), *RAC2* rs13058338 (n=271) and *RARG* rs2229774 (n=273).

4.6.4 Validation Sequencing

Genotyping results were validated using Sanger sequencing and 5% of the entire selection of seven SNPs were sequenced. Statistical significance is achieved when $p < 0.05$ therefore 5% was used as a threshold for validation sequencing.

Electropherograms derived from the genetic analyser were assessed for accuracy of sequencing and to validate variants found when carrying out SNP genotyping (Fig. 38).

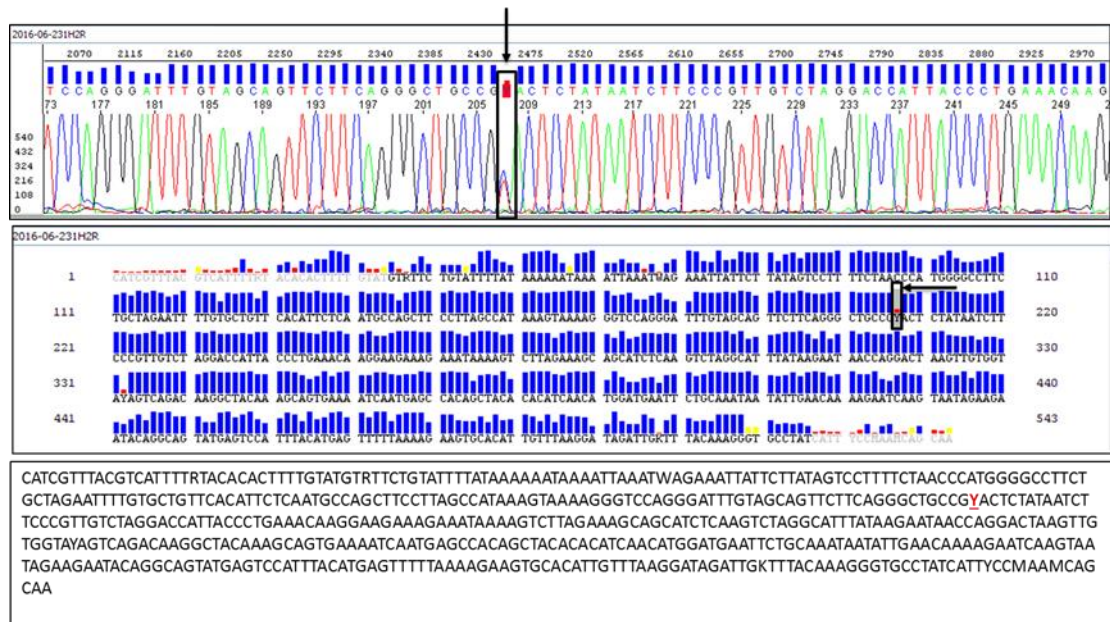


Figure 38: Representation of electropherogram (top panel), sequence coverage (middle panel) and sequence (bottom panel) derived from Sanger sequencing conducted to validate SNaPshot® genotyping assay results. Patient 249.1JAN's genotyping results obtained from the SNaPshot® genotyping assay was validated using Sanger/Direct Cycle sequencing. The arrow on the top and middle panel show the location of the SNP for *ABCC2* rs8187710 (572bp), Y indicates a heterozygote (C/T)

The genotyping primer designed for the SNaPshot® Assay for the detection of the *ABCC2* rs8187710 variant was in the forward direction with expected genotypes of GG/GA/AA however since the reverse PCR primer was found to be optimal for sequencing, the resulting electropherogram trace and sequence (Fig.38) was reverse complemented. Therefore Patient 249.1JAN's genotype according to SNaPshot® was G/A which translates to C/T which was obtained by confirmatory sequencing.

Each region of amplification and SNP was confirmed to be correct by the utilisation of the nucleotide basic local alignment search tool (BLAST) ¹³⁸.

The context sequence (Fig.39) was correlated to the reverse complement sequence that was already amplified (Fig.38).



Figure 39: Representation of nucleotide blast results for *ABCC2* rs8187710 validating both the target gene and corresponding SNP

4.7 Statistical Analysis

4.7.1 Genotype and Allele frequencies

Genotype counts and minor allele frequencies for each of the seven SNPs are listed in Table 34.

Table 34: Distribution of genotypes and minor allele frequencies for seven SNPs focusing on differences in population groups

<u>Gene Variants</u>	<u>**Genotypic Distribution</u>					<u>Minor Allele Frequencies</u>					<u>P value*</u>	<u>P value*</u>	<u>P value*</u>
	Lit ⁸¹	All	IA	MA	Caucasian	Lit ⁸¹	All	IA	MA	Caucasian			
ABCC1 rs246221	934/1013/557	80/123/67	6/19/22	68/100/45	6/4/0	0.42	0.48	0.67	0.45	0.2	0.0737	<0.0001* 0.6951 0.1275	0.0009*
ABCC2 rs17222723	2321/179/4	201/54/5	34/11/1	158/42/4	9/1/0	0.04	0.12	0.14	0.12	0.05	<0.0001*	<0.0001* 0.9566	0.0352*
ABCC2 rs8187710	2181/306/17	153/98/16	19/23/4	125/74/12	9/1/0	0.07	0.24	0.34	0.23	0.05	<0.0001*	<0.0001* 0.9508	0.0285*
HNMT rs17583889	1922/516/66	206/29/15	41/0/2	157/28/13	8/1/0	0.13	0.12	0.05	0.14	0.06	0.7682	0.0741 0.9241 0.6474	0.0152*
NCF4 rs1883112	938/1059/507	124/91/44	30/14/1	91/73/40	3/4/3	0.41	0.35	0.18	0.38	0.5	0.0106*	<0.0001* 0.3068 0.7378	0.0009*
RAC2 rs13058338	1794/91/619	200/65/6	42/5/0	152/57/5	6/3/1	0.16	0.14	0.05	0.16	0.25	0.5561	0.0192* 0.9831 0.5488	0.0113*
RARG rs2229774	2101/367/36	217/49/5	40/7/0	168/41/5	9/1/0	0.09	0.11	0.07	0.12	0.05	0.4798	0.9043 0.0921 0.8379	0.0226*

= p-value derived from a chi-square test with a 95% confidence interval where the MAFs of all the SNPs under investigation were compared to the MAFs of these SNPs reported in the literature; # = p values derived from a Chi-square test with 95% confidence interval where the MAFs of each population group was compared to literature; += p values after 2-way ANOVA with 95% confidence interval to determine whether population group MAFs are significantly different to each other

**Genotypic Distribution: Ratios indicate homozygous major/ heterozygous/ homozygous minor allele

Table 34 shows that the *ABCC2* rs17222723, *ABCC2* rs8187710 and *NCF4* rs1883112 polymorphisms had minor allele frequencies (MAF) in our patient cohort that were statistically different from literature. The MAFs of all the SNPs were statistically different when compared between the three population groups with the MAFs for IAs for the following SNPs: *ABCC1* rs246221, *ABCC2* rs17222723, *ABCC2* rs8187710, *NCF4* rs1883112 and *RAC2* rs13058338 all being significantly different from the literature. Only *ABCC2* rs17222723 and *ABCC2* rs8187710 in the MA population were statistically significant from literature with none of the variants in the CA cohort being statistically different to literature.

Hardy-Weinberg calculations indicated that both *HNMT* rs17583889 and *NCF4* rs1883112 are not in Hardy-Weinberg equilibrium whereas all the other SNPs that were included in the final analysis were in HWE (Table 35).

Table 35: Patient population allele frequencies and Pearson's Chi-Square test for HWE

Gene Variant	Alleles	Allele Frequency	HWE χ^2 value	p-value*
<i>ABCC1</i> rs246221	A	0.52	2.61	0.12
	G	0.48		
<i>ABCC2</i> rs17222723	A	0.88	1.01	0.4
	T	0.12		
<i>ABCC2</i> rs8187710	G	0.76	0.01	1
	A	0.24		
<i>HNMT</i> rs17583889	C	0.88	36.86	9.99e ⁻⁰⁵
	A	0.12		
<i>NCF4</i> rs1883112	G	0.65	12.71	4e ⁻⁰⁴
	A	0.35		
<i>RAC2</i> rs13058338	A	0.86	0.03	1
	T	0.14		
<i>RARG</i> rs2229774	G	0.89	1.25	0.34
	A	0.11		

*simulated p-value based on 1000 replicates using R

Both the D' and r^2 values were used to interpret LD – *ABCC2* rs8187710 and *ABCC2* rs17222723 indicate that there was very little to no recombination between markers ($D'=0.954$) and that they were in fairly strong LD ($r^2=0.414$). The other variants analysed showed some degree of recombination and very weak LD (Table 36).

Table 36: Testing for LD of genetic variants using R ¹⁰¹ and the SHESIS Program
132

Pairwise LD			LD Test			
Variant 1	Variant 2	D'	X ²	p-value	N	r ²
rs17583889	rs8187710	0.451	4.216	0.04*	248	0.009
rs17583889	rs1883112	0.129	1.970	0.16	236	0.004
rs17583889	rs13058338	0.318	1.101	0.29	247	0.002
rs17583889	rs246221	0.143	1.192	0.27	246	0.002
rs17583889	rs17222723	0.152	0.210	0.65	240	0.000
rs17583889	rs2229774	0.124	7.125	0.008*	248	0.015
rs8187710	rs1883112	0.310	8.066	0.005*	251	0.016
rs8187710	rs13058338	0.180	0.930	0.34	263	0.002
rs8187710	rs246221	0.160	4.746	0.03*	263	0.009
rs8187710	rs17222723	0.954	212.547	0	257	0.414
rs8187710	rs2229774	0.0180	0.007	0.93	265	0.000
rs1883112	rs13058338	0.106	1.870	0.17	257	0.004
rs1883112	rs246221	0.121	3.574	0.05*	255	0.007
rs1883112	rs17222723	0.151	0.848	0.36	245	0.002
rs1883112	rs2229774	0.176	3.740	0.05*	257	0.007
rs13058338	rs246221	0.004	0.002	0.97	267	0.000
rs13058338	rs17222723	0.026	0.307	0.58	257	0.001
rs13058338	rs2229774	0.040	0.620	0.43	269	0.001
rs246221	rs17222723	0.225	4.170	0.04*	259	0.008
rs246221	rs2229774	0.116	0.959	0.33	269	0.002
rs17222723	rs2229774	0.011	0.052	0.82	259	0.000

All seven SNPs were utilised to generate both an LD plot and haplotype analysis (Fig.40). Figure 40 shows that cumulatively all the SNPs are not in strong LD and not inherited as a single haplotype.

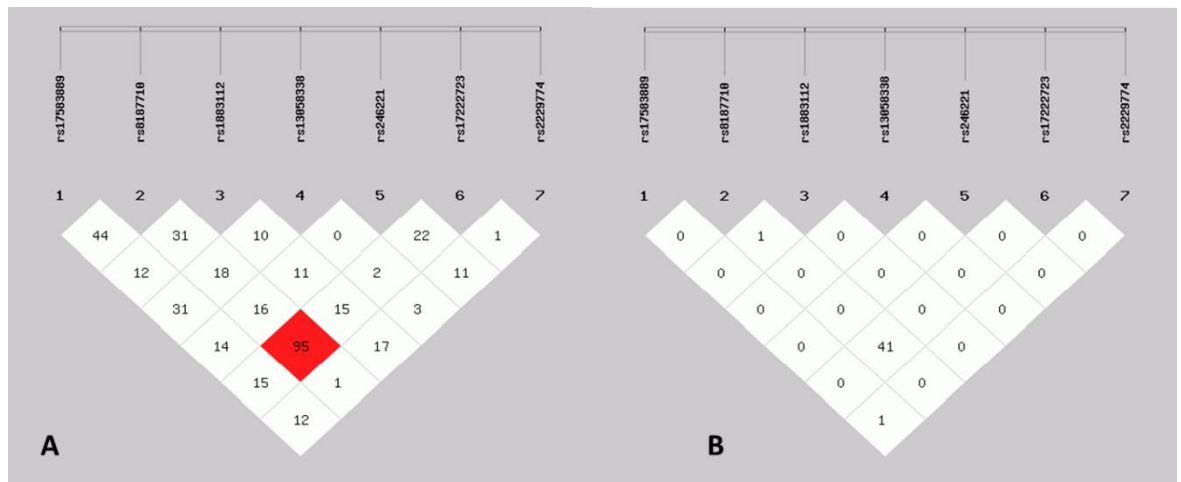


Figure 40: LD plot (A) and Haplotype analysis (B) generated by the SHEsis program ¹³² using all seven SNPs

4.7.2 Association testing

Patient status was significantly associated with *RARG* rs2229774 ($p=0.049$, Chi-square test; $p=0.05$, Fisher's exact test). No association was found between patient status and other variants - *ABCC1* rs246221 ($p=0.56$), *ABCC2* rs17222723 ($p=0.95$), *ABCC2* rs8187710 ($p=0.44$), *HNMT* rs17583889 ($p=0.18$), *NCF4* rs1883112 ($p=0.28$) and *RAC2* rs13058338 ($p=0.53$).

The more accurate logistic regression was used to determine whether any of the variants predicted clinical status. As previously mentioned, logistic regression was found to be better suited to our needs due to its ability to model the determinants of and predict the likelihood of an outcome compared to descriptive correlation for which chi-square tests are most apt. None of the SNPs showed any significant association with patient clinical status (Table 37).

Severity score was significantly associated with *ABCC2* rs8187710 ($p=0.004$, Chi-square test) and *ABCC2* rs17222723 ($p=0.006$, Chi-square test). However no association was found between patient severity score and other variants - *ABCC1* rs246221 ($p=0.21$), *HNMT* rs17583889 ($p=0.72$), *NCF4* rs1883112 ($p=0.07$) *RAC2* rs13058338 ($p=0.89$) and *RARG* rs2229774 ($p=0.66$).

Logistic regression models were computed firstly for genotype related to the outcome of status and then genotype together with total dose related to the outcome of clinical status.

Table 37: Logistic Regression Co-efficients used to determine Odds Ratios using Genotype to Predict Outcome

Covariates	Test Statistic	Odds Ratio^	p-value
<i>HNMT</i> rs17583889 C/A	-0.014	2.19e ⁻⁰⁷⁺	0.989
<i>HNMT</i> rs17583889 C/C	-0.015	1.17e ⁻⁰⁷⁺	0.988
<i>ABCC2</i> rs8187710 G/A	1.055	1.98 (0.49-6.65)	0.291
<i>ABCC2</i> rs8187710 G/G	1.261	2.20 (0.57-7.05)	0.207
<i>NCF4</i> rs1883112 G/A	0.671	1.46 (0.46-4.35)	0.502
<i>NCF4</i> rs1883112 G/G	-0.572	0.75 (0.26-1.9)	0.568
<i>RAC2</i> rs13058338 A/T	-1.105	0.65 (0.31-1.43)	0.269
<i>RAC2</i> rs13058338 T/T	-0.286	0.73 (0.11-14.23)	0.775
<i>ABCC1</i> rs246221 A/G	-1.037	0.64 (0.26-1.45)	0.300
<i>ABCC1</i> rs246221 G/G	-0.368	0.83 (0.31-2.26)	0.713
<i>ABCC2</i> rs17222723 A/T	-0.235	0.90 (0.40-2.25)	0.814
<i>ABCC2</i> rs17222723 T/T	-0.217	0.78 (0.12-15.34)	0.828
<i>RARG</i> rs2229774 G/A	-0.012	1.5e ⁻⁰⁶⁺	0.990
<i>RARG</i> rs2229774 G/G	-0.014	3.2e ⁻⁰⁷⁺	0.989

^odds ratios with 95% CI; +sample size too small to compute 95% CI

Odds ratios indicate that despite the genotype, total dose had a statistically significant contribution to the outcome of clinical status (Table 38).

Table 38: Logistic Regression Co-efficients used to determine Odds Ratios using Genotype and Dose Covariates

Covariates	Test Statistic	Odds Ratio [^]	p-value
<i>HNMT</i> rs17583889 and Total Dose	2.430	1.002 (1.0006-1.004)	0.015*
<i>ABCC2</i> rs8187710 and Total Dose	2.553	1.002 (1.0005-1.004)	0.011*
<i>NCF4</i> rs1883112 and Total Dose	2.163	1.002 (1.0003-1.004)	0.031*
<i>RAC2</i> rs13058338 and Total Dose	2.363	1.002 (1.0004-1.004)	0.018*
<i>ABCC1</i> rs246221 and Total Dose	2.355	1.002 (1.0004-1.004)	0.019*
<i>ABCC2</i> rs17222723 and Total Dose	2.433	1.002 (1.0004-1.004)	0.015*
<i>RARG</i> rs2229774 and Total Dose	2.247	1.002 (1.0003-1.004)	0.025*

*statistically significant; [^]odds ratios with 95% CI

The genetic models of variants was examined in the context of their allelic frequency and contribution to outcome (affected cardiac status due to ACT) in Table 39.

Table 39: Overview of genetic variants, their genetic model and contribution to phenotype

Gene Variants	Minor Allele Frequency		p-value [#]	Covariates	Odds Ratio	p-value [^]	Type of Genetic Model
	Lit	Study					
HNMT rs17583889	0.13	0.12	0.7682	HNMT rs17583889 C/A	2.19e ⁻⁰⁷	0.989	Multifactorial/ Polygenic
				HNMT rs17583889 C/C	1.17e ⁻⁰⁷	0.988	
ABCC2 rs8187710	0.07	0.24	<0.0001*	ABCC2 rs8187710 G/A	1.98	0.291	Multifactorial/ Polygenic
				ABCC2 rs8187710 G/G	2.20	0.207	
NCF4 rs1883112	0.41	0.35	0.0106*	NCF4 rs1883112 G/A	1.46	0.502	Multifactorial/ Polygenic
				NCF4 rs1883112 G/G	0.75	0.568	
RAC2 rs13058338	0.16	0.14	0.5561	RAC2 rs13058338 A/T	0.65	0.269	Multifactorial/ Polygenic
				RAC2 rs13058338 T/T	0.73	0.775	
ABCC1 rs246221	0.42	0.48	0.0737	ABCC1 rs246221 A/G	0.64	0.300	Multifactorial/ Polygenic
				ABCC1 rs246221 G/G	0.83	0.713	
ABCC2 rs17222723	0.04	0.12	<0.0001*	ABCC2 rs17222723 A/T	0.90	0.814	Multifactorial/ Polygenic
				ABCC2 rs17222723 T/T	0.78	0.828	
RARG rs2229774	0.09	0.11	0.4798	RARG rs2229774 G/A	1.5e ⁻⁰⁶	0.990	Multifactorial/ Polygenic
				RARG rs2229774 G/G	3.2e ⁻⁰⁷	0.989	

Chapter 5: Discussion

5.1 Summary of Main Findings

“Anthracycline-induced cardiotoxicity, while dose-dependent, may be attributed to inherent genetic differences in treated patients” was the thesis statement specified at the beginning of the study. This study sought to discover differences between treated patients to allow for the minimisation of cardiotoxicity due to anthracycline-based chemotherapy.

The risk of ACT has been estimated, according to GLOBOCAN, at 10-26% ¹⁵. The retrospective (79/402=19.7%) and prospective cohorts (38/272=14%) in the present study showed that approximately 17.35% of patients here in the Western Cape were likely affected with ACT. This incidence of ACT may be an underestimation since some patients with initial subclinical damage may later progress to irreversible cardiac damage and subsequent symptoms ¹⁷, and perhaps not be related back to their chemotherapy. The extent to which different population groups were affected with ACT seemed distinguishable – IAs had the highest overall incidence of ACT (20% and 19%), MA patients had a relatively lower incidence (19.8% and 13%) and CA patients had the lowest overall incidence of ACT (16.7% and 10%), in both the retrospective and prospective cohorts, respectively. Therefore, patient risk with regard to clinical co-morbidities were investigated.

Clinical co-morbidities such as hypertension, diabetes, cardiac disease and smoking have previously been associated with increased risk of developing ACT ^{10,24,48}. In the retrospective and prospective cohorts, the incidence of hypertension was the highest (40% and 43%, respectively) with pre-existing cardiac disease (5% and 7%, respectively) having the lowest incidence. These clinical co-morbidities were stratified into population group in both the retrospective and prospective cohorts; MA patients had the highest overall risk of developing ACT due to clinical co-morbidities with IA patients having a fairly low to low risk. Therefore, these risk factors were not predictive of the outcome of ACT.

Previously, the type of anthracycline-based chemotherapy and dose were reported to be associated with ACT and therefore investigated in the Cape Town cohort ^{24,25,46,51}. Patients in both cohorts were analysed for type and dose of anthracycline and it was found that in the retrospective cohort, CA patients were most likely to be prescribed doxorubicin and at higher median doses compared to their MA counterparts whereas in the prospective cohort, both MA and IA patients were prescribed doxorubicin at

higher median doses compared to their CA counterparts. Logistic regression showed that both type and dose of anthracyclines were significantly associated with ACT for both the retrospective and prospective cohorts.

The motivation for the investigation of genetic variants associated with susceptibility/resistance to ACT was for a range of reasons which included: that ACT was evident at different incidences in the three local populations of cancer patients receiving anthracycline-based chemotherapy; (ii) previous literature indicating pharmacogenetic association with ACT ; and (iii) evidence of IA women being more susceptible to cardiotoxicity due to ethnically variant polymorphisms pertinent to anthracycline metabolism ^{6-8,139,140}.

Prospectively recruited patients (n=272) were genotyped for seven SNPs: *ABCC1* rs246221; *ABCC2* rs17222723; *ABCC2* rs8187710; *HNMT* rs17583889; *NCF4* rs1883112; *RAC2* rs13058338 and *RARG* rs2229774. A simple illustration of genetic diversity between the three local populations was evident from statistically significant differences of the MAFs for these markers when compared to literature – while the local CA patients showed no significant differences, the MA patients had 2 SNPs (*ABCC2* rs17222723 and *ABCC2* rs8187710) and the IA patients had 5 SNPs (*ABCC1* rs246221, *ABCC2* rs17222723, *ABCC2* rs8187710, *NCF4* rs1883112 and *RAC2* rs13058338) with significantly different allele frequencies compared to that reported (generally for CA) in the literature. Furthermore, SNPs interrogated in the patient population had shown previous association to ACT however the only SNP that showed an association with patient clinical ACT status was *RARG* rs2229774, which corroborated an earlier Canadian GWAS investigating ACT in childhood cancer ⁷. This significance however was lost when the more robust logistic regression to predict outcome was applied.

5.2 Retrospective Cohort Analysis

Data analysis was performed on the entire cohort (n=402) and stratified into the local population groups. The recruitment sites, two government hospitals in Cape Town, South Africa, were attended by predominantly individuals of MA and to a lesser degree, IAs and CA individuals. MA refers to an admixed population of origins as diverse as European (including Dutch, French, German and English), Asian and indigenous Khoisan, whereas IA refers to a population group of native or indigenous Africans with various ethnicities such as Zulu and Xhosa, and CA refers to a population group of European origin, mentioned earlier ¹⁴¹. Not only does population stratification improve accuracy for larger scale association studies, but it may also aid

in delineating extreme phenotypes due to the unique genotypes of the constituent local populations ^{6,142}.

There were only seven males in this cohort – this was due to the fact that they are only rarely affected with breast cancer, the prevalence is reported to be approximately 1% in the literature ^{14,34}.

Additional demographic factors such as age and BSA were analysed. While the overall median age at diagnosis for this cohort was 51 years, which was in agreement with South African Census statistics ¹⁴³, this is comparatively younger than the published worldwide statistics of 65 years and older ¹⁵. The IA cohort had a median age of only 44 years. Young age at diagnosis in the IA patient cohort may be attributed to a range of factors which is outside of the scope of this research but may include risk factors such as delayed onset of childbirth and genetic influences where hereditary factors such as *BRCA1/2* mutations (amongst those in other genes) may be a contributing factor ^{144,145}. Similarly, BSA and by extension, body mass index (BMI), were found to be consistently higher than normal especially in the MA and IA sub-cohorts which may be attributed to two possibilities – i) ethnic differences in body form for local populations that do not correlate with worldwide standards, therefore making a universal cut-off value inapplicable, and/or ii) the possibility of the adoption of an unhealthier lifestyle due to e.g. urbanisation and modernization ^{146,147}.

Clinical co-morbidities such as hypertension, diabetes, cardiac disease and smoking, shown to increase the risk of developing ACT previously, were also investigated. Logistic regression models based on our retrospective data did not substantiate these findings ^{24,26,36,148}. Nevertheless, both MA and IA patients had higher rates of these co-morbidities compared to their CA counterparts which may indicate shared risk factors (including genetic) in these two groups (i.e. MA and IA) resulting in greater susceptibility to certain lifestyle-induced diseases, or perhaps due to inadequate access to healthcare due to socioeconomic circumstances.

Risk factors such as type and dose of anthracycline were also assessed. The anthracyclines, doxorubicin and epirubicin, have different safety profiles. Due to a shorter terminal half-life and more rapid total body clearance ^{22,26,30}, epirubicin is considered “safer” and given at increased doses. However, our analysis shows that neither of these agents are entirely safe – 138 patients were treated with doxorubicin and 37 were affected (27%) compared to 264 patients treated with epirubicin, 42 of whom were affected (16%). This relative (minimal) improvement (i.e. 16% versus 27%) in ACT-affectation status warrants the investigation of alternatives such as

liposomal-encapsulated anthracyclines or the parallel provision of a cardio-protectant
75,76,98.

Patients' clinical status in terms of ACT was either 'affected' or 'unaffected' based on numerous factors which included LVEF decline. It emerged that IAs at 20% may be marginally more susceptible compared to MA at 19.8%, with Caucasians at 16.7% being the relatively least susceptible. Previous evidence of ethnically variant polymorphisms that influence doxorubicin pharmacokinetics and pharmacodynamics suggest that population-based differences may be expected ^{6,139,140}.

Although relied on heavily in this study, LVEF, as a measure of cardiac function may prove to be unreliable, whereby 56/402 patients (14%) had significant decreases in LVEF ($\geq 10\%$) yet only seven out of the 56 patients exhibited clinical signs and symptoms of cardiac dysfunction. Conversely, 79/402 patients (20%) were deemed to be clinically "affected" post-treatment (i.e. exhibiting signs of cardiac dysfunction/impairment) – however, only 56 out of the 79 patients had significant LVEF decline – a failure rate of 29%, indicating that LVEF may be ineffective as both an early and sensitive measure of cardiac dysfunction, specifically ACT. Despite LVEF being the widely accepted measure of cardiac function, its lack of sensitivity and inherent variability has been mentioned previously ^{149,150} and other alternatives such as the measurement of global longitudinal strain as a more sensitive and reproducible prognostic indicator of ACT has been suggested ^{69,151}.

Therefore, in this study, the "unaffected" status of patients was not deemed definitive without an echocardiography to provide confirmation. Some measure of association could be lost due to the potential inaccuracy in phenotyping. In trying to circumvent this issue and provide clarity, the severity score or classifier was developed based on previous literature (CTCAE grading) and the clinical phenotype of the cohort ^{51-54,152}.

Logistic regression models developed using retrospective patient data pointed to the following factors contributing to the final phenotype: hypertension, smoking, type of chemotherapy (i.e. total dose of anthracyclines: either doxorubicin, or epirubicin), and the change in LVEF from baseline to after chemotherapeutic administration, which have all been previously indicated ^{24,51,87,148}. However, in a multivariable model, the only factor that showed robustness was the LVEF decline – nevertheless this still does not indicate its utility as an early indicator of cardiotoxicity as LVEF decline was used for determining clinical status and the severity score of patients.

ANOVA type II tests showed that pre-chemo LVEF combined with population group contributed to the post-chemo LVEF measure which may indicate that different LVEF

ranges for different population groups may be more accurate in determining cardiac clinical status. Furthermore, when the pre-chemo LVEF was combined with severity score, population group and type of first-line chemotherapy, a fairly robust model of prediction of post-chemo LVEF emerged. This may have utility in financially-constrained hospital settings where only one measure of LVEF (pre-chemo) is possible.

5.3 Prospective Cohort Analysis

Anthracycline-naïve patients (n=272) were prospectively recruited from both GSH and TBH Hospitals in the Western Cape Province of South Africa.

Similar to the retrospective cohort analysis, patient clinical histories were extensively analysed. Infiltrating or invasive ductal carcinoma was found to be most frequently diagnosed in both cohorts (71% of the entire cohort), in accordance with worldwide statistics ¹⁵³. The median age of diagnosis in this cohort was 50 years with the IA cohort again being significantly younger (44 years) compared to both the MA (51 years) and CA (59 years) patients. The BSA of this cohort was also higher and in this instance, to a greater degree for IA (1.81m²) and CA (1.84m²) compared to their MA counterparts (1.74m²) (See Table 30). Age at diagnosis and BSA are similar to the trends observed in the retrospective patient cohort.

While the retrospective cohort showed a high number of patients with unknown HIV status, the prospective cohort showed a higher proportion of IA women (43%) with HIV. This may reveal easier accessibility and increased testing which is useful for patient care and management. However, the differential between HIV positivity in the cohort (43%) and the general reported incidence of 18% in this province is worthy of note¹⁵⁴.

The co-morbidities present in this cohort, which include hypertension, diabetes mellitus, cardiac disease and smoking status provided interesting insights when they were analysed within the population groups. IA patients were, on average, younger, but they were also found to be at the lowest risk for hypertension, diabetes and smoking. However, baseline cardiac incidental findings were highest in this group (13%). These cardiac incidental findings could be attributed to poor previous clinical care and subsequent subclinical cardiac dysfunction and/or the increased genetic likelihood of cardiac insufficiency ^{155,156}.

Incidental cardiac findings were both of interest and a confounding factor that could not be disregarded as they had a bearing on the outcome phenotype (cardiac status).

These findings ranged from the more serious left ventricular hypertrophy where ACT would be potentially greatest, to the lesser but still serious rhythm abnormality. Despite this, LVEF for all these patients were 'normal' allowing for treatment to be initiated – only one patient had an inconclusive LVEF measure and this was presumably in response to rhythm abnormality.

The patient standard of care at the beginning of the study included LVEF measurement at both baseline (before chemotherapy) and again after three or four cycles of chemotherapy. However, protocol changes due to change in management and an overburdened healthcare system resulted in only one LVEF measurement (baseline) recorded for a number of the prospective cohort (68%). Furthermore, patient overload on the Department of Nuclear Medicine at TBH and GSH resulted in some patients without any LVEF measure. Chemotherapy was administered regardless of cardiac status (either before or after treatment) as the treatment was deemed to be of greater need i.e. to treat cancer compared to the potential danger of cardiotoxicity. This, of note, is the standard of care in most public hospitals in the country.

However, the number of cardiac incidental findings in seemingly healthy patients (Table 32) at baseline together with significant rates of post-chemotherapy affected (ACT) patients (exhibiting signs of cardiotoxicity) emphasises the need for instituting effective measures of cardiac function and, specifically, repeated measures of LVEF.

The model of prediction of post-chemotherapy LVEF was developed using retrospective patient data – notably the following variables: pre-chemotherapy LVEF, severity score, population group and type of first-line chemotherapy. This statistical model was validated in prospective patients (n=87) with no missing variables and allowed for a fairly utilizable estimation of post-chemotherapy LVEF with an accuracy of 82%. The prediction of post-chemotherapy LVEF could allow for the change in LVEF and subsequent clinical cardiac status (i.e. dysfunction/impairment) to be ascertained. This predictive model could be utilised in patients with missing secondary LVEF measures (post-chemotherapy LVEF) for improved patient outcomes and may ultimately warrant further development.

There were 14% affected individuals in this cohort. However this may be an underestimation due to the likelihood of subclinical damage which can manifest later and both LVEF measure and clinical symptoms may not be indicative at the stage that patients were being assessed ^{56,58,106}. Nevertheless, IAs may have an increased risk of ACT as they were proportionally most affected (19%) compared to MA (13%) and

CA (10%), which is also in agreement with the retrospective cohort findings and the literature ^{6,140}.

After patient history, and patient status regarding ACT, genotyping of patient DNA was undertaken for an association study. Firstly, SNP MAFs for each population group were compared to MAFs (Reference population: ALL) derived from both dbSNP and Ensembl ⁸¹. The allelic frequencies of five SNPs (*ABCC1* rs246221, *ABCC2* rs17222723, *ABCC2* rs8187710, *NCF4* rs1883112 and *RAC2* rs13058338) in IAs and two SNPs (*ABCC2* rs17222723 and *ABCC2* rs8187710) in MA patients were significantly different compared to literature and Ensembl ⁸¹ reiterating the need for the inclusion of African and/or local populations in worldwide databases ¹⁵⁷. The MAFs of the investigated SNPs for the CA patients in this study were in accordance with the MAFs reported in both Ensembl and dbSNP (Population: ALL). Secondly, Hardy-Weinberg Equilibrium calculations were conducted and two SNPs – *HNMT* rs17583889 and *NCF4* rs1880112 were found not to be in Hardy-Weinberg Equilibrium in the cohort. While genotyping error is an improbable reason for these deviations (as confirmed by Sanger sequencing), the relatively small cohort size may explain this deviation.

The variant, *RARG* rs2229774 was found to have a strong association with anthracycline-induced cardiotoxicity in a genome-wide association study conducted by Aminkeng *et al.* ⁷ on childhood cancer patients of both European and non-European (including Asian, African-American and Hispanic) ancestry assessing cardiac function using the CTCAE grading and ECHO measures. The present study also found a statistically significant association of *RARG* rs2229774 with clinical status pertaining to ACT (Chi-square test, p=0.049). However, the more accurate logistic regression models found no association with this variant or any of the other variants and ACT status.

ABCC1 rs246221 was not associated with clinical status pertaining to ACT in this study, however a previous study by Semsei *et al.* ¹⁵⁸ found this variant to be associated with anthracycline-induced left ventricular dysfunction in Hungarian paediatric patients with acute lymphoblastic leukaemia. Aside from a different population and the use of ECHOs to show diminished cardiac function, patients were followed for a median of 6.3 years. Therefore the lack of association of this variant with ACT in our study may indicate that it would be worth following up on our patients longer term, and assessing for ACT (our patients were only followed for 1-3 years). Similarly, Vulsteke *et al.* ¹⁵⁹ found *ABCC1* rs246221 to be associated with an LVEF

decline of >10% in a European CA cohort of breast cancer patients treated with epirubicin and followed for a median of 3.62 years. While our study cohort had breast cancer patients, treatment with epirubicin and the outcome of LVEF decline >10%, our cohort consisted of mostly African-derived populations.

Wojnowski *et al.*⁸ found the variants *NCF4* rs1883112, *RAC2* rs13058338 and *ABCC2* rs8187710 to be associated with ACT in a German patient population treated with anthracyclines for non-Hodgkin lymphoma (NHL), and followed up for a median of more than three years, where arrhythmias and cardiac failure were classified as acute and chronic ACT, respectively. Again the divergent European-based population and longer follow up time may explain the lack of association with these variants and ACT in the present study. Similarly, Leong *et al.*¹⁰⁵ found an increased risk of ACT associated with *RAC2* rs13058338 and *ABCC2* rs8187710.

The variant, *ABCC2* rs17222723, had been previously associated with acute cardiotoxicity^{83,137,160} due to its role in drug transportation of cytotoxic agents into and out of the cell. However, the present study failed to find an association between this SNP and cardiotoxicity despite its sensitivity to acute ACT.

Similarly, the variant *HNMT* rs17583889, was found to have an association with ACT in Canadian paediatric cancer patients where cardiac function was assessed using both CTCAE guidelines and ECHOs¹⁰. However, in the current study of adult women, this variant showed no association with ACT and this may be explained by not only ancestry of the population compared to our cohort but also that paediatric cases may have greater susceptibility to cardiac damage due to the developing heart. It has been shown that paediatric hearts have inadequate compensatory mechanisms for cardiomyocyte loss allowing cardiac damage from anthracyclines to be potentially progressive thereby resulting in significant morbidity and/or mortality¹⁶¹.

Furthermore as suggested in the Aminkeng *et al.*⁶ article, genetic differences in key genes in African populations may account for increased sensitivity to both ACT and CHF. Differences in MAF as shown in the study between IA patients and literature illustrates these genetic dissimilarities. Beyond the variants discussed in this study, Aminkeng *et al.*⁶ showed that CYP enzymes', involved in the metabolism of 40-60% of all drugs, varied expression due to genetic differences may contribute to predisposition to several ADRs and poor response rates in African compared to European populations. The pharmacogenomic heterogeneity of African populations across different ethnic groups and geographical regions may contribute to differences in drug efficacy and safety profiles.

Variables that appeared to increase the odds of the outcome (patient clinical status) included significant LVEF decline ($>10\%$) and total anthracycline dose ($p=9.9e^{-05}$ and $p=0.0164$, respectively). The logistic regression of a multivariable model with both these factors was found to have an odds ratio of 1.704 and a p-value of 0.000164 thereby indicating a strong association of LVEF change and total anthracycline dose to level of cardiotoxicity (i.e. patient clinical status related to cardiotoxicity). Despite the inadequacy of LVEF as a sensitive measure of ACT, it has some utility in predicting the outcome of cardiotoxicity. Similarly, the dose of anthracycline, also predicts the outcome of cardiotoxicity – a finding that has been supported previously^{24,51,53}.

5.4 Study Limitations

General limitations of the study were:

- i) relatively small sample size – despite the recruitment of 272 prospective patients, their population stratification may have decreased statistical power of certain associations;
- ii) short median follow-up – the study in fulfilment of a PhD with a finite completion period included the recruitment of prospective patients before anthracycline-based treatment as well as follow-up after treatment which may have been too short a timeframe to assess progressive late-onset ACT;
- iii) the lack of information pertaining to lifestyle factors such as stress and exercise which may have had a bearing on cardiac function and/or susceptibility to cardiotoxicity. For example, studies indicate that aerobic exercise may mitigate cardiovascular dysfunction^{162,163};
- iv) lack of two LVEF measures for every patient – despite the insensitivity of the LVEF measure in some instances, the lack of a second measure complicated patient phenotyping with regard to ACT;
- v) attributing differences in genotypes to self-reported ethnicity – which may decrease population-specific significance. Ancestry Informative markers may have been useful in delineating the different population groups rather than the reliance on self-reporting¹⁶⁴. The limitation of attributing differences in genotypes to self-reported ethnicity is that SNPs with population-specific significance may be lost or diluted in the sub-cohorts (stratified according to population group). Furthermore, patient follow-up at a later stage could reveal late-onset ACT and therefore an affected case which may

contribute to non-associated SNPs finding statistical significance, particularly within the heterogeneous local population groups.

5.5 Recommendations

Despite the study's focus on the development of ACT, other issues related to patient health emerged. The lack of HIV status in a significant fraction of the retrospective cohort, is a concern given that South Africa has one of the largest epidemics in the world ¹⁵⁴. As was noted in the prospective cohort – up to 43% of women in the IA sub-cohort were HIV positive. Although not focused on in this thesis – HIV status or perhaps the status of an individual's immune system (e.g. AIDs versus non-AIDs in HIV positive subset) may contribute to ACT-susceptibility, and makes for a reasonable follow-up project with public health relevance.

In terms of managing ACT, patients with suspected or potential cardiotoxicity may be at a critical point whereby reversible cardiac damage may progress to irreversible, chronic or sometimes life-threatening cardiomyopathy, yet few patients were referred to cardiology clinics for follow-up and confirmatory ECHOs ^{25,60}. The inherent variability and lack of sensitivity of LVEF as a measure of cardiac function warrants the consideration of alternatives such as ECHOs or tissue-doppler imaging as a truer measure of cardiotoxicity. We therefore recommend routine ECHOs before and after chemotherapy as standard of care in the government setting for improved patient outcomes and decreased chronic cardiac care costs.

5.6 Future Directions

While this study provided valuable insights into the genetic heterogeneity of our African populations and their increased risk of developing ACT, this is merely a good starting point for future work.

Confirmed affected and non-affected (normal) patients' DNA may be utilised for GWAS to determine the nuances of their susceptibility to ACT. Patients will be stratified according to population group, confirmed by ancestry informative markers and their GWAS data analysed.

Additional patients may be recruited with the aim of improving cardiac assessment – ECHOs before and after treatment as well as submitting patient samples to a panel of biomarkers. These patients cardiac status can then be correlated to genotyping for the SNPs discussed in this study. Furthermore, the model developed in this study may be validated using actual post-chemotherapy cardiac measures.

While a genotypic change provides information that may be pertinent to susceptibility or protection, the level of expression may confer to what extent this is the case. Quantitative PCR may provide valuable insight/s into expression of genes associated with ACT.

Chapter 6: Supplementary Study – Testing of Biomarkers as a Measure of Cardiac Injury

6.1 Introduction:

Cardiac biomarkers found in blood had been initially used to detect cardiotoxicity in animal models and in pilot clinical studies, however they have the potential to be a more accurate measure of early cardiotoxicity in the routine management of patients^{17,18,22,37,69}. The advantages of biomarker assays is that they are standardized thereby minimizing technical variability to some extent, and they are also minimally invasive and easily repeated. Serial monitoring of serum biomarker concentrations have been proposed as a more specific and sensitive modality of cardiotoxicity detection^{24,69}, perhaps in place of LVEF (and the means of currently measuring this parameter), as discussed earlier in the thesis. Biomarkers that are currently being utilised in the assessment and detection of cardiotoxicity include: natriuretic peptides, troponins, and the ST2 cardiac biomarker^{161,165-167}, which are reviewed hereunder

6.1.1 Brain Type Natriuretic Peptide (BNP)

Natriuretic peptides play an important regulatory role in cardiovascular (Fig. 41) and renal homeostasis, as well as fatty acid metabolism and subsequent maintenance of body weight¹⁶⁸. Natriuretic peptides belong to a group of structurally similar yet genetically heterogeneous peptide hormones, namely: atrial, brain and C-type (ANP, BNP, CNP respectively)^{69,168}.

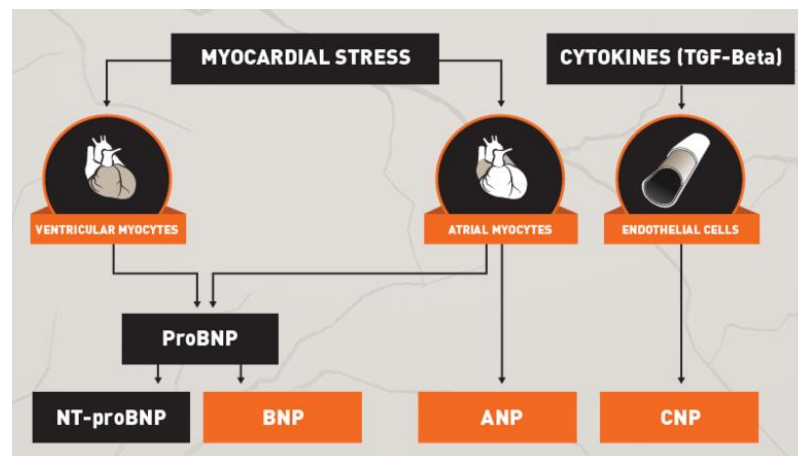


Figure 41: Natriuretic peptides involved in Cardiac Failure¹⁶⁹

All three peptides (Fig. 42) contain a 17 amino acid disulphide ring with variable C and T terminal regions¹⁷⁰.

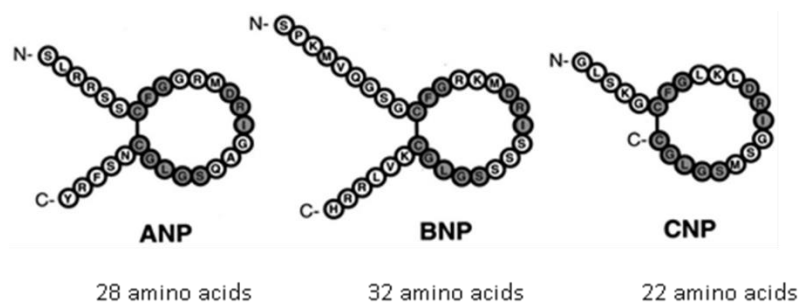


Figure 42: Natriuretic peptides ANP, BNP and CNP adapted from Suzuki et al ¹⁷⁰
Conserved residues are shaded and the amino acids are indicated by their single letter code

Specifically, B-type natriuretic peptide (BNP) is a hormone involved in cardiac homeostasis (natriuresis, diuresis, vasorelaxation and inhibition of aldosterone and renin secretion) and is preferentially expressed in response to cardiac stress or injury which manifests as increased filling pressures and volume overload ^{168,171,172}.

The prohormone, proBNP is converted to an inactive N-terminal pro B-type natriuretic peptide (NT-proBNP) and the active BNP ¹⁷³. Mature BNP consists of 108 amino acids, however BNP has a cleavable signal sequence allowing for variable BNP fragments in circulation ¹⁶⁸.

Elevated levels of NT-proBNP and BNP have been associated with CF and therefore have been previously used as a predictive marker of this phenotype (CF) ^{127,173-175}. While the increased concentration of BNP is associated with CF, these levels may be sensitive to other factors such as patient age, gender, renal insufficiency and obesity ¹²⁷. Evidence shows that natriuretic peptide deficiencies may contribute to both hypertension and diabetes ¹⁶⁴. Previous findings indicate an inverse correlation between BNP levels and obesity – therefore patients with diabetes may have lower BNP levels ¹²⁷.

Although data is limited, the literature indicates that ethnicity may have an effect on BNP levels ¹²⁷. Krim *et al.* ¹²⁷ found that both Asian and Black patients had higher median BNP levels compared to their Hispanic and CA counterparts. Conversely, Gupta *et al.* ¹⁶⁴ found that African American patients' NT-proBNP levels were below the limit of detection, and that this was significantly lower independent of other factors. It was also found that lower NT-proBNP levels were associated with the male gender, higher BMI, heart rate, blood glucose and diastolic blood pressure whereas higher NT-proBNP levels were associated with increased age, smoking, beta-blocker use and systolic blood pressure ¹⁶⁴. Furthermore, a genetic basis was used to associate ethnicity with NT-proBNP levels ¹⁶⁴. Genetic polymorphisms in the *NPBB* and *Corin*

genes, involved in NT-proBNP processing, have been suggested as plausible explanations for lowered NT-proBNP levels in African Americans, where these functional variants exist at a higher frequency ¹⁶⁴.

During the first three months of chemotherapy, increased levels of BNP were reported to be associated with abnormal LV thickness-to-dimension ratio which may indicate LV remodelling; in this regard, studies have shown abnormal LV structure years after chemotherapy ^{24,136}.

However Plana *et al.* ⁶⁹ found that the association between BNP levels and LV function were prone to inconsistencies.

6.1.2 Troponin T

Cardiomyocyte damage results in the increase of circulating cardiac troponin in the blood allowing for plasma and serum to be utilized for biomarker testing to assess cardiac health ¹³⁶. Cardiac troponin T-levels are generally undetectable in healthy individuals but are elevated where there is myocardial injury, possibly indicating irreversible cardiomyocyte necrosis ^{24,39,136}. Negative troponin concentrations have been shown to be indicative of low risk of cardiomyopathy – pointing to the sensitivity of troponin T as a measure of even early or subclinical cardiac damage which may allow for treatment while damage is still reversible ^{37,136,176}.

Troponins are proteins found in both cardiac and skeletal muscle. The troponin complex consists of thin filaments in striated muscle which is complexed to actin. There exist three types of troponins: Troponin T which is tropomyosin binding, Troponin I which inhibits binding between actin and myosin, and Troponin C which is calcium binding allowing for muscle contraction ¹⁷⁷.

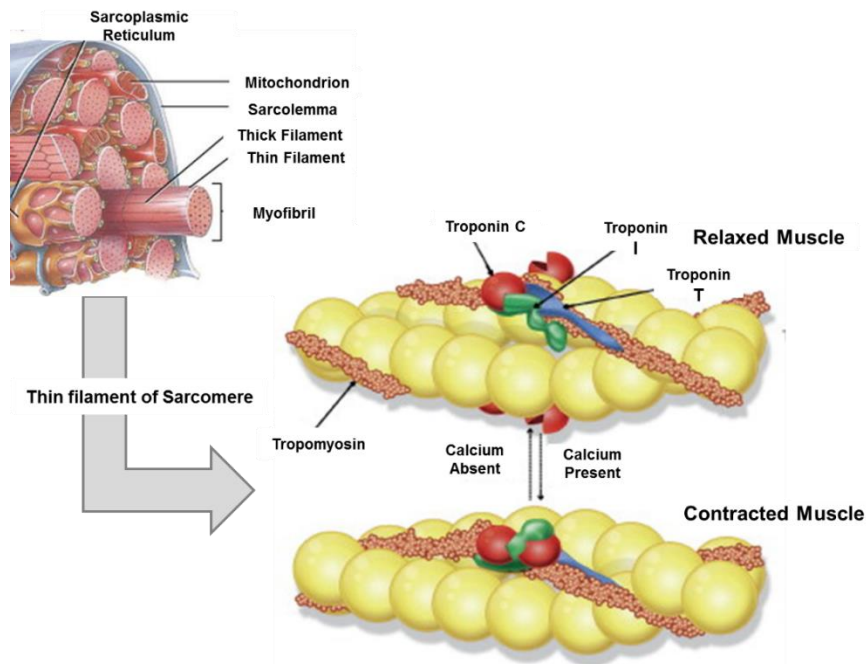


Figure 43: Visualization of cardiac muscle and the different Troponin molecules, adapted from Shave *et al.*¹⁷⁷

Despite females reportedly having a greater risk of developing ACT, males are more likely to have increased cardiac troponin levels due to anthracyclines indicating that together with the difference in LV mass between the sexes, an attempt should be made to devise population and gender based Troponin T values correlated with cardiac assessment/function¹³⁶. Furthermore, in addition to cardiac troponin levels being significantly elevated in males, especially those with irradiation near the heart, this biomarker was raised in correlation with higher cumulative doses of anthracyclines¹³⁶.

Cheung *et al.*¹³⁶ were not able to elucidate if troponin release was due to anthracycline-induced apoptosis of cardiomyocytes or due to consistent myocardial injury causing troponin release into the bloodstream.

Nevertheless, genotyping revealed that the *CYBA* rs4693 CT/TT genotype was significantly associated with increased cardiac troponin levels compared to the CC genotype, whereas the variants in *RAC2* (rs13058338) and *NCF4* (rs1883112) had no association with troponin levels¹³⁶. The *CYBA* rs4673 CT/TT genotype has been associated with high sensitivity cardiac troponin levels which functionally translate to worse left ventricular longitudinal strain¹³⁶.

6.1.3 Suppression of Tumorigenicity 2 (ST2)

The “Suppression of Tumorigenicity 2” or ST2 marker is an interleukin-33 receptor, part of the interleukin-1 receptor family, and is a cytokine secreted in response to cellular damage, particularly cardiovascular stress and fibrosis ¹⁶⁶. While it has a cardiovascular role, ST2 is also involved in inflammatory and immune processes ¹⁶⁶.

While severe cardiotoxicity during anthracycline-based therapy may result in its early discontinuation, cardiotoxicity may also present years after treatment ^{24,41}. Cardiac troponin T as a measure of acute cardiotoxicity, may benefit from an additional, sensitive biomarker such as ST2; the latter of which is a powerful predictor for death due to CF, and may be especially useful to detect late onset ACT ^{41,166}.

While careful monitoring of cardiac function, utilisation of a specific type of anthracycline and limiting cumulative anthracycline dose may mitigate risk of developing ACT, it is likely that cardiotoxicity may still occur regardless of these efforts. Therefore, other measures need to be utilized for the reduction or prevention of cardiotoxicity at the clinical level.

This aspect of the study was to determine whether biomarkers, in this instance NT-proBNP or BNP may serve as a more accurate measure of cardiac injury and cardiotoxicity.

6.2 Materials and Methods:

6.2.1 The Study Cohort:

Forty-two patients from the prospective cohort with adequate biological specimen before and after chemotherapy were selected for the biomarker study.

Peripheral whole blood (3ml) was collected in Greiner Bio-One Vacuette Venous Blood Tubes (Lavender K₃EDTA) from patients which enable an intact and stable specimen to be collected for plasma for biomarker testing.

6.2.2 Determination of cardiac biomarker of injury levels using peripheral blood

The Biomedica® Competitive Enzyme Immunoassay (Biomedica Immunoassays, Austria) was used to detect level of NT-proBNPs in order to determine the extent of cardiac injury.

6.2.2.1 Principle of ELISA

The method of Enzyme-Linked Immunosorbent Assays (ELISA) or Enzyme Immunoassays (EIA) dates to the 1960s and utilises the combined specificity and sensitivity of antibodies and/or antigens and enzymes allowing for inferences of either antigen or antibody concentration to be made ¹⁷⁸⁻¹⁸⁰. ELISAs can be either used to detect the presence of antigens specifically recognized by an antibody or vice-versa. A generalized ELISA consists of the following: Microtiter plates are first coated with antigen, unbound sites are then blocked to prevent non-specific binding, primary antibodies are added to the wells and finally a secondary antibody which is conjugated to an enzyme, is added ¹⁷⁹. The enzyme acts as the reporter label ¹⁷⁸. This conjugate usually produces a colour change when a substrate is added that ultimately indicates a positive result that can be more accurately quantified with an ELISA plate-reader.

There are four types of ELISA that can be used depending on the object of the experiment: Direct ELISA, Indirect ELISA, Competitive ELISA and Sandwich ELISA ¹⁷⁹. Direct ELISAs involve antigen attachment to the microtiter plate and the addition of an enzyme-linked antibody, allowing for a rudimentary measurement of sample concentrations ¹⁷⁹. Similarly, Indirect ELISAs involve antigen attachment to the solid phase, but the addition of an unlabelled primary antibody with the addition of an enzyme-linked secondary antibody allows for greater specificity in antibody detection ¹⁷⁹. Greater specificity is achieved with Competitive ELISAs whereby “competing” antibodies or proteins are added ¹⁷⁹. The last type of ELISA is both sensitive, specific and amenable to high-throughput platforms – Sandwich ELISAs involve a solid phase coated with capture antigen, the addition of samples with known or unknown antigens in a matrix or buffer followed by the addition of an enzyme-conjugated antibody that allows for a quantifiable detection signal ¹⁷⁹.

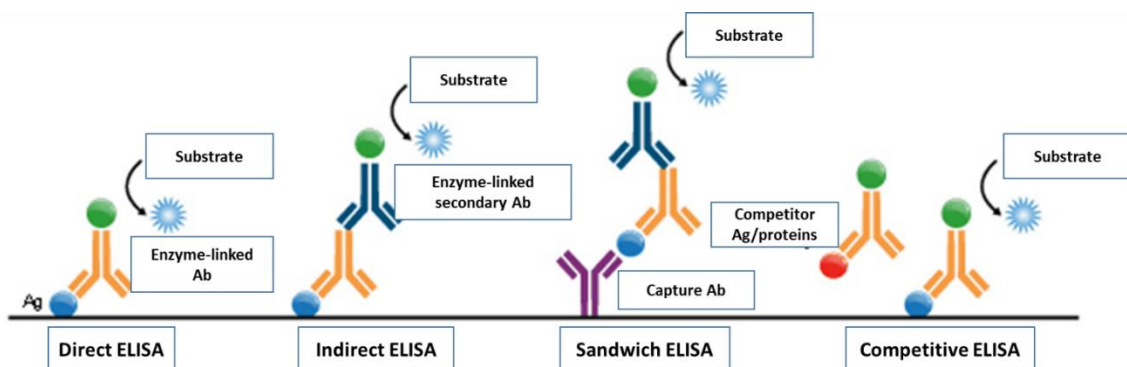


Figure 44: Schematic illustration of the generalized principles of the four types of ELISAs (Image adapted from ¹⁸¹)

6.2.2.2 Technique of Detection of N-terminal pro B-Type Natriuretic Peptide (NT-proBNP) using a Competitive ELISA

Peripheral blood was centrifuged at 2500 rpm for 20 minutes at 4°C allowing for separation of plasma. BNP fragments are stable in plasma and serum and therefore centrifugation occurred soon after procurement of sample. Plasma was then stored at -80°C until needed. The plasma may be subjected to five freeze-thaw cycles without compromising sample integrity. The reliability of haemolysed blood samples in determining levels of NT-proBNP is disputed¹⁸²; samples which were suspected of haemolysis were therefore collected and recorded as such, and utilized nevertheless.

The Biomedica assay was performed according to manufacturer's instructions¹⁶⁸. The wash buffer, standard and control were reconstituted before use. The wash buffer was diluted 1:20 and both the standards (synthetic human BNP fragment at various concentrations (pmol/l) and control (synthetic human BNP fragment) were reconstituted with 200ul of distilled water for 20 min at room temperature, mixed gently and then stored at -25°C. A volume of 150ul of Assay Buffer was added to all wells except the blank in a plate coated with polyclonal anti-BNP fragment antibody followed by 30ul of either samples, control or standards to each well except the blank. This was followed by the addition of 50ul of conjugate (synthetic BNP fragment –HRPO with red dye) to each well except for the blank. The plate was then well covered and incubated overnight at 4°C in darkness. The wells were then aspirated and washed four times with 300ul of diluted wash buffer using an ELISA plate washer (Biotek® Microplate Washer, USA). A volume of 200ul of substrate [Tetramethylbenzidine (TMB) solution] was then added to each well and then incubated for 20 minutes at room temperature in the dark. Subsequently, 50ul of stop solution (Sulphuric acid, 0.18M) was added to each well, shaken well and then placed on the ELISA plate reader capable of determining absorbance at 450nm with a correction wavelength at 630nm. The stop solution can alter the pH therefore inactivating the enzyme and halting the reaction. The correction wavelength allows for non-specific emissions and interference signals to be eliminated thereby giving the correct absorbance of proteins of interest. The assay was performed in duplicate.

6.2.2.3 Statistical Analysis for the determination of NT-proBNP levels

Results were analysed by measurement of the optical density (OD) of each well. OD values derived from the standards were used to construct the standard curve. Raw data was transformed and analysed using the 4PL algorithm (GraphPad Prism 6) and unknown samples were interpolated using the standard curve. Sample concentrations

were then derived from the antilog of interpolated values. Reference ranges derived from the standards for the assay were specific to the run and could not be utilised across assay runs.

NT-proBNP levels were assessed as transformed log values and as quartiles specific to population as previously done ¹²⁷.

6.3 Results:

Incidental cardiac findings and the missing LVEF measures for some patients prompted a pilot study for the assessment of a sub-group of patients at baseline and after chemotherapy, and where blood samples were collected at these two time points, using a cardiac biomarker to determine if there was any cardiac injury in asymptomatic patients.

6.3.1 Determination of cardiac biomarker of injury levels using EDTA-plasma

Forty two patients were assessed at both baseline and post-chemotherapy for BNP levels using EDTA-plasma from peripheral blood. Raw values from the ELISA were log-transformed and patient concentrations of NT-proBNP were inferred from the fourth-party logistics (4PL) Algorithm using GraphPad Prism 6 ¹⁸³. Multivariable linear regression was utilized for the association between population group (predictor) and biomarker levels (outcome). Covariates for the multivariable models included: population group, age, BMI, hypertension, diabetes and smoking status.

6.3.2 NT-pro B-Natriuretic Peptide (NT-proBNP) concentration

Patients were stratified according to their hypertensive status (Table 40) as hypertension due to ventricular stretching of the myocardium may increase the release of BNPs ¹⁷⁵.

Table 40: Clinical, demographic and experimental information pertaining to the patients assessed for BNP levels

<u>Patient ID</u>	<u>Age at Diagnosis</u>	<u>Population Group</u>	<u>Pre-existing CD</u>	<u>Diabetes</u>	<u>Smoking</u>	<u>Other Meds</u>	<u>LVEF Pre</u>	<u>Type of Chemo</u>	<u>Dose</u>	<u>Clinical Symptoms Post</u>	<u>BNP Concentration</u>	
											<u>Pre</u>	<u>Post</u>
<u>Non-Hypertensives</u>												
ACT217	53	MA	N	N	Y	None	57	Epi	690	Severe SOB	571.6	647.8
ACT219	55	MA	N	N	N	None	65	Dox	420	.	363.3	281.1
ACT220	61	MA	N	N	N	None	68	Dox	400	DECEASED	OR	296.1
ACT222	50	MA	N	N	Y	None	65	Dox	480	.	187.2	276.2
ACT227	41	MA	N	N	Y	None	60	Dox	460	.	112.4	188.1
ACT228	50	IA	N	N	N	None	65	Dox	400	.	227.9	562.1
ACT229	54	MA	N	N	N	None	68	Dox	440	.	344.9	55.2
ACT230	58	MA	N	N	N	None	67	Dox	330	.	343.8	267.4
ACT232	69	MA	N	N	N	None	55	Epi	440	Borderline ECG	218.8	415.3
ACT234	68	MA	N	N	N	None	55	Dox	600	.	176.2	288.1
ACT238	52	MA	N	N	N	None	60	Dox	330	.	593.6	402.6
ACT240	30	MA	N	N	N	None	55	Dox	285	Confirmed LVH	500.5	513.3
ACT241	51	MA	N	N	Y	None	67	Dox	600	.	397.9	386.8
ACT245	57	MA	N	N	N	None	60	Dox	270	Borderline ECG	161.0	113.1
ACT246	49	IA	N	N	N	None	60	Dox	330	Potential LVH	662.0	224.3
ACT248	44	IA	N	N	N	None	60	Dox	460	.	206.5	386.8
ACT252	73	MA	N	N	Y	None	53	Epi	330	Confirmed Acute MI	366.3	95.8
ACT259	43	MA	N	N	Y	None	58	Epi	840	.	895.8	440.8
ACT260	63	MA	Y	Y	N	NIDDM meds	55	Dox	345	Chest pain	247.2	151.9
ACT263	43	MA	N	N	N	None	60	Dox	460	.	OR	95.8
ACT264	57	MA	N	N	N	None	55	Epi	375	.	312.7	43.8
ACT272	44	MA	N	N	Y	ARVs	69	Dox	320	.	738.4	540.8
<u>Hypertensives</u>												
ACT215	62	MA	N	N	N	HCTZ, Atenolol, Enalapril, Zocar, Amlidopine	73	Dox	400	.	432.9	48.5
ACT221	63	MA	N	N	N	Hypertensive meds, Simvastatin	77	Dox	420	.	290.0	175.4
ACT223	37	IA	N	N	N	Amlidopine, ARV	55	Epi	520	.	89.5	146.0
ACT224	58	MA	N	Y	N	Hypertensive meds	67	Dox	400	.	146.0	1015.6

Table 40 continued: Clinical, demographic and experimental information pertaining to the patients assessed for BNP levels

ACT225	54	MA	N	N	N	Dispirin, Amlidopine	60	Dox	380	.	159.7	217.0
ACT226	50	MA	N	N	Y	Ridaq, Pharmapress	67	Dox	330	Abnormal ECG; Sinus Tachycardia	93.7	465.5
ACT231	44	MA	N	N	Y	None	65	Dox	330	.	387.8	392.3
ACT244	47	MA	N	N	N	Ridaq	55	Epi	540	Abnormal ECG; Prolonged QT	324.2	140.9
ACT249	56	MA	N	Y	Y	Ridaq, Pharmapress, Glibendamide	58	Epi	780	.	362.3	43.1
ACT250	43	IA	N	N	N	Ridaq, Atenolol, Zocar; Simvastatin, Enalapril	none	Dox	440	.	362.3	436.4
ACT251	63	MA	N	N	N	Ridaq, Atenolol	60	Epi	500	Borderline ECG	187.1	129.3
ACT253	51	MA	N	N	Y	TB Drug Regimen 1; Ridaq, Atenolol	71	Dox	380	Potential MI	523.2	715.5
ACT254	48	MA	N	N	N	Ridaq, Atenolol	66	Dox	345	.	234.5	139.0
ACT255	63	MA	N	N	Y	Hypertensive Meds	60	Dox	400	.	276.8	305.2
ACT257	40	MA	N	N	N	Ridaq, Pharmapress, Atenolol	65	Dox	460	.	568.6	203.2
ACT261	67	IA	N	N	N	None	65	Dox	450	.	388.2	289.0
ACT265	38	MA	N	N	N	Pharmapress	65	Dox	400	.	550.5	490.3
ACT266	60	MA	Y	N	N	Atenolol	60	Dox	400	.	345.0	236.8
ACT269	45	MA	N	N	Y	ARVs, Pharmapress	64	Dox	360	.	132.2	496.5
ACT273	43	MA	N	N	N	Ridaq, Pharmapress	50	Dox	400	Potential LVH	1139.8	676.5

*SOB = shortness of breath; ECG= echocardiogram; LVH= left ventricular hypertrophy; MI= myocardial infarction; NIDDM= non-insulin dependent diabetes mellitus;

ARVs= antiretroviral; HCTZ = hydrochlorothiazide; QT = time between start of Q wave and end of T wave; TB = tuberculosis

6.3.3 Statistical Analysis

Patients were analysed as a combined cohort as well as after stratification into population groups. The median age of this sub-cohort was 51.5 years, which, when stratified showed MA patients with a median age of 53.5 years compared to the younger IA cohort with a median age of 46.5 years. Despite the younger age of the IA cohort, their median BMI at 31.6 was higher and in the obese category compared to the median BMI of the MA cohort at 28.2 - in the overweight category.

While the IA cohort had a higher incidence of hypertension (0.5) compared to the MA cohort (0.44), the MA cohort had more pre-existing cardiac disease (0.03), diabetes (0.08) and more smokers (0.33) compared to a zero incidence of these factors in the IA cohort. These risk factors have been shown to increase the likelihood of ACT^{24,26,36}. This would essentially translate to the MA cohort being at higher risk of cardiotoxicity and therefore likely to have higher expected levels of BNPs. However, the median baseline LVEF for the combined, MA and IA cohort was 60% which is in the normal or healthy heart range⁶⁴.

Cumulative chemotherapeutic dose relies on type and stage of cancer as well as the BSA which relies on both weight and height¹⁸⁴. While BMI is a crude but relatable measure, the IA cohort with a higher median BMI received overall, a higher median cumulative dose of doxorubicin – i.e. 440mg/m² compared to the MA cohort with a median dose of 400mg/m² in this pilot biomarker cohort. Only one IA patient was administered epirubicin so a similar deduction could not be made for this drug. However, when both cohorts were analysed for median dose of anthracycline-based chemotherapy, the IA sub-cohort received a higher dose – 445mg/m² compared to the MA cohort's cumulative median dose of 400mg/m².

While the increased concentration of BNP is associated with CF, a major limitation of this measure is that BNP levels may be sensitive to other factors such as patient age, gender and obesity, as well as population-specific variants resulting in increased sensitivity to chemotherapy^{127,139,140}. Therefore, BNP baseline levels were stratified according to population group (Fig.45).

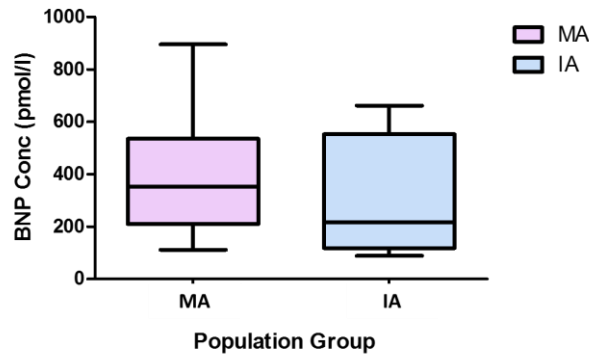


Figure 45: Comparison of baseline BNP concentrations in both the MA and IA cohorts with the exclusion of all hypertensive patients (n=40, p=0.4369, Unpaired t-test)

Hypertensive patients were excluded from this analysis as hypertension may cause ventricular stretching which can cause increases in BNP levels (Fig. 45, Table 41) ¹⁷⁵.

Table 41: Comparison of median baseline BNP concentrations before the administration of anthracycline based chemotherapy and stratified per the type of chemotherapy administered, population group and hypertensive status of patient

Patient Cohort	Type of Anthracycline	BNP Concentration (mg/m ²)		Population Group	p-value
		Median	Range		
All	Doxorubicin	344.4	93.7-1139.8	MA	<0.0001*
		362.3	206.5-662	IA	
	Epirubicin	343.3	187.1-895.8	MA	
		89.5 [^]	n/a	IA	
	Both	344.4	93.7-1139.8	MA	
		295.1	89.5-662	IA	
Hypertensive	Doxorubicin	290	93.7-1139.8	MA	<0.0001*
		375.3	362.3-388.2	IA	
	Epirubicin	324.2	187.1-362.3	MA	
		89.5 [^]	n/a	IA	
	Both	307.1	93.7-1139.8	MA	
		362.3	89.5-388.2	IA	
Not Hypertensive	Doxorubicin	344.9	112.4-738.4	MA	-+
		227.9	227.9-662	IA	
	Epirubicin	366.3	218.8-895.8	MA	
		n/a	n/a	IA	
	Both	354.1	112.4-895.8	MA	
		227.9	227.9-662	IA	

*Chi-square Test, *Not computed due to no IA, non-hypertensive patients administered Epirubicin, p-value_{both} <0.0001 therefore statistically significant, [^]Only one Indigenous African patient was administered epirubicin

Overall, hypertensive IA patients had higher baseline BNP levels compared to their MA counterparts. However, MA patients (both hypertensive and non-hypertensive

combined) had higher baseline BNP concentrations compared to IA patients (Table 41). Chi-square test analysis shows that this difference is statistically significant ($p_{\text{overall}} < 0.0001$).

The BNP concentration of the entire cohort before and after chemotherapy is illustrated in Figure 46.

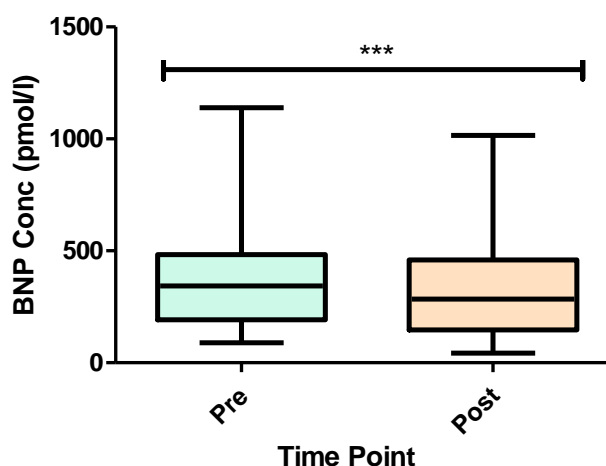


Figure 46: BNP Concentration of the entire cohort before (pre) and after (post) chemotherapy (n=42), ($p < 0.001$, Chi-square Test)

While the differences in BNP levels for the combined populations (pre vs post, both hypertensive and non-hypertensive) are statistically significant, Figure 46 indicates that anthracycline-based chemotherapy decreases BNP concentration after administration, which is counterintuitive. Anthracycline-based chemotherapy is known to be cardiotoxic and was therefore expected to increase BNP levels rather than show a decrease. Therefore, the BNP concentration of the entire cohort was re-analysed, excluding the hypertensive patients, in case the decreased BNP levels after chemotherapy is as a result of the use of anti-hypertensives ^{185,186}.

The BNP concentration of the non-hypertensive patients in the cohort were compared before and after chemotherapy and illustrated in Figure 47.

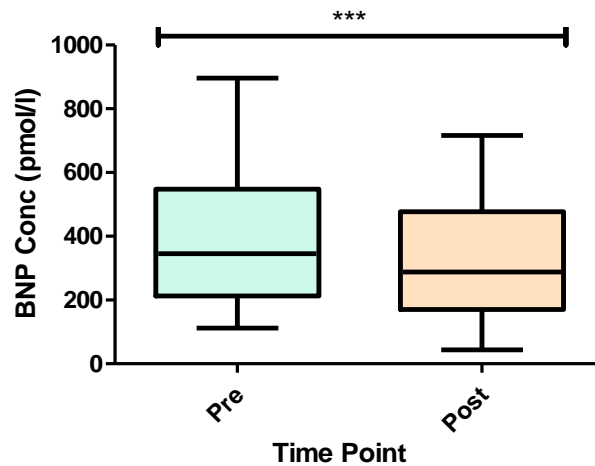


Figure 47: BNP Concentration of the non-hypertensive patients in the cohort before and after chemotherapy (n=21), ($p < 0.001$, Chi-square Test)

Despite the exclusion of hypertensive patients, there was still a uniform decrease in BNP levels after the administration of chemotherapy (Fig. 47). This shows that this trend is not due to hypertension and the use of anti-hypertensives. Therefore, as previously discussed (Fig. 45), stratification of the cohort into population group before the analysis of BNP concentration levels may allow for a more accurate analysis as seen in Figure 48.

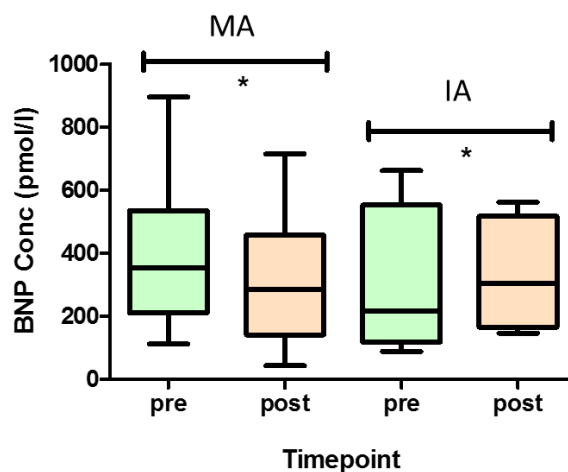


Figure 48: Comparison of BNP levels at baseline (pre) and after (post) chemotherapy for both MA and IA patients with the exclusion of hypertensive patients ($p < 0.0001$ statistically significant change from baseline to after chemotherapy, chi-square test for both MA and IA)

Figure 48 demonstrated a statistically significant change from baseline to after chemotherapy in BNP concentration levels in both populations. While BNP levels decreased in the MA population after the administration of chemotherapy as it has

with the previous analyses (Figs.45 & 48), it shows a posttreatment increase in the IA cohort, indicating possible quantifiable cardiac dysfunction (Fig. 49). Furthermore, this pilot analysis shows that BNP levels may be ethnicity dependent and that the anthracycline-based chemotherapy has potential cardiotoxic effect in the IA population.

This effect was interrogated further whereby pre- and post-treatment measures were analysed taking account of the type of anthracycline administered in each of the MA and IA ethnic groups.

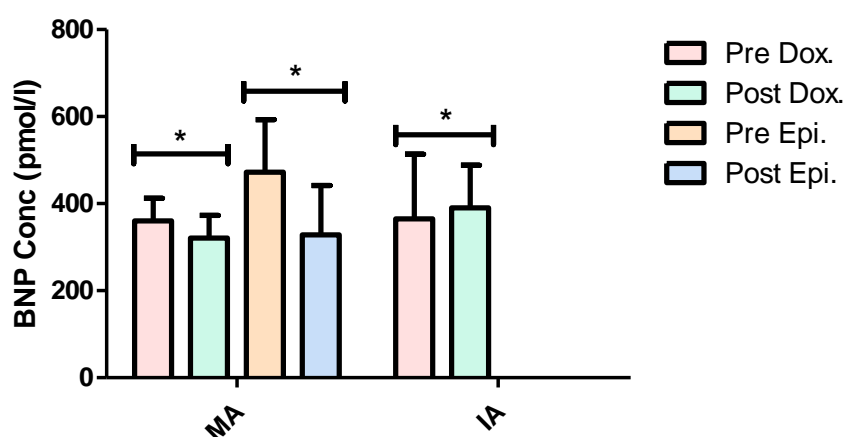


Figure 49: Comparison of BNP levels at baseline and after chemotherapy for both MA and IA patients with the exclusion of hypertensive patients and stratified into type of anthracycline-based chemotherapy administered

Within the MA cohort, BNP levels were found to be significantly different (i.e. decreased) from baseline to post-chemotherapy in patients treated with doxorubicin and as well as in patients treated with epirubicin ($p < 0.0001$, Chi-Square Test, Fig. 49). In this MA cohort, there is a trend toward BNP levels decreasing after treatment with doxorubicin. The MA patients scheduled for epirubicin had a higher BNP concentration at baseline than the patients scheduled for doxorubicin.

Similarly, within the IA cohort, BNP levels were found to be significantly different from the baseline time-point to the time-point after the administration of chemotherapy in patients treated with doxorubicin ($p < 0.0001$, Chi-Square Test, Fig. 48). IA patients scheduled for doxorubicin had slightly higher baseline BNP levels compared to their MA counterparts. This observation is interesting given that the IA cohort had a lower clinical risk in terms of co-morbidities (Table 41). The trend for doxorubicin is an increase of BNP levels after the administration of treatment indicating that IA may be more susceptible to cardiotoxic chemotherapy as previously inferred to (Fig. 48).

Because of the small sample size – this observation does need to be interpreted with caution.

While the assessment of BNP levels at specific time-points (pre- vs post chemotherapy) is of value, it is important to correlate these levels with patient clinical status in order to ascertain if BNP concentrations are indicative of cardiac physiological insult or dysfunction.

6.3.4 Correlation between Routine Measures, Biomarkers and Cardiac Function Decline

As previously mentioned, a severity score was established where patients were stratified in terms of anthracycline-induced cardiotoxicity. The score was based on the Common Technology Criteria for Adverse Events v3.0 (CTCAE) which has been utilised previously^{7,10}. This score or grading was based on change in LVEF if available and clinical phenotype after the administration of chemotherapy.

Table 42: Severity Score established using LVEF measure and patient clinical phenotype

Severity Score	Change in LVEF	Clinical Phenotype
0	No change	Normal
1	No LVEF decline	Chest pain, shortness of breath, palpitations
2	LVEF decline <10%	Chest pain, shortness of breath, palpitations, chemotherapy dose change or decrease
3	LVEF decline <10%	Suspected CCF, LV Dilation, Cardiomegaly, raised Troponin T
4	LVEF decline ≥ 10%	Congestive Heart Failure, Myocardial Infarction

Due to the progressive nature of cardiac dysfunction, it was necessary to take certain clinical characteristics beyond LVEF into account⁵¹⁻⁵⁴.

Cumulatively (in both population groups), the change in BNP concentration levels (post – pre) was not normally distributed ($W=0.938$; $p=0.029$). The median BNP change is -59 pmol/l indicating that there was an overall average decrease of 59 pmol/l from pre-chemotherapy levels to post-chemotherapy levels. In terms of the extremes in BNP levels change – this ranged from a decrease of 463.2 pmol/l to an increase of 869.6 pmol/l.

The change in BNP was analysed in terms of clinical status of the patient after the conclusion of chemotherapy and the following emerged: despite there being evidence

of the patient having some measure of cardiac dysfunction, there was no statistically significant difference in change in BNP levels between the unaffected and affected groups (Fig. 50a, Chi-square test, $p=0.426$).

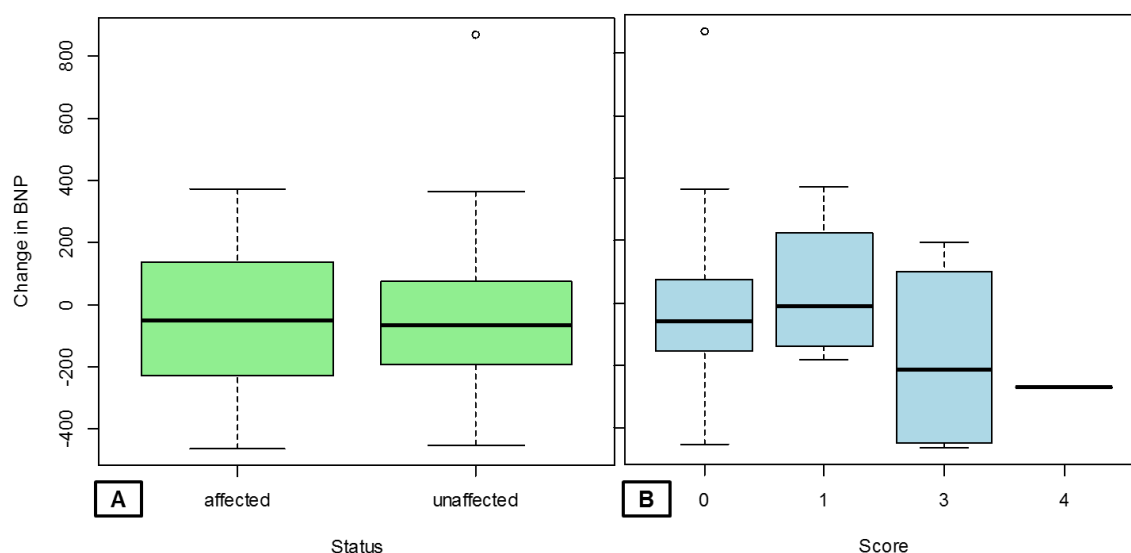


Figure 50: Comparison of change in BNP based on both patient status (A) and severity score (B)

Figure 50A demonstrates that despite the clinical status of patients after treatment, there is no difference in change in BNP levels. Figure 50B shows that while there are differences depending on the severity score, these differences indicate that BNP levels decrease in patients with a higher severity score (i.e. BNP levels after chemotherapy have a greater decrease in patients with signs of cardiac dysfunction) which is counterintuitive.

Patients were then stratified into population group and assessed for change in BNP compared to their cardiac clinical status (affected vs unaffected).

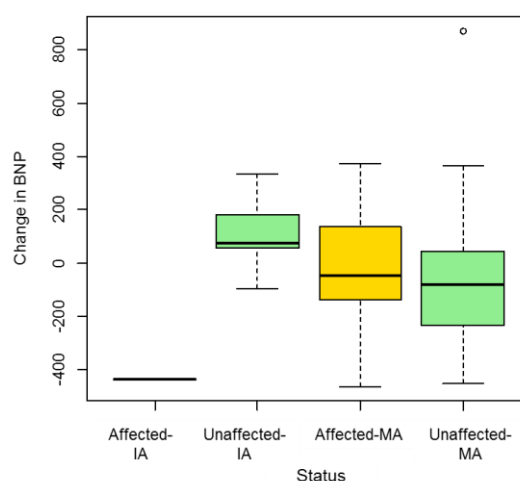


Figure 51: Comparison of change in BNP in both IA and MA affected (yellow) and unaffected (green) individuals

While there is no discernible difference in the change in BNP between affected and unaffected MA individuals, there is a difference between affected and unaffected IAs (Fig. 51).

Furthermore, patients with baseline cardiac incidental findings (Table 43) were analysed together with their levels of BNP and clinical status.

Table 43: Patients with baseline cardiac incidental findings analysed for both BNP levels and clinical status

<u>Patient ID</u>	<u>Pre LVEF</u>	<u>Cardiac Baseline</u>	<u>HPT</u>	<u>Pre</u>	<u>BNP</u>		<u>Score</u>	<u>Status</u>
					<u>Post</u>	<u>Change</u>		
ACT223	55	LVH	Y	89.5	146.0	56.5	0	unaffected
ACT232	55	Impaired relaxation LV	N	218.8	415.3	196.5	0	affected
ACT234	55	Impaired relaxation, elevated atrial filling pressures	N	176.2	288.1	111.8	0	unaffected
ACT238	60	Impaired relaxation LV, aortic regurgitation	N	593.6	402.6	-191.1	0	unaffected
ACT251	60	Tricuspid regurgitation	Y	187.1	129.3	-57.8	0	affected
ACT260	55	LVH	N	247.2	151.9	-95.3	1	affected

Table 43 shows patients with both baseline cardiac incidental findings and measurement of BNP levels before and after chemotherapeutic administration – despite potential diminished cardiac function, increases in BNP levels were not indicative of clinical status. This lack of association was illustrated in Figure 52.

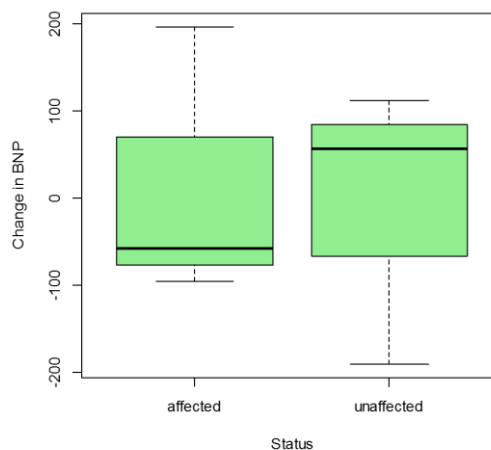


Figure 52: BNP changes in patients with baseline cardiac incidental findings compared to their clinical status after the administration of chemotherapy

Chi-square test for change in BNP levels compared to status (Fig. 52) showed non-significant differences ($p=0.3062$).

6.4 Discussion

Given the inadequacy of LVEF, this prompted the validation and utilisation of BNP concentration as a measure of cardiac dysfunction and to improve the accuracy of gauging the cardiac phenotype^{62,93,165}. Ideally, the entire cohort would have undergone BNP analysis, however, the combined cost of 272 patients at two time points limited the study to prioritisation of those without a second LVEF measure; so at best the present study is a pilot.

Data derived from our cohort of 42 patients, treated for breast cancer, indicated that, in general, BNP levels decrease after the administration of a cardiotoxic treatment. This is of interest as it can be erroneously inferred that anthracyclines may improve cardiac function or, more rationally, that the measurement of BNP concentration as a surrogate marker of cardiac function is limited. However, this trend persisted even after the removal of hypertensive patients (as BNP may be released in response to ventricular stretching of the myocardium¹⁷⁵), as well as when the data was further stratified into the type of regimen (i.e. doxorubicin versus epirubicin). It was found that there was a discernible and significant increase in BNP concentration for the IA cohort – indicating that despite the limitation of BNP levels, the cardiac effect of the anthracyclines may have been sufficient to show impairment in this population group. Although the IA cohort was relatively small, this trend may suggest that African women may be more sensitive to chemotherapy which is plausible considering previous

evidence of ethnically variant polymorphisms that influence doxorubicin pharmacokinetics and pharmacodynamics ^{127,139}.

While the lowered levels of BNP after the administration of cardiotoxic chemotherapy, was unexpected – numerous studies have also found conflicting results correlating BNP and/or NT-proBNP levels with chemotherapy ¹⁸⁷⁻¹⁹⁰. This may be explained by the difference in BNP versus Troponin – Troponin is released due to cardiac myocyte damage and/or death whereas BNP is released due to stretching of the ventricular myocardium ^{191,192}. Additionally, maintained preload reserve may explain the unchanged or decreased BNP levels after the administration of chemotherapy – compensatory mechanisms that preserve stroke volume and cardiac output thereby preventing excess expansion and pressure overload and subsequent release of BNP may explain this phenomenon ¹⁸⁶.

BNP levels are not only sensitive to functional genetic variants which may be population specific, but also to patient age, gender, obesity and hypertension ^{127,139,140}. While hypertensive patients may exhibit higher levels of BNP due to ventricular stretching and therefore not be as informative as a predictor of cardiac dysfunction, hypertensive medications such as angiotensin inhibitors and β -blockers, may preserve cardiac function particularly in patients treated with a sufficiently high dose of the drug ^{69,185}. It is hypothesized that the progressive nature of myocardial injury enabling the asymptomatic cardiac decline to become irreversible, symptomatic cardiac dysfunction may be slowed or even halted by the concomitant administration of anti-hypertensive medications ¹⁸⁵.

It is also likely that patients may not have left ventricular remodelling, causing systolic dysfunction, thereby not showing an increase in BNP levels. There was a difference in IA patients (Fig.51), which indicated that clinically unaffected (i.e. relating to CF) individuals have higher BNP levels after chemotherapy compared to baseline. Against this background - the one affected individual who had lower BNP levels after chemotherapy compared to before the administration of chemotherapy – suggests that BNP levels are not indicative of cardiac dysfunction but could point to ventricular stretching without cardiomyocyte death. However, we cannot exclude ACT related to cardiomyocyte death using BNP levels which is more closely related to cardiac stress and contractile dysfunction than cardiomyocyte death, as previously discussed.

While the correlation of BNP levels to patient clinical status proved to be inconclusive, the severity score, developed for increased accuracy in patient phenotyping also failed to show an association with BNP levels, suggesting that the BNP biomarker

may not be an early predictor of ACT. Furthermore, the cardiac incidental findings at baseline were compared to BNP levels and also showed no association despite there being quantifiable cardiac compromise.

6.4.1 Study Limitations:

Limitations related to the use of BNP analysis for the assessment of cardiac function include:

- i) lack of two LVEF measures for every patient – despite the insensitivity of the LVEF measure in some instances, the lack of a second measure complicated the correlation of BNP measures to cardiac function;
- ii) attributing differences in biomarker levels to self-reported ethnicity – which may decrease population-specific significance . Ancestry Informative markers may have been useful in delineating the different population groups rather than the reliance on self-reporting ¹⁶⁴, and
- iii) lack of biomarker analysis for the entire cohort – although BNP had limited utility, data on the entire cohort may have provided more useful insight.
- iv) the use of only one blood sample at each time-point due to the patients in the study being outpatients, whereas previous studies used serially collected blood samples to determine BNP concentration ¹⁹⁰. Therefore, as indicated previously in literature, BNP levels may increase in response to chemotherapy (first 72 hours) but as the damage may be transient, will then decrease and return to a “normal” range compared to persistently high BNP levels only being present in patients with irreversible cardiac dysfunction ^{187,190};
- v) The haemolysis of some patient samples were then looked at as a reason for the exaggerated baseline BNP levels. Haemolysis of a blood sample is defined as the pink or red colour of plasma or serum after centrifugation, specifically a free haemoglobin concentration of more than 0.3g/L ¹⁸². While haemolysis of blood was thought to invalidate the results of biomarker assays owing to a lag time between when peripheral blood was obtained up to its usage, more recent findings have indicated otherwise. Daves *et al.* ¹⁸² demonstrated that moderate haemolysis had no effect on the reliability of cardiac biomarker results. *In vitro* haemolysis occurs in approximately 3.3% of all routinely collected samples and is the leading cause of up to 70% specimen rejection, by laboratories ¹⁸². It is important to quantify the effect of moderately haemolysed samples on cardiac biomarker testing as it has ramifications on the potentially unnecessary rejection of patient specimens and the clinical

management of such patients pertaining to diagnosis and treatment ¹⁸². Essentially, the level of haemolysis needs to be gauged accurately so that severely haemolysed samples that may invalidate biomarker results are discarded.

vi) Epirubicin treatment has been shown to be less cardiotoxic than doxorubicin treatment ². Possibly due to the small number of patients, our sub-study failed to conclude on any treatment-type effect (epirubicin vs. doxorubicin). For instance, out of six patients in the IA cohort, only one patient was treated with epirubicin; and

vii) the lack of an echocardiographic evaluation after chemotherapy preventing the correlation of BNP levels to quantitative measure – routine clinical management of patients in a resource-poor environment does not always include a post-chemotherapy echocardiography.

6.4.2 Recommendations:

This pilot study has been inconclusive about the use of BNP as a measure of irreversible cardiac damage as a result of chemotherapy. However, there is every indication for expanding the study, especially focussing on ethnicities towards establishing valid population-relevant baseline measures, as well as potential changes and factors which influence this, including anthracycline as a chemotherapeutic. This would also be an opportunity to gauge whether Troponin, and perhaps ST2 and other biomarkers may be a better marker of early cardiotoxicity ^{188,192}. The excellent collaboration that has been established with the Department of Cardiology, here at the University of Cape Town for the preliminary study presented here, will facilitate the design of such a comprehensive study.

Chapter 7: Concluding Remarks

Despite genotypes not emerging as a predictor of ACT in this study, the increased susceptibility of the IA population to ACT as well as increased BNP levels after chemotherapy, demands a closer look. Furthermore, the interrogation of IA patient genomes for novel variants of susceptibility to ACT are recommended; this requires building up of a substantial cohort from this population group, which would likely require collaboration with a number of South African health care institutions.

Furthermore, this study illustrates the need for clinical trials for new and existing drugs to be conducted in Africa on local populations. Both the present study and literature^{6,139,140} show that local populations may have both increased risk of adverse drug reactions and/or reduced efficacy compared to their CA counterparts whose risk is already established in historical clinical trials.

The development of both the patient scoring system and statistical model to predict post-chemo LVEF may warrant further development and utilisation in a resource-poor setting.

Findings derived from this study indicate the need for refined patient management of ACT in a South African population to potentially allow for treatment with minimised risk and event-free breast cancer survival.

References

1. Duan, S. et al. Mapping Genes that Contribute to Daunorubicin-Induced Cytotoxicity. *Cancer Research* **67**, 5425-5433 (2007).
2. Horenstein, M.S., Van der Heide, R.S. & L'Ecuyer, T.J. Molecular Basis of Anthracycline-Induced Cardiotoxicity and Its Prevention. *Molecular Genetics and Metabolism* **71**, 436-444 (2000).
3. Leon, E., de Jager, S. & Toop, J. Chemotherapy. in *Oncology for Health-Care Professionals* (eds. Pervan, V., Cohen, L.H. & Jaftha, T.) 197-229 (Juta & Co, Ltd, Cape Town, 1995).
4. FoodAndDrugAdministration. Adriamycin (Doxorubicin HCl) for Injection, USP. (2012).
5. Kumar, S., Marfatia, R., Tannenbaum, S., Yang, C. & Avelar, E. Doxorubicin-Induced Cardiomyopathy 17 years after Chemotherapy. *Texas Heart Institute Journal* **39**, 424-427 (2012).
6. Aminkeng, F. et al. Higher frequency of genetic variants conferring risk for ADRs for commonly used drugs treating cancer, AIDS and tuberculosis in persons of African descent. *The Pharmacogenomics Journal - Nature* **14**, 160-170 (2014).
7. Aminkeng, F. et al. A coding variant in RARG confers susceptibility to anthracycline-induced cardiotoxicity in childhood cancer. *Nat Genet* **47**, 1079-1084 (2015).
8. Wojnowski, L. et al. NAD(P)H oxidase and multidrug resistance protein genetic polymorphisms are associated with doxorubicin-induced cardiotoxicity. *Circulation* **112**, 3754-3762 (2005).
9. Deng, S. & Wojnowski, L. Genotyping the risk of anthracycline-induced cardiotoxicity. *Cardiovascular Toxicology* **7**, 129-134 (2007).
10. Visscher, H. et al. Pharmacogenomic Prediction of Anthracycline-Induced Cardiotoxicity in Children. *Journal of Clinical Oncology* **30**, 1422-1428 (2012).
11. Hershman, D. et al. Racial disparities in treatment and survival among women with early-stage breast cancer. *J Clin Oncol* **23**, 6639-46 (2005).
12. Cascales, A. et al. Association of anthracycline-related cardiac histological lesions with NADPH oxidase functional polymorphisms. *Oncologist* **18**, 446-53 (2013).
13. AmericanCancerSociety. Breast Cancer. (2016).
14. Weiss, J.R., Moysich, K.B. & Swede, H. Epidemiology of Male Breast Cancer. *Cancer Epidemiology Biomarkers & Prevention* **14**, 20-26 (2005).
15. GLOBOCAN 2012: Estimated Cancer Incidence, Mortality and Prevalence Worldwide in 2012. (IARC WHO, 2012).
16. Gianni, L. et al. Anthracycline Cardiotoxicity: From Bench to Bedside. *Journal of Clinical Oncology* **26**, 3777-3784 (2008).
17. Eschenhagen, T. et al. Cardiovascular side effects of cancer therapies: a position statement from the Heart Failure Association of the European Society of Cardiology. *European Journal of Heart Failure* **13**, 1-10 (2011).
18. Valachis, A., Nilsson, C. Cardiac risk in the treatment of breast cancer: assessment and management. *Breast Cancer: Targets and Therapy*, 21-35 (2015).
19. AmericanCancerSociety. Early Detection, Diagnosis and Staging. in *Breast Cancer* (2016).
20. Stedman's Medical Dictionary, (Lippincott Williams & Wilkins, Philadelphia, 2005).
21. Blackhall, F.H., Howell, S. & Newman, B. Pharmacogenetics in the management of breast cancer - prospects for individualised treatment. *Familial Cancer* **5**, 151-157 (2006).

22. Carvalho, C. et al. Doxorubicin: The Good, the Bad and the Ugly Effect. *Current Medicinal Chemistry* **16**, 3267-3285 (2009).
23. Vanderpuye, V.D.N.K., Olopade, O.I. & Huo, D. Pilot Survey of Breast Cancer Management in Sub-Saharan Africa. *Journal of Global Oncology* **3**, 194-200 (2017).
24. Raj, S., Franco, V.I. & Lipshultz, S.E. Anthracycline-Induced Cardiotoxicity: A Review of Pathophysiology, Diagnosis and Treatment. *Curr Treat Options Cardio Med* **16**(2014).
25. Volkova, M., Russell, R. Anthracycline Cardiotoxicity: Prevalence, Pathogenesis and Treatment. *Current Cardiology Reviews* **7**, 214-220 (2011).
26. Mordente, A., Meucci, E., Silvestrini, A., Martorana, G.E. & Giardina, B. New developments in Anthracycline-Induced Cardiotoxicity. *Current Medicinal Chemistry* **16**, 1656-1672 (2009).
27. Thorn, C.F. et al. Doxorubicin pathways: pharmacodynamics and adverse effects. *Pharmacogenetics and Genomics* **21**, 440-446 (2011).
28. National Center for Biotechnology Information. in PubChem Compound Database.
29. Levine, M. The First Pharmacia & Upjohn Pan European Investigators Forum. *Medscape* (2000).
30. Minotti, G., Menna, P., Salvatorelli, E., Cairo, G. & Gianni, L. Anthracyclines: Molecular Advances and Pharmacologic Developments in Antitumor Activity and Cardiotoxicity. *Pharmacological Reviews* **56**, 185-229 (2004).
31. DrugBank. Daunorubicin. (Accessed: 15 January 2018).
32. DrugBank. Valrubicin. (Accessed: 15 January 2018).
33. DrugBank. Mitoxantrone. (Accessed: 15 January 2018).
34. Bains, O.S. et al. Two allelic variants of aldo-keto reductase 1A1 exhibit reduced in vitro metabolism of daunorubicin. *Drug Metab Dispos* **36**, 904-10 (2008).
35. Smith, L. et al. Cardiotoxicity of anthracycline agents for the treatment of cancer: Systematic review and meta-analysis of randomised controlled trials. *BMC Cancer* **10**, 337 (2010).
36. Lipshultz, S.E., Alvarez, J.A. & Scully, R.E. Anthracycline associated cardiotoxicity in survivors of childhood cancer. *Heart* **94**, 525-533 (2008).
37. Dolci, A., Dominici, R., Cardinale, D., Sandri, M.T. & Panteghini, M. Biochemical Markers for Prediction of Chemotherapy-Induced Cardiotoxicity. *American Journal of Clinical Pathology* **130**, 688-695 (2008).
38. Lefrak, E.A., Pitha, J., Rosenheim, S. & Gottlieb, J.A. A clinicopathologic analysis of adriamycin cardiotoxicity. *Cancer* **32**, 302-314 (1973).
39. Jain, D. Cardiotoxicity of doxorubicin and other anthracycline derivatives. *Journal of Nuclear Medicine* **7**, 53-62 (2000).
40. von Hoff, D.D. et al. Risk factors for doxorubicin-induced congestive heart failure. *Annals of Internal Medicine* **91**, 710-717 (1979).
41. Holmgren, G. et al. Identification of novel biomarkers for doxorubicin-induced toxicity in human cardiomyocytes derived from pluripotent stem cells. *Toxicology* **328**, 102-111 (2015).
42. AmericanHeartAssociation. What is Heart Failure. in http://www.heart.org/idc/groups/heart-public/@wcm/@hcm/documents/downloadable/ucm_300315.pdf.
43. McKenna, W.J., Elliot, Perry. The Cardiomyopathies: hypertrophic, dilated, restrictive and right ventricular. in *Oxford Textbook of Medicine* (5 ed.) (ed. Warrell, D.A., Cox, Timothy. M., Firth, John. D) (2015).
44. Wang, X., Sun, C-L., Quinones-Lombrana, A., Singh, Purnima., Landier, W., Hageman, L. et al. CELF4 Variant and Anthracycline-Related Cardiomyopathy: A Children's Oncology Group Genome-Wide Association Study. *Journal of Clinical Oncology* **34**(2016).

45. Mulrooney, D.A. et al. Cardiac outcomes in a cohort of adult survivors of childhood and adolescent cancer: retrospective analysis of the Childhood Cancer Survivor Study cohort. *BMJ* **339**(2009).
46. Grenier, M.A., Lipshultz, S.E. Epidemiology of anthracycline cardiotoxicity in children and adults. *Seminars in Oncology* **25**, 72-85 (1998).
47. Blanco, J.G. et al. Genetic Polymorphisms in the Carbonyl Reductase 3 Gene CBR3 and the NAD(P)H: Quinone Oxidoreductase 1 Gene NQO1 in Patients Who Developed Anthracycline-related Congestive Heart Failure After Childhood Cancer. *Cancer* **112**, 2789-2795 (2008).
48. Kremer, L.C. & Caron, H.N. Anthracycline Cardiotoxicity in Children. *New England Journal of Medicine* **351**, 120-121 (2004).
49. Curigliano, G. et al. Cardiotoxicity of anticancer treatments: Epidemiology, detection, and management. *CA: A Cancer Journal for Clinicians* **66**, 309-325 (2016).
50. Bradshaw, P.T. et al. Cardiovascular Disease Mortality Among Breast Cancer Survivors. *Epidemiology* **27**, 6-13 (2016).
51. Barrett-Lee, P.J., et al. Expert opinion on the use of anthracyclines in patients with advanced breast cancer at cardiac risk. *Annals of Oncology* **20**, 816-827 (2009).
52. Ryberg, M., Nielsen, D. & Skovsgaard, T. Epirubicin cardiotoxicity: an analysis of 469 patients with metastatic breast cancer. *J Clin Oncol* **16**, 3502-3508 (1998).
53. Swain, S.M., Whaley, F.S. & Ewer, M.S. Congestive heart failure in patients treated with doxorubicin: a retrospective analysis of three trials. *Cancer* **97**, 2869-2879 (2003).
54. Von Hoff, D.D., Layard, M.W., Basa, P., et al. Risk factors for doxorubicin-induced congestive heart failure. *Annals of Internal Medicine* **91**, 710-717 (1979).
55. Aminkeng, F. et al. Higher frequency of genetic variants conferring risk for ADRs for commonly used drugs treating cancer, AIDS and tuberculosis in persons of African descent. *The Pharmacogenomics Journal - Nature* **14**, 160-170 (2013).
56. Sandhu, H., Maddock, H. Molecular basis of cancer-therapy-induced cardiotoxicity: introducing microRNA biomarkers for early assessment of subclinical myocardial injury. *Clinical science* **126**, 377-400 (2014).
57. Ebashi, S., . Ohtsuki, I. Troponin: Structure, Function and Dysfunction. in *Regulatory Mechanisms of Striated Muscle Contraction* (2007).
58. Blanco, J.G. et al. Anthracycline-Related Cardiomyopathy After Childhood Cancer: Role of Polymorphisms in Carbonyl Reductase Genes - A Report From the Children's Oncology Group. *Journal of Clinical Oncology* **30**, 1415-1421 (2012).
59. Ashley, N. & Poulton, J. Mitochondrial DNA is a direct target of anti-cancer anthracycline drugs. *Biochemical and Biophysical Research Communications*, **378**, 450-455 (2009).
60. Khasraw, M., Bell, R. & Dang, C. Epirubicin: Is it like doxorubicin in breast cancer? A clinical review. *The Breast* **21**, 142-149 (2012).
61. Price, D.J.A., Wallbridge, D.R. & Stewart, M.J. Tissue Doppler imaging: current and potential clinical applications. *Heart* **84**, ii11-ii18 (2000).
62. Kittiwarawut, A., Vorasettakarnkij Y Fau - Tanasanvimon, S., Tanasanvimon S Fau - Manasnayakorn, S., Manasnayakorn S Fau - Sriuranpong, V. & Sriuranpong, V. Serum NT-proBNP in the early detection of doxorubicin-induced cardiac dysfunction. *Asia Pac J Clin Oncol* **9**, 155-61 (2013).
63. Skovgaard, D., Hasbak, P. & Kjaer, A. BNP Predicts Chemotherapy-Related Cardiotoxicity and Death: Comparison with Gated Equilibrium Radionuclide Ventriculography. *PLoS ONE* **9**, e96736 (2014).

64. Ejection Fraction. (ed. Clinic, C.) (2016).
65. Vorobiof, G. & Silverstein, C. Non-invasive cardiac imaging for evaluation of cardiotoxicity in cancer patients - early detection and follow-up. *SA Heart* **9**, 264-272 (2012).
66. Maleki, M. & Esmaeilzadeh, M. The Evolutionary Development of Echocardiography. *Iranian Journal of Medical Sciences* **37**, 222-232 (2012).
67. Echocardiogram. (ed. Medicine, J.H.) (2016).
68. Blanco, J.G. et al. Anthracycline-Related Cardiomyopathy After Childhood Cancer: Role of Polymorphisms in Carbonyl Reductase Genes - A Report From the Children's Oncology Group. *Journal of Clinical Oncology* **30**, 1415-1421 (2011).
69. Plana, J.C. et al. Expert consensus for multimodality imaging evaluation of adult patients during and after cancer therapy: a report from the American Society of Echocardiography and the European Association of Cardiovascular Imaging. *European Heart Journal - Cardiovascular Imaging* **15**, 1063-1093 (2014).
70. Magnetic Resonance Imaging (MRI) - Cardiac. (2016).
71. van Dalen, E.C., van der Pal, H.J.H., Caron, H.N., Kremer, L.C.M. Different dosage schedules for reducing cardiotoxicity in cancer patients receiving anthracycline chemotherapy. *Cochrane Database of Systematic Reviews* (2009).
72. Van Dalen, E.C., Michiels, E.M., Caron, H.N. & Kremer, L.C. Different anthracycline derivatives for reducing cardiotoxicity in cancer patients. *Cochrane Database System of Review* **5**(2010).
73. Weiss, R.B. The anthracyclines: will we ever find a better doxorubicin? *Seminars in Oncology* **19**, 670-686 (1992).
74. Demain, A.L. & Vaishnav, P. Natural products for cancer chemotherapy. *Microbial biotechnology* **4**, 687-699 (2011).
75. Salvatorelli, E., Menna, Lusini, M., Covino, E. & Minotti, G. Doxorubicinolone formation and efflux: A salvage pathway against epirubicin accumulation in human heart. *Journal of Pharmacology and Experimental Therapeutics* **329**, 175-184 (2009).
76. Hershman, D. & Shao, T. Anthracycline cardiotoxicity after breast cancer treatment. *Oncology* **23**, 227-234 (2009).
77. Lipshultz, S.E. et al. Continuous Versus Bolus Infusion of Doxorubicin in Children With ALL: Long-term Cardiac Outcomes. *Pediatrics* **130**, 1003-1011 (2012).
78. Bovelli, D., Plataniotis, G., Roila, F. & On behalf of the, E.G.W.G. Cardiotoxicity of chemotherapeutic agents and radiotherapy-related heart disease: ESMO Clinical Practice Guidelines. *Annals of Oncology* **21**, v277-v282 (2010).
79. Kunicka, T. et al. Non-coding Polymorphisms in Nucleotide Binding Domain 1 in ABCC1 Gene Associate with Transcript Level and Survival of Patients with Breast Cancer. *PLoS ONE* **9**(2014).
80. Ng, P.C. & Henikoff, S. SIFT: predicting amino acid changes that affect protein function. *Nucleic Acids Research* **31**, 3812-3814 (2003).
81. Flicek, P. et al. Ensembl2014. *Nucleic Acids Research* **42**, D749-D755 (2014).
82. ENCODE. An integrated encyclopedia of DNA elements in the human genome. *Nature* **489**, 57-74 (2012).
83. PharmGKB. PharmGKB- The Pharmacogenomics Knowledgebase. (Stanford University, 2001-2016).
84. Aminkeng, F. et al. Pharmacogenomic screening for anthracycline-induced cardiotoxicity in childhood cancer. *Br J Clin Pharmacol* **83**, 1143-1145 (2017).
85. Zhang, S. et al. Identification of the molecular basis of doxorubicin-induced cardiotoxicity. *Nat Med* **18**, 1639-42 (2012).

86. WeizmannInstituteofScience. GeneCards^R Human Gene Database. (1996-2016).
87. Lipshultz, S.E. et al. Impact of hemochromatosis gene mutations on cardiac status in doxorubicin-treated survivors of childhood high-risk leukemia. *Cancer* **119**, 3555-3562 (2013).
88. Cairo, G., Recalcati, S.,. Iron-regulatory proteins: molecular biology and pathophysiological implications. *Expert Reviews in Molecular Medicine* **9**(2007).
89. Picano, E. Economic and biological costs of cardiac imaging. *Cardiovascular Ultrasound* **3**(2005).
90. World Bank and Lending Groups. (2016).
91. What are the costs or price of Echocardiograms?
92. How much does a troponin test cost?
93. Heidenreich, P.A. et al. Cost-effectiveness of screening with B-type natriuretic peptide to identify patients with reduced left ventricular ejection fraction. *Journal of the American College of Cardiology* **43**, 1019-1026 (2004).
94. Brouwer, E.D. et al. Provider costs for prevention and treatment of cardiovascular and related conditions in low- and middle-income countries: a systematic review. *BMC Public Health* **15**, 1-17 (2015).
95. Smallhorne, M. The true cost of cancer. in *Fin24* (2013).
96. Younis, T., Rayson, D. & Skedgel, C. The cost-utility of adjuvant chemotherapy using docetaxel and cyclophosphamide compared with doxorubicin and cyclophosphamide in breast cancer. *Current Oncology* **18**, e288-e296 (2011).
97. Ojeda, B., de Sande, L.M., Casado, A., Merino, P. & Casado, M.A. Cost-minimisation analysis of pegylated liposomal doxorubicin hydrochloride versus topotecan in the treatment of patients with recurrent epithelial ovarian cancer in Spain. *Br J Cancer* **89**, 1002-7 (2003).
98. Bates, M., Lieu, D., Zagari, M., Spiers, A. & Williamson, T. A pharmacoeconomic evaluation of the use of dexrazoxane in preventing anthracycline-induced cardiotoxicity in patients with stage IIIB or IV metastatic breast cancer. *Clin Ther.* **19**, 167-84 (1997).
99. Dunlay, S.M. et al. Lifetime Costs of Medical Care After Heart Failure Diagnosis. *Circulation: Cardiovascular Quality and Outcomes* **4**, 68-75 (2011).
100. GraphPad Prism version 5.00 for Windows. in *GraphPad Software 5 edn* (San Diego California USA).
101. R_Core_Team. R: A language and environment for statistical computing. (ed. Computing, R.F.f.S.) (Vienna Austria, 2015).
102. Kruglyak, L. & Nickerson, D.A. Variation is the spice of life. *Nature Genetics* **27**, 234-236 (2001).
103. Brookes, A.J. The essence of SNPs. *Gene* **234**, 177-186 (1999).
104. Rebello, G. *Gene Annotation script*. (1997).
105. Leong, S.L., Chaiyakunapruk, N. & Lee, S.W. Candidate Gene Association Studies of Anthracycline-induced Cardiotoxicity: A Systematic Review and Meta-analysis. *Sci Rep* **7**, 39 (2017).
106. Rajic, V. et al. Influence of the polymorphism in candidate genes on late cardiac damage in patients treated due to acute leukemia in childhood. *Leuk. Lymphoma* **50**, 1693-8 (2009).
107. WorldMedicalAssociation. World Medical Association Declaration of Helsinki: ethical principles for medical research involving human subjects. *JAMA* **310**, 2191-4 (2013).
108. GreinerBioOneInternational. K3E K3EDTA. in *EDTA Vol. 2016* (2016).
109. Miller, S.A., Dykes, D.D. & Polesky, H.F. A simple salting out procedure for extracting DNA from human nucleated cells. *Nucleic Acids Research* **16**, 1215 (1988).

110. Aaij, C., Borst, P. The Gel Electrophoresis of DNA. *Biochemica et Biophysica Acta - Nucleic Acids and Protein Synthesis* **269**, 192-200 (1972).
111. ThermoFisherScientific. Technical Reference Library. (2016).
112. Saiki, R.K., et al. Primer-directed enzymatic amplification of DNA with a thermostable DNA polymerase. *Science* **239**(1988).
113. EncyclopædiaBritannicaOnline. Polymerase Chain Reaction. (2016).
114. Ralser, M., Querfurth, R., Warnatz, H-J., Lehrach, H., Yaspo, M-L., Krobisch, S. An efficient and economic enhancer mix for PCR. *Biochemical and Biophysical Research Communications* **347**, 747-751 (2006).
115. Frackman, S., Kobs, G., Simpson, D., Storts, D. Betaine and DMSO: Enhancing Agents for PCR. *Promega Notes* **65**, 27 (1998).
116. Promega. PCR Amplification. in Resources (2016).
117. Korbie, D.J. & Mattick, J.S. Touchdown PCR for increased specificity and sensitivity in PCR amplification. *Nat. Protocols* **3**, 1452-1456 (2008).
118. ABM. Polymerase Chain Reaction (PCR) - Variations to the System. in Knowledge_Base (2015).
119. ThermoFisherScientific. SNaPshot Multiplex System for SNP Genotyping. in Product Bulletin (Applied Biosystems, 2012).
120. ThermoFisherScientific. FastAP Thermosensitive Alkaline Phosphatase (1 U/μL). in PCR & Cloning Enzymes (2016).
121. ThermoFisherScientific. GeneScan™ 120 LIZ™ dye Size Standard. in DNA/RNA Ladders (2016).
122. ThermoFisherScientific. SNP Genotyping Analysis Using TaqMan® Assays. in Real-Time PCR Assays Vol. 2016 (Applied Biosystems, 2014).
123. Sanger, F., Nicklen, S., Coulson, A.R. DNA Sequencing with chain-terminating inhibitors. *Proc. Natl. Acad. Sci* **74**, 5463-5467 (1977).
124. Zeugin, J.A., Hartley, J.L. Ethanol Precipitation of DNA. *Focus* **7**, 1-2 (1985).
125. Hall, T.A. BioEdit: a user-friendly biological sequence alignment editor and analysis program for Windows for 95/98/NT. *Nucl. Acids. Symp. Ser* **41**, 95-98 (1999).
126. Introduction to SAS. (ed. Group, U.S.C.).
127. Krim, S.R. et al. Racial/Ethnic Differences in B-Type Natriuretic Peptide Levels and Their Association with Care and Outcomes Among Patients Hospitalized with Heart Failure: Findings From Get With The Guidelines - Heart Failure. *JACC: Heart Failure* **1**, 345-352 (2013).
128. Fisher, R.A. & Yates, F. Statistical Tables for Biological Agricultural and Medical Research. (Oliver & Boyd, Ltd., Edinburgh).
129. Szumilas, M. Explaining Odds Ratios. *Journal of the Canadian Academy of Child and Adolescent Psychiatry* **19**, 227-229 (2010).
130. Montana, G. Statistical methods in genetics. *Briefings in Bioinformatics* **7**, 297-308 (2006).
131. Li, Z. et al. A partition-ligation-combination-subdivision EM algorithm for haplotype inference with multiallelic markers: update of the SHESis (<http://analysis.bio-x.cn>). *Cell Res* **19**, 519-523 (2009).
132. Shi, Y.Y. & He, L. SHESis, a powerful software platform for analyses of linkage disequilibrium, haplotype construction, and genetic association at polymorphism loci. *Cell Res* **15**, 97-98 (2005).
133. Calculator.net.
134. Steyn, R., Boniaszczuk, J. & Geldenhuys, T. Comparison of estimates of left ventricular ejection fraction obtained from gated blood pool imaging, different software packages and cameras. *Cardiovascular Journal of Africa* **25**, 44-49 (2014).
135. Romero, A. et al. Glutathione S-transferase P1 c.313A>G polymorphism could be useful in the prediction of doxorubicin response in breast cancer patients. *Annals of Oncology*, 1-7 (2011).

136. Cheung, Y.-f. et al. Plasma High Sensitivity Troponin T Levels in Adult Survivors of Childhood Leukaemias: Determinants and Associations with Cardiac Function. *PLoS ONE* **8**, e77063 (2013).
137. Vulsteke, C., Lambrechts, D., Dieudonne', A., Hatse, S., Brouwers, B., van Brussel, T., Neven, P., Belmans, A., Schoffski, P., Paridaens, R., Wildiers, H. Genetic variability in the multidrug resistance associated protein-1 (ABCC1/MRP1) predicts hematological toxicity in breast cancer patients receiving (neo-)adjuvant chemotherapy with 5-fluorouracil, epirubicin and cyclophosphamide (FEC). *Ann Oncol* **24**, 1513-25 (2013).
138. Altschul, S.F., Gish W Fau - Miller, W., Miller W Fau - Myers, E.W., Myers Ew Fau - Lipman, D.J. & Lipman, D.J. Basic local alignment search tool. *J Mol Bio* **215**, 403-410 (1990).
139. Lal, S. et al. Novel SLC22A16 polymorphisms and influence on doxorubicin pharmacokinetics in Asian breast cancer patients. *Pharmacogenomics* **8**, 567-575 (2007).
140. Fan, L. et al. Genotype of human carbonyl reductase CBR3 correlates with doxorubicin disposition and toxicity. *Pharmacogenetics and Genomics* **18**, 621-631 (2008).
141. Pickering, R. *The Use of Forensic Anthropology*, (CRC Press, 2009).
142. Tian, C., Gregersen, P.K. & Seldin, M.F. Accounting for ancestry: population substructure and genome-wide association studies. *Human Molecular Genetics* **17**, R143-R150 (2008).
143. *Cancer Statistics*. (ed. Health, N.I.f.O.) (2012).
144. Kruger, W.M. & Apffelstaedt, J.P. Young breast cancer patients in the developing world: incidence, choice of surgical treatment and genetic factors. *SA Fam Pract* **49**, 18-24 (2007).
145. Gabriel, C.A. & Domchek, S.M. Breast Cancer in Young Women. *Breast Cancer Research* **12**, 212 (2010).
146. Morris, A.G. Fatter and fatter: South Africa's rise in body mass index. *S Afr J Sci* **107**(2011).
147. Rahman, M. & Berenson, A.B. Accuracy of current body mass index obesity classification for white, black and Hispanic reproductive-age women. *Obstetrics and gynecology* **115**, 982-988 (2010).
148. Reinbolt, R.E. et al. Risk factors for anthracycline-associated cardiotoxicity. *Supportive care in cancer : official journal of the Multinational Association of Supportive Care in Cancer* **24**, 2173-2180 (2016).
149. Tan, T.C. & Scherrer-Crosbie, M. Assessing the Cardiac Toxicity of Chemotherapeutic Agents: Role of Echocardiography. *Current cardiovascular imaging reports* **5**, 403-409 (2012).
150. Jiji, R.S., Kramer, C.M. & Salerno, M. Non-invasive imaging and monitoring cardiotoxicity of cancer therapeutic drugs. *Journal of Nuclear Cardiology* **19**, 377-388 (2012).
151. Mornos, C. et al. The value of left ventricular global longitudinal strain assessed by three-dimensional strain imaging in the early detection of anthracyclinemediated cardiotoxicity. *Hellenic Journal of Cardiol* **55**, 235-244 (2014).
152. National Cancer Institute: Cancer Therapy Evaluation Program: Common Terminology Criteria for Adverse Events, Version 3.
153. AmericanCancerSociety. *Cancer Facts and Figures 2012*. (American Cancer Society, Atlanta, 2012).
154. AVERT. *HIV and AIDS in South Africa*. (2015).
155. Damasceno, A., Cotter G Fau - Dzudie, A., Dzudie A Fau - Sliwa, K., Sliwa K Fau - Mayosi, B.M. & Mayosi, B.M. Heart failure in sub-saharan Africa: time for action. *J Am Coll Cardiol* **50**, 1688-1693 (2007).

156. Bloomfield, G.S., Barasa, F.A., Doll, J.A. & Velazquez, E.J. Heart Failure in Sub-Saharan Africa. *Current Cardiology Reviews* **9**, 157-173 (2013).
157. May, A. et al. Genetic diversity in black South Africans from Soweto. *BMC Genomics* **14**, 644-644 (2013).
158. Semsei, A.F. et al. ABCC1 polymorphisms in anthracycline-induced cardiotoxicity in childhood acute lymphoblastic leukaemia. *Cell Biology International* **36**, 79-86 (2012).
159. Vulsteke, C. et al. Clinical and genetic risk factors for epirubicin-induced cardiac toxicity in early breast cancer patients. *Breast Cancer Research and Treatment* **152**, 67-76 (2015).
160. Brown, S.-A., Sandhu, N. & Herrmann, J. Systems biology approaches to adverse drug effects: the example of cardio-oncology. *Nat Rev Clin Oncol* **12**, 718-731 (2015).
161. Lipshultz, S.E. et al. Predictive Value of Cardiac Troponin T in Pediatric Patients at Risk for Myocardial Injury. *Circulation* **96**, 2641-2648 (1997).
162. Chen, J.J., Wu, P.T., Middlekauff, H.R. & Nguyen, K.-L. Aerobic Exercise in Anthracycline-Induced Cardiotoxicity: A Systematic Review of Current Evidence and Future Directions. *American Journal of Physiology - Heart and Circulatory Physiology* (2016).
163. Scott, J.M. et al. Modulation of Anthracycline-Induced Cardiotoxicity by Aerobic Exercise in Breast Cancer: Current Evidence and Underlying Mechanisms. *Circulation* **124**, 642-650 (2011).
164. Gupta, D.K. et al. Racial Differences in Circulating Natriuretic Peptide Levels: The Atherosclerosis Risk in Communities Study. *J Am Heart Assoc* **4**, 1-8 (2015).
165. Dodos, F., Halbsguth, T., Erdmann, E. & Hoppe, U. Usefulness of myocardial performance index and biochemical markers for early detection of anthracycline-induced cardiotoxicity in adults. *Clinical Research in Cardiology* **97**, 318-326 (2008).
166. Villacorta, H. & Maisel, A.S. Soluble ST2 Testing: A Promising Biomarker in the Management of Heart Failure. *Arquivos Brasileiros de Cardiologia* **106**, 145-152 (2016).
167. Kouloubinis, A. et al. ProANP and NT-proBNP levels to prospectively assess cardiac function in breast cancer patients treated with cardiotoxic chemotherapy. *Int J Cardiol* **122**, 195-201 (2007).
168. Biomedica. BNP Fragment EIA. in *Enzyme Immunoassay for the Quantitative Determination of BNP Fragment in Human Serum, Citrate Plasma, EDTA Plasma or Heparin Plasma* 1-12 (2013).
169. NovartisPharmaceuticals. *Heart Failure*. (2015).
170. Suzuki, T., Yamazaki, T., Yazaki, Y. The role of the natriuretic peptides in the cardiovascular system in *Cardiovascular Research* (ed. Sipido, K.R.) 489-494 (2001).
171. Mueller, T., Gegenhuber, A., Poelz, W. & Haltmayer, M. Comparison of the Biomedica NT-proBNP Enzyme Immunoassay and the Roche NT-proBNP Chemiluminescence Immunoassay: Implications for the Prediction of Symptomatic and Asymptomatic Structural Heart Disease. *Clinical Chemistry* **49**, 976-979 (2003).
172. Soon, E. et al. Log-transformation improves the prognostic value of serial NT-proBNP levels in apparently stable pulmonary arterial hypertension. *Pulmonary Circulation* **1**, 244-249 (2011).
173. Ichiki, T., Huntley, B.K. & Burnett Jr, J.C. BNP Molecular Forms and Processing by the Cardiac Serine Protease Corin. *Adv Clin Chem.* **61**, 1-31 (2013).

174. Seino, Y. et al. Application of NT-proBNP and BNP measurements in cardiac care: a more discerning marker for the detection and evaluation of heart failure. *European Journal of Heart Failure* **6**, 295-300 (2004).
175. Maisel, A.S. et al. Rapid measurement of B-type natriuretic peptide in the emergency diagnosis of heart failure. *New England Journal of Medicine* **347**, 161-167 (2002).
176. Auner, H.W., Tinchon, C. & Linkesch, W. Prolonged monitoring of troponin T for the detection of anthracycline cardiotoxicity in adults with hematological malignancies. *Annals of Hematology* **82**, 218-222 (2003).
177. Shave, R. et al. Exercise-Induced Cardiac Troponin Elevation Evidence, Mechanisms, and Implications. *Journal of the American College of Cardiology* **56**, 169-176 (2010).
178. Lequin, R.M. Enzyme Immunoassay (EIA)/Enzyme-Linked Immunosorbent Assay (ELISA). *Clinical Chemistry* **51**, 2415-2418 (2005).
179. SinoBiologicalInc. ELISA Principle. in *ELISA Encyclopedia*.
180. Engvall, E. & Perlmann, P. Enzyme-linked immunosorbent assay (ELISA) quantitative assay of immunoglobulin G. *Immunochemistry* **8**, 871-874 (1971).
181. Abnova. Support - Resources. in *ELISA Pairs Kit* (2016).
182. Daves, M. et al. Influence of hemolysis on routine laboratory cardiac marker testing. *Clin Lab* **58**, 333-6 (2012).
183. Min, H., Liang, R., Ming, C. & Yan, C. Modeling and optimizing of 4PL routing optimization problem based on goal programming. *Proceedings of the 25th Chinese Control and Decision Conference (CCDC '13)*, 2348-2352 (2013).
184. Gurney, H. How to calculate the dose of chemotherapy. *British Journal of Cancer* **86**, 1297-1302 (2002).
185. Gulati, G. et al. Prevention of cardiac dysfunction during adjuvant breast cancer therapy (PRADA): a 2 x 2 factorial, randomized, placebo-controlled, double-blind clinical trial of candesartan and metoprolol. *European Heart Journal* **37**, 1671-1680 (2016).
186. Yun, S., Vincelette, N.D. & Abraham, I. Cardioprotective role of B-blockers and angiotensin antagonists in early-onset anthracyclines-induced cardiotoxicity in adult patients: a systematic review and meta-analysis. *Postgrad Med J* **91**, 627-633 (2015).
187. Suzuki, T. et al. Elevated B-type natriuretic peptide levels after anthracycline administration. *Am Heart J* **136**, 362-363 (1998).
188. Sandri, M.T. et al. N-terminal pro-B-type natriuretic peptide after high-dose chemotherapy: a marker predictive of cardiac dysfunction? *Clin Chem* **51**, 1405-1410 (2005).
189. Romano, S. et al. Serial measurements of NT-proBNP are predictive of not-high-dose anthracycline cardiotoxicity in breast cancer patients. *Br J Cancer* **105**, 1663-1668 (2011).
190. Aydogan, M. et al. The reasons of higher NT-proBNP depend on very different conditions. *Annals of the Rheumatic Diseases* (2013).
191. Daubert, M.A. & Jeremias, A. The utility of troponin measurement to detect myocardial infarction: review of the current findings. *Vasc Health Risk Manag* **6**, 691-699 (2010).
192. Squara, P., Estagnasie, P., Belliard, O., Squara, F. & Dib, J.C. Preload Reserve is Restored in Patients with Decompensated Chronic Heart Failure who Respond to Treatment. *Congestive Heart Failure* **19**, 207-213 (2013).

Appendices

Appendix A: Gene Annotation and Primer Design Protocol

Before annotation of your genes, you will need to prepare files and your information will come from NCBI and Ensembl.

It is simplest to create a gene annotation folder, and create subfolders of each gene of interest which will contain the files specific to that gene.

NCBI (www.ncbi.nih.gov)

- Navigate to the NCBI website
- Select Gene under “All Databases” and type the gene name in the search box
- Select for the Homo Sapiens in your gene search results
- This will open a page with a “Summary” for the gene
- Copy and Paste the gene summary (until Genomic Context) into a Word Document and label it GeneName_Summary and save in the specific gene folder that you already created. Save and Close
- Scroll down to Genomic Regions, Transcripts and Products and make sure the Reference Sequence Primary Assembly is selected and select Genbank where “Go to Nucleotide” is shown
- This will open a page with the gene details followed by the sequence (the selected region should be sufficient for SNP genotyping purposes)
- Copy the page from “LOCUS....” Till “//” and paste in Notepad and save in your gene folder as GeneName.seq
- The SEQ file must be edited to allow for accurate annotation later so please do the following:
 - o Note the Gene ID, the orientation of the strand and transcript ID – this information can be gathered from the NCBI gene page that you first navigated to as well as the link on that page called “SNP: GeneView”
 - o SNP:GeneView will also allow you to double check the validity of your SNPs as well as orientation and transcript ID
 - o With this information, go through the gene, mRNA, CDS, misc_RNA info and for those with different gene and transcript IDs, insert a space...for example mRNA becomes m RNA etc. Also, spaces can be inserted to STS if any
 - o Save and close when done – this file is ready for annotation

Ensembl (www.ensembl.org)

- Navigate to the Ensembl website
- Under “All Species” select Human and type the gene name in the Search Box next to it
- Find the version of the gene you require and select (ie Human Gene version)
- This will open up a page where a Transcript table is visible, find the longest transcript (Note down the Gene ID (ENSG...), Transcript ID (ENST...) and orientation of strand for later)

- Select the longest transcript
- On the left hand side of the page, click on “Export Data” which will open a pop-up, select the following:
 - o Select GenBank format
 - o Select Feature Strand
 - o Select 10000 bases upstream and 10000 bases downstream
 - o Under “Options for GenBank”, select only “Variation Features”, “Marker Features” and “Gene Information”
 - o Click Next
 - o Select Text
- This will open up another page in your browser with the required information
- Select all, copy and paste into Notepad. Save the file in your gene folder as GeneName.e.seq
- Again, this SEQ file must be edited before annotation:
 - o With the Gene and Transcript IDs noted earlier, go through the text and insert spaces to genes, mRNA, misc_RNA that are not needed
 - o Save and Close

PERLV5

For the PerlV5 first timer:

After installing PerlV5 on your laptop or PC

Create a PerlV5 folder in your C drive, every time you create new NCBI and Ensembl gene SEQ files, add them to this folder (after editing!)

- Click the start icon, search for cmd and select
- This opens up the command line for Windows
- For command line: cd.. will navigate you back a directory; to check what is in a directory you may type in dir
- Navigate to the C:\>
- You may check if your PerlV5 folder is there by typing dir so that it looks like this C:\>dir and press Enter
- If your PerlV5 folder shows on the list then you may proceed further
- Type in cd perl5 so that it looks like this **C:\>cd perl5**, press Enter
- Type in pre-perl so that it looks like this **C:\Perl5>pre-perl**, press Enter
- The next line will look like this **C:\Perl5>**
- You are ready to annotate!
- For NCBI:
 - o For forward strand orientation (plus strand), type the following:
 - o perl annotv9.pl gene.seq gene.annot s
 - o it will look like this: **C:\Perl5>perl annotv9.pl gene.seq gene.annot s**
 - o Press Enter and if the next line is **C:\Perl5>** then it has worked!
 - o For reverse strand orientation (minus strand), type the following:
 - o perl annotv9.pl gene.seq gene.annot sr
 - o it will look like this: **C:\Perl5>perl annotv9.pl gene.seq gene.annot sr**
 - o Press Enter and if the next line is **C:\Perl5>** then it has worked!

- For Ensembl:
 - For forward strand orientation, type the following:
 - perl annotv9ev2.pl genee.seq genee.annot s
 - it will look like this: **C:\Perl5>perl annotv9ev2.pl genee.seq genee.annot s**
 - Press Enter and if the next line is **C:\Perl5>** then it has worked!
 - For reverse strand orientation, type the following:
 - perl annotv9ev2.pl genee.seq genee.annot sr
 - it will look like this: **C:\Perl5>perl annotv9ev2.pl genee.seq genee.annot sr**
 - Press Enter and if the next line is **C:\Perl5>** then it has worked!

Appendix B: Informed Consent

Consent Document

Consent to Participate in Research:

Good Day Madam/Sir

Prof Raj Ramesar (Human Genetics, UCT), A/Prof H. Simonds (Radiation Oncology, Tygerberg Hospital) and Miss H.Naidoo (Human Genetics, UCT) will be the researchers on this study. Miss H.Naidoo will be using this research project to obtain her Doctorate.

This study will focus on damage caused to the heart by chemotherapy and its genetic basis.

You have been asked to participate in this research study by allowing us access to two tubes of your blood to run tests on and allow us access to your medical history so that we may monitor your response to treatment. Your samples will be stored securely in the Human Genetics Laboratory with access only to the investigators for a period of 3 years. At the end of the study, all samples will be destroyed. Patient samples will not be used for other studies unless new ethical approval is applied for and obtained.

Your HIV status will be made available only to the researchers and will be kept confidential.

Your personal and medical details will be kept confidential and you will remain anonymous in the study. You will not be at any risk by being part of this study and will not need to pay any money for the additional laboratory tests. One extra tube of blood at diagnosis and again after 3 cycles of chemotherapy will be taken with your routine blood draw at no extra risk. The unlikely risks of any blood draw include: pain, infection, bruising and minor bleeding after blood is taken.

Your participation in this research is voluntary and you will not be given any compensation for your involvement in the study. Furthermore, you will not be penalized or lose benefits if you refuse to participate or decide to stop at any time. If you agree to participate, you will be given a signed copy of this document and information about the research.

The benefit of this study will be information on the genes responsible for damage to the heart when cancer patients receive chemotherapy.

You have been informed about the study by.....

You may contact Horacia Naidoo at 021 406 6501 at any time if you have questions about the research. You may also contact the Human Research Ethics Committee if you have any concerns or queries on 021 406 6338 or email sumayah.ariefdien@uct.ac.za.

The research study, including the above information, has been described to me orally. I understand what my involvement in the study means and I voluntarily agree to participate. I have been given an opportunity to ask any questions that I might have about participation in the study.

Please tick if you agree to allow us to run more tests on your blood samples _____

Please tick if you agree to allow us access to your medical files _____

.....
Signature of Participant	Date

.....
Signature of Translator (if applicable)	Date

.....
Signature of Witness	Date

Appendix C: Ethics Approval – UCT

UNIVERSITY OF CAPE TOWN



Faculty of Health Sciences
Faculty of Health Sciences Human Research Ethics Committee
Room E52-24 Groote Schuur Hospital Old Main Building
Observatory 7925
Telephone [021] 406 6338 • Facsimile [021] 406 6411
e-mail: sumayah.ariefeldien@uct.ac.za
www.health.uct.ac.za/research/humanethics/forms

08 February 2013

HREC REF: 650/2012

Ms H Naidoo
c/o Prof R Ramesar
Human Genetics
FHS

Dear Ms Naidoo

PROJECT TITLE: THE GENETICS OF ANTHRACYCLINE-INDUCED CARDIOTOXICITY IN CANCER PATIENTS

Thank you for addressing the issues raised by the committee.

It is a pleasure to inform you that the HREC has formally approved the above mentioned study.

Approval is granted for one year till the 28 February 2014.

Please submit a progress form, using the standardised Annual Report Form, if the study continues beyond the approval period. Please submit a Standard Closure form if the study is completed within the approval period.

Please note that the ongoing ethical conduct of the study remains the responsibility of the principal investigator.

Please quote the REC. REF in all your correspondence.

Yours sincerely

signature removed

PROFESSOR M BLOCKMAN
CHAIRPERSON, HSF HUMAN ETHICS

Federal Wide Assurance Number: FWA00001637.
Institutional Review Board (IRB) number: IRB00001938

sAriefeldien

Appendix D: Ethics Approval – GSH



GROOTE SCHUUR HOSPITAL

Enquiries: Dr Bhavna Patel

E-mail : Bhavna.Patel@westerncape.gov.za

Ms Horacia Naidoo
C/o Dr Hannah Simonds
Radiation Oncology Department
LE33 – New Main Building

E-mail: Hannah.simonds@uct.ac.za & raj.ramesar@uct.ac.za

Dear Ms Naidoo

RESEARCH: The Genetics of Anthracycline-induced Cardiotoxicity in Cancer Patients

Your recent letter to the hospital refers.

You are hereby granted permission to proceed with your research.

Please note the following:

- a) Your research may not interfere with normal patient care
- b) Hospital staff may not be asked to assist with the research.
- c) No hospital consumables and stationary may be used.
- d) **No patient folders may be removed from the premises or be inaccessible.**
- e) Please introduce yourself to the person in charge of an area before commencing.
- f) Please discuss the study with the Head of Radiation Oncology before commencing.
- g) Confidentiality must be maintained at all times.

I would like to wish you every success with the project.

Yours sincerely

signature removed

DR BHAVNA PATEL
SENIOR MANAGER: MEDICAL SERVICES
Date: 15 February 2013

C.C. Dr B. Eick
Professor R. Abratt

G46 Management Suite, Old Main Building,
Observatory 7925

Private Bag X,
Observatory, 7935

Appendix E: Ethics Approval – SUN/TBH



UNIVERSITEIT • STELLENBOSCH • UNIVERSITY
jou kennisvennoot • your knowledge partner

Approval Notice

New Application

25-Mar-2015
Naidoo, Horacia H

Ethics Reference #: S15/02/032

Title: The genetics of anthracycline-induced cardiotoxicity in cancer patients.

Dear Ms Horacia Naidoo,

The **New Application** received on 27-Feb-2015, was reviewed by members of **Health Research Ethics Committee 2** via Expedited review procedures on 18-Mar-2015 and was approved.

Please note the following information about your approved research protocol:

Protocol Approval Period: 25-Mar-2015 -25-Mar-2016

Please remember to use your **protocol number** (S15/02/032) on any documents or correspondence with the HREC concerning your research protocol.

Please note that the HREC has the prerogative and authority to ask further questions, seek additional information, require further modifications, or monitor the conduct of your research and the consent process.

After Ethical Review:

Please note a template of the progress report is obtainable on www.sun.ac.za/rds and should be submitted to the Committee before the year has expired. The Committee will then consider the continuation of the project for a further year (if necessary). Annually a number of projects may be selected randomly for an external audit.

Translation of the consent document to the language applicable to the study participants should be submitted.

Federal Wide Assurance Number: 00001372
Institutional Review Board (IRB) Number: IRB0005239

The Health Research Ethics Committee complies with the SA National Health Act No.61 2003 as it pertains to health research and the United States Code of Federal Regulations Title 45 Part 46. This committee abides by the ethical norms and principles for research, established by the Declaration of Helsinki, the South African Medical Research Council Guidelines as well as the Guidelines for Ethical Research: Principles Structures and Processes 2004 (Department of Health).

Provincial and City of Cape Town Approval

Please note that for research at a primary or secondary healthcare facility permission must still be obtained from the relevant authorities (Western Cape Department of Health and/or City Health) to conduct the research as stated in the protocol. Contact persons are Ms Claudette Abrahams at Western Cape Department of Health (healthres@pgwc.gov.za Tel: +27 21 483 9907) and Dr Helene Visser at City Health (Helene.Visser@capetown.gov.za Tel: +27 21 400 3981). Research that will be conducted at any tertiary academic institution requires approval from the relevant hospital manager. Ethics approval is required BEFORE approval can be obtained from these health authorities.

We wish you the best as you conduct your research.

For standard HREC forms and documents please visit: www.sun.ac.za/rds

Appendix F: Reagent Preparation

Primer Preparation:

1x TE Buffer:

10mM Tris added to 1mM EDTA at pH 8.0 makes up a 10x TE Buffer stock solution. A dilution of 1:10 with distilled water will produce 1x TE Buffer.

DNA Isolation:

Red Blood Cell Lysis Buffer (RBC Lysis Buffer):

8.28g of Ammonium Chloride (NH_4Cl), 0.79g of Ammonium Bicarbonate powder (NH_4HCO_3), 0.2ml of EDTA (0.5M, pH 7.4) made up to 1L with distilled water.

- 0.5M EDTA:

18.612g of EDTA in 60ml of dH_2O , adjust pH to 7.4 and make up to total volume of 100ml.

Cell Lysis Buffer:

25ml of Tris-HCl (1M, pH 7.5), 16.7ml of 3M NaCl and 1ml of 0.5 M EDTA made up to 500ml with distilled water.

- 1M Tris-HCl:

12.1g of Tris in 60ml of dH_2O , adjust pH to 7.5 and make up to total volume of 100ml

- 3M NaCl:

17.532g of NaCl in 100ml of dH_2O

- 0.5M EDTA:

18.612g of EDTA in 60ml of dH_2O , adjust pH to 7.4 and make up to total volume of 100ml

20% SDS:

2g Sodium Dodecyl Sulfate in 10ml of dH_2O

20mg/ml Proteinase K:

0.02g Proteinase K in 1000ul of 1mM CaOAc at pH 8

6M NaCl:

35.064 g NaCl in 100ml of dH₂O

Agarose Gel Electrophoresis:

10x Tris-Borate-EDTA (TBE) Buffer:

108g Tris, 55g Boric Acid and 7.4g EDTA (pH 8) made up to 1L using distilled water.

Appendix G: Multiplex PCR Protocol

Aim of the experiment: Allow for the exponential amplification of a targeted sequence for SNaPshot Genotyping

	bp	tm	cond	Change/exp peak	
HNMT	325	55		C/A (black to green)	MXA
ABCC2 rs818	572			G/A (blue to green)	
RAC2	341	56		A/T (green to red)	MXB
NCF4	725			G/A (blue to green)	
ABCC1 rs246	595	60	Tchdwn, Gly	A/G (green to blue)	MXC
*ABCC2 rs172	761			A/T (green to red)	

Date:

Preparation of Mastermix

Materials:

	Volume for 1 reaction (µl) – 1x	Volume for mastermix (µl) - x	Volume of Mastermix (ul) – x	Volume of Mastermix (ul) – x
Taq Reaction Buffer (5X)	5 (1X)			
dNTPs (5mM)	1 (200uM)			
MgCl ₂ (50mM/ul)	1.5 (1mM)			
F and R primer (20uM)	0.5 each (10pmol each)			
Glycerol	0 or 0.25			
dH ₂ O	14.4 or 14.15			
Taq Polymerase (5U/ul)	0.1 (0.02U/ul)			
DNA template (100ng/ul)	2 (100ng)			
TOTAL	25			

- DNA samples and 1 negative control (water)
- Clean bench area with biocide; have all reagents on ice
- Set up master-mix without DNA and remember to add Taq last
- Add 23µl master mix to each PCR tube or plate as well as 2µl of DNA template
- Include a **control** containing 2µl master-mix and 2µl of dH₂O
- Edit the machine program: 94°C for 3min, 94°C for 3sec, **T_m = 55°C for MX1, 2, & 3, T_m = 58°C for MX4, T_m = 60°C for MX5, T_m = 60°C touchdown for MX6 and Singleplex**
- 72°C for 1min repeated for 30 cycles
- 72°C for 10min at the end
- Set the sample volume to 25µl and Run!
- Once completed – remove samples of PCR products. Use in the designated post-PCR areas or store in the fridge appropriately. Post PCR area= Zone

Electrophoresis of PCR products for correct temp

Materials:

- Loading Dye - Thermoscientific (Lot No: 00148043)
- 1x TBE Tank Buffer
- Molecular Weight Marker-Thermoscientific (Lot No: 00149428)
- NuSieve Agarose – Lonza (ME, USA) (Lot No: 0000313053)

For 3% (w/v) Agarose gel (50ml or 100ml), use 1.5g or 3g agarose respectively and mix into 50ml or 100ml 1X TBE Buffer respectively. Dissolve by microwave heating. Allow to cool, add 5ul or 10ul of SyBr Safe, pour into casting tray with a well comb and allow to solidify (1-2hr min).

Immerse gel into tank buffer. Load first well with 7ul of MWM and 3ul LD or mix 200ul lab LD with 25ul of MWM and 125ul water and store in fridge and use 7ul in gel. Load 7-8ul of PCR product onto gel. Electrophorese at 90V for 50-60minutes. For larger gels, allow for run in of samples as loading proceeds. If GoTaq Reaction buffer used then no LD needed.

For the analysis:

- Assess sharpness and specificity of band at different temps by visualizing under UV Doc, photograph and label.

Appendix H: Patient DNA Isolations

Table 1: Patient DNA Isolations at Diagnosis and after Cycle 3 of Anthracycline-based Chemotherapy

DNA Number	Pre-treatment Sample	Post-treatment Sample	Notes
ACT 1.1ANN	848.62	150.69	
ACT 2.1FLO	908.33	591.97	
ACT 3.1FAI	286.03	249.69	
ACT 4.1SUK	285.79	69.73	
ACT 5.1JUL	1204.09	806.91	
ACT 6.1GER	332.81	616.3	
ACT 7.1VUY	535.19	198.97	
ACT 8.1 LYN	860.98	1509.22	
ACT 9.1HEN	1472.8	291.65	
ACT 10.1SHA	948.92	131.2	
ACT 11.1CHA	2357.47	310.74	
ACT 12.1NAD	101	374.3	
ACT 13.1NOM	1671.5	965.99	
ACT 14.1GAY	1517.7	331.52	
ACT 15.1BER	1269.04	379.99	
ACT 16.1BON	546.74	793.25	
ACT 17.1MON	285.05	144.67	
ACT 18.1CHA	385.35	835.29	
ACT 19.1CHE	949.22	426.34	
ACT 20.1MYM	1017.5	619.58	
ACT 21.1NON	1209.6	765.63	
ACT 22.1VER	929.33	562.76	
ACT 23.1SHI	748.93	577.21	
ACT 24.1MER	321.74		Patient deceased before sample 2 procured
ACT 25.1MAR	927.17	587.09	
ACT 26.1RHO	284.81	108.5	
ACT 27.1LUC	916.28	180.9	
ACT 28.1NOE	1155.7		Patient defaulted
ACT 29.1GAD	231.58	648.42	
ACT 30.1TAN	135.93	335.36	
ACT 31.1DOR			DNA Isolation failed for sample 1; patient defaulted for sample 2
ACT 32.1SHA	395.24	420.3	
ACT 33.1SYL	151.08		Chemotherapy regimen changed
ACT 34.1NEL	307.32	328.47	
ACT 35.1INTO	1168.9		Patient defaulted

ACT 36.1NAT	228.77	323.22	
ACT 37.1KUL	131.21		No treatment administered
ACT 38.1MAR	820.18	333.33	
ACT 39.1SUS	879.15	1078.84	
ACT 40.1MON	101.57	190.86	
ACT 41.1PHE	239.3		Patient defaulted
ACT 42.1LIE	383.96		Patient defaulted
ACT 43.1DEN	508.37	214.14	
ACT 44.1HEL	778.58	520.41	
ACT 45.1NOK	594.36	662.52	
ACT 46.1ELI	153.71	402.42	
ACT 47.1SHA	180.16	346.74	
ACT 48.1YAL	275.37		Patient defaulted
ACT 49.1NOS	260.96	44.9	
ACT 50.1PAM	452.16	103.2	
ACT 51.1BON	54.78	92.54	
ACT 52.1ANN	45.41		Patient defaulted
ACT 53.1DEB	81.21		Patient defaulted
ACT 54.1BAR	229.35	53.64	
ACT 55.1MAR	332.43		Patient defaulted
ACT 56.1FEL	55.2		Patient defaulted
ACT 57.1OLI	24.96	73.5	
ACT 58.1DOR	78.4		Patient defaulted
ACT 59.1JAN	28.3	149.09	
ACT 60.1MAR	155.93	54.8	
ACT 61.1LAT	102.7	120.5	
ACT 62.1THA	65.6	57.6	
ACT 63.1ELI	25.1	68.8	
ACT 64.1NOK	29.8	147.7	
ACT 65.1MAR	88.62	52.9	
ACT 66.1RAC	162.72	154.2	
ACT 67.1TES	356.67	51.1	
ACT 68.1MAR	308.62	87.4	
ACT 69.1NOB	118.7		Patient defaulted
ACT 70.1KAR	193.1	139.02	
ACT 71.1SHI	147.3		Sample 2 stored as buffy
ACT 72.1MON	49.6		Sample 2 stored as buffy
ACT 73.1ALY	65.3		Sample 2 stored as buffy
ACT 74.1RAG	176.01		Sample 2 stored as buffy
ACT 75.1ZUK	56.42		Sample 2 stored as buffy
ACT 76.1DEL	138.23		Sample 2 stored as buffy
ACT 77.1CHR	190.57		Sample 2 stored as buffy
ACT 78.1BON	95.6		Sample 2 stored as buffy
ACT 79.1VER	82.86		Sample 2 stored as buffy
ACT 80.1MAR	169.89		Sample 2 stored as buffy

ACT 81.1ELI	248.69		Sample 2 stored as buffy
ACT 82.1PAT	69		Sample 2 stored as buffy
ACT 83.1YVO	302.16		Sample 2 stored as buffy
ACT 84.1EUA	67.21		Sample 2 stored as buffy
ACT 85.1CHR	82.11		Sample 2 stored as buffy
ACT 86.1YOL	231.57		Sample 2 stored as buffy
ACT 87.1JOL	103.35		Sample 2 stored as buffy
ACT 88.1TAN	225.67		Sample 2 stored as buffy
ACT 89.1MAR	171.46		Sample 2 stored as buffy
ACT 90.1ANT	550.46		Sample 2 stored as buffy
ACT 91.1LIZ	340.34		Sample 2 stored as buffy
ACT 92.1JAM	118.76		Sample 2 stored as buffy
ACT 93.1NAZ	71.24		Sample 2 stored as buffy
ACT 94.1AVR	47.61		Sample 2 stored as buffy
ACT 95.1VUY	183.76		Sample 2 stored as buffy
ACT 96.1FAG	66.63		Sample 2 stored as buffy
ACT 97.1MAG	29.89		Sample 2 stored as buffy
ACT 98.1AVR	21.94		Sample 2 stored as buffy
ACT 99.1PAT	27.78		Sample 2 stored as buffy
ACT 100.1 NOM	52		Sample 2 stored as buffy
ACT 101.1MAR	177.93		Sample 2 stored as buffy
ACT 102.1PAU	286.96		Sample 2 stored as buffy
ACT 103.1INS	75.08		Sample 2 stored as buffy
ACT 104.1NOT	57.78		Sample 2 stored as buffy
ACT 105.1NAN	58.26		Sample 2 stored as buffy
ACT 106.1ELL	19.51		Sample 2 stored as buffy
ACT 107.1NOM	20.02		Sample 2 stored as buffy
ACT 108.1CHR	72.82		Sample 2 stored as buffy
ACT 109.1SAN	40.38		Sample 2 stored as buffy
ACT 110.1JEA	150.19		Sample 2 stored as buffy
ACT 111.1THE	25.68		Sample 2 stored as buffy
ACT 112.1RUB	189.17		Sample 2 stored as buffy
ACT 113.1JEA	117.57		Sample 2 stored as buffy
ACT 114.1PAM	33.72		Sample 2 stored as buffy
ACT 115.1ANN	23.25		Sample 2 stored as buffy
ACT 116.1SHI	28.37		Sample 2 stored as buffy
ACT 117.1VIO	62.99		Sample 2 stored as buffy
ACT 118.1GLE	133.19		Sample 2 stored as buffy
ACT 119.1ROW	116.77		Sample 2 stored as buffy
ACT 120.1VAL	93.94		Sample 2 stored as buffy
ACT 121.1MAR	91.54		Sample 2 stored as buffy
ACT 122.1GRA	59.51		Sample 2 stored as buffy
ACT 123.1LUL	50.23		Sample 2 stored as buffy
ACT 124.1NCU	186.94		Sample 2 stored as buffy
ACT 125.1SHA	105.63		Sample 2 stored as buffy

ACT 126.1GEO	67.88		Sample 2 stored as buffy
ACT 127.1AME	11.15		Sample 2 stored as buffy
ACT 128.1CHR	176.37		Sample 2 stored as buffy
ACT 129.1AME	111.99		Sample 2 stored as buffy
ACT 130.1MIN	121.62		Sample 2 stored as buffy
ACT 131.1ELI	102.25		Sample 2 stored as buffy
ACT 132.1NIC	89.01		Sample 2 stored as buffy
ACT 133.1AMA	153.66		Sample 2 stored as buffy
ACT 134.1ADR	103.7		Sample 2 stored as buffy
ACT 135.1FIO	107		Sample 2 stored as buffy
ACT 136.1JUR	93.76		Sample 2 stored as buffy
ACT 137.1CYN	95.41		Sample 2 stored as buffy
ACT 138.1JEA	44.63		Sample 2 stored as buffy
ACT 139.1HEN	74.48		Sample 2 stored as buffy
ACT 140.1URS	32.27		Sample 2 stored as buffy
ACT 141.1MAR	42.28		Sample 2 stored as buffy
ACT 142.1ALE	115.33		Sample 2 stored as buffy
ACT 143.1DES	102.58		Sample 2 stored as buffy
ACT 144.1NOK	43.19		Sample 2 stored as buffy
ACT 145.1JAC	110.64		Sample 2 stored as buffy
ACT 146.1ELI	52.1		Sample 2 stored as buffy
ACT 147.1SHI	158.18		Sample 2 stored as buffy
ACT 148.1GER	76.9		Sample 2 stored as buffy
ACT 149.1ZEL	287.11		Sample 2 stored as buffy
ACT 150.1KAT	47.43		Sample 2 stored as buffy
ACT 151.1AMA	94		Sample 2 stored as buffy
ACT 152.1ALE	40.94		Sample 2 stored as buffy
ACT 153.1SOF	240.04		Sample 2 stored as buffy
ACT 154.1SHA	18.09		Sample 2 stored as buffy
ACT 155.1TAN	131.21		Sample 2 stored as buffy
ACT 156.1LUC	37.16		Sample 2 stored as buffy
ACT 157.1LIL	250.23		Sample 2 stored as buffy
ACT 158.1NOM	56.89		Sample 2 stored as buffy
ACT 159.1WIL	99.1		Sample 2 stored as buffy
ACT 160.1MYR	5.17		Sample 2 stored as buffy
ACT 161.1MIC	83.91		Sample 2 stored as buffy
ACT 162.1LYN	37.72		Sample 2 stored as buffy
ACT 163.1JOH	25.27		Sample 2 stored as buffy
ACT 164.1EVA	68.35		Sample 2 stored as buffy
ACT 165.1JEN	85.04		Sample 2 stored as buffy
ACT 166.1SUS	49.55		Sample 2 stored as buffy
ACT 167.1LUN	19.95		Sample 2 stored as buffy
ACT 168.1RAC	39.83		Sample 2 stored as buffy
ACT 169.1NOK	102.67		Sample 2 stored as buffy
ACT 170.1NOV	163.38		Sample 2 stored as buffy

ACT 171.1NOK	688.71		Sample 2 stored as buffy
ACT 172.1MAR	261.47		Sample 2 stored as buffy
ACT 173.1LEA	344.45		Sample 2 stored as buffy
ACT 174.1JOA	68.97		Sample 2 stored as buffy
ACT 175.1JOH	281.45		Sample 2 stored as buffy
ACT 176.1MAR	987.31		Sample 2 stored as buffy
ACT 177.1ANN	110.75		Sample 2 stored as buffy
ACT 178.1RAC	349.14		Sample 2 stored as buffy
ACT 179.1NAZ	419.74		Sample 2 stored as buffy
ACT 180.1MIC	168.29		Sample 2 stored as buffy
ACT 181.1LAU	137.91		Sample 2 stored as buffy
ACT 182.1THA	657.25		Sample 2 stored as buffy
ACT 183.1WEN	96.84		Sample 2 stored as buffy
ACT 184.1SAR	96.31		Sample 2 stored as buffy
ACT 185.1FLO	976.93		Sample 2 stored as buffy
ACT 186.1VER	590.32		Sample 2 stored as buffy
ACT 187.1RUK	371.95		Sample 2 stored as buffy
ACT 188.1LOR	75.43		Sample 2 stored as buffy
ACT 189.1LEL	136.21		Sample 2 stored as buffy
ACT 190.1BAD	1281.4		Sample 2 stored as buffy
ACT 191.1PET	777.44		Sample 2 stored as buffy
ACT 192.1INTO	313.3		Sample 2 stored as buffy
ACT 193.1FRA	782.92		Sample 2 stored as buffy
ACT 194.1YOL	747.9		Sample 2 stored as buffy
ACT 195.1LOR	694.16		Sample 2 stored as buffy
ACT 196.1JUD	560.45		Sample 2 stored as buffy
ACT 197.1PET	183.82		Sample 2 stored as buffy
ACT 198.1ALV	192.12		Sample 2 stored as buffy
ACT 199.1PAT	106.45		Sample 2 stored as buffy
ACT 200.1KAR	440.13		Sample 2 stored as buffy
ACT 201.1INTO	66.91		Sample 2 stored as buffy
ACT 202.1JAC	196.86		Sample 2 stored as buffy
ACT 203.1BEA	155.92		Sample 2 stored as buffy
ACT 204.1MUR	22.42		Sample 2 stored as buffy
ACT 205.1ZUR	521.45		Sample 2 stored as buffy
ACT 206.1NOA	282.67		Sample 2 stored as buffy
ACT 207.1MAG	305.56		Sample 2 stored as buffy
ACT 208.1RAC	233.67		Sample 2 stored as buffy
ACT 209.1VEN	49.16		Sample 2 stored as buffy
ACT 210.1JOH	212.56		Sample 2 stored as buffy
ACT 211.1VER	440		Sample 2 stored as buffy
ACT 212.1ALI	216.81		Sample 2 stored as buffy
ACT 213.1DES	312.04		Sample 2 stored as buffy
ACT 214.1SHI	130.27		Sample 2 stored as buffy
ACT 215.1GER	555.82		Sample 2 stored as buffy

ACT 216.1FUN	646.26		Sample 2 stored as buffy
ACT 217.1MIE	97.86		Sample 2 stored as buffy
ACT 218.1PAT	271.82		Sample 2 stored as buffy
ACT 219.1MAG	468.66		Sample 2 stored as buffy
ACT 220.1MAU	199.7		Sample 2 stored as buffy
ACT 221.1BER	413.44		Sample 2 stored as buffy
ACT 222.1STE	201.95		Sample 2 stored as buffy
ACT 223.1PLI	75.69		Sample 2 stored as buffy
ACT 224.1FLO	100.25		Sample 2 stored as buffy
ACT 225.1KAR	454.62		Sample 2 stored as buffy
ACT 226.1SER	92.82		Sample 2 stored as buffy
ACT 227.1LUC	243.93		Sample 2 stored as buffy
ACT 228.1DUN	47.05		Sample 2 stored as buffy
ACT 229.1ROS	56.45		Sample 2 stored as buffy
ACT 230.1WIL	513.23		Sample 2 stored as buffy
ACT 231.1ELS	634.41		Sample 2 stored as buffy
ACT 232.1ALE	638.29		Sample 2 stored as buffy
ACT 233.1ANI	465.57		Sample 2 stored as buffy
ACT 234.1CHR	299.49		Sample 2 stored as buffy
ACT 235.1ELI	267.6		Sample 2 stored as buffy
ACT 236.1RUT	174.89		Sample 2 stored as buffy
ACT 237.1ELI	152.36		Sample 2 stored as buffy
ACT 238.1BEU	581.08		Sample 2 stored as buffy
ACT 239.1BUS	1742.5		Sample 2 stored as buffy
ACT 240.1TAR	670.17		Sample 2 stored as buffy
ACT 241.1CAT	407.82		Sample 2 stored as buffy
ACT 242.1EME	520.35		Sample 2 stored as buffy
ACT 243.1CHR	696.28		Sample 2 stored as buffy
ACT 244.1LYD	578.75		Sample 2 stored as buffy
ACT 245.1RAC	290.01		Sample 2 stored as buffy
ACT 246.1SUS	97.36		Sample 2 stored as buffy
ACT 247.1ELI	263.33		Sample 2 stored as buffy
ACT 248.1BUS	246.17		Sample 2 stored as buffy
ACT 249.1JAN	543.42		Sample 2 stored as buffy
ACT 250.1THA	89.19		Sample 2 stored as buffy
ACT 251.1WEN	600.6		Sample 2 stored as buffy
ACT 252.1JOH	306.36		Sample 2 stored as buffy
ACT 253.1FRA	369.31		Sample 2 stored as buffy
ACT 254.1JON	328.43		Sample 2 stored as buffy
ACT 255.1VAN	704.44		Sample 2 stored as buffy
ACT 256.1CAR	507.32		Sample 2 stored as buffy
ACT 257.1ANN	705.13		Sample 2 stored as buffy
ACT 258.1BER	497.99		Sample 2 stored as buffy
ACT 259.1CAR	611.26		Sample 2 stored as buffy
ACT 260.1NAO	257.88		Sample 2 stored as buffy

ACT 261.1FLO	570.03		Sample 2 stored as buffy
ACT 262.1LEZ	413.59		Sample 2 stored as buffy
ACT 263.1SUZ	59.54		Sample 2 stored as buffy
ACT 264.1ANN	454.65		Sample 2 stored as buffy
ACT 265.1EST	406.05		Sample 2 stored as buffy
ACT 266.1SAR	380.05		Sample 2 stored as buffy
ACT 267.1JOH	197.99		Sample 2 stored as buffy
ACT 268.1CAT	503.42		Sample 2 stored as buffy
ACT 269.1HAZ	489.64		Sample 2 stored as buffy
ACT 270.1NOM	439.12		Sample 2 stored as buffy
ACT 271.1MOI	657.32		Sample 2 stored as buffy
ACT 272.1MAR	232.58		Sample 2 stored as buffy
ACT 273.1THE	503.84		Sample 2 stored as buffy
ACT 274.1MER	1871		Sample 2 stored as buffy
ACT 275.1CAR	317.49		Sample 2 stored as buffy

Appendix I: Spectrophotometric quantitation of DNA

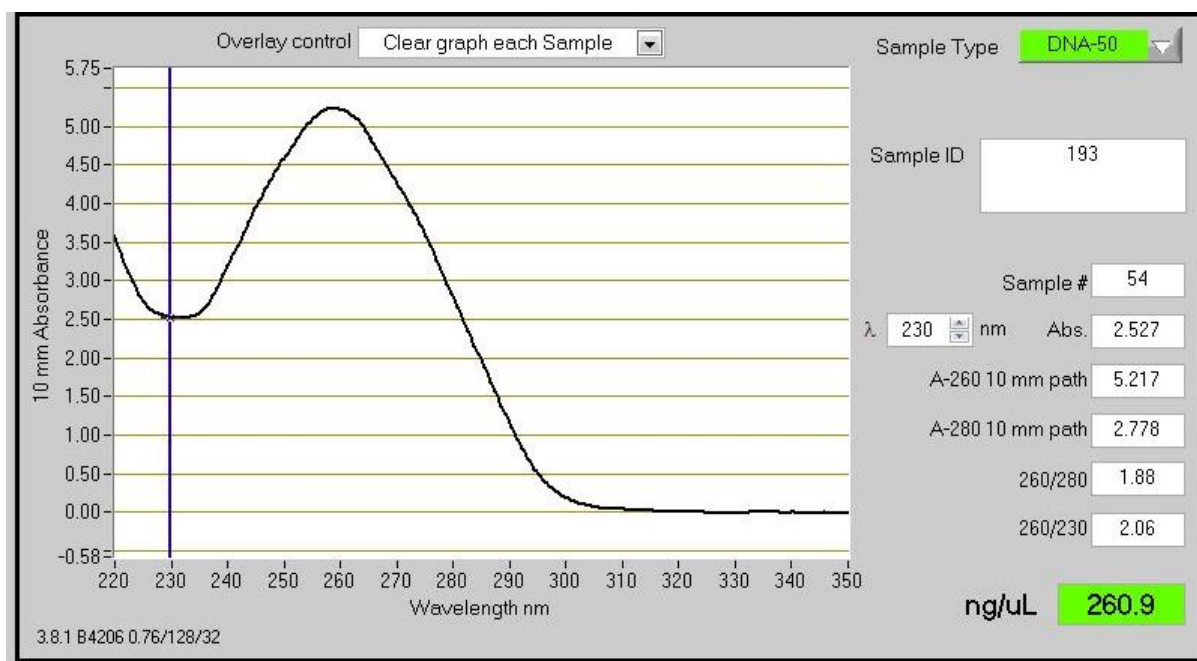


Figure 1: Representation of the spectrophotometric quantitation of patient DNA samples (ACT 193.1FRA) using the NanoDrop ND-1000 (Nanodrop Technologies, USA)

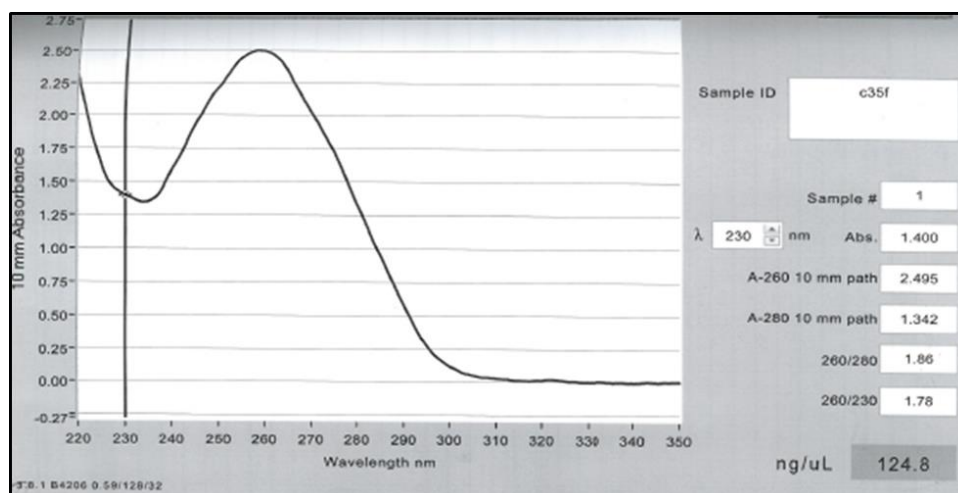


Figure 2: Representation of the spectrophotometric quantitation of a control DNA sample (C35F) before being utilized in the optimisation of the TaqMan™ Genotyping Assay using the NanoDrop ND-1000 (Nanodrop Technologies, USA)

